Physical patterns and *post-hoc* measures of wildfire behaviour in grassland.

Relevance of forensic indicators in wildfire investigations.

Matthew Danckwerts

Thesis presented in fulfilment of the requirements for the degree of Master of Science in the Department of Botany and Zoology, at Stellenbosch University

Supervisor: Guy Midgley

Co-supervisor: Heath Beckett

December 2022

DECLARATION

By submitting this thesis electronically, I declare that the entirety of the work contained therein is my own original work, that I am the authorship owner thereof (unless to the extent explicitly otherwise stated) and that I have not previously in its entirety or in part submitted it for obtaining any qualification.

The Author

ABSTRACT

Wildland fires are an intrinsic feature of seasonal grassland and savanna ecosystems, and are thus guaranteed to occur at some frequency in these systems. In addition, fire managers and practitioners in southern Africa use fire as a management tool in these rangeland systems to achieve an array of management goals for ecological, agricultural, and safety purposes. The occurrence of uncontrolled fires potentially attributable to human agency and accompanied by damage to property and associated litigation is an inevitable outcome in these wildland fire systems. The fields of fire litigation and forensics are, however, under-developed for such wildfire systems in which the inference of deliberate, accidental, and natural contributors to events is critical. *Post-hoc* physical indicators of wildfire pattern and spread, as well as fire behaviour prediction models are used by experts to determine origin, spread, and behaviour of fires in forensic wildland fire investigations conducted in contemplation of litigation.

A review of *post-hoc* wildfire behaviour indicators relevant to forensic wildfire investigations, detailing application, reliability, and limitations, identified a suite of indicators of potential value in such circumstances. Selected *post-hoc* indicators and prediction models of fire behaviour were then tested for their suitability and utility across a range of fuel and weather conditions in montane grassland systems of the Greater Winterberg region, Eastern Cape, South Africa.

Real-time fire behaviour data were gathered from 143 fires across seven sites and compared with corresponding post-fire indicator expression and prediction model outputs. Slope proved to be a critical driver of fire behaviour in the mountainous Eastern Cape grassland systems. Fire behaviour models (encompassing a wide range of fuel model configurations constructed for southern African grassland systems), did not suitably predict (or retrodict) actual fire conditions, generally under-predicting rate of spread, fire intensity, & flame length values. McArthur models, derived from field-based data, proved to be the most suitable predictors of fire behaviour in Eastern Cape montane grasslands. It is recommended that current fuel model and input assumptions which exist for southern African grassland and savanna systems be re-evaluated.

Residual ash colour, curling, spalling, and residual ash organic carbon content were found to be unreliable forensic indicators of wildfire pattern and spread. Foliage freeze, cupping of grass tussocks, consumption depth of grass tussocks, amount of residual unburnt plant litter, protection, sooting, & staining were considered reliable, but in some cases may be site specific and need to be applied in conjunction with each other to draw accurate and reliable conclusions of fire pattern and spread. The presence of undercut culms and leeside charring on pole-type fuels are almost unequivocal indicators of back fires and wind direction, respectively.

These findings suggest that certain *post-hoc* wildland fire pattern and spread indicators must be re-evaluated, and practitioners are advised to adopt an adaptive approach to indicator interpretation,

applying fire behavioural science of the processes and drivers of indicator formation and expression, while collectively incorporating several indicators in conjunction with each other before forming conclusions on origin, cause, and spread of ‘runaway’ wildfires.

OPSOMMING

Veldbrande is 'n intrinsieke kenmerk van seisoenale grasveld en savanne ekosisteme, en is dus gewaarborg om op 'n sekere frekwensie in hierdie stelsels te voorkom. Daarbenewens gebruik brandbestuurders en praktisyns in Suider-Afrika vuur as 'n bestuursinstrument in hierdie weiveldstelsels om 'n verskeidenheid bestuursdoelwitte vir ekologiese, landbou en veiligheidsdoeleindes te bereik. Die voorkoms van onbeheerde brande moontlik toeskryfbaar aan menslike agentskap wat gepaard gaan met skade aan eiendom en regseise is 'n onvermydelike uitkoms in hierdie veldbrandstelsels. Die onderwerpe van brandlitigasie en forensiese ondersoeke is egter onderontwikkel vir sulke veldbrandstelsels waarin die afleiding van doelbewuste, toevallige en natuurlike bydraers tot gebeure krities is. Post-hoc fisiese aanwysers van veldbrandpatroon en verspreiding, sowel as brandgedragvoorspellingsmodelle word deur kundiges gebruik om oorsprong, verspreiding en gedrag van brande te bepaal in forensiese veldbrandondersoeke wat uitgevoer word in oorweging van litigasie.

'n Lieteraturr-oorsig van post-hoc veldbrandgedrag-aanwysers wat relevant is vir forensiese veldbrandondersoeke, met besonderhede oor toepassing, betroubaarheid en beperkings, het 'n reeks aanwysers van potensiële waarde in sulke omstandighede geïdentifiseer. Geselekteerde post-hoc aanwysers en voorspellingsmodelle van brandgedrag is getoets vir hul geskiktheid en bruikbaarheid oor 'n reeks brandstof- en weerstoestande in berggrasveldstelsels van die Groter Winterberg-streek, Oos-Kaap, Suid-Afrika.

Brandgedragdata is van 143 brande oor sewe terreine versamel en vergelyk met ooreenstemmende na-brand-aanwyseruitdrukking en voorspellingsmodeluitsette. Helling was 'n kritieke drywer van brandgedrag in die bergagtige Oos-Kaapse grasveldstelsels. Brandgedragmodelle (wat 'n wye reeks brandstofmodelkonfigurasies insluit wat vir Suider-Afrikaanse grasveldstelsels gebou is), het werklike brandtoestande nie behoorlik voorspel (of teruggespel) nie, gewoonlik onder voorspelling van verspreidingstempo, brandintensiteit en vlamlengtewaardes. McArthur-modelle, afgelei van veldgebaseerde data, het geblyk die mees geskikte voorspellers van brandgedrag in Oos-Kaapse berggraslande te wees. Dit word aanbeveel dat huidige brandstofmodel en insetaannames wat bestaan vir Suider-Afrikaanse grasveld- en savannestelsels herevalueer word.

Daar is gevind dat oorblywende askleur, krul, spatsels en oorblywende as-organiese koolstofinhoud onbetroubare aanwysers van veldbrandpatroon en verspreiding is. Blaarvriesing, opvul van graspolle, verbruiksdiepte van graspolle, hoeveelheid oorblywende onverbrande plantrommel, beskerming, roeting en kleuring is as betroubaar beskou, maar kan in sommige gevalle plekspesifiek wees en moet in samewerking met mekaar toegedien word om maak akkurate en betroubare gevolgtrekkings van brandpatroon en verspreiding. Die teenwoordigheid van ondersnyde halms en verkooling op paaltipe brandstowwe is byna onomwonde aanduidings van onderskeidelik terugbrande en windrigting.

Hierdie bevindings dui daarop dat sekere post-hoc veldbrandpatroon en verspreidingsaanwysers herevalueer moet word, en praktisyns word aangeraai om 'n aanpasbare benadering tot aanwyserinterpretasie aan te neem, deur brandgedragswetenskap van die prosesse en dryfvere van aanwyservorming en uitdrukking toe te pas, terwyl hulle gesamentlik verskeie aanwysers in samewerking met mekaar in te sluit voordat gevolgtrekkings gemaak word oor oorsprong, oorsaak en verspreiding van 'weghol' veldbrande.

ACKNOWLEDGEMENTS

My sincerest thanks goes out to the following people for all their valuable contributions towards this MSc, without whom this would not have been possible:

Mark Wienand, Colin Bennett, Bradley & Dale Emslie for kindly allowing me to sit in on your prescribed burns and conduct my experiments on your farms, thank you for your flexibility and gracious hospitality.

Jock Danckwerts for all your valuable contributions and ideas — the inspiration for this MSc project.

To my parents and all at Saxfold Park for funding my MSc. Your support and encouragement through this period has been most sincerely appreciated.

Winston Trollope for all your valuable advice and mentoring, which has contributed significantly towards my understanding of fire behaviour and ecology. May we continue to "push back the frontiers of ignorance".

To all those whom I have failed to mention, who have helped in one way or another, thank you.

Lastly, thank you to my supervisors Guy Midgley and Heath Beckett, for all your teachings, guidance, and patience throughout this period.

For my father Jock,
who has gifted me with an analytical mind,
sparked my interest in science,
and inspires me to keep pushing back the frontiers of ignorance.

"Clouds of smoke ascended from behind every hill, and one vast fire was seen near Winter Berg, which we never lost sight of."

– William Somerville, 1800

CONTENTS

LIST OF FIGURES

LIST OF TABLES

LIST OF ABBREVIATIONS

Order in which they appear in text

NFPA	—	National Fire Protection Association
NWCG	—	National Wildlife Coordinating Group
IAFC	—	International Association of Fire Chiefs
ROS	—	Rate of spread
FM	—	Fuel moisture
SA/V	—	Surface area to volume ratio
FMC	—	Fuel moisture content
FDI	—	Fire danger index
TOC	—	Total organic carbon
SD	—	Standard deviation
DPM	—	Disc pasture meter
MOE	—	Moisture of extinction
GAM	—	General additive model
DFM	—	Dead fuel moisture
TC	—	Total carbon
TIC	—	Total inorganic carbon
se	—	Standard error of mean

Chapter 1:
GENERAL INTRODUCTION

Wildfires have been burning across the planet since at least the early Eocene (Bond & Keeley, 2005; Trollope *et. al*., 2007). Over the past 8 million years, wildfire has played an integral part in shaping and maintaining ecosystems in some of the world's major biomes (Bond *et. al*., 2005; Bond & Keeley, 2005; Pausas & Keeley, 2009; Trollope, 2011; Staver *et al.*, 2011a, 2011b). The global ecological importance of fire has not perhaps been fairly represented and recognised in the past (Trollope *et. al.*, 2004; Bond *et. al*., 2005; Bond & Keeley, 2005; Pausas & Keeley, 2009), especially in the general public's perception (Durigan, 2020, Fidelis, 2020). In recent years, however, it has become a topic of growing interest for scientists (Trollope *et. al.*, 2004; Bond & Keeley, 2005; Pausas & Keeley, 2009), particularly in the context of a changing global climate (Bowman *et. al*., 2009; Flannigan *et. al*., 2009; Whitlock *et. al*., 2010; Moritz *et. al*., 2012; Archibald *et. al*., 2013). It is now widely accepted fires can, in many cases, play a beneficial role rather than a destructive one, that some species are fire-enhancing, and some ecosystems are fire-dependent (Bond et. al., 2005; Bond & Keeley, 2005; Trollope *et. al*., 2007; Pausas & Keely, 2009). Misunderstanding and misinterpretation of the role wildfires play, by scientists and the general public alike, may now be beginning to change (Durigan, 2020; Fidelis, 2020).

In the Central Grassland Biome, montane grasslands and many savanna systems of southern Africa, fire managers and pastoralists endeavour to emulate, regulate and control the natural effects of fire which maintain these systems, by implementing controlled fire regimes. There is a long history of wildfire management in southern Africa. While there is broad evidence to support human influences on African fire regimes for the past ten thousand years or more (Archibald *et. al.*, 2012), more recent observations relevant to southern African grasslands reveal South African pastoralists implementing prescribed burning (as a management tool), at least as early as the 15th century (Alberti, 1968; Wilson, 1969; Bradlow & Bradlow, 1979; Forbes, 1986; Trollope, 2011). The use of fire as a management tool in southern Africa likely extends many hundreds to thousands of years prior to these historical accounts. It is interesting to note, given the above, that Archibald *et. al.*, (2013) found that of all the continents, Africa has the highest representation of cooler, frequent fires of smaller extent.

An account by William Somerville during late winter/early spring 1800, of his trip to the Tarka region of the Eastern Cape, observed "*Clouds of smoke ascended from behind every hill, and one vast fire was seen near Winter Berg which we never lost sight of*." "*In many places we found the plains burned by locals – a common practice before the rainy season…*" (Bradlow & Bradlow, 1979, p.46). *"…the sour mountain grassland was burnt by Nguni pastoralists in winter so as to provide palatable spring grazing for their cattle.*" (Wilson, 1969, p.108).

Carl Peter Thunberg, on his trip to the Eastern Cape during the spring and summer (Sept - Jan) of 1772, also observed *"In many places…" "…the land to have been set on fire for the purpose of clearing it…" "Diverse plains here, produce a very high sort of grass, which being too coarse in nature, and unfit food for cattle, is not consumed and thus prevents fresh verdure from shooting up…" "Such a piece of land as this, therefore, is set on fire, to the end that new grass may spring up from the roots."* (Forbes, 1986, p.83).

Ludwig Alberti's account of the high rainfall (sour) grassland systems of the Eastern Cape in 1807 perhaps best describes fire management at the time: *"…the grass, which reaches an uncommon height there, is nearly everywhere, in the utmost degree, sour. In consequence of this characteristic, it attains such harshness after a long journey, that it cannot be eaten by any animal, which is why the…"* local pastoralists *"…go in for burning such grass so as to cause young growth to come in. Without such precautions they would not be able, owing to lack of nourishment for their cattle, to live in this stretch of country."* (Alberti, 1968, p.16).

These same practices are still implemented today, by fire managers and pastoralists alike, to much of the same end. Today it is widely recognised by both commercial and communal land users in Africa that fire can be used to manage vegetation for domestic livestock and wildlife (Trollope, 2011). In addition to removal of moribund and unpalatable vegetation, the use of fire as a management tool extends to the control of bush encroachment, management of wildlife conservation areas, pest control of ticks (Trollope, 1989; Trollope, 2011), as well as a variety of other uses (Nieman *et. al*., 2021). Extensive research into the effects of fire in savanna and grassland ecosystems has resulted in comprehensive, effective, and practical guidelines for the use of fire as a management tool in commercial livestock farming and ecological management practices (Trollope, 1989; Trollope, 2011).

Notwithstanding the important ecological role fire plays in shaping and maintaining ecosystems, anthropogenic settlement, accompanied by infrastructural development has resulted in inevitable damage to property when fires occur. The consequence is often, numerous claims for damages, incurred as a result of runaway fires, and many of these lead to litigation. Examples of such range from:

- Prethart Maatskappy (PTY) LTD vs Transnet SOC LTD (Free State Division of the High Court of South Africa, case no: 1839/2015), where more than **1600 ha** were burnt, and the quantum of claim was **R149 813.96**.
- Andries Cornelis de Klerk vs Eskom Holdings SOC LTD (Eastern Cape Division of the High Court of South Africa, case no: 2662/2018), where more than **1000 ha** were burnt, and the quantum of claim was in excess of **R600 000**. (The investigative report of which I was a co-author).
- Dirk Jakobus du Plessis vs Eskom Holdings SOC LTD (Free State Division of the High Court of South Africa, case no: 1459/2015), where more than **10 000 ha** were burnt, and the quantum of claim was in excess of **R1 600 000**.

- Pieter Nicolaas Oosthuizen & 2 Others vs Schalk Willem Vorster (Eastern Cape Division of the High Court of South Africa, case no: 1491/2016), where more than **2700 ha** were burnt, and the quantum of claim was in excess of **R7 million**.
- Corpinvest 60 (Pty) LTD & 11 Others vs Erinvale Country Estate & Others (Western Cape Division of the High Court of South Africa, case no: 17998/2011), where the cumulative quantum of claim was in excess of **R80 million**.
- Narciso Comes & 15 Others vs Zebula Country Club Sabel-Fauna Farming (Gauteng Division of the High Court of South Africa, case no: 43084/2013), where two **human lives were lost**.

The incidence, intensity and impact of these wildfires is expected to increase significantly with the changing climate and rapidly expanding wildland-urban interface (Trollope *et. al.*, 2004; Bowman *et. al*., 2009; Flannigan *et. al*., 2009; Moritz *et. al*., 2012; Jolly *et. al.*, 2015; Doerr & Santin, 2016).

To face and overcome these challenges, modern fire managers and pastoralists need to be mindful of when and when not to burn, taking into account the weather and fuel conditions in their considerations of the dangers and risks involved when conducting prescribed burns (Van Wilgen & Wills, 1988; Trollope *et. al.*, 2004). When making decisions in this regard, fire managers and pastoralists, need to be equipped with appropriate data and information, as well as skills and knowledge to interpret these data (Van Wilgen & Wills, 1988; Trollope *et. al.*, 2004).

With the onset of these 'modern' problems, come modern solutions. Fire danger rating systems and fire behaviour prediction models arm fire managers and pastoralists with a tool from which a range of important management strategies and safety decisions can be made (Van Wilgen & Wills, 1988; Anderson *et. al.*, 2011; Andrews, 2018).

While fire danger rating systems and fire behaviour prediction models have been developed and well researched for many years, rapid advances in technological advancement and the emergence of open-access software have increased the range, scope, availability, and promptness of fire behaviour mapping and forecasting. However, despite tremendous recent modelling advances, basic empirical fire research into the mechanics and processes of fire behaviour and spread has largely been neglected (Finney *et. al.*, 2013). Given the risks involved in conducting prescribed burns, it is important that predictions be considered accurate and reliable for subject site. To achieve this, fuel models based on site-appropriate fuel properties of dominant vegetation, need to be constructed (Van Wilgen & Wills, 1988; Trollope *et. al*., 2004). Therefore, before model-based management decisions can be made, site-specific empirical research is required.

Predictive mechanistic models need to be based on fundamental fire behaviour theory (Finney *et. al.*, 2013). Many models are based on a variety of assumptions, making it difficult to accurately represent real fire conditions (Finney *et. al.*, 2013). It has further been noted that there seems to be a lack of common understanding of what processes occur, and how they occur (Finney *et. al.*, 2013). Authors

have identified a serious lack of quantitative data on factors influencing fire behaviour in Africa, compared to Australia and the USA (Trollope *et. al*., 2004). Finney *et. al.*, (2013), emphasized the need for work on theory that provides a better understanding of wildfire behaviour.

Given their increasing credibility and value in predicting and forecasting fire behaviour, mathematical models should also be useful tools for the retrodiction* of fire conditions and aid in the reconstruction of fire behaviour. Given fuel and weather boundary conditions for any past fire event, it should be possible to reconstruct the behaviour and passage of past wildfires. Application of this technique could be a useful aid in the forensic investigation of wildfires (Danckwerts J.E. (PhD), personal communication, 2019). However, for this to be successful, fire behaviour prediction models' output values need to accurately retrodict actual fire conditions, and a clear idea of which variables are critical for credible retrodiction (simulation) is needed.

Legal teams rely on experts in wildland fire behaviour to investigate the origin, cause, spread and other pertinent aspects of the fire to gain a better understanding of potential liability. These investigations are conducted on a *post-hoc* basis and rely on physical evidence left by the fire. When conducting investigations in this regard, wildland fire investigators follow a stepwise and systematic process, first determining the direction of spread of the fire and then tracing their way back through the direction of spread, towards the approximate point of origin of the wildfire, where the backing fire meets the heading fire (Cheney & Sullivan, 2008; NFPA, 2017). Piecing together physical evidence, the path of a fire's spread can be reconstructed by examining the directional pattern shown by *post-hoc* wildland fire pattern indicators (NWCG, 2016; NFPA, 2017). These physical indicators of wildfire pattern, spread and behaviour are a fire investigator's primary evidence in origin and cause determination.

There is a need from legal teams for litigation relevant evidence to be considered credible in the court of law. Determination of the origin, cause and spread of wildfires, therefore need to be accurate and reliable, if possible (Simeoni *et. al*., 2017). To ensure this, it is necessary that the indicators from which identification of point of origin, cause and spread are determined, are empirically evaluated and based on quantified data.

Post-hoc wildland fire pattern indicators have variously been defined as the physical objects or visual remains persisting after a fire's passage, that display the physical effects of fire and collectively reveal the progress, action, and overall pattern of the fire (NWCG, 2016; NFPA, 2017; Simeoni *et. al*., 2017; NWCG, 2018). These visual fire effects are the observable or measurable changes caused to partially burned fuels and incombustible objects when exposed to heat, flame and/or the by-products of combustion (NWCG, 2016). Fire effects may, *inter alia*, include differential damage, char patterns, discolouration, carbon staining, shape, location, and condition of residual unburnt fuel (NFPA, 2017).

**** Retrodiction.*** *n. The act of making a "prediction" about the past.*

Close inspection and interpretation of individual wildfire pattern indicators can reveal a host of information pertaining to the behaviour and spread of fire can be inferred from individual wildfire pattern indicators. This information can, however, be simplified to indicate at least one of the following**:** **direction of fire passage**; **wind direction**; and **fire spread type** (heading, backing or flanking fire).

The field of wildfire forensics in southern Africa is still in its infancy, but there is a growing need from litigants for the development of a reliable scientifically and evidence-based practice, based on good theory and observation. There has also been a paucity of wildfire modelling work in Eastern Cape montane grasslands. The purpose of this study is to contribute to resolving these identified gaps and needs. I aimed to do this by gathering empirical data for a number of controlled burns in Eastern Cape montane grasslands and using this information to evaluate and assess the reliability, accuracy, and suitability of various fire models and pos*t-hoc* indicators to predict and retrodict actual wildfire conditions in this ecosystem. This information and analysis provide new insights into wildfire behaviour, which may lead to a better understanding of fire effects in montane grasslands, and help managers and investigators make informed decisions.

Thesis structure

A thorough review of wildfire investigation literature is covered in **Chapter 2**, including an overview of the science of combustion as it relates to wildfire investigations, a review of various fire behaviour prediction models and their use in fire investigations, an introduction to wildfire investigations, and an extensive list of *post-hoc* wildfire indicators, their descriptions, uses and limitations, as well as some proposed 'novel' indicators.

Chapter 3 is a short overview of the study sites, prescribed fires, fuel, and weather conditions.

In **Chapter 4**, I examine how various configurations of several fire behaviour prediction models compare with recorded grassfire conditions. I also explore various fuel model and input assumptions and investigate which configurations are best suited to the conditions of the Eastern Cape montane grasslands.

I hypothesised that the critical input parameters (primary drivers of fire behaviour) required for accurate simulation of fire behaviour in Eastern Cape montane grasslands, will not differ significantly from those in other similar grassland and savanna systems in southern Africa.

I hypothesised further, that models developed either specifically for grassland conditions, using data collected from numerous field trials, or for wildland fires in general, from artificially reconstructed fuel conditions, will differ significantly in their ability to project and thus to retrodict actual wildfire behaviour (recorded fire conditions).

Chapter 5 is an assessment of the reliability and accuracy of *post-hoc* wildland fire pattern indicators to reveal aspects of actual fire behaviour conditions. Specific conditional requirements (weather, fuel, environmental, or fire behavioural) for indicator formation and expression is also examined.

My primary hypothesis is that some of the selected indicators will be more sensitive and reliable for the purposes of reconstructing and interpreting wildfire behaviour, and my objective is to determine which of these have utility for forensic purposes.

Finally, **Chapter 6** is a synthesis of the above topics, discussing the results in the context of wildland fire management and with specific reference to wildfire investigations conducted in preparation for litigation. The practicality of indicator and model application in this field is discussed, as well as the relative reliability and credibility expected from this evidence. Study limitations, potential and proposed improvements, as well as areas of research required in future studies are also discussed.

Chapter 2:
A REVIEW OF WILDFIRE FORENSICS AS AN EVIDENCE BASED PRACTICE

Before one can delve into the study and analysis of wildfire forensics, it is important to have an understanding of the critical concepts behind the principles of combustion, such as what drives fire behaviour, the chemistry, physical science, and fluid dynamics (heat transfer) of combustion, types and structures of fires, fire intensity and severity, rate of spread, fuel moisture and curing. Many of these concepts are circular, feeding back into each other and ultimately explain the formation and expression of forensic indicators of wildfire behaviour. The following section delves into these aspects of fire behaviour, providing a thorough review of the relevant science and literature.

2.1 Some pertinent aspects of fire behaviour as it relates to fire investigations:

There are three main components which collectively influence the **general behaviour** of wildfires: weather, topography, and fuels (Teie, 2003; Cochrane & Ryan, 2009; Scott *et. al*., 2014; NWCG, 2016; Leavell *et. al*., 2017). These three elements are sometimes referred to as the fire behaviour triangle (Teie, 2003; Cochrane & Ryan, 2009; Scott *et. al*., 2014; NWCG, 2016; Leavell *et. al*., 2017).

There are numerous measures of fire behaviour, comprising many metrics, both quantitative and qualitative. Some notable measures relevant to this study include fire intensity, severity, rate of spread, and fire spread type.

2.1.1 Fire spread type:

Fire spread type (head, back & flank) is a vector value describing the direction of fire spread, usually in relation to wind direction (**FIGURE 2.1**). While in progress, a moving wildfire burns roughly in an elliptical or oval shape (As a fire evolves from a point of ignition, under a steady wind, the perimeter will spread forwards, laterally and backwards developing the typical elliptical or oval shape (isochrone)) (Cheney & Sullivan, 2008; Scott *et. al*., 2014) (**FIGURE 2.1 & FIGURE 2.10**).

Fire spread type is determined by both direction of fire passage and wind direction. Three types of fire spread can be described according to their respective positions along the fire perimeter – **heading**, **backing** and **flanking** fires (Cheney & Sullivan, 2008; NFPA, 2017).

Wind (speed and direction) therefore, is considered to be the predominant factor influencing wildfire **spread** (particularly in cured grasslands) (Cheney *et. al.*, 1993; Teie, 2003; Trollope *et. al.*, 2004; Cheney & Sullivan, 2008; NWCG, 2016).

After wind, slope is considered to be the second dominant factor influencing wildfire spread (NWCG, 2016). Irrespective of wind, a fire moving up a slope will tend to behave like a heading fire, spreading rapidly, whereas a fire moving down a slope will behave like backing fire, spreading at a slower rate (Luke & McArthur, 1978; Trollope, 1984; Cheney & Sullivan, 2008; NWCG, 2016; Leavell *et. al*., 2017; NFPA, 2017). This is because fuel upslope of the fire is preheated more rapidly as the flames lean into the slope, reducing distance between the flames and fuel (Trollope, 1984; NWCG, 2016; Leavell *et. al*., 2017; NFPA, 2017). Conversely, fuel downslope of the fire is preheated less rapidly as flames lean away from the fuel, into the slope, increasing distance between the flames and fuel (Trollope, 1984; NWCG, 2016; Leavell *et. al*., 2017; NFPA, 2017).

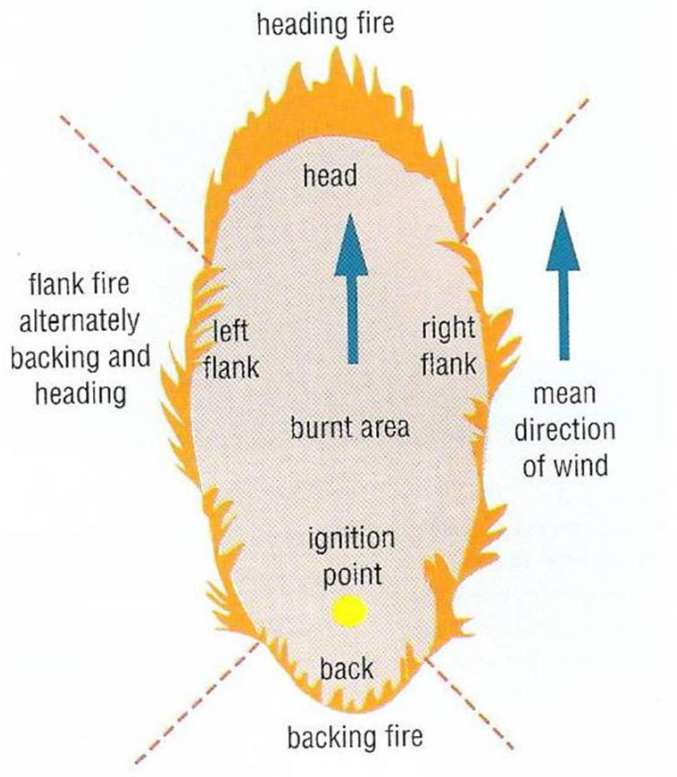

FIGURE 2.1: *The parts of a moving fire; flames of a heading fire lean over the unburnt fuel; flames of a backing fire lean over burnt ground; flames of flank fires may lean over either unburnt fuel or burnt ground depending on local fluctuation in wind direction. While grassfires more commonly burn in an oval shape (heading region widens at a greater rate than backing region), for the purpose of this figure, the fire is depicted in an elliptical shape. Reprinted from "*Grassfires: fuel, weather and fire behaviour (1st ed.)", *by Cheney, P., & Sullivan, A., 1997, pp. 13, Australia: CSIRO Publishing. Copyright 1997 by CSIRO.*

The influence of fuel on fire spread should not be disregarded. Fuel parameters such as fuel load (mass per unit area), size, (fine or heavy), moisture content, and flammability characteristics have considerable influence on fire behaviour measures such as intensity and rate of spread (Trollope *et. al*., 2004; Cheney & Sullivan, 2008; Scott *et. al*., 2014). Typically, fuel has little influence on the direction of spread of wildland fires, however, in cases where fuel is not continuous, or there are abrupt changes in fuel conditions, fire spread may deviate from the typical elliptical or oval shaped pattern of spread (Danckwerts J.E. (PhD), personal communication, 2019). Put simply, fires follow fuel. This is particularly relevant in back fires, which may be halted by even minor influences in fuel continuity. Importantly, fuel conditions do not influence fire spread type (head, back, or flank).

In fire behaviour literature head fires have typically been defined as those that burn in the same direction as the prevailing wind (and *vice versa* with regards to backfires) (Beaufait, 1965; Trollope, 1978; Trollope, 1981; Trollope, 1984; IAFC *et. al*., 2018; NWCG, 2018). Cheney & Sullivan, in their 2008 book *Grassfires: fuel, weather and fire behaviour* (2nd ed.), perhaps more appropriately, distinguish between fire spread types by the angle at which the flames are burning in relation to direction of spread. This definition accounts for the influence of both wind and topography.

A **heading fire**, usually positioned along the portion of the oval (**FIGURE 2.1**) furthest from the point of ignition (Cheney & Sullivan, 2008), is defined as the part of the fire moving most rapidly (Trollope *et. al.*, 2004; NFPA, 2017). They are also known as advancing fires (NFPA, 2017), and are characterised by having flames which lean towards the unburnt fuel (**FIGURE 2.2 & FIGURE 2.3**) (Trollope *et. al.*, 2004; Cheney & Sullivan, 2008). This arises by the fire burning either with the wind (Trollope, 1978; NFPA, 2017) or up a slope (**FIGURE 2.3**) (Trollope *et. al.*, 2004). The rapid nature of combustion in head fires means that they are more intense than other fire spread types (Trollope, 1984; NFPA, 2017), but also less efficient, often resulting in incomplete combustion of plant material (Trollope *et. al.*, 2004; Cheney & Sullivan, 2008). In addition, the heat load in head fires is at a higher elevation in the fuel bed (Trollope, 1984), further contributing to the reduced consumption of plant material (less severe) (Trollope *et. al.*, 2004; Cheney & Sullivan, 2008). Large billows of black smoke are often characteristic of the more intense advancing fires, ensuing from rapid, incomplete combustion (**FIGURE 2.2**) (Cheney & Sullivan, 2008).

FIGURE 2.2: *A typical head fire. Black smoke indicates incomplete combustion. Experimental fire A091, NT, Australia, 4 August 1986. Reprinted from "*Grassfires: fuel, weather and fire behaviour (2nd ed.)", *by Cheney, P., & Sullivan, A., 2008, pp. 22, Australia: CSIRO Publishing. Copyright 2008 by CSIRO.*

FIGURE 2.3: *Separate head and back fires approaching each other. Head fire burning up slope and with wind. Back fire burning down slope and against wind. Prescribed burn BE3, Katberg, EC, South Africa, 8 November 2019.*

In contrast to heading fires, **backing fires** are usually positioned along the portion of the oval (**FIGURE 2.1**) closest to the point of ignition (Cheney & Sullivan, 2008), moving in the opposite direction to the head fire (NFPA, 2017). Back fires are slow moving (Cheney & Sullivan, 2008; NFPA, 2017) and are characterised by having flames which lean over burnt ground (**FIGURE 2.3 & FIGURE 2.4**) (Trollope *et. al.*, 2004; Cheney & Sullivan, 2008). This arises by fires burning, either against the wind (Trollope, 1978; NFPA, 2017) or down a slope (**FIGURE 2.3**) (Trollope *et. al.*, 2004; NFPA, 2017). Backing fires have smaller flames (Trollope, 1984) and are less intense (Trollope, 1984; Trollope *et. al.*, 2004; NFPA, 2017), but are more severe than head fires, as they burn close to the ground, consuming most of the plant material (Trollope *et. al*., 2004; Cheney & Sullivan, 2008). However, back fires are often more intense at ground level and less severe higher up in the fuel bed (canopy) (Trollope, 1989), as their smaller flames do not reach the branches of trees and tall bushes, leaving them unburnt (**FIGURE 2.5**). The slow rate of spread of backing fires means that combustion is also more complete than in head fires (Trollope *et. al.*, 2004; Cheney & Sullivan, 2008). The efficiency of back fire combustion results in less smoke production than that of head fires (**FIGURE 2.4**) (Trollope *et. al.*, 2004; Cheney & Sullivan, 2008).

FIGURE 2.4: *A typical back fire. Note flames burning from the base of the fuel bed and leaning over burnt ground. Experimental fire A011, NT, Australia, 30 July 1986. Reprinted from "*Grassfires: fuel, weather and fire behaviour (2nd ed.)", *by Cheney, P., & Sullivan, A., 2008, pp. 23, Australia: CSIRO Publishing. Copyright 2008 by CSIRO.*

FIGURE 2.5: *Unburnt canopy after back fire passage. Reprinted from the "*Guide to wildland fire origin and cause determination (2016 ed.)*", by NWCG, 2016, pp. 68, USA: National Wildlife Coordinating Group.*

Flanking fires are usually positioned along the portion of the oval (**FIGURE 2.1 & FIGURE 2.10)** either side of head and back fires (Cheney & Sullivan, 2008), parallel to the main direction of spread of the fire (Trollope *et. al.*, 2004; NFPA, 2017). Also known as lateral fires (NFPA, 2017), they are characterised by having flames which lean up and down the flank (Cheney & Sullivan, 2008). The flame front in flank fires will alternate between heading and backing fire progression in response to fluctuations in wind direction (**FIGURE 2.6**) (Trollope *et. al.*, 2004; Cheney & Sullivan, 2008).

During a fire's progression, changes in wind direction may cause heading, backing or flanking fire spread to occur along any portion of the perimeter of the fire (Cheney & Sullivan, 2008). While burning, the three types of fire spread behave differently (differing intensity, severity) (Cheney & Sullivan, 2008). As a result, they leave distinctly different remains in the fire scar (Cheney & Sullivan, 2008). The characteristics of each fire spread type need to be taken into consideration when analysing post-fire physical evidence (Cheney & Sullivan, 2008). Differentiating between areas of backing and heading fires is one of the more important aspects of wildfire origin and cause investigation, as it allows the investigator to identify an approximate point of origin (Cheney & Sullivan, 2008; NFPA, 2017).

FIGURE 2.6: *A flank fire, showing sections of both heading (right) and backing (left) fires along a section of the flank. NT, Australia. Reprinted from "*Grassfires: fuel, weather and fire behaviour (2nd ed.)", *by Cheney, P., & Sullivan, A., 2008, pp. 25, Australia: CSIRO Publishing. Copyright 2008 by CSIRO.*

2.1.2 Combustion chemistry:

The science of combustion forms the basis on which the literature and theory of wildfire pattern indicators is built and provides a technical background to assist in understanding how wildfires start and spread.

Combustion is an oxidation process which is closely related to photosynthesis (Brown & Davis, 1973; Trollope, 1984; Trollope *et. al.*, 2004; Van Wagtendonk, 2006; Cochrane & Ryan, 2009; Scott *et. al*., 2014). Photosynthesis is the production of plant material and oxygen from carbon dioxide and water together with sunlight (Scott *et. al*., 2014). Combustion of plant fuels is essentially the photosynthetic process in reverse (Trollope, 1984; Trolllope *et. al.*, 2004; Van Wagtendonk, 2006; Cochrane & Ryan, 2009; Scott *et. al*., 2014). Plant material (usually cellulose and hemicellulose) in the presence of heat, is converted to flammable hydrocarbons (Cochrane & Ryan, 2009; Scott *et. al*., 2014). These are oxidised to produce carbon dioxide, water, and energy (heat and light) (Byram, 1959; Van Wagtendonk, 2006; Cochrane & Ryan, 2009; Scott *et. al*., 2014). Byram (1959) presented the chemical equation for combustion, by approximating the carbon, hydrogen, and oxygen content of plant material (cited by Van Wagtendonk, 2006):

$$\mathbf{4C_6H_9O_4 + 25O_2 \rightarrow 18H_2O + 24CO_2 + 5{,}264{,}729\ kJ.}$$

Or simply:

Cellulose + O_2 + Kindling Temperature → CO_2 + H_2O + Thermal Energy

(Trollope *et. al.*, 2004; Scott *et. al.*, 2014)

Unlike photosynthesis, the combustion process is chaotic (Scott *et. al*., 2014), and in wildfires is often incomplete.

2.1.3 Phases of combustion:

In wildfires, there are three phases of combustion: Preheating; flaming combustion; and glowing combustion (Trollope, 1984; Van Wagtendonk, 2006; Cochrane & Ryan, 2009):

- **Preheating** is an endothermic process, where fuel temperature is raised to ignition point (Trollope, 1984; Cochrane & Ryan, 2009; Scott *et. al*., 2014). As temperature rises, the fuel loses moisture and dries out, gases are partially distilled and cellulose begins to breakdown and produce flammable hydrocarbon gases (pyrolysis) (Byram, 1959; Trollope, 1984; Trollope *et. al.*, 2004; Van Wagtendonk, 2006; Cheney & Sullivan, 2008; Cochrane & Ryan, 2009; Scott *et. al*., 2014).

- **Flaming combustion** is an exothermic process in which the flammable hydrocarbon gasses generated during the pre-heating phase are ignited and oxidise very rapidly to produce flame (Byram, 1959; Trollope, 1984; Van Wagtendonk, 2006; Cochrane & Ryan, 2009; Scott *et. al*., 2014). During the oxidation process, photons of light are released for each atom of carbon that is oxidised to CO_2 (Cochrane & Ryan, 2009). When this process (flaming combustion) is rapid, the photons are seen as flames; when the process is slow, the fuel appears to be glowing (Cochrane & Ryan, 2009). For pyrolysis to remain self-sustaining, heat energy must be sufficient, and oxidation must occur in the presence of oxygen (Cochrane & Ryan, 2009; Scott *et. al*., 2014). When the flaming combustion phase is very rapid (*e.g.*, intense head fires), oxygen supply is limited as it is consumed faster than it is replaced and the breakdown of cellulose is chaotic (Cheney & Sullivan, 2008), culminating in production of large volumes of less flammable hydrocarbons such as tars and molecular carbon (Cheney & Sullivan, 2008). In such cases, combustion is incomplete, and the products of partial combustion are seen as billows of smoke (**FIGURE 2.2**) (Van Wagtendonk, 2006; Cheney & Sullivan, 2008; Cochrane & Ryan, 2009). Conversely, in cases where flaming combustion occurs at a slower rate (*e.g.*,

back fires), oxidation can be very efficient (Cheney & Sullivan, 2008). The slow rate of combustion allows oxygen to mix sufficiently with the fuel, allowing for complete combustion to occur, and resulting in little or no smoke being emitted (Cheney & Sullivan, 2008). Furthermore, advancing flame fronts of back fires may experience a 'fanning' effect from the oncoming wind, enhancing the supply of oxygen to the combustion zone. The exothermic reaction in flaming combustion releases energy and preheats the adjacent fuel, allowing the fire to continue to spread in a positive feedback system.

- **Glowing combustion**. This phase occurs when all, or most of the flammable hydrocarbon gasses have been burned off the fuel (Trollope *et. al.*, 2004; Cochrane & Ryan, 2009; Scott *et. al*., 2014). Following the consumption of the hydrocarbon gases, the residual fuel comprises charcoal, which continues to combust, oxidising on the surface of the fuel (Byram, 1959; Trollope, 1984; Van Wagtendonk, 2006; Cochrane & Ryan, 2009; Scott *et. al*., 2014). Glowing combustion is exothermic and allows pyrolysis to continue in a positive feedback system, however, oxidation occurs at a much slower rate than in flaming combustion (Cochrane & Ryan, 2009). This combustion phase can be very efficient and emit little to no smoke (Cheney & Sullivan, 2008), as long as the supply of oxygen and heat is not limited.

$$\mathbf{C + O_2 \rightarrow CO_2 + Thermal\ Energy}$$

(Cheney & Sullivan, 2008)

Glowing combustion should not be confused with the phenomenon that occurs when heavy or compacted fine fuels remain smouldering in a fire scar after the fire front has passed. The process of smouldering is a combination of all three combustion phases but constrained to a very slow rate by fuel characteristics and/or micro-environmental conditions (Cheney & Sullivan, 2008). The combustion reaction nears equilibrium and the positive feedback reaction is constrained by declining temperature and limited oxygen (Cheney & Sullivan, 2008; Cochrane & Ryan, 2009). Flammable hydrocarbons are released so slowly that the flames are essentially invisible (Scott *et. al*., 2014), and/or the photons of light emitted during the oxidation process are masked by ash covering the combusting material, resulting in not even a glow being seen (Cheney & Sullivan, 2008). Such combustion may be very efficient (Cheney & Sullivan, 2008), resulting in very little (wisps) (Cheney & Sullivan, 2008; Scott *et. al*., 2014) or no smoke being emitted. There is considerable variation in the amount of heat energy released by different size fuels during combustion (Trollope, 1984). Large fuels usually release more energy, at a slower rate, during glowing combustion (Brown & Davis, 1973; Trollope, 1984; Trollope *et. al.*, 2004). Fine fuels release less energy, but at a rapid rate, and almost all of it during flaming combustion (Trollope, 1984; Trollope *et. al.*, 2004). As the fire front advances in a wildland

fire, all three phases of combustion may overlap and can usually be observed occurring simultaneously in three distinguishable zones (Trollope, 1984; Trollope *et. al.*, 2004). This is sometimes referred to as the **fourth phase of combustion (smouldering combustion)**, which may, but does not always occur. As indicated, technically a combination of the three phases of combustion occurring together, but at a slow rate.

The preheating phase of combustion is crucial to the spread of wildland fires, since for fire to spread from one point to another point, the heat generated in the combustion zone must preheat the adjacent fuel until it releases flammable hydrocarbons (Trollope, 1984; Cochrane & Ryan, 2009; Scott *et. al.*, 2014). In the early stages of a point ignition, this is not always easy, since preheating the adjacent fuel is an endothermic process, and the heat energy released from the combustion zone is often insufficient to extract the flammable hydrocarbon gasses from the adjacent fuel and maintain a positive feedback reaction.

2.1.4 Heat transfer:

In wildland fires, heat energy is transferred from the combustion zone to the adjacent fuel in three ways: conduction; convection; and radiation (**FIGURE 2.7**) (Trollope, 1984; Teie, 2003; Trollope *et. al.*, 2004; Van Wagtendonk, 2006; Cheney & Sullivan, 2008; Cochrane & Ryan, 2009; Scott *et. al.*, 2014).

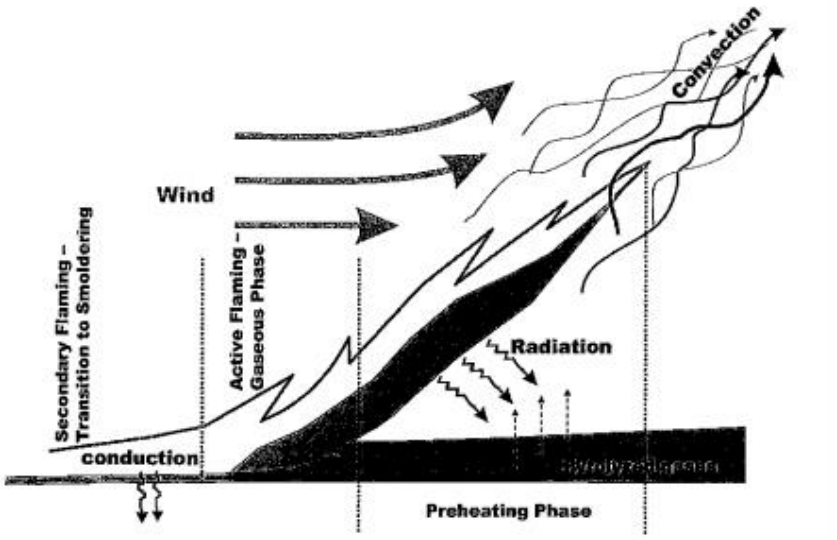

FIGURE 2.7: *Schematic diagram illustrating the mechanisms of heat transfer. Reprinted from "*Fire and fire ecology: Concepts and principles, in Cochrane, M. A. (ed.), Tropical fire ecology*", by Cochrane, M. A., & Ryan, K. C., 2009, pp. 28, Heidelberg, Germany: Springer. Copyright 2009 by Springer.*

- **Conduction** is the transfer of heat energy through matter, from one molecule to another and from an area of high temperature to an area of lower temperature (Teie, 2003; Trollope *et. al.*, 2004; Van Wagtendonk, 2006; Cochrane & Ryan, 2009; Scott *et. al*., 2014). Conduction usually occurs through solids (Cochrane & Ryan, 2009), but also occur when flames are in contact with objects (Van Wagtendonk, 2006). The structural make up of plant matter means that conduction has little influence on the spread of wildland fires (Teie, 2003; Trollope *et. al.*, 2004; Scott *et. al*., 2014), especially in grassfires. It is, however, important during ignition (Cochrane & Ryan, 2009), in ground fires (see **Section 2.1.5** below), and in the combustion of large woody fuels such as stumps, logs and roots (Teie, 2003; Cochrane & Ryan, 2009; Scott *et. al*., 2014). Conduction is important within the fuel, where heat transfer raises the temperature of the fuel, drying it out (Van Wagtendonk, 2006). Large, dense fuels such as stumps and logs are often difficult to ignite, because they are relatively efficient conductors, which rapidly transfer heat to the centre of the fuel, keeping the surface cool (Cochrane & Ryan, 2009).

- **Convection** is the transfer of heat energy through a moving fluid, such as gas or liquid (Teie, 2003; Trollope *et. al.*, 2004; Van Wagtendonk, 2006; Cochrane & Ryan, 2009; Scott *et. al*., 2014). The heated air molecules are less dense (Cochrane & Ryan, 2009), moving upwards (Van Wagtendonk, 2006; Cochrane & Ryan, 2009; Scott *et. al*., 2014) and importantly downwind. In wildland fires, convection is the most effective form of heat transfer and has the biggest influence on fire spread (Trollope, 1984; Teie, 2003; Scott *et. al*., 2014). Convective heat currents preheat fuels which are elevated and in front of the angled flames and therefore is the primary driver inducing head fires (spreading with the wind or upslope) and crown fires (see **Section 2.1.5** below) (Trollope, 1984; Teie, 2003; Trollope *et. al.*, 2004; Van Wagtendonk, 2006; Cochrane & Ryan, 2009; Scott *et. al*., 2014). Convection is also an important contributor in the phenomenon known as spotting, the process whereby firebrands are deposited ahead of the fire to kindle a new fire in front of the original fire front (Trollope, 1984; Teie, 2003; Van Wagtendonk, 2006; Cochrane & Ryan, 2009; Scott *et. al*., 2014).

- **Radiation** is the electromagnetic transfer of heat energy in a straight line, through a free space, to its surroundings (Teie, 2003; Trollope *et. al.*, 2004; Van Wagtendonk, 2006; Cochrane & Ryan, 2009; Scott *et. al*., 2014). After convection, radiation has the next biggest influence on fire spread (Trollope, 1984; Scott *et. al*., 2014). Radiation is most effective in preheating fuels which are perpendicular to the radiative energy (Cochrane & Ryan, 2009) and can cause spontaneous ignition (Van Wagtendonk, 2006). Radiation contributes almost entirely to the preheating of adjacent fuel in back fires (Scott *et. al*., 2014). For this reason, head fires (with the wind or upslope), which transfer heat in the direction of spread by both radiation and convection, spread much more rapidly than back fires (against the wind or downslope).

When a fire is ignited at a point, initially, the total amount of heat energy produced is low. The endothermic and exothermic reactions are almost in equilibrium. There is, therefore, a limited amount of energy available to preheat the adjacent fuel, meaning that the initial spread of the fire is slow. This is known as the incubation or embryonic period, and typically lasts around seven minutes (Scott *et. al*., 2014). The rate of this process accelerates as the heat generated by the exothermic reaction exceeds that required for the endothermic reaction, allowing pyrolysis to continue as a positive feedback system. The forward spread of head fires is determined by weather (temperature, relative humidity and wind speed), fuel conditions, topography and width of fire front (Trollope, 1984; Cheney & Sullivan, 2008). Interestingly however, wind speed does not affect the rate of spread of backing fires (Trollope, 1984; Cheney & Sullivan, 2008). This is because wind speed affects convective heat transfer and transfer of heat in back fires is almost entirely radiative (Scott *et. al*., 2014). While Cheney & Sullivan, (2008), found that in grassfires, terminal rate of spread can take between 12 minutes and over an hour to be reached, they also noted that in most cases, terminal rate of spread is reached within 30 minutes. The relevance of this with respect to fire control, is that for a fire to be contained effectively, it is important that it be contained within the incubation period and importantly before the forward spread reaches terminal velocity (McArthur, 1968; Scott *et. al*., 2014).

2.1.5 Types of fires:

Fires can further be distinguished by where in the fuel layer they burn (Brown & Davis, 1973; Luke & McArthur, 1978; Trollope, 1984; Trollope *et. al.*, 2004; Scott *et. al*., 2014). This distinction is mostly recognised in the USA and Australia, where three fire types are identified: crown fires; surface fires; and ground fires (Brown & Davis, 1973; Luke & McArthur, 1978; Trollope, 1984; Scott *et. al*., 2014).

- **Crown fires** burn in the canopies of tall vegetation, such as trees and shrubs (Trollope, 1981; Trollope, 1984; Trollope *et. al.*, 2004; Scott *et. al*., 2014).

- **Surface fires** burn in the surface vegetation, most commonly grass, but also small shrubs (Luke & McArthur, 1978; Trollope, 1981; Trollope, 1984; Trollope *et. al.*, 2004; Scott *et. al*., 2014). Surface fires are the most common fire type in South Africa (Trollope, 1984).

- **Ground fires** burn through organic matter below the surface of the ground (Luke & McArthur, 1978; Trollope, 1984; Trollope *et. al.*, 2004; Scott *et. al*., 2014). Southern Africa has a relatively dry climate, and there are few soils containing high levels of organic carbon (Soil Classification Working Group, 1991), and thus few occurrences of ground fires (Trollope, 1984).

All three fire types can occur both simultaneously and independent of each other (Brown & Davis, 1973; Trollope, 1984).

2.1.6 Flame zone structures:

A general knowledge of flame zone structures and characteristics is necessary for wildfire behaviour studies. Flame height is the vertical height of flames above the ground (**FIGURE 2.8**) (Van Wilgen, 1986; Trollope *et. al.*, 2004; Cheney & Sullivan, 2008; Scott *et. al*., 2014). Flame length is measured from the base of the flame on the ground to the tip (**FIGURE 2.8**) (Van Wilgen, 1986; Trollope *et. al.*, 2004; Cheney & Sullivan, 2008; Scott *et. al*., 2014). Flame flashes are not included in measurements of flame length. Flashes of flame are detached envelopes of combustible gas in flame (**FIGURE 2.8**) (Cheney & Sullivan, 2008). Flame angle is largely determined by wind and slope (**FIGURE 2.8**) (Cheney & Sullivan, 2008). Flame depth is the distance along the ground behind the fire front covered by flame (**FIGURE 2.8**) (Cheney & Sullivan, 2008). This does not include isolated islands of flaming or smouldering fuels which continue to combust after the fire has passed (Cheney & Sullivan, 2008). Much of the smoke that is produced by a grassfire often comes from smouldering combustion behind the flame front (Cheney & Sullivan, 2008). Residence time is the length of time flames remain burning over a patch of ground (Cheney & Sullivan, 2008).

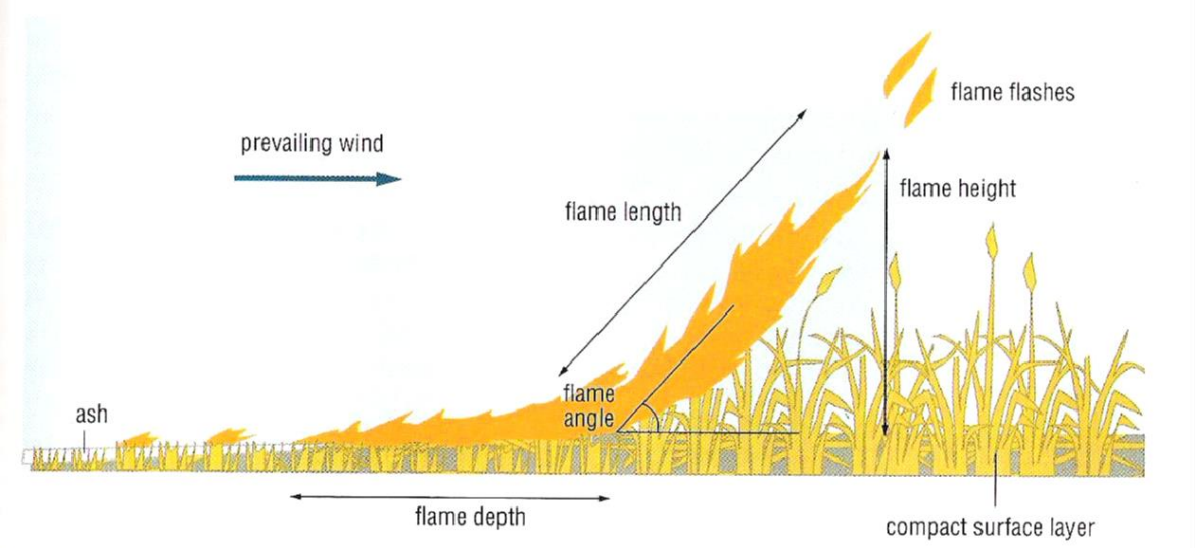

FIGURE 2.8: *Stylised cross-section through a heading fire. The tall flames at the front result from the combustion of the standing grass. Flashes of flame indicate detached envelopes of combustible gas. The depth of flame is largely determined by the amount of material in the compacted surface layer. Reprinted from* "Grassfires: fuel, weather and fire behaviour (1st ed.)", *by Cheney, P., & Sullivan, A., 1997, pp. 15, Australia: CSIRO Publishing. Copyright 1997 by CSIRO.*

2.1.7 Intensity and severity:

Fire intensity is considered to be the most important wildfire behaviour parameter (Trollope, 1981; Andrews, 1986; Van Wilgen, 1986; Kremens *et. al.*, 2003; Trollope *et. al.*, 2004). Despite this, there seems to be confusion with regards to usage, terminology, and definitions of intensity (Schwilk, 2003; Keeley, 2009; Scott *et. al*. 2014). Fire intensity is variably defined as the (rate of) energy output or heat release from a fire (Byram, 1959; Trollope, 1981; Teie, 2003; Keeley, 2009; Scott *et. al*., 2014). A widely accepted, implemented and practical measure for intensity (one of many measures of fire intensity), is Byrams' (1959), concept of **Fireline Intensity** (Van Wilgen, 1986; Trollope *et. al*., 2004; Keeley, 2009; Scott *et. al*., 2014). Byram, (1959), describes fireline intensity as the rate of heat release per meter of fire front (kJ/s/m). Trollope, (1981), recommends that units of fireline intensity be expressed as kJ/s/m rather than kW/m, as fireline intensity is a measure of the rate of heat energy release, and thus, is conceptually more meaningful when expressed as energy per duration (kJ/s), than as a unit of power (kW) (Trollope *et. al*., 2004). Importantly, fire intensity should not be confused with temperature at which fires burn.

Byram, (1959), and subsequently various other authors, have noted the existence of a correlation between fireline intensity and flame length (Chandler *et. al.*, 1983; Van Wilgen *et. al.*, 1985; Van Wilgen, 1986; Kremens *et. al.*, 2003; Cochrane & Ryan, 2009; Scott *et. al*., 2014; Andrews, 2018).

The parameters which influence fire intensity are the amount of **available heat energy (kJ/m^2)** (released) and the **rate of combustion** (rate of heat energy release) (Byram, 1959; Luke & McArthur, 1978; Trollope, 1984). The amount of available heat energy (kJ/m^2) is dependent on **fuel load (kg/m^2)** and **heat of combustion (kJ/kg)** (total amount of heat energy contained per unit mass of fuel) (Byram, 1959; Luke & McArthur, 1978; Trollope, 1984).

Heat of combustion differs between various species and fuel types and is dependent on the chemical make-up of the fuel (Byram, 1959). Some species contain highly flammable metabolites such as terpenes, which may burn readily, even at high fuel moistures (Luke & McArthur, 1978). The maximum available heat energy contained within a fuel stand of a specific load and heat of combustion, can be termed as the 'potential' heat energy available for release.

In practice, not all 'potential' energy is released from the fuel during the combustion process (Byram, 1959; Trollope, 1984; Cheney & Sullivan, 2008). Some heat energy (heat of combustion) is 'lost' in driving off fuel moisture and raising fuel temperature to ignition point (Byram, 1959; Luke & McArthur, 1978; Trollope, 1984; van Wagtendonk, 2006; Cheney & Sullivan, 2008). Further energy losses are incurred from incomplete (inefficient) combustion, as potential energy is lost in smoke, unburnt material remains and ash (Byram, 1959; Luke & McArthur, 1978; Trollope, 1984; van Wagtendonk, 2006; Cheney & Sullivan, 2008).

Therefore, the amount of energy released per unit mass of fuel is always somewhat less than the total amount of heat energy contained per unit mass of fuel (heat of combustion) (Byram, 1959; Luke & McArthur, 1978; Trollope, 1984; Cheney & Sullivan, 2008). This parameter is known as **Heat Yield** and is equal to the heat of combustion minus heat energy losses (Byram, 1959; Trollope, 1984).

Some energy also remains within the unburnt fuel (*e.g.*, grass stubble), as the amount of fuel consumed is always somewhat less than the fuel load. The actual amount heat energy released ('realised' energy) is equal to the product of Heat Yield (kJ/kg) and the amount of fuel consumed (kg/m^2) (Byram, 1959). In summary, the potential heat energy contained within a particular fuel stand is always somewhat less than the realised heat energy released during combustion under natural conditions.

'Potential' Energy (kJ/m^2) = Fuel Load (kg/m^2) * Heat of Combustion (kJ/kg)

'Realised' (released) Energy (kJ/m^2) = Amount of Fuel consumed (kg/m^2) * Heat Yield (kJ/kg)

The rate of combustion (rate of heat energy release) has not been dealt with in much detail within fire behaviour literature. There does not appear to be a clear and widespread understanding of the concept (Trollope, 1984). The rate of heat energy release is measured practically as the linear rate of spread of the fire front (m/s) (Byram, 1959; Trollope, 1984; Scott *et. al*., 2014). Some measures of rate of combustion have also included residence time as a contributory factor.

Fire severity should not be confused with fire intensity. Similar to intensity, definitions of severity vary, and are often misused (Kremens *et. al*., 2003; Keeley, 2009; Scott *et. al*., 2014). Some authors have broadly defined fire severity as the ecosystem impacts from fire (Kremens *et. al*., 2003; Bond & Keeley, 2005; Cochrane & Ryan, 2009; Keeley, 2009). This is problematic, as it has left room for interpretation (Keeley, 2009). However, empirical studies have perhaps more usefully described fire severity as the amount of organic material consumed in a fire (Trollope *et. al.*, 2004; Cochrane & Ryan, 2009; Keeley, 2009; Scott *et. al*., 2014).

2.1.8 Rate of spread:

Rate of spread (ROS) of fires can be measured in several ways, notably: instantaneous rate of spread of fire front; vector rate of spread from one point to another; and mean rate of spread for a given area (ROS = Area burnt / period of flaming combustion * mean length of fire front) (Trollope *et. al*., 2004). It is important to note that the vector ROS from one point to another (*e.g.*, ignition point to final destination), in a linear direction (axis of the fire), will always be somewhat slower than the actual ROS of the fire front between the same two points. This is because wind direction is variable in the short term and changes overall direction over time (Cheney & Sullivan, 2008). As a result, head fires do not burn in a straight line, but rather follow a variable path (**FIGURE 2.9**) (Cheney & Sullivan, 2008), and

therefore take longer to travel between two points than would be the case if it burnt in a linear direction. Similarly, the instantaneous ROS of a fire front, at any point along the fire axis may vary with constantly changing wind conditions (Cheney & Sullivan, 2008).

The most important factors that influence rate of spread in grass fires are wind speed, fuel moisture (FM), percentage of dead fuel, topography, humidity, temperature, and fuel continuity (Trollope *et. al.*, 2004; Cheney & Sullivan, 2008). Other factors include fuel size (surface area to volume ratio (SA/V)) and extent of fuel compaction (fuel bed depth, grass sward density, and vertical structure) (Rothermel, 1972; Andrews, 1986; Cheney & Sullivan, 2008; Andrews, 2018), however, these factors are less relevant in grass fires (Cheney & Sullivan, 2008). One reason for this, is that subtropical grassland fuels generally have similar physical structure (Cheney *et. al.*, 1993), unlike macchia and forest fuels. Extensive experimental grassfires in Australia (incl. 2500ha, Northern Territory, 1986) could not return any significant influence of fuel size, fuel height, and fuel density on rate of spread in ungrazed pastures (Cheney *et. al.*, 1993; Cheney & Sullivan, 2008). Interestingly, fuel load (not to be confused with fuel size) itself does not directly influence rate of spread of grass fires, unless changes in fuel load also reflect changes in fuel condition (Cheney *et. al.*, 1993; Cheney & Sullivan, 2008; Cruz *et. al.*, 2016).

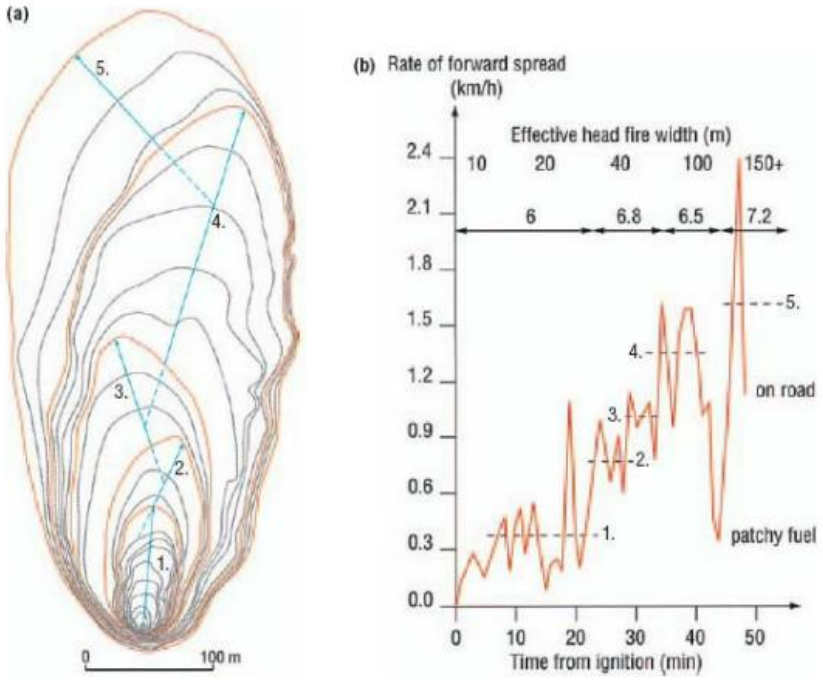

FIGURE 2.9: *Illustration (a)(left) showing growth of a fire from a point ignition and responding to changes in wind direction. Isochrones (fire perimeter) at 2-minute intervals. Blue lines indicate changes in direction of spread for duration of fire. Graph (b)(right) shows changes in forward rate of spread of fire responding to changes in wind speed, fuel continuity, and various other factors. Dashed lines (- - -) represent mean rates of forward spread for corresponding directional classes on (a). Mean wind speeds for corresponding periods are shown above (←→). Vector rate of spread for entire period was approximately 0.6km/h. Experimental fire No. 50 in open forest at Gunn Point, NT, Australia. Reprinted from "Grassfires: fuel, weather and fire behaviour (2nd ed.)", by Cheney, P., & Sullivan, A., 2008, pp. 33, Australia: CSIRO Publishing. Copyright 2008 by CSIRO.*

2.1.9 Fuel moisture and curing:

Fuel moisture content (FMC) is one of the most important, yet one of the least understood fuel characteristics influencing fire behaviour, particularly ROS (Finney *et. al*., 2013; Cruz *et. al*., 2015). It is expressed as the ratio (percentage) of the amount water contained within the fuel to its dry weight (Teie, 2003; Cochrane & Ryan, 2009; Finney *et. al*., 2013; Scott *et. al*., 2014). FMC can be divided into the proportion of moisture contained within the live and dead portions of the fuel (Cochrane & Ryan, 2009; Scott *et. al*., 2014). Dead fuels can be divided further, into size classes (1-hour, 10-hour, 100-hour fuels, 1000-hour fuels, and 10 000-hour, grouped according to diameter of the fuel (< ¼ in; ¼ - 1 in; 1 - 3 in; 3 - 8 in; > 8 in, respectively) (Cochrane & Ryan, 2009; NWCG, 2018). Size classes are based on the time lag related to moisture transfer (wetting and drying) in and out the fuel (Cochrane & Ryan, 2009; NWCG, 2016; NWCG, 2018).

In grassy fuels, **curing state** (the extent of senescence) is a crucial measure of fuel conditions for fire behaviour prediction (Cheney & Sullivan, 2008; Anderson *et. al*., 2011; Cruz *et. al*., 2015; Kidnie *et. al*., 2015). Curing refers to the senescence process whereby herbaceous plants (usually grasses) come to the end of their annual or seasonal lifecycle after the production of flowering culms (Danckwerts, 1989; Anderson *et. al*., 2011). Once the existing herbaceous plant material (tillers) begin to senesce (die), the process cannot be reversed — (plant material cannot 'green-up') (Anderson *et. al*., 2011). Entire plants do not necessarily die, as new growth (tillers) usually begins to sprout from the basal meristematic tissue, at the onset of the new season, or following rainfall events (Danckwerts, 1989). It is noted that *Themeda triandra*, — (one of, if not the most important grass species in southern Africa (Danckwerts, 1989)) — might appear to be cured or partially cured (and subsequently 'green-up'), when in fact, it is not (Danckwerts J.E. (PhD), personal communication, 2019). This is due to the presence of anthocyanin in the leaves giving the grass a reddish colour (Rooigras) (Danckwerts J.E. (PhD), personal communication, 2019).

Percent curing (or degree of curing) is defined as the proportion of dead (cured) plant material within the fuel sward (Cheney & Sullivan, 2008; Anderson *et. al*., 2011; Cruz *et. al*., 2015; Kidnie *et. al*., 2015). Percent curing is a proxy for live and bulk fuel moisture content of herbaceous fuel (Cheney & Sullivan, 2008; Anderson *et. al*., 2011; Cruz *et. al*., 2015), while the fuel moisture content of dead grass fuel is largely influenced by relative humidity (Trollope *et. al.*, 2004; Cheney & Sullivan, 2008; Anderson *et. al*., 2011; NWCG, 2016). This is because the stomata on cured (dead) grass fuel are no longer functional, so moisture can transfer in and out of the cured portion of the (porous) fuel with relative ease.

2.2 A review of various wildfire behaviour prediction models:

Fire behaviour prediction models have a wide variety of applications and uses. Models have been developed for use at a range of different spatial and temporal scales. These include fire danger warning systems, safety and prevention measures, fire suppression planning and strategies, environmental and ecological research, fire management strategies, and planning prescribed burns (Cheney *et. al*., 1998; Trollope *et. al*., 2004; Anderson *et. al*., 2011).

Prediction models are frequently applied as fire danger rating systems, offering numerical and categorical fire risk or danger ratings based on a number of input values including topography, fuel, and weather conditions (Cheney *et. al.*, 1993; Cheney *et. al.*, 1998; McCaw & Catchpole, 1997; Sullivan *et. al*., 2014). Many of these fire danger indices (FDIs) are implemented in countries such as Australia, New Zealand, USA, Canada and South Africa as warning systems, by regional and national governments, and fire protection associations (Sullivan *et. al.*, 2014).

As well as FDIs used for safety purposes, specific aspects of fire behaviour, such as intensity and rate of spread, can also be predicted by fire behaviour prediction models. These predicted parameter values are used by fire managers and researchers alike to investigate fire behavioural activity in past, active, and potential fires. Fire managers wanting to emulate or achieve specific fire conditions (*e.g.*, minimum fire intensity required for top-kill of woody species) (Teie, 2003; Trollope, 2011; Nieman *et. al*., 2021) use fire behaviour prediction models to accurately predict and plan for prescribed burns (Van Wilgen & Wills, 1988 Van; Anderson *et. al.*, 2011; Andrews, 2018).

These models use a range of input variables (fuel, weather, topography) to predict the same or similar specific fire behaviour parameters (*e.g.*, rate of spread & fire intensity). Some notable differences between models include: 1) The method of data collection used in development of models (Weise & Biging, 1997); 2) The perceived weighted influence (or interactions) predictor variables (fuel, weather, & topographic inputs) (input variables) have on fire behaviour; 3) The input variables required by each model; & 4) The manner in which models handle topographic influences on fire behaviour (Sharples, 2008; Sullivan *et. al*., 2014).

Fire behaviour varies significantly between crown fires in forests and surface fire in grasslands (Trollope *et. al.*, 2004). Various models are developed for and suited to these different particular fuel types.

Some well recognised and widely used wildfire behaviour prediction models by rangeland fire practitioners include:

- **Rothermel (1972)** developed a mathematical model for predicting fire spread in wildland fuels. The model was one of the first wildfire behaviour prediction models developed, and to date, is the

most widely applied fire model available (Andrews, 2014; Andrews, 2018). The Rothermel (1972) model forms the basis from which many fire behaviour prediction models are developed (Finney, 1998; Andrews, 2014; Vacchiano & Ascoli, 2015; Andrews, 2018). Its extensive acceptance as a fire behaviour prediction model is based on its ability to predict fire behaviour under a wide range of fuel conditions (Sneeuwjagt & Frandsen, 1977). The model predicts rate of spread (ROS) and fire intensity of wildfires (Sneeuwjagt & Frandsen, 1977). Adaptations of the model have been made to predict various other fire behaviour parameters (Andrews, 2018).

- **BEHAVE and BEHAVEPLUS** (Andrews & Bevins, 2018) are flexible, site-specific fire behaviour prediction models based on Rothermel's, (1972), fire model, which estimate wildfire behaviour from fuel, weather and topography (Burgan, 1984; Andrews, 1986; Van Wilgen & Wills, 1988; Andrews, 2014; Andrews, 2018). These 'user-friendly' applications have been used worldwide for fire behaviour parameter prediction and risk assessment (Trollope *et. al.*, 2004). BehavePlus and Rothermel (1972) based models make fire behaviour predictions based on fuel models (Van Wilgen & Wills, 1988). In these systems, fuel characteristics are summarized into pre-set fuel models – sets of values based on predefined fuel characteristics for specific fuel/ecosystem types (Van Wilgen & Wills, 1988). The SURFACE module of the BEHAVEPLUS program (Andrews & Bevins, 2018) can calculate up to 14 different fire behaviour and fire related parameters (Trollope *et. al.*, 2004). A unique feature of the BehavePlus model is its ability to scale wind and slope influence relative to fire spread direction, by accepting directional vectors as input parameters (Andrews & Bevins, 2018). The primary outputs of the BehavePlus Surface module are rate of spread; heat per unit area; fireline intensity; flame length; & reaction intensity (Trollope *et. al.*, 2004).

- **McArthur Mk3, Mk5, & CSIRO-modified Mk4 grassland models** (McArthur, 1966; McArthur, 1967; McArthur, 1977; CSIRO, 1999). Unrelated to the Rothermel (1972) model, Australian researcher A.G. McArthur developed fire behaviour and surface spread models suited to specific fuel types, namely grassland, northern Australia vegetation, and eucalypt forests (Cheney *et. al.*, 1993; McCaw & Catchpole, 1997; Cheney *et. al*., 1998). These various models developed by McArthur (1966; 1967; 1977), CSIRO, and others, do not require fuel model selection or fuel model input. Rather direct input of fuel characteristics pertaining to relevant fuel type (grassland, northern Australia vegetation, and eucalypt forests) are entered into a model calculator (CSIRO, 1999), equations (Noble *et. al.*, 1980), circular slide rules (McArthur, 1977), or CSIRO published nomograms (Cheney & Sullivan, 2008). Standard meteorological observations of weather conditions are also incorporated (Noble *et. al.*, 1980; CSIRO, 1999; Cheney & Sullivan, 2008). The attractiveness of the McArthur Mk3 & Mk5 model equations (Noble *et. al.*, 1980) and associated

CSIRO-modified McArthur Mk4 grassland model (CSIRO, 1999) lies in its simple, easy to use, and accurate simulations of basic behavioural parameters, such as ROS, flame length, spotting distance, and fire danger rating. The McArthur grassland spread models and related modifications have been widely used in Australia and accepted by the Bureau of Meteorology and most State Fire Authorities (Cheney *et. al*., 1998). Variations of the McArthur models have also been incorporated into the grassland module of the Canadian Fire Danger Rating System (Van Wagner *et. al.*, 1992; Cheney *et. al*., 1998).

The main differences between the Australian McArthur based models and Rothermel, (1972), based models, concerns fuel parameters and the influences fuel characteristics have on fire behaviour calculations, most notably, how fuel moisture is accounted for (Cheney *et. al*., 1998; Cheney & Sullivan, 2008; Anderson *et. al*., 2011). Rothermel, (1972), based fire modelling systems do not consider the degree of curing as a direct input variable (Cruz *et. al*., 2015), but rather require direct fuel moisture input values for each size class (Andrews & Bevins, 2018; Vacchiano & Ascoli, 2015). The McArthur based Australian models account for fuel moisture through temperature, relative humidity, and curing input variables (Noble *et. al*., 1980; McCaw & Catchpole, 1997; Cheney & Sullivan, 2008). It has, however, been acknowledged that methods of indirect fuel moisture estimation from meteorological data (*i.e.*, function for fuel moisture determination) are not always accurate and effective (Dexter & Williams, 1976; Noble *et. al.*, 1980). Other fuel parameters which are required by Rothermel based models but not McArthur based models include fuel surface area to volume ratios and dead fuel moisture of extinction values.

The curing state of grasses is considered to be a crucial determinant of fire behaviour in grassland fuel types (Cheney *et. al*., 1998; Anderson *et. al.*, 2011; Cruz *et. al*., 2015), where fuel moisture is largely determined by seasonality (percentage of live material) and the transfer of moisture between fine fuels and the atmosphere (humidity and temperature). For this reason, Australian McArthur grassland models have been favoured over Rothermel (1972) based models when predicting fire behaviour in grasslands.

The Australian McArthur models and Rothermel (1972) based models also differ in terms of the method of data collection used for the development of the models (Weise & Biging, 1997). The Australian McArthur models were derived from field data collected from multiple fire trials (McArthur, 1966; McArthur, 1967; Weise & Biging, 1997), while the Rothermel (1972) model — and therefore subsequent models based on Rothermel, (1972) — were developed using data collected from fire tunnels (Cheney *et. al*., 1993). Fire tunnels make use of harvested fuel, collected from the field and placed in the tunnel to recreate a desired fuel type (Cheney *et. al.*, 1993). Fire tunnels are far removed from field conditions, and for that matter, may be far removed from reality (Weise & Biging, 1997; Trollope W.S.W. (PhD), personal communication, 2019).

Several fire behaviour prediction models have been applied to a range of fire prone veld types in southern Africa, with varying success (Van Wilgen *et. al*., 1985; Van Wilgen, 1986; Van Wilgen & Wills, 1988; Trollope *et. al*., 2004). Although research into ground-truthing these various models against wildfires in southern African fuel types is limited. What is important to note from these studies, is that it is recommended that South African fuel models be locally developed for southern African fuel/ecosystem types (Trollope *et. al.*, 2004). This is crucial for various reasons. Firstly, for most models, fuel characteristics cannot be entered via direct input (Trollope *et. al.*, 2004). Secondly only a few North American fuel models can be applied to southern African conditions (Trollope *et. al.*, 2004). This is mostly due to the pronounced curing period after summer rainfall experienced in southern African grasslands, and due to southern African woodlands and forests differing significantly from those in North America in terms of fuel characteristics (Trollope *et. al.*, 2004). Lastly, model algorithms, formulae and regressions developed based on North American fuel conditions may not extrapolate well to other fuel types worldwide, where fire behaviour and the drivers of fire behaviour may differ significantly. Fuel model construction, and fire behaviour prediction model ground-truthing as of yet, has not been developed or conducted for Eastern Cape montane grasslands.

2.3 Wildfire investigation:

A number of fire investigation handbooks have been published which provide guidance on the systematic approach to conducting wildland fire origin and cause investigations (*e.g.*, Ford, 1971; Bourhill, 1982; Ford, 1995; Anon, 2001; NFPA & IAAI, 2005; Cheney & Sullivan, 2008; De Haan & Icove, 2013; De Ronde & Goldammer, 2015; NWCG, 2016; NFPA, 2017; IAFC *et. al.*, 2018) and, in most cases, are widely accepted by fire investigators as the 'standard' (Simeoni *et. al.*, 2017).

These handbooks contain lists of *post-hoc* wildland fire pattern indicators which can be used in origin and cause investigation, describe what information can be deduced from each indicator and how that information should be used to determine specific behavioural aspects of the fire. Upon review, however, these guides and handbooks are often inconsistent with one another, and in some cases, factually incorrect (as explained below). They have differing views and focus on different aspects of wildfire investigation. The differing views and indicator descriptions are perhaps influenced by the focus audience/target market that they were compiled for, and as a result focus on indicators and aspects of wildfire behaviour pertaining to the predominant vegetation type in those areas or countries in which they were included.

An example where established science of fire behaviour seems to be reliably applied is, the chapter on wildfire investigations in the Australian book *Grassfires: fuel, weather and fire behaviour* (2nd ed.) by Cheney and Sullivan, 2008. It focuses essentially on grasslands, occasionally mentioning aspects related to heathland and shrubland and only very briefly touches on eucalypt forests. While it should be interpreted within an Australian context, the principles can be applied to regions with similar vegetation types such as Southern African, since the conclusions drawn are based on sound principles of fire behaviour, and not on anecdotal or unsubstantiated observations. A number of South African wildfire investigators and researchers often refer to this science during investigation reports and deem this book to be most useful (Danckwerts J.E. (PhD), personal communication, 2019; Du Toit J.C.O. (PhD), personal communication, 2019).

Other handbooks such as the *NFPA 921, guide for fire and explosion investigations* (2017 ed.), the *Guide to wildland fire origin and cause determination* (2016 ed.) and *Fire Investigator: Principles and Practice to NFPA 921 and 1033* (5th ed.) (2018) are American, and while they do, in some cases, deal with aspects relating to grassfire investigation, focus more on crown fires in conifer forests. This is important to keep in mind as an investigator in Southern Africa (dealing more with surface fires in grassland and savanna ecosystems), as the behavioural aspects and patterns left behind by surface and crown fires may differ significantly (Trollope, 1984). Despite the lessened focus on grassfires and anecdotal assumptions, these three handbooks (NWCG, 2016; NFPA, 2017; IAFC *et. al.*, 2018) are thorough, and have more detailed list of indicators than *Grassfires: fuel, weather and fire behaviour* (2nd ed.) (Cheney & Sullivan, 2008). The *NFPA 921, guide for fire and explosion investigations* (2017

ed.) chapter on wildfire investigation is often considered to be the 'standard' for wildfire investigators (Simeoni *et. al*., 2017), however, by its own admission is intended as a basic introduction (NFPA, 2004; NFPA, 2017) and is not an expert account nor comprehensive document. The *Guide to wildland fire origin and cause determination* (2016 ed.) focuses exclusively on wildfire investigation and is a more detailed document (Simeoni *et. al*., 2017).

Investigations of structural fires on the other hand, have much more clarity, incorporating scientific principles, protocols, and investigative procedures, and have a wide array of information on the topic in the literature (Babrauskas, 2003; De Haan & Icove, 2013; NFPA, 2017; IAFC; 2018). This is somewhat understandable, as structural fires have greater impacts on human lives and therefore more money made available for scientific studies and research. Studies on wildfire investigation have largely been neglected in the scientific literature, especially with regards to *post-hoc* wildland fire pattern indicators.

While the use of wildland fire pattern indicators in origin, cause and behaviour determination is not a novel topic, the literature and knowledge on the topic is almost entirely anecdotal. Research on the relatively simple science behind wildfire origin and cause determination has largely been neglected. An extensive literature review found only a single peer reviewed study on the reliability of *post-hoc* wildland fire pattern indicators: *A preliminary study of wildland fire pattern indicator reliability following an experimental fire* by Simeoni *et. al*., (2017). There have been no quantitative studies on the efficacy of these indicators in determining wildfire pattern and spread. There is therefore a need for further studies in this field. Authors of *NWCG Guide to wildland fire origin and cause determination* (2016 ed.) emphasise that fire pattern indicators should be tested to determine their reliability. In addition, Trollope *et. al.*, in *Wildland fire management handbook for Sub-Sahara Africa* (2004), highlight a serious lack of quantitative data on various factors of fire behaviour in Africa. A review by Prestemon *et. al.*, (2013) found that enhanced wildfire investigation knowledge may be an effective long-term method to reduce rates of accidental and incendiary anthropogenic fires.

A possible explanation for the lack of empirical research on this topic, may be, in part, due to the difficulties surrounding experimentation. Aside from the regular complications that may arise when conducting prescribed burns and fire experiments, sampling and recording of indicators and localised fire conditions pose particularly inconvenient obstacles. It is difficult to monitor fire spread direction, type, and other fire behaviour characteristics across multiple plots, over vast area of (often rugged) terrain, and while visibility is hindered by smoke. *Post-hoc* physical indicators (visual remains) are directly influenced by the specific and localised behaviour of combustion that occurred on, or near the indicator. It is therefore crucial that the specific behaviour of the fire is recorded as it passes each indicator or plot, rather than recording generalised fire conditions across the entire fire. This is not an

easy task. Deployment of supporting items, recreation of specific fire conditions, and inconsistencies within the fire scar pose additional problems.

The work done by Simeoni *et. al*., 2017 was a crucial first step in ground truthing the theory behind several *post-hoc* wildland fire pattern indicators. While the importance of their study cannot be understated, the preliminary nature of the study means that the novelty was inevitably accompanied by drawbacks and shortcomings. The superficial nature of the Simeoni *et. al*., (2017) study needs to be elaborated, towards achieving a quantifiable basis for fire investigation. Although their preliminary study aimed to assess the reliability of wildfire pattern indicators, it failed to quantify or statistically analyse the reliability of these indicators. Further methodological errors arise with regards to replication and representation. Only one prescribed burn site was used in the study by Simeoni *et. al*., (2017), with few replicates, clustered together within a small portion of the entire burn site. Additionally, the study was conducted within a conifer forest, typically conducive to very different fire behaviour to that of grassland, savanna and fynbos (chaparral/macchia), giving limited information about indicators associated with those vegetation types.

Simeoni *et. al*., 2017 stated that the focus of their study was to provide a first analysis and scale of reliability for the different *post-hoc* wildland fire pattern indicators where they appear. Their study aimed to develop an experimental database that would be large enough to support a statistical analysis of the reliability of wildfire pattern indicators (Simeoni *et. al*., 2017). They further noted that the analysis of wildfire pattern indicators, together with the measurement of fire properties, offer a scientific framework that can be used in the further study of the reliability of indicators (Simeoni *et. al*., 2017). Moreover, they stressed the need for further work in this field, in the hope that a better understanding of the reliability of wildland fire pattern indicators could help aid in their use by investigators (Simeoni *et. al*., 2017).

2.4 Post-hoc wildland fire pattern indicators:

This study will follow on from the work done by Simeoni *et. al*., (2017). Specifically, conduct a first quantitative assessment of the reliability and accuracy of wildland fire pattern indicators as aids in wildfire origin and cause investigation and, in doing so, to provide a scientific framework and procedure for quantitative assessment of indicators in future studies. This review also presents a centralised list of wildland fire pattern indicators, incorporating a number of well recognised wildfire investigation handbooks, in the hope that some newfound clarity and consistency will be provided.

Catalogued below is a list of *post-hoc* indicators of wildland fire pattern and spread that are commonly thought to be important in wildfire investigation. The indicator list provided was compiled from multiple fire investigation handbooks. There is inconsistency in the literature, and in pursuit of clarity, terminology has, where appropriate, been reworded, grouped together, or sub-divided. This was done only where needed. The handbooks and guides considered in the compilation process of the following list were chosen according to the following criteria: relevance; recognition amongst wildfire investigators; and availability. Four books and publications have been used to compile a list of wildfire pattern indicators: *Grassfires: fuel, weather and fire behaviour* (2nd ed.) by Cheney & Sullivan, 2008; *NFPA 921, guide for fire and explosion investigations* (2017 ed.); *Guide to wildland fire origin and cause determination* (2016 ed.); *Fire Investigator: Principles and Practice to NFPA 921 and 1033* (5th ed.) (2018).

***Post-hoc* physical indicators of wildfire pattern and spread:**

1.) *Shape of fire scar*
2.) *Degree of damage*
3.) *Partial burning in fire scar*
4.) *Leeside charring on pole type fuels*
5.) *Crown damage*
6.) *Foliage freeze*
7.) *Curling*
8.) *Consumption depth of grass tussocks*
9.) *Undercutting*
10.) *Ash colour and pattern*
11.) *Die-out pattern*
12.) *Cupping*
13.) *Depth of char*
14.) *Protection*
15.) *Sooting*
16.) *Staining*
17.) *Spalling*

While the following descriptions of wildfire pattern indicators may appear to be thorough and accurate, there are in fact many scientific inconsistencies within the literatures' descriptions of these indicators. Some of these inconsistencies and factual errors are addressed below each relevant indicator description. These listed inconsistencies and factual errors further highlight the need for empirical research on the reliability of *post-hoc* wildfire pattern indicators.

2.4.1 Shape of fire scar:

The first indicator used in origin and cause investigation is the shape of the remaining fire scar. By looking at the shape of the fire scar, together with weather data (specifically wind speed and direction), topography, and barriers (IAFC *et. al*., 2018), deductions on the spread and overall passage of fire can be made (Cheney & Sullivan, 2008). The mean direction of spread of the fire can be inferred from the overall axis of the scar (Cheney & Sullivan, 2008). While shape of a burning fire in progress is roughly elliptical or oval (**FIGURE 2.1 & FIGURE 2.10**) (Cheney & Sullivan, 2008), the scar that remains after the fire has burnt often leaves a distinctive V or U shape (**FIGURE 2.11 & FIGURE 2.12**) (NWCG, 2016; NFPA, 2017; IAFC *et. al*., 2018).

As a fire advances under steady wind (or slope), the head and flank portions of the fire expand at a more rapid rate than the backing portion of the fire (**FIGURE 2.1 & FIGURE 2.9**) (Cheney & Sullivan, 2008). After the head extinguishes, is suppressed, or encounters a barrier, the flanks continue to burn out sideways, to produce the typical U or V shape often encountered in fire scars (**FIGURE 2.11 & FIGURE 2.12**). This shape is well documented in fire behaviour scientific literature (*e.g.*, Cheney & Sullivan, 1997 & 2008). The significance of this, is that the approximate origin of a wildfire can be identified from fire scars depicting the distinctive V or U shape (NWCG, 2016; NFPA, 2017; IAFC *et. al*., 2018). Typically, the point of ignition would be near the base of the U of V and the burn-out area opens into the U or V shape in a downwind direction. A small area may burn back from the point of ignition as a back fire into the apex of the U or V.

FIGURE 2.10: *Shape of a fire in progress from a point ignition. Experimental fire C064, NT, Australia 18 August 1986. Reprinted from* "Grassfires: fuel, weather and fire behaviour *(2nd ed.)", by Cheney, P., & Sullivan, A., 2008, pp. 27, Australia: CSIRO Publishing. Copyright 2008 by CSIRO.*

FIGURE 2.11: *V-shaped burn pattern in fire scar. Reprinted from the "*Guide to wildland fire origin and cause determination (2016 ed.)*", by NWCG, 2016, pp. 94, USA: National Wildlife Coordinating Group.*

FIGURE 2.12: *Example of extreme V-shaped burn pattern in fire scar, influenced by high wind speed. Reprinted from the* "Guide to wildland fire origin and cause determination (2016 ed.)", *by NWCG, 2016, pp. 96, USA: National Wildlife Coordinating Group.*

Of course, these typical shapes may be affected and modified by fire suppression activities (NWCG, 2016) and barriers to fire spread, such as cultivated lands and bodies of water, which might alter the shape of isochrones in actively burning fires, or the final shape of fire scar after extinction. The reliability of this indicator often reduces with decreasing wind speeds and slope. Under no wind or slope a fire will theoretically spread at an equal rate in all directions (in a circular shape). Under low wind conditions (or slope) an indistinctive shape of fire scar may be formed.

While the above comments on reliability of this indicator may be self-evident, it is noted that, apart from fire suppression activities (NWCG, 2016), the literature fails to acknowledge these conditions (which are not unusual) which frequently effect reliability of this indicator. From personal wildfire investigation experience, as well as that of colleagues (Danckwerts J.E. (PhD), personal communication, 2019), it is our observation that with expanding cultivated agriculture (as opposed to rangeland agriculture) and increased human-wildfire interface, it is not unusual for wildland fire scars to be affected or modified by fire suppression activities or barriers to spread, and as a result, not form the typical U or V shape.

2.4.2 Degree of damage:

Degree of damage is not an individual *post-hoc* indicator of wildland fire pattern *per se*, but rather a fundamental principle that dictates how investigators interpret most of the indicators (NWCG, 2016). The degree of damage is the change that occurs to non-combustible objects, or the amount of combustible material lost from the fire (NWCG, 2016). The damage differential to fuels and non-combustible objects is an indication of the intensity, duration, and the direction of fire passage (NWCG, 2016; NFPA, 2017; IAFC *et. al*., 2018).

The degree of damage is one of the most important principles used in determining fire spread type (NFPA, 2017). By comparing and contrasting the degree of damage in different areas, an investigator can determine regions of backing, flanking and heading fires (NWCG, 2016). One can also determine the direction of fire passage by looking at which side of the fuel or object show the greatest damage (NWCG, 2016; NFPA, 2017). In most cases, the side of the fuel or object that displays the greatest damage, faces the direction in which the fire approached (NWCG, 2016; NFPA, 2017; IAFC *et. al*., 2018). This is with the exception of indicators such as leeside charring (see **Section 2.4.4, *Leeside charring on pole type fuels*** below) and crown damage (see **Section 2.4.5, *Crown damage*** below).

The literature (fire investigation handbooks etc.) however, fails to recognise that the side of the fuel or object that displays the most damage is not always the side from which the fire approached.

2.4.3 Partial burning in fire scar:

Partial burning in the fire scar manifests itself as narrow strips of burnt lines (often non continuous) in a field which can be seen from above (aerial photographs) (**FIGURE 2.13**) (Cheney & Sullivan, 2008). This indicator occurs only when high wind speeds prevail during the fire, and usually in sparse grasslands with little fuel (Cheney & Sullivan, 2008). When a fire starts under these conditions, the strong force of the wind causes the head fire to advance rapidly, regularly forming multiple heads and spotting freely (Teie, 2003). The flank fires, however, spread laterally at a much slower rate, usually run out of fuel, and die out. As a result, narrow strips of burnt lines indicating the direction of the wind are formed in in the fire scar (**FIGURE 2.13**) (Cheney & Sullivan, 2008).

Partial or patchy burning may also occur under unfavourable fire conditions. When conditions are not conducive to the spread of wildland fires (*e.g.*, high fuel moisture and humidity, low temperatures and wind speeds), combustion is often incomplete, resulting in patchy or partial burning in the fire scar.

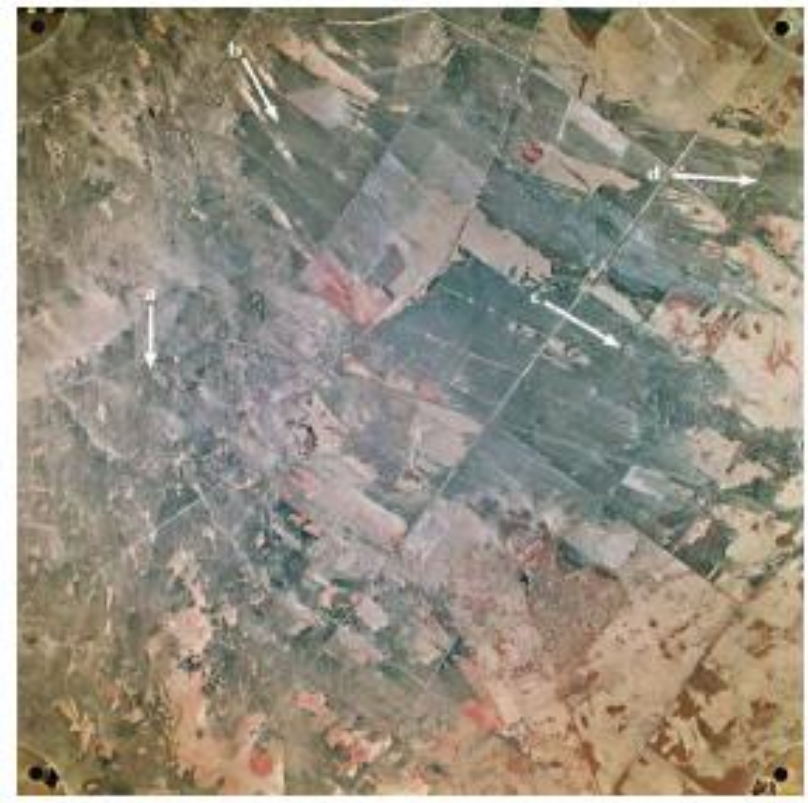

FIGURE 2.13: *Partial burning in fire scar as seen from above. a, b, c, & d show direction of prevailing wind (and spread of fire) at different times throughout the fire. Note the narrow strips of burnt grass in the direction of fire spread and wind. Aerial photograph of the Narraweena fire, Australia, 16 February 1983. Reprinted from "*Grassfires: fuel, weather and fire behaviour *(2nd ed.)", by Cheney, P., & Sullivan, A., 2008, pp. 108, Australia: CSIRO Publishing. Copyright 2008 by CSIRO.*

2.4.4 Leeside charring on pole type fuels:

Leeside charring occurs when flames are drawn into an eddy zone on the leeward side of pole type fuels (**FIGURE 2.14**), such as trees and posts, charring higher up the leeside than on the windward side (**FIGURE 2.16**) (Cheney & Sullivan, 2008; NWCG, 2016; NFPA, 2017; IAFC *et. al*., 2018). As a fire progresses, the flames lean at an angle, either over burnt (back fire) or unburnt fuel (head fire) (Cheney & Sullivan, 2008). The angle in which the flames lean is primarily influenced by wind, but also slope (Luke & McArthur, 1978; Trollope, 1984; Cheney & Sullivan, 2008; NWCG, 2016). As flames burn at an angle past a pole type fuel, an eddy zone vortex generates flame-wrap on the side in which the flames are leaning (**FIGURE 2.14**), leaving a characteristic angle of char (**FIGURE 2.16**) (Cheney & Sullivan, 2008; NWCG, 2016; NFPA, 2017).

FIGURE 2.14: *Flames drawn into an eddy zone vortex flame wrap on the leeward side of two tree trunks. Note how the flames extend higher on the leeward side (right) than the windward side (left). Reprinted from "*Grassfires: fuel, weather and fire behaviour (2nd ed.)", *by Cheney, P., & Sullivan, A., 2008, pp. 107, Australia: CSIRO Publishing. Copyright 2008 by CSIRO.*

In typical circumstances, when wind primarily determines flame angle, the highest point of charring will be on the leeward side, directly opposite the oncoming wind (**1 in FIGURE 2.15**), indicating the direction the wind was blowing as the fire front passed (and importantly, not necessarily an indication of the direction of fire passage) (Cheney & Sullivan, 2008). However, slope and the fire's convection through the combustion zone can also influence the pattern of charring (Cheney & Sullivan, 2008; NFPA, 2017; IAFC *et. al*., 2018). When a fire burns up a slope with the wind, charring will be higher

on the upslope side of the pole type fuel, with the angle of char greater than the angle of slope (**2 in FIGURE 2.15**) (NFPA, 2017; IAFC *et. al*., 2018). When a fire burns down a slope against the wind, charring will be higher on the upslope side of the pole type fuel, with the angle of char nearly parallel to the angle of slope (**4 in FIGURE 2.15**) (NFPA, 2017; IAFC *et. al*., 2018). When a fire burns down a slope with the wind, charring will be higher on the downslope side of the pole type fuel as a result of the eddy zone vortex flame-wrap (NFPA, 2017; IAFC *et. al*., 2018). When a fire burns up a slope against the wind, charring will be nearly parallel to the angle of slope, however, char damage will be much greater on the downslope side of the pole type fuel (NFPA, 2017; IAFC *et. al*., 2018).

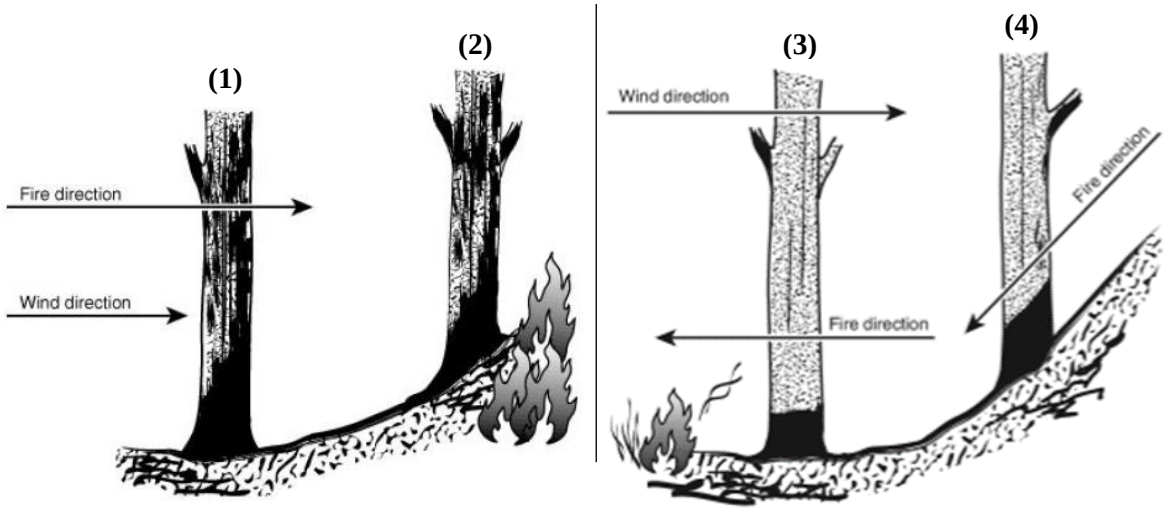

FIGURE 2.15: *Fire burning with the wind (1) and/or uphill (2) create leeside char patterns at an angle greater than slope of ground. Fire burning against the wind (3) and downslope (4) create char patterns parallel to slope of ground. Adapted from the "*NFPA 921: guide for fire and explosion investigations (2017 ed.)*", by NFPA, 2017, pp. 329 & 330, Quincy, Massachusetts, USA: National Fire Protection Association. Copyright 2016 by National Fire Protection Association.*

In some instances, the width of the head fire and positions of either flank can be roughly inferred from the directional leeside charring on pole type fuels placed in a transect across the fire (Cheney & Sullivan, 2008). This indicator is usually more prominent in heading regions of the fire than backing regions (**3 in FIGURE 2.15**) (NWCG, 2016).

FIGURE 2.16: *Example of leeside charring on a pole type fuel. Fire passage and wind direction right to left. One-meter ruler for scale. Prescribed burn BE3, Katberg, EC, South Africa, 8 November 2019.*

While the authors of *Grassfires: fuel, weather and fire behaviour* (2nd ed.) (Cheney & Sullivan, 2008) are explicitly clear that leeside charring is an indicator of the wind direction at the time of pole type fuel combustion, the *NFPA 921, guide for fire and explosion investigations* (2017 ed.); the *Guide to wildland fire origin and cause determination* (2016 ed.); & *Fire Investigator: Principles and Practice to NFPA 921 and 1033* (5th ed.) (2018) are not as clear, and in some cases are factually incorrect. They state that leeside charring is an indication of direction of fire passage (NFPA, 2017) and fire spread type (head fire) (NWCG, 2016), asserting that leeside charring does not occur in backing fires (NWCG, 2016).

The biggest driver of leeside charring is wind, drawing the flames into an eddy zone vortex on the leeward side of the pole type fuel (Cheney & Sullivan, 2008). Therefore, leeside charring could occur on the leeward side of a pole type fuel, while the passage of fire was perpendicular to wind direction (*i.e.*, flank fire). This affirms the notion that leeside charring is an indicator of wind direction (at the time of pole type fuel combustion) and not direction of fire passage.

While leeside charring is more prominent in advancing regions of the fire (NWCG, 2016), it should not be assumed that this indicator is limited to head fires, as the principals surrounding the formation of eddy zonal vortex flame wrap do not change for back fires. One would, however, expect less incidence and prominence of leeside charring in back fires, due to the smaller flame size. Deductions can be made about fire spread type by looking at the intensity and pattern of char (**FIGURE 2.15**), but one should be careful not to base conclusions about direction of fire passage and fire spread type on leeside charring without first looking at other more appropriate indicators.

Evidently, Simeoni *et. al.*, (2017), noted in their study that convective heat currents may play a greater role in the formation of leeside charring than was previously understood. The literature attributes the formation of this indicator to wind and slope (Cheney & Sullivan, 2008; NWCG, 2016; NFPA, 2017; Simeoni *et. al.*, 2017; IAFC *et. al.*, 2018), yet Simeoni *et. al.*, (2017), recorded many tree trunks in their study displaying leeside charring, despite low mean wind speeds (1.4 m/s) and gentle gradients. They did, however, record high fire intensities, and attributed the vortex flame wrap and subsequent formation of leeside charring in their trial to 'wind' created by convective heat currents from the advancing fire (Simeoni *et. al.*, 2017).

2.4.5 Crown damage:

Crown damage is the charring that occurs in foliage crowns of trees and shrubs. As a fire progresses through a standing fuel, convection and radiation will preheat the lower limbs of trees and bushes (Trollope, 1984; Van Wagtendonk, 2006; Scott *et. al*., 2014), igniting and spreading upward through the canopy, scorching or charring fuels at an angle in the direction of the fire's travel (**FIGURE 2.17**) (NFPA, 2004; NFPA, 2017). In advancing areas of a fire, the flame front will enter low on the side facing the oncoming fire and exit high on the opposite side, leaving a triangular unburned portion of crown on the side of the approaching fire (**FIGURE 2.18**) (NWCG, 2016; NFPA, 2017). This pattern is an indication of the direction of fire spread and the type of fire spread (head fire) (NWCG, 2016; NFPA, 2017). Due to the lack of convective heat transfer in back fires (Van Wagtendonk, 2006; Scott *et. al*., 2014), the crown damage will be parallel to the ground, indicating backing fire spread type (NWCG, 2016; NFPA, 2017).

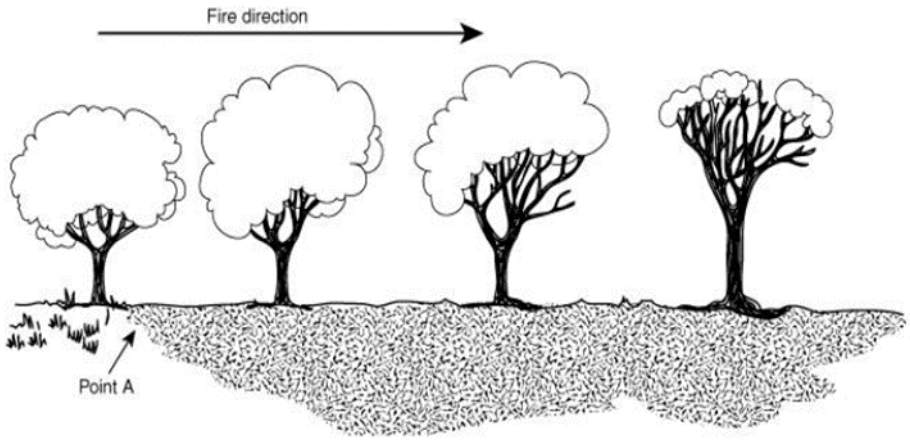

FIGURE 2.17: *Progressive crown damage from point of origin. Reprinted from the "*NFPA 921: guide for fire and explosion investigations (2017 ed.)", *by NFPA, 2017, pp. 331, Quincy, Massachusetts, USA: National Fire Protection Association. Copyright 2016 by National Fire Protection Association.*

FIGURE 2.18: *Angle of char on a tree crown. Reprinted from the "*Guide to wildland fire origin and cause determination (2016 ed.)*", by NWCG, 2016, pp. 60, USA: National Wildlife Coordinating Group.*

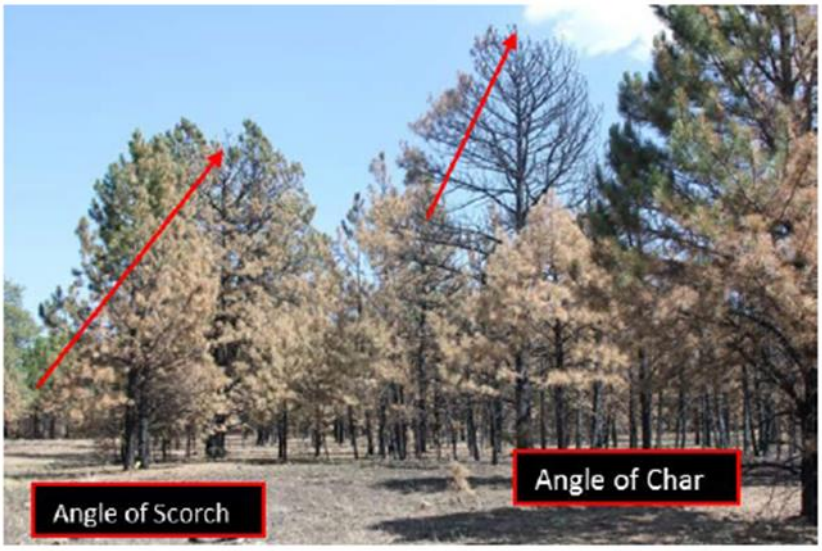

FIGURE 2.19: *Angle of scorch and angle of char in foliage crown. Reprinted from the "*Guide to wildland fire origin and cause determination (2016 ed.)*", by NWCG, 2016, pp. 58, USA: National Wildlife Coordinating Group.*

This indicator is most accurately identified closer to the point of origin, where the angle of char is more prominent, as the lower branches and surface fuels are burnt, while the foliage crown is usually unburnt (**FIGURE 2.19**) (NFPA, 2017). As the fire advances further from the point of origin, the angle of char

becomes less clear as more of the foliage crown is burned as the fire intensifies (**FIGURE 2.17**) (NFPA, 2017). The height of char in the foliage crown can be an indication of fire intensity (Cheney & Sullivan, 2008; NFPA, 2017), which may help an investigator differentiate between areas of backing and heading fires (Cheney & Sullivan, 2008). Unlike leeside charring on pole type fuels, crown damage does not necessarily indicate the wind direction.

2.4.6 Foliage freeze:

Foliage freeze (often referred to as leaf freeze) is the scorching of green leaves, needles or young branches in the direction the wind was blowing when the fire passed through (Cheney & Sullivan, 2008; NWCG, 2016; NFPA, 2017; IAFC *et. al*., 2018). The process occurs when green material, usually leaves, are rapidly heated, becoming soft and pliable and bend in the direction the wind is blowing (NWCG, 2016; NFPA, 2017; IAFC *et. al*., 2018). Following the passage of the fire, the leaves begin to cool and stiffen ('freeze') in the direction the wind was blowing (**FIGURE 2.20**) (NWCG, 2016; NFPA, 2017; IAFC *et. al*., 2018).

FIGURE 2.20: *Foliage freeze. Wind blew left to right. Prescribed burn MW2, Boschberg, EC, South Africa, 17 September 2019.*

It is important to note that (a) foliage freeze shows the direction the wind was blowing at the time the fire passed through (Cheney & Sullivan, 2008), it does not show the direction of the prevailing wind for the duration of the entire wildfire; and that (b) foliage freeze does not necessarily show the direction of fire spread (Cheney & Sullivan, 2008; NWCG, 2016; NFPA, 2017). Occasionally, leaves may be found frozen vertically (Cheney & Sullivan, 2008; NWCG, 2016; NFPA, 2017). This is a result of strong upward convective drafts created by the fire (Cheney & Sullivan, 2008; NWCG, 2016; NFPA, 2017), which usually occurs in an area where fuel is concentrated and likely to burn intensely (Cheney & Sullivan, 2008). For this reason, the use of this indicator is recommended on isolated and exposed trees and shrubs and on fires which have burned under very windy conditions (Cheney & Sullivan, 2008).

This indicator is most commonly observed in advancing areas of a fire (NWCG, 2016; NFPA, 2017; IAFC *et. al.*, 2018), but is not uncommon in lateral (flank) areas (NWCG, 2016). Foliage freeze is less common in backing areas of the fire, due to reduced convective heat transfer onto unburnt fuel (Scott *et. al*., 2014; NWCG, 2016).

Similar to *leeside charring on pole type fuels*, Simeoni *et. al.*, (2017), noted that convective heat currents play an important role in the formation of leaf freeze. While convection induced foliage freeze is not uncommon, in their prescribed burn, Simeoni *et. al.*, (2017), found that crown freezing was, for the most part, an indicator of the direction of fire spread (ENE) and not the wind direction (ESE). Pointing toward convective heat currents playing a greater role in the formation of directional leaf freeze than wind. Simeoni *et. al.*, (2017), recognized this as a common occurrence (NWCG, 2016) and attributed their scenario to the low mean wind velocity (1.4 m/s) on the day. Adding that short wind gusts would not be able to change the direction of foliage freezing (Simeoni *et.al.*, 2017). The high fire intensities estimated (7 350 ± 3 480 to 12 590 ± 5 870 kW/m) during the burn may be an additional explanation for Simeoni *et. al.*, (2017) findings. At these intensities, the 'wind' created by the convective updrafts may well have been greater than the mean wind velocity. It should also be noted that the trial conducted by Simeoni *et. al.*, (2017), took place in a dense pitch pine (*Pinus rigida* Mill.) forest. Cheney & Sullivan, (2008), recommend that the *foliage freeze* indicator be used on isolated and exposed trees and shrubs and on fires which have burned under very windy conditions, in order to avoid convective heat current effects.

2.4.7 Curling:

In some ways similar to *foliage freeze*, curling occurs when green leaves are heated, dry out and shrink on the side facing the heat source, causing the edges to curl towards the direction the fire came from (**FIGURE 2.21**) (NWCG, 2016; NFPA, 2017; IAFC *et. al*., 2018). Curling indicates the direction of fire passage. Less likely to be present in advancing areas of the fire or under high wind speeds, curling

usually occurs when foliage freeze does not. Curling is most commonly observed in slow moving, low intensity burns associated with backing and flanking fires (NWCG, 2016; NFPA, 2017; IAFC *et. al*., 2018).

FIGURE 2.21: *Curling. Fire passage from left to right. Leaves curled towards left. Reprinted from the "*Guide to wildland fire origin and cause determination (2016 ed.)*", by NWCG, 2016, pp. 75, USA: National Wildlife Coordinating Group.*

The literature, in some cases (NWCG, 2016; NFPA, 2017; IAFC *et. al*., 2018), contradicts itself with regards to the directional indication of *curling*. The descriptions state that curling is most prevalent in back fires, and that leaves curl towards heat source as well as in direction fire approached from (NWCG, 2016; NFPA, 2017; IAFC *et. al*., 2018). However, in back fires, the majority of heat (convection) moves (is blown) over burnt ground. By this rationale, if curling were to occur in direction of heat source, leaves should curl in direction of fire spread, after the fire has passed. On the other hand, perhaps curling is induced by radiative heat energy, in which case the literature would be correct. Further research and clarity is needed on this matter.

2.4.8 Consumption depth of grass tussocks:

Differentiating between areas of backing and heading fires is one of the more important aspects of wildfire origin and cause investigation, as it allows the investigator to identify an approximate point of origin. The differences in intensity, severity and behaviour of heading and backing fires leave distinctly different charred or unburnt remains (indicators) (Cheney & Sullivan, 2008; NWCG, 2016; NFPA, 2017). In grasslands the depth of consumption (height differences) of the remaining grass tussocks allow investigators to confidently distinguish between regions of heading and backing fires (Cheney & Sullivan, 2008). Back fires burn close to the ground, leaving short grass tussocks and very little litter

remaining (Trollope *et. al.*, 2004; Cheney & Sullivan, 2008). Conversely, when an advancing head fire passes, the grass tussocks are typically not entirely consumed (Trollope *et. al.*, 2004; NFPA, 2017), leaving lengths of residual basal grass stalks protruding well above the ground (**FIGURE 2.22**) (Cheney & Sullivan, 2008; NFPA, 2017).

FIGURE 2.22: *Example of lengths of residual basal grass stalks left unburnt after a head fire. Prescribed burn MW1, Boschberg, EC, South Africa, 13 September 2019.*

The heat load in head fires is at a higher elevation than is the case with back fires. In head fires, flames are angled over the unburnt fuel (Cheney & Sullivan, 2008), which is ignited well above the ground (Cheney & Sullivan, 2008). This is a result of both forward and upward convective (and to a lesser extent radiative) preheating (Trollope, 1984; Van Wagtendonk, 2006; Scott *et. al.*, 2014). As a fire continues to burn rapidly forwards and upwards, it also progressively burns into the lower layers, slowly dying out due to inefficient combustion, leaving unburnt stubble and litter remaining (Cheney & Sullivan, 2008).

In contrast, in back fires, the flames lean over the burnt ground, and as the fire progresses (against the wind or down a slope) it ignites the fuel in its path at, or near, ground level (Cheney & Sullivan, 2008). The fuel is preheated by radiation only, with no upward convective heat transfer (Van Wagtendonk, 2006; Scott *et. al.*, 2014). Back fires burn slowly and close to ground level, and because there is enough time for thorough mixing of oxygen with flammable material, they burn much more efficiently than head fires, leaving little residual partially combusted material (with the exception of heavy fuels which

are not sufficiently pre-heated to catch alight, and elevated fuels which cannot be reached by the short flames) (Trollope *et. al.*, 2004; Cheney & Sullivan, 2008).

Another indication of a head fire having passed through is the presence of grass tussocks exhibiting protection (see **Section 2.4.14, *Protection*** below) (**FIGURE 2.35 & FIGURE 2.36**) (NFPA, 2017). The grass stalks are burned at an angle, leaving the remaining tussocks sloping upwards, in the direction of the advancing fire front (**FIGURE 2.36**) (NWCG, 2016; NFPA, 2017). The remaining grass tussocks may also exhibit cupping (see **Section 2.4.12, *Cupping*** below) (**FIGURE 2.29**) (NWCG, 2016; NFPA, 2017), as well as sooting (see **Section 2.4.15, *Sooting*** below) (NWCG, 2016).

Exceptions to this indicator (which have not been stated in the literature) may occur in cases where head fires advance upslope and with the wind. With both wind and gradient causing the flames to lean into the slope, the fire may burn close to the ground, leaving little residual unburnt material remaining.

2.4.9 Undercutting of flowering culms:

Undercutting refers to the process where flowering culms of grasses are undercut by a back fire and blown back by the wind to fall into the already burnt area, where they remain unburnt (**FIGURE 2.23**) (NWCG, 2016; NFPA, 2017; IAFC *et. al*., 2018). As a back fire progresses, the flames lean over the burnt ground (Cheney & Sullivan, 2008), preheating the fuel by radiation only, with no upward convective heat transfer (Van Wagtendonk, 2006; Scott *et. al*., 2014). The flames will first ignite the grass tussocks in its path at, or near the base (Cheney & Sullivan, 2008; NFPA, 2017), collapsing the flowering culms (**FIGURE 2.23**) (NFPA, 2017). Culms that fall ahead of, or adjacent to the flame front are burned (NFPA, 2017), while undercut culms that are blown, or fall behind the flame front into the already burnt fire scar, often remain unburnt (**FIGURE 2.23**) (NFPA, 2017), and point in the approximate direction the fire came from (NWCG, 2016; NFPA, 2017; IAFC *et. al*., 2018).

Thus, in back burn areas, although the grass sward (leafy material) is more completely combusted (Cheney & Sullivan, 2008), unburnt grass culms are commonly found scattered in the burnt area (**FIGURE 2.24**) (NWCG, 2016; NFPA, 2017; IAFC *et. al*., 2018).

In contrast, the heat load in head fires is at higher elevation (Cheney & Sullivan, 2008), and grass culms are usually completely combusted (NFPA, 2017). The presence or absence of unburnt grass culms in the burn area is thought to be one of the most reliable indicators of back and head fires respectively (**FIGURE 2.25**). Additionally, the direction in which the majority of the culms are pointing indicates where the back fire approached from (**FIGURE 2.24**) (NWCG, 2016; NFPA, 2017; IAFC *et. al*., 2018).

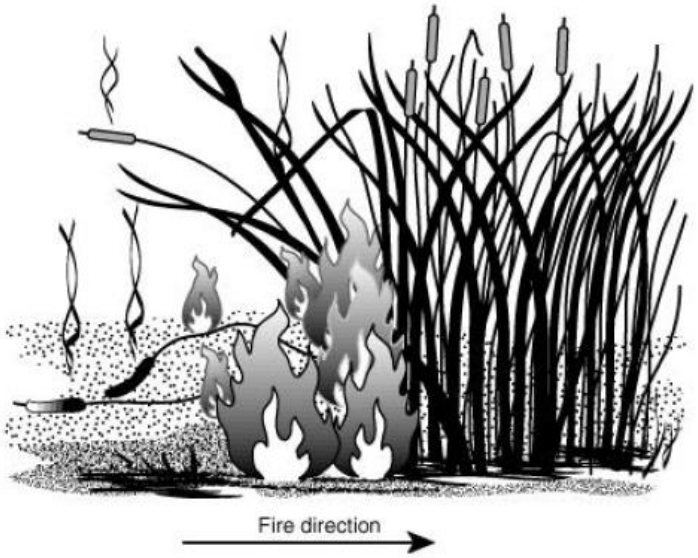

FIGURE 2.23: *The process of undercutting. Flowering culms are cut at the base by back fire and fall onto burnt ground. Littered culms point in general direction of fire's approach. Reprinted from the "*NFPA 921: guide for fire and explosion investigations (2017 ed.)*", by NFPA, 2017, pp. 329, Quincy, Massachusetts, USA: National Fire Protection Association. Copyright 2016 by National Fire Protection Association.*

FIGURE 2.24: *Backing area showing littering of culms pointing back in general direction of fire's approach. Arrow showing direction of fire passage. Reprinted from the "*Guide to wildland fire origin and cause determination (2016 ed.)*", by NWCG, 2016, pp. 50, USA: National Wildlife Coordinating Group.*

FIGURE 2.25: *Picture of a clean burn showing no culms in advancing area (outlined), with culms outlining the lateral and backing areas. Arrows showing direction of head fire passage. Reprinted from the "*Guide to wildland fire origin and cause determination (2016 ed.)*", by NWCG, 2016, pp. 48, USA: National Wildlife Coordinating Group.*

2.4.10 Ash colour and pattern:

Ash is the unconsumed remains of the combustion process and the by-product of incomplete combustion (Bodi *et. al.*, 2011; Smith & Hudak, 2005; Hudak *et. al.*, 2013; NWCG, 2016). The colour and pattern of ash in the fire scar varies according to the nature of combustion and behaviour of the fire (Cheney & Sullivan, 2008; Bodi *et. al.*, 2014; Dlapa *et. al.*, 2015). When the combustion process is incomplete, such as in rapidly moving head fires, some of the complex mixture of organic compounds such as cellulose, hydrocarbons, tars and molecular carbon are left unconsumed, in the form of dark ash and soot (Lentile *et. al.*, 2006; Cheney & Sullivan, 2008; Bodi *et. al.*, 2011). Conversely, when combustion is more complete, most of the organic carbon is consumed, leaving inorganic carbon and other elements in the form of white ash remaining (Lentile *et. al.*, 2006; Cheney & Sullivan, 2008; Bodi *et. al.*, 2011; NWCG, 2016). This is because, inorganic carbon requires higher temperatures (roughly 600 – 800^{o}C) than organic carbon (roughly 150 – 400^{o}C) to combust (Bodi *et. al.*, 2014).

The corollary to this, is that in back fires, where combustion is slow and often complete, white ash is left behind in the fire scar (Cheney & Sullivan, 2008; Trollope, 1983). While, in head fires, on the other hand, combustion is often rapid, chaotic, and incomplete, leaving dark ash and black soot remaining in the fire scar (Cheney & Sullivan, 2008; Trollope, 1983). Ash colour is therefore considered an indicator of fire spread type (Cheney & Sullivan, 2008).

The pattern of ash deposition can also reveal behavioural aspects of the fire and help build a time frame of fire spread (Cheney & Sullivan, 2008). In some instances, differential burning along the fire

perimeter and fluctuations between heading and backing fires along the flank, may leave ash patterns or lines of different colours (**FIGURE 2.26**) (Cheney & Sullivan, 2008). It is, however, rare to find complete isochrones (ellipses/ovals) of ash patterns (**FIGURE 2.26**) (Cheney & Sullivan, 2008). This is because, a head fire is usually always heading, even during lulls in wind (Cheney & Sullivan, 2008). These patterns of ash deposition as an indicator of fire shape, origin and spread (Cheney & Sullivan, 2008). In order to properly interpret ash patterns, they usually have to be viewed from above (aerial photograph) (Cheney & Sullivan, 2008).

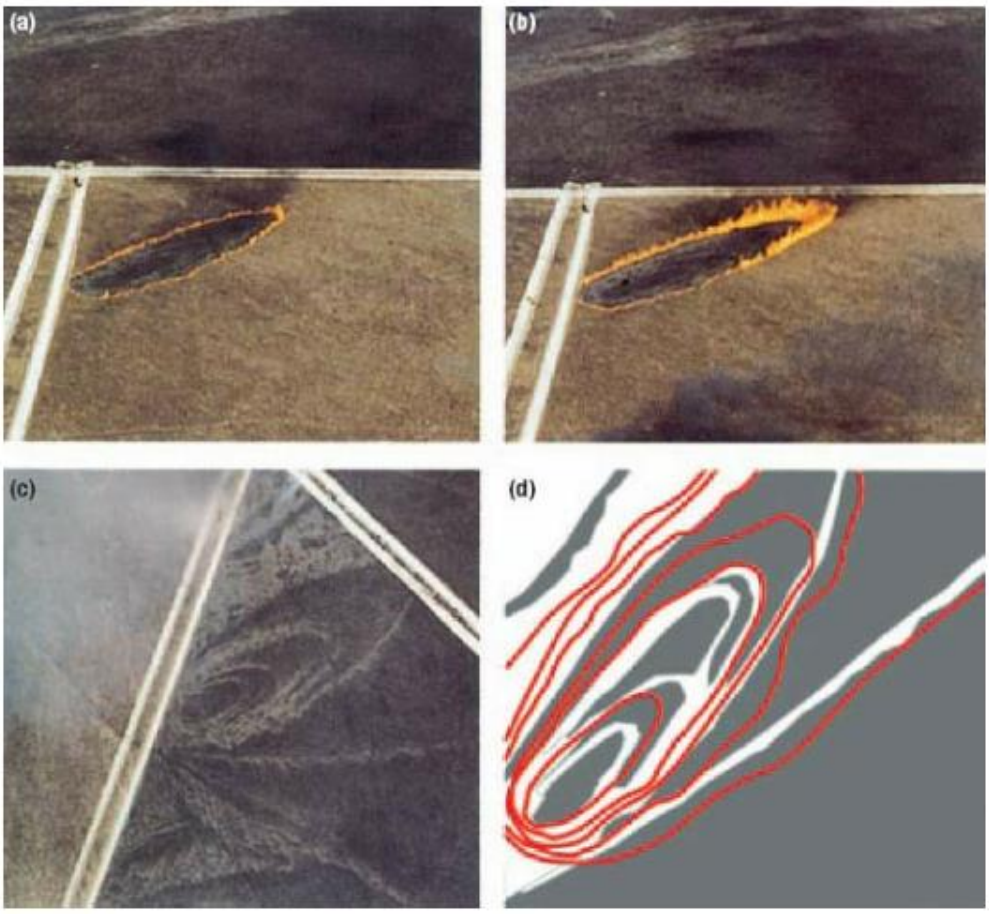

***FIGURE 2.26**: Deposition of ash patterns in consecutive isochrones, as a result of fluctuations between heading (b) and backing (a) fires. Periods of backing (a) fire deposit white ash as isochrones seen in (c). Experimental fire E26, NT, Australia, 20 August 1986. Reprinted from* "Grassfires: fuel, weather and fire behaviour (2nd ed.)*", by Cheney, P., & Sullivan, A., 2008, pp. 110, Australia: CSIRO Publishing. Copyright 2008 by CSIRO.*

Light, white ash can also be picked up by wind and deposited on objects (NWCG, 2016; NFPA, 2017). Deposition downwind usually occurs on the windward sides of objects (**FIGURE 2.27**) (NWCG, 2016; NFPA, 2017). White ash deposits are generally a reliable indicator of wind direction (NWCG, 2016;

NFPA, 2017). However, under fluctuating and changing wind conditions, it may be an unreliable indicator of the general prevailing wind conditions (NWCG, 2016).

Ash colour and pattern indicators do not last long in the fire scar (NWCG, 2016; NFPA, 2017), and usually need to be viewed within a day or two of the fire (Cheney & Sullivan, 2008). Ash indicators may begin to degrade immediately under certain whether conditions (rain and wind) (NFPA, 2017).

Exceptions around ash colour and pattern indicators may occur with regards to fuel (Bodi *et. al.*, 2014; Dlapa *et. al.*, 2015; NWCG, 2016). It is important to note that there are many components that effect ash colour, other than fire behaviour (Bodi *et. al.*, 2014; Dlapa *et. al.*, 2015). One of the most important of these, is the amount, combustibility, and type of fuel (Bodi *et. al.*, 2014; Dlapa *et. al.*, 2015). Different species, as well as fine and heavy fuels may leave differential ash colour and patterns.

FIGURE 2.27: *Example of white ash deposits blown by wind onto windward side of stem. Reprinted from the* "Guide to wildland fire origin and cause determination *(2016 ed.)", by NWCG, 2016, pp. 90, USA: National Wildlife Coordinating Group.*

The literature on ash colour and pattern indicators does, in many cases have mixed views. The *NFPA 921, guide for fire and explosion investigations* (2017 ed.) and the *Guide to wildland fire origin and cause determination* (2016 ed.), state that white ash deposition is a result of exposure to heat and flame, and more prevalent in heading regions of the fire. However, while the *Guide to wildland fire origin and cause determination* (2016 ed.), states that white ash is a by-product and result of complete combustion, they fail to recognise that ash colour may be an indicator of fire spread type. In fact, rather contradictorily, the authors clearly state that backing areas of fires will exhibit less white ash overall (NWCG, 2016). Trollope, (1983), observed the opposite pattern of ash distribution, with dark ash deposited in areas of heading fires, and lighter ash remaining on the ground surface after back fire passage.

2.4.11 Die-out pattern:

As a fire burns across a landscape, it may move into new areas comprising less fuel, different fuel types, increased fuel moisture, or other conditions which may cause decreased rate of spread and intensity. In these areas, the fire may begin to die out, leaving distinct patterns (NFPA, 2017; IAFC *et. al*., 2018). These distinct patterns offer insights into how the fire behaved and help us establish general fire progression (NFPA, 2017). As a fire progresses, the flanks experience fluctuations in wind direction, alternating between backing and heading fires (Cheney & Sullivan, 2008). During periods of heading fire the vegetation completely defoliates and blackens (Cheney & Sullivan, 2008). Conversely, during periods of backing fire the vegetation is scorched leaving foliage intact and occasionally unburned (Cheney & Sullivan, 2008; NFPA, 2017). These fluctuations between back and head fires leave narrow strips or fingers of unburned or partially burned fuels, indicating areas of lateral fire progression (Cheney & Sullivan, 2008; NFPA, 2017). Die-out patterns are best observed in shrublands or heathlands with dense, uniform fuels (Cheney & Sullivan, 2008).

2.4.12 Cupping:

Cupping indicators are divided into two groups based on the types of fuel on which they occur. Cupping is the concave or cup shaped pattern of charring that occurs (1) on small stumps (< 25cm diameter) (**FIGURE 2.28**) and whole tussocks of grass (**FIGURE 2.29**), as well as (2) on the terminal ends of thin branches (< 1cm diameter) (**FIGURE 2.30**) and grass stems (**FIGURE 2.32**) (NWCG, 2016; NFPA, 2017; IAFC *et. al.*, 2018). The windward side of the fuel is exposed to the most heat, charring deeply, burning the tips off twigs and branches and leaving a rounded or blunted end (NWCG, 2016; NFPA, 2017; IAFC *et. al.*, 2018).

In the case of grass tussocks and small stumps (1), an angled cup shape will be charred into the fuel, with the low end of the cup on the windward side (**FIGURE 2.28 & FIGURE 2.29**) (NWCG, 2016; NFPA, 2017). The leeward side of the fuel remains relatively cooler and protected (see **Section 2.4.14, *Protection*** below) (NWCG, 2016; NFPA, 2017; IAFC *et. al.*, 2018), with flames charring at an angle from underneath or above, creating sharp, tapered points (NWCG, 2016; NFPA, 2017).

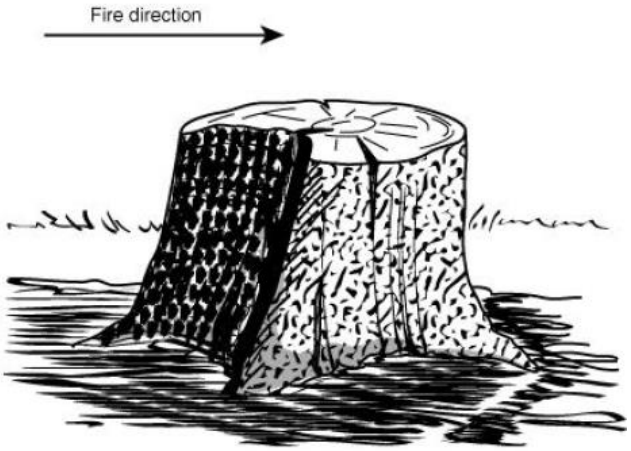

FIGURE 2.28: *Illustration of cupping shown on a small tree stump (<25cm diameter). Fire passage left to right. Reprinted from the "*NFPA 921: guide for fire and explosion investigations (2004 ed.)*", by NFPA, 2004, pp. 431, Quincy, Massachusetts, USA: National Fire Protection Association. Copyright 2004 by National Fire Protection Association.*

FIGURE 2.29: *Example of cupping on grass tussocks. Fire passage left to right. Adapted from the "*Guide to wildland fire origin and cause determination (2016 ed.)*", by NWCG, 2016, pp. 49 & 65, USA: National Wildlife Coordinating Group.*

In the case of individual grass stems and thin branches (2), sharp, tapered points will be on the higher and protected (leeward) side of the cup (NWCG, 2016; NFPA, 2017). Thus, cupping indicates wind direction when the fire passed through, with the blunt or cupped side of the fuel pointing into the wind and the sharp tapered side indicating the direction in which the wind blew (**FIGURE 2.30 & FIGURE 2.31**) (NWCG, 2016; NFPA, 2017; IAFC *et. al.*, 2018). In scenarios where cupping on tussocks is difficult to identify by eye, one can examine the indicator more closely by rubbing their hand over the tussock, feeling for a rough and smooth side **(FIGURE 2.32**) (NFPA, 2004).

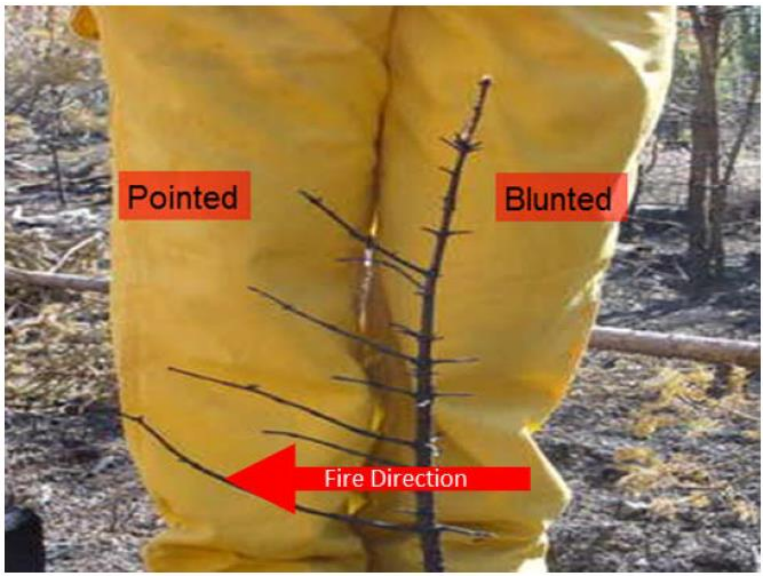

FIGURE 2.30: *Example of cupping on a small bush. Fire passage right to left. Note the blunted branches on the entry side and the pointed branches on the exit side. Reprinted from the "*Guide to wildland fire origin and cause determination (2016 ed.)*", by NWCG, 2016, pp. 93, USA: National Wildlife Coordinating Group.*

FIGURE 2.31: *Example of sharp tapered branch on the side of the bush the fire exited. Fire progressed left to right. Prescribed burn MW2, EC, South Africa, 17 September 2019.*

FIGURE 2.32: *Example of cupped grass stems. Fire passage right to left. Note grass stems are smooth on entry side and pointed on exit side. When rubbing one's hand over the tussock, it would feel smooth from right to left and rough from left to right. Prescribed burn MW1, Boschberg, EC, South Africa, 11 September 2019.*

Large stumps and branches are not considered when investigating this indicator, as their long fire residency means they continue to burn after the fire front has passed (NWCG, 2016; NFPA, 2017). Cupping is typically associated with advancing fire areas and is not a common occurrence in slow moving and severe back fires (NWCG, 2016; NFPA, 2017), where the fuel is almost entirely consumed (Cheney & Sullivan, 2008).

Concerning cupping in grass tussocks, exceptions to this indicator may occur when curing of tussocks is not uniform. Many tussock grasses cure from the centre out, with new growth (tillers) developing along the outer edges of the tussock (Danckwerts, 1989). This means that a tussock often does not have uniform distribution of moisture content, with less flammable, green outer tillers. The consequence of this with regards to cupping, is that incomplete combustion or reduced consumption of outer tillers may occur. This may result in a pattern of consumption inconsistent with the expected pattern of cupping that would have resulted from flame angle and angle of combustion.

2.4.13 Depth of char:

Charring on woody material such as branches, trunks, logs, and poles appears scaly and fissured in appearance (NFPA, 2017; IAFC *et. al*., 2018). As the woody materials are heated and burn, they lose mass through release moisture (Byram, 1959; Van Wagtendonk, 2006; Scott *et. al*., 2014) and breakdown and combustion of cellulose (Byram, 1959; Scott *et. al*., 2014), shrinking and forming a scaly surface (NFPA, 2017; IAFC *et. al*., 2018). The side with the deepest charring typically indicates the direction in which the fire advanced from (NFPA, 2017; IAFC *et. al*., 2018).

This is with the exception of *leeside charring on pole type fuels* (which have not been stated in the literature). Depth of char indicators may be more applicable on fuels close to or on the ground, such as felled trees and stumps.

2.4.14 Protection:

Protection is when fuels on the opposite side of the approaching fire (unexposed/ protected side) are shielded from heat damage by another object (NWCG, 2016; NFPA, 2017; IAFC *et. al*., 2018). The fuel may be protected by non-combustible objects such as rocks and cans (**FIGURE 2.33**), less combustible objects such as stumps and logs (**FIGURE 2.34**), or the fuel itself (*e.g.,* exposed side of grass tussock protects unexposed side) (**FIGURE 2.35 & FIGURE 2.36**) (NWCG, 2016; NFPA, 2017; IAFC *et. al*., 2018). Protection usually occurs close to, or on the surface of the ground. Fuels on the protected side will be unburnt or display less damage than fuels or objects on the side of the approaching fire (exposed side) (NWCG, 2016; NFPA, 2017; IAFC *et. al*., 2018). The exposed side of fuels and objects will display more charring, sooting, staining, white ash and defined, clean burn lines on the ground surface (**FIGURE 2.33 & FIGURE 2.34**) (NWCG, 2016; NFPA, 2017). The burn line on the protected side will be ragged, uneven and less defined, creating a 'shadow' of the object (**FIGURE 2.33 & FIGURE 2.34**) (NWCG, 2016; NFPA, 2017). While protection is an accurate indicator of the direction of fire passage, exceptions may occur in pole type fuels, when flames are drawn into an eddy zone, wrapping around the fuel and charring on the leeward side (NWCG, 2016).

FIGURE 2.33: *Pictures showing protection. Clean and protected burn lines clearly visible after non-combustible object removed (glass bottle). Adapted from the "*Guide to wildland fire origin and cause determination (2016 ed.)*", by NWCG, 2016, pp. 39, USA: National Wildlife Coordinating Group.*

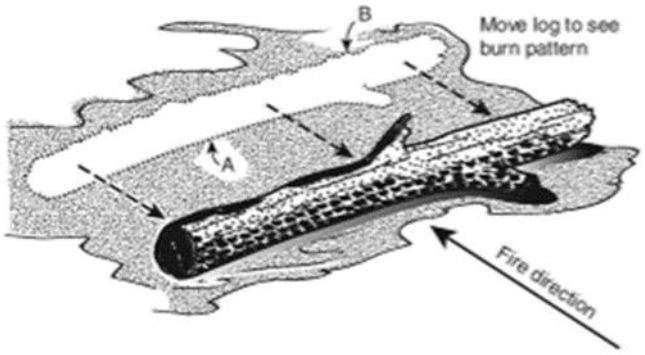

FIGURE 2.34: *Illustration of protection on less combustible object. Clean burn line on the entry side (A) and a ragged burn line (B) on the exit side. Reprinted from the "*NFPA 921: guide for fire and explosion investigations (2017 ed.)*", by NFPA, 2017, pp. 332, Quincy, Massachusetts, USA: National Fire Protection Association. Copyright 2016 by National Fire Protection Association.*

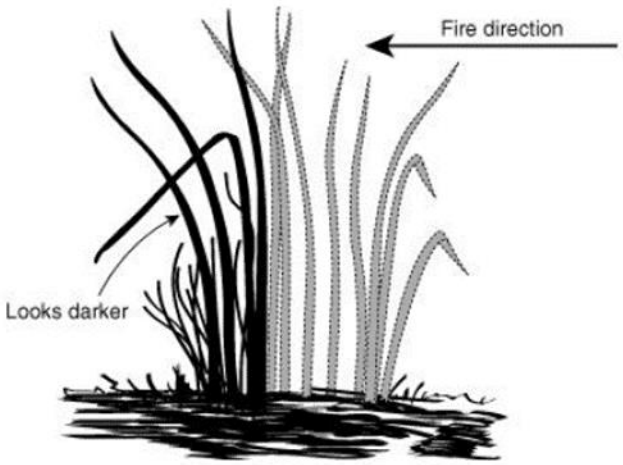

FIGURE 2.35: *Illustration showing how highly combustible material such as grass may experience protection. Vegetation on the side of the approaching fire may protect vegetation on the exit side. Reprinted from the "*NFPA 921: guide for fire and explosion investigations (2004 ed.)*", by NFPA, 2004, pp. 434, Quincy, Massachusetts, USA: National Fire Protection Association. Copyright 2004 by National Fire Protection Association.*

FIGURE 2.36: *Picture showing example of protection in grass tussocks. Reprinted from the "*Guide to wildland fire origin and cause determination (2016 ed.)*", by NWCG, 2016, pp. 40, USA: National Wildlife Coordinating Group.*

2.4.15 Sooting:

Sooting is the deposition of black, carbon-based particulates onto the surface of various objects, such as rocks, cans, fences, posts, wire, and unburnt vegetation (**FIGURE 2.37**) (Cheney & Sullivan, 2008; NWCG, 2016; NFPA, 2017). The airborne particles which cause sooting are a complex mixture of organic compounds that arise from the incomplete combustion of hydrocarbons in the fuel (Cheney & Sullivan, 2008; NWCG, 2016; NFPA, 2017; IAFC *et. al*., 2018). This process is pronounced in fast moving head fires, when the combustion process is very rapid, leading to the chaotic breakdown of cellulose and culminating in the production of large volumes of less flammable hydrocarbons such as tars, as well as molecular carbon, as billows of smoke (**FIGURE 2.2**) (Byram, 1959; Van Wagtendonk, 2006; Cheney & Sullivan, 2008; Cochrane & Ryan, 2009; Scott *et. al*., 2014)**.**

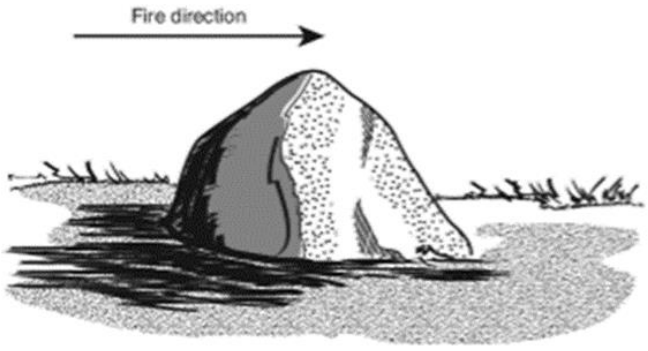

FIGURE 2.37: *Illustration of sooting on a non-combustible object (rock) Soot is deposited on the side facing the oncoming fire. Reprinted from the "*NFPA 921: guide for fire and explosion investigations (2017 ed.)*", by NFPA, 2017, pp. 332, Quincy, Massachusetts, USA: National Fire Protection Association. Copyright 2016 by National Fire Protection Association.*

This occurrence is as a result of the following manifestations: In a head fire, flames are blown towards the unburnt fuel (Cheney & Sullivan, 2008), which is pre-heated by means of convection (and to a lesser extent radiation) (Trollope, 1984; Van Wagtendonk, 2006; Cochrane & Ryan, 2009; Scott *et. al*., 2014). Because the convective movement of heat is both forwards, and upwards (Trollope, 1984; Scott *et. al*., 2014), the fuel in the path of the fire is ignited well above the ground (Cheney & Sullivan, 2008). The fire continues to burn forwards, but also progressively into the lower layers (Cheney & Sullivan, 2008). This pattern of burning can be quite inefficient, and combustion is often incomplete, particularly under strong wind conditions when the fuels are pre-heated and ignited too rapidly for the flammable hydrocarbon gasses to mix sufficiently with oxygen (Cheney & Sullivan, 2008). This is often compounded when the organic residue (hydrocarbons & molecular carbon) from above is deposited on the unburnt fuel below, further limiting the mixture of combusting fuel with oxygen (Cheney & Sullivan, 2008). The carbon soot appears dull and black in colour and can often be rubbed off when

touched (**FIGURE 2.38**) (Cheney & Sullivan, 2008; NWCG, 2016; NFPA, 2017; IAFC *et. al*., 2018). Deposition typically occurs more heavily on the side facing the oncoming fire, indicating the direction the fire approached from (NWCG, 2016; NFPA, 2017; IAFC *et. al.*, 2018).

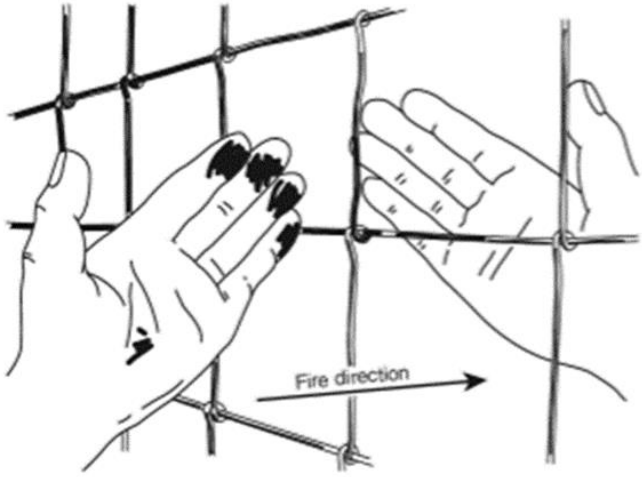

FIGURE 2.38: *Illustration of soot deposited on the side of a fence facing the approaching fire. The soot can be noticed by rubbing a hand along the wire. Reprinted from the "*NFPA 921: guide for fire and explosion investigations (2017 ed.)", *by NFPA, 2017, pp. 332, Quincy, Massachusetts, USA: National Fire Protection Association. Copyright 2016 by National Fire Protection Association.*

While this wildfire pattern indicator may occur in all three fire types, sooting is usually less pronounced in areas of backing fire due to the lower intensities and increased completeness of combustion associated with backing fires (Cheney & Sullivan, 2008; NWCG, 2016).

The literature (NWCG, 2016; NFPA, 2017; IAFC *et.al.*, 2018) states that sooting is an indicator of direction of fire spread, adding that deposition of soot should occur on the side of surfaces facing the approaching fire. While this is a perfectly reasonable postulation for head fires, it may not be the case for back fires. In back fires, the flames lean back over the burnt ground (Cheney & Sullivan, 2008). One might therefore reasonably assume that in back fires, carbon-based particulates would be blown and deposited onto the side of objects opposite the oncoming fire.

2.4.16 Staining:

In some ways similar to sooting, staining is the condensation of vapourised volatile resins and oils in the flame and smoke column, onto the cooler surfaces of non-combustible objects, such as metal cans, glass bottles and rocks, to form a shiny film, yellow-to-brown in colour (**FIGURE 2.39**) (NWCG, 2016;

NFPA, 2017; IAFC *et. al*., 2018). These stains cannot be rubbed off and when touched, may feel tacky (NWCG, 2016; NFPA, 2017). In some instances, light-weight fire debris such as white ash, may adhere to it (NWCG, 2016; NFPA, 2017). Staining will typically appear darker on the side exposed to the flames (NWCG, 2016; NFPA, 2017; IAFC *et. al*., 2018), indicating the direction in which the flames were leaning. Often a subtle indicator of wildfire pattern, staining requires close examination, especially in areas of backing fire, where it is usually less pronounced (NWCG, 2016). The staining process does not often occur on large objects (NWCG, 2016) and happens on a smaller scale to sooting.

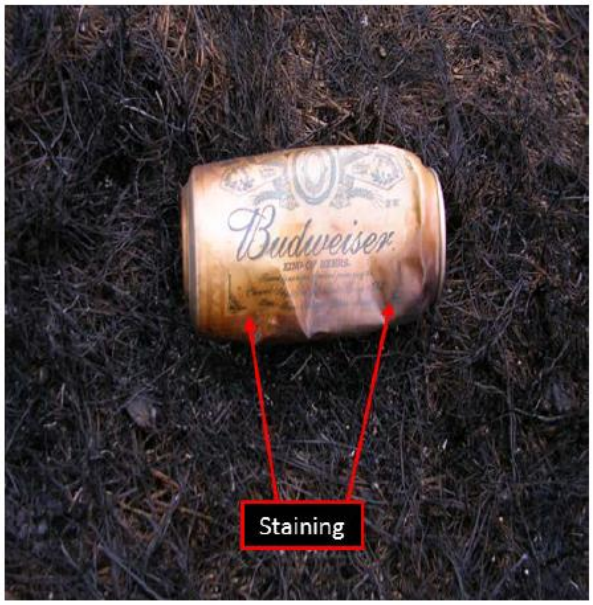

FIGURE 2.39: *Staining on a can. Reprinted from the "*Guide to wildland fire origin and cause determination (2016 ed.)*", by NWCG, 2016, pp. 80, USA: National Wildlife Coordinating Group.*

Similar to *sooting*, the literature (NFPA, 2017; IAFC *et.al.*, 2018) states that staining is an indicator of direction of fire spread, adding that deposition of volatile resins and oils should occur on the side of surfaces facing the approaching fire. Once again, while this is a perfectly reasonable postulation for head fires, it may not be the case for back fires, where the flames lean back over the burnt ground (Cheney & Sullivan, 2008) and one might expect volatile resins and oils to be blown and deposited onto the side of objects opposite the oncoming fire. However, somewhat contradictory to the *NFPA 921, guide for fire and explosion investigations* (2017 ed.) and *Fire Investigator: Principles and Practice to NFPA 921 and 1033* (5th ed.) (2018), the *Guide to wildland fire origin and cause determination* (2016 ed.) states that staining occurs on the side of objects exposed to flames. This description would be suitable for both heading and backing fires.

In their study, Simeoni *et. al.*, (2017), noted that only one stone (of more than 30) was stained enough to record a direction. The stained stone indicated the fire spread direction at an offset angle (Simeoni *et. al.*, 2017).

2.4.17 Spalling:

Spalling (fire-induced) is the exfoliation or chipping of rocks after exposure to heat (Shakesby & Doerr, 2006; NWCG, 2016; NFPA, 2017; IAFC *et. al*., 2018; Buckman *et. al.*, 2021). The process occurs after exposure to intense heat causes the tensile strength on the surface of the rock to fail (NWCG, 2016; NFPA, 2017; IAFC *et. al*., 2018). Being poor conductors of heat, the outside of the rock heats up much faster than the inside (NWCG, 2016). The higher temperatures of the rock's surface lead to differential expansion, causing sub surface shear stress and ultimately breakage (NWCG, 2016). The thin layers of rock usually break off after the fire front has passed, leaving shallow, light coloured craters (**FIGURE 2.40 & FIGURE 2.41**) (Shakesby & Doerr, 2006; NWCG, 2016; NFPA, 2017; IAFC *et. al*., 2018). These are often surrounded by sooting or staining (**FIGURE 2.40 & FIGURE 2.41**) (NWCG, 2016) and accompanied by small chips or pieces of stone at the base of the rock (**FIGURE 2.40 & FIGURE 2.41**) (NWCG, 2016; NFPA, 2017; IAFC *et. al*., 2018).

FIGURE 2.40: *Example of fire-induced spalling surrounded by sooting. Reprinted from the "*Guide to wildland fire origin and cause determination (2016 ed.)*", by NWCG, 2016, pp. 71, USA: National Wildlife Coordinating Group.*

This indicator should be investigated in conjunction with sooting and staining in order to discern whether the chipping occurred before or after the fire passed through (Shakesby & Doerr, 2006). The absence of sooting or staining within the crater (and presence of sooting or staining around the crater) rules out the possibility that the chipping occurred by other means, before the fire passed through (Shakesby & Doerr, 2006; NWCG, 2016). However, in cases where sooting does not occur, it is difficult to determine whether chipping occurred as a result of fire-induced spalling or by other means.

FIGURE 2.41: *Example of fire-induced spalling on a rock. Fire passage bottom to top. Reprinted from the "*Guide to wildland fire origin and cause determination (2016 ed.)*", by NWCG, 2016, pp. 73, USA: National Wildlife Coordinating Group.*

Spalling will typically appear on the side exposed to the flames (NWCG, 2016; NFPA, 2017; IAFC *et. al*., 2018), indicating the direction in which the flames were leaning. In instances of high fire intensity and when fire residence time is prolonged, spalling may occur on both sides of rocks (NWCG, 2016).

Inconsistencies with regards to the type of rock, moisture content and pre-existing cracks may also affect the presence or absence of spalling (Shakesby & Doerr, 2006; NWCG, 2016).

This indicator is most commonly observed in advancing areas of a fire (NWCG, 2016; NFPA, 2017; IAFC *et. al.*, 2018) and may most likely be explained by the higher intensities and temperatures associated with head fires, which are more conducive to the formation of spalling. Fire-induced spalling is less prolific in backing areas of the fire, where temperatures are too cool to cause differential expansion and chipping (NWCG, 2016).

While it has been stated that spalling is more prolific in head fires than back fires (NWCG, 2016; NFPA, 2017; IAFC *et. al.*, 2018), it must be noted that heat moves upwards and away from the ground in head fires. It might therefore be reasonably assumed that spalling would be rare on stones and rocks in the first 40cm of the fuel structure, and more common on large boulders and rocks that sit higher up in the fuel structure. In fact, it is not uncommon for hares and other small mammals to survive the passing of a head fire, as they escape most of the heat by taking cover close to the ground (Danckwerts J.E. (PhD), personal communication, 2019; Trollope W.S.W. (PhD), personal communication, 2019).

In their study, Simeoni *et. al.*, (2017), recorded very few incidents of fire-induced spalling. Of what little spalling was observed, there was no indication of any specific fire direction (Simeoni *et. al.*, 2017).

2.5 Potential 'novel' indicators:

In addition to the 17 indicators listed in the literature, I have included a review of four additional indicators of fire behaviour, which may prove useful in wildfire investigations. **Unburnt plant litter**, **char and scorch height**, **skeleton damage**, and **total organic carbon content of ash** need to be tested for their suitability and feasibility as indicators of fire behaviour for wildfire investigations. While the use of these methods as indicators of fire behaviour is not novel *per se* (used by researchers), their use as indicators in wildfire investigations is not yet mentioned in the literature.

2.5.1 Unburnt plant litter:

Unburnt plant litter are the loose remains of partially combusted plant material which fall to the ground after the fire has passed. They should not be confused with grass stubble, tussocks, bush skeletons, and other unburnt or partially burnt plants left intact after the fire has passed. Similar to *consumption depth of grass tussocks*, amount of unburnt plant litter is an indicator closely linked to the efficiency and completeness of combustion. The differences in intensity, severity and behaviour of heading and backing fires leave distinctly different charred or unburnt remains (indicators) (Cheney & Sullivan, 2008; NWCG, 2016; NFPA, 2017). The rapid and inefficient nature of combustion in head fires means plant material is often only partially combusted, falling to the ground as loose plant litter (Trollope *et. al.*, 2004; Cheney & Sullivan, 2008). In contrast, back fires burn more slowly and efficiently, combusting plant material more completely, leaving little residual loose plant litter remaining (Trollope *et. al.*, 2004; Cheney & Sullivan, 2008).

2.5.2 Char and scorch height:

The charring and leaf scorch height on trees has been proposed as a useful p*ost-hoc* indicator of flame length and fire intensity for researchers and land managers (Williams *et. al.*, 2003). Based off data collected from a series of fire experiments between 1990 and 1994 in eucalypt savannas at the Kapalga research site, Australia, Williams *et. al.*, (2003), showed that the height of char and scorch on savanna trees (including various other metrics) were both associated with fireline intensity. These relationships, as well as the relationship between flame length and fireline intensity have been corroborated in the literature (Byram, 1959; Chandler *et. al.*, 1983; Van Wilgen *et. al.*, 1985; Van Wilgen, 1986; Kremens *et. al.*, 2003; Cochrane & Ryan, 2009; Andrews, 2018). While these are not typical forensic indicators, they could offer valuable post-hoc insight into aspects of fire behaviour.

FIGURE 2.42: *Loose residual unburnt plant litter prior collection within a 29 x 25cm quadrat with rounded edges (725cm^2). Note that remaining grass tussocks and other intact plants are not included in collection. Prescribed burn BE3, Katberg, EC, South Africa, 8 November 2019.*

2.5.3 Skeleton damage:

Similar to char and scorch height, following principals similar to those proposed by Williams *et. al.*, (2003), the degree of damage (unburnt, scorched or charred) on bush skeletons in a fire scar, may be a useful indicator of fire intensity. In encroached montane grasslands and in macchia (fynbos) there is a smaller proportion of grassy component as supporting items for indicators to form. Bush and macchia indicators, such as cupping, become important for fire investigators in these scenarios. Extent and proportion of skeleton damage throughout a fire scar may offer insights into the intensity or severity of fire.

2.5.4 Total organic carbon content of ash:

As mentioned previously, wildfire ash is the unconsumed plant remains after the combustion process (Bodi *et. al.*, 2011; Smith & Hudak, 2005; Hudak *et. al.*, 2013; NWCG, 2016). Ash is largely comprised of organic carbon and inorganic elements. This composition is affected by fire conditions as well as amount, combustibility, and type of fuel (Bodi *et. al.*, 2014; Dlapa *et. al.*, 2015). Organic carbon in wildland fire ash is generally consumed as completeness of combustion increases (Bodi *et. al.*, 2014; Dlapa *et. al.*, 2015). The colour of ash is largely determined by the amount of organic carbon remaining after combustion. For this reason, ash colour has widely been used to gauge combustion efficiency (Lentile *et. al.*, 2006; Robichaud *et. al.*, 2007; Keeley, 2009; Bodi *et. al.*, 2011; Hudak *et. al.*, 2013). In numerous controlled grassfire burns in the Eastern Cape, South Africa, Trollope, (1983), noted that after back fires passage, ash residue was generally grey in colour, while after head fire passage, black ash (soot) was produced. Trollope, (1983), attributed this difference in residual ash colour to variance in carbon content of ash, and thus combustion completeness of grass fuel. However, subsequent research has found that ash colour was only weakly corelated with total organic carbon (TOC), indicating that other factors may play a role in ash colour determination (Bodi *et. al.*, 2011). The challenging nature of quantifying colour makes comparative statistical analyses of ash colour difficult. Measuring ash TOC content may, therefore, perhaps be a more accurate and precise method of determining completeness of combustion.

This has become a widely accepted relationship, especially in recent years, with a growing number of studies focussing on wildland fire ash (Bodi *et. al.*, 2011; Bodi *et. al.*, 2014; Dlapa *et. al.*, 2015). Nevertheless, there is still little known about the composition and properties of wildfire ash, as well as the relationship between ash TOC content, colour and severity (Bodi *et. al.*, 2011; Bodi *et. al.*, 2014; Dlapa *et. al.*, 2015).

Chemical indicators of wildland fire behaviour are typically not favoured by wildfire investigators, due to time constraints, availability of equipment and monetary costs. Instead, grassfire investigators use *post-hoc* physical indicators, as they are low cost, time and labour efficient (deductions can be made almost immediately, while in the field), and require no lab equipment and little analysis. However, the TOC content of ash may be a potential 'new', low cost, time efficient chemical indicator of fire severity. At the very least, wildland fire ash TOC content analyses may offer insights into the mechanisms surrounding fire severity, completeness of combustion and ash colour.

Similar to chemical indicators, satellite imagery tends to be more time and labour intensive, costs more, and often offer less detail on fire behaviour than physical indicators. Some satellites and databases, such as geostationary satellites, MODIS data and the Advanced Fire Information System (AFIS) database, are useful in identifying the presence or absence of fire, or actively burning wildfires. This can help with establishing a timeline of the fire and ultimately understand how the fire behaved. Though, satellite

imagery is rarely used to track the origin and cause of wildland fires, as they are usually limited by temporal and spatial resolution. While some satellites such as Landsat and Sentinal-2 can offer high resolution imagery, poor temporal resolution prevents them from being reliable data sources. However, in large enough fires, such as the Knysna fires of 2017, satellite imagery can be helpful in establishing an approximate region of fire origin, which can then be followed up with investigation on the ground.

Chapter 3:
STUDY SITES AND PRESCRIBED FIRES

3.1 Vegetation, topography & climate:

The study was conducted on seven controlled burn sites across the Eastern Cape province of South Africa, for the duration of three months, from early September to mid November 2019. For the purpose of this study, burn sites comprised mostly of mesic montane grassland and occasional savanna vegetation (sites 1, 2 & 6), with a focus on grass fires. Each burn site contained between 14 and 22 ten-by-ten-meter (100 m^2) experimental burn plots (143 in total). The seven prescribed burns took place on the following days of 2019: 11th & 17th September; 15th & 16th October; 4th, 8th & 12th November.

Burn sites are located along the Greater Winterberg Escarpment in the Eastern Cape, from the Boschberg near Somerset East, through the Winterberg peak, to the Katberg in the East. These burn sites are located on high rainfall grassland livestock farms, predominantly grazed by sheep (vegetation units – Amathole Montane Grassland & Amathole Mistbelt Grassland (Mucina *et. al.,* 2006); veld types – Dohne Sourveld & Highland Sourveld, possibly bordering on *Themeda* - *Festuca* Alpine Veld at very high altitudes of sites 3, 4 & 5, & Karroid *Merxmuellera* Mountain Veld on rocky, dry aspects (Acocks, 1975)).

Usually, paddocks are burnt every three to five years to promote fresh growth and control and remove unpalatable moribund herbaceous material and invasive and undesirable woody species. The use of fire as a management tool to achieve this, has been well documented (Trollope, 2011; Nieman *et. al*., 2021). This area has a high altitude (± 1500 m), sub-tropical to temperate climate, with a frost season of about six months, occasional winter snowfalls and predominant summer rainfall. Mean annual rainfall varies between 800 mm in the Boschberg, 900 mm near the Winterberg peak and 1000 mm in the Katberg mountain range.

The use of large agricultural rangeland paddocks (comprising natural vegetation) as experimental burn plots in this study was favoured over typical experimental burn plots usually found on nature reserves or research stations, as these rangeland paddocks are more representative of real-life conditions under which litigation relevant runaway veld fires occur (damage to agricultural property, loss of grazing, *etc*.). The burn plots (sites) used in this study are subject-specific examples (as opposed to reproductions) of typical rangeland paddocks which are encountered by litigation relevant runaway veld fires, and are therefore appropriate for this study.

3.1.1 Boschberg fires:

Sites 1 & 2 are located in the Boschberg mountain range (32.72300ºS; 25.75100ºE & 32.72400ºS; 25.73100ºE respectively). These paddocks have areas of 54.2 ha and 20 ha respectively. Elevation varies from 900–1300 m above sea level and paddock gradients are very steep (up to 150%). Dominant grass species (composition) include: *Themeda triandra; Cymbopogon* species; *Eragrostis* species (*racemosa, obtusa, plana*); *Sporobolis africanus;* & *Festuca* species. *Cliffortia paucistamina* is dominant on steep, Southern aspect slopes. Other notable woody plant species include: *Leucosidea sericea; Rubus* species; *Helichrysum* species; & *Vachellia karoo* on Northern aspect slopes and low-lying areas.

Biomass composition (available fuel) at the time of controlled burns, however, was dominated by *Cymbopogon* species, followed by *Cliffortia paucistamina* and *Leucosidea sericea.* This may be explained by several reasons, one of which is because the more palatable species, such as *Themeda triandra,* had been selectively grazed by livestock. This is at its worst, at the end/beginning of the burn cycle (3–5 years), as the less palatable species (*Cymbopogon* & *Festuca* species) have grown tall and wide (selectively under-grazed by livestock), gaining competitive advantage over, and limiting resource availability to, the more heavily grazed, palatable species (*Themeda triandra*).

3.1.2 Katberg fires:

Sites 3, 4, 5 & 6 are located in the Katberg mountain range (32.50600ºS; 26.57700ºE, 32.45200ºS; 26.64000ºE, 32.46100ºS; 26.64100ºE, & 32.41000ºS; 26.57400ºE respectively). These paddocks have areas of 91.8 ha, 62.3 ha, 57.7 ha and 24 ha respectively. Elevation varies from 1300–1800 m above sea level. Site 6 is at the lower extent of the elevation range, while sites 3, 4 & 5 are at the higher extent. Paddock gradients are very steep for sites 3, 4 & 6 (up to 125%), while site 5 has a considerably gentler gradient range. Dominant grass species include: *Themeda triandra; Festuca* species; *Elionurus muticus*; & *Eragrostis* species (*racemosa, obtusa, plana*). Site 6 however, has little *Festuca,* but does have *Sporobolis africanus,* which sites 3, 4 & 5 have little to none of. *Cliffortia paucistamina* was more prevalent in site 5 than in sites 1, 2, 3 & 4, and was widespread throughout the paddock. Site 6 had few, if any, *Cliffortia paucistamina.* Other notable woody plant species include: *Leucosidea sericea; Rubus* species; & *Helichrysum* species. Site 6 also has a scattering of *Vachellia karoo* throughout the paddock.

Biomass composition (available fuel) for sites 3, 4 & 5, at the time of prescribed burn, was dominated by moribund *Festuca* species, followed by *Cliffortia paucistamina, Elionurus muticus, Leucosidea sericea* and *Rubus* species. Reasons for this biomass composition are similar to those mentioned above for sites 1 & 2.

FIGURE 3.1: *Photographs showing upper (A) and lower (B) slopes of Site 1, Boschberg, Eastern Cape, dominated by Cymbopogon, Cliffortia paucistamina, & Leucosidea sericea. Vachellia karoo becomes more prevalent at lower altitudes (B). Note in photograph B, south facing slope (left) comprising a larger component of Cliffortia paucistamina, & Leucosidea sericea, and north facing slope (right) comprising a larger component of Cymbopogon and Vachellia karoo. Woody slope at top and centre of photograph B (west facing) is at lower altitude and was not part of prescribed burning operation.*

FIGURE 3.2: *Photograph showing Festuca dominated south facing slope of Site 4, Katberg, Eastern Cape. Photograph taken in a westerly direction.*

3.1.3 Winterberg fires:

Site 7 is located near the Wintergerg peak (32.37600°S; 26.30500°E). This paddock has an area of 26.6 ha. Elevation varies from 1700–1900 m above sea level, with very steep paddock gradients (up to 150%). Dominant grass species include: *Themeda triandra; Festuca* species; & *Elionurus muticus*, with few *Eragrostis* species (*racemosa; obtusa; plana*). Site 7 has few, if any, woody plant species. Biomass composition (available fuel) for site 7, at the time of prescribed burn, was dominated almost completely by moribund *Festuca* species, followed by *Elionurus muticus*.

FIGURE 3.3: *Photograph showing moribund Festuca atop Site 7, Winterberg, Eastern Cape.*

TABLE 3.1: *Summary of experimental set up, including various total, mean, and standard deviation (SD) values for environmental and fuel conditions for each burn site in the Greater Winterberg Escarpment, Eastern Cape, South Africa. Altitudinal and gradient data were extracted remotely from a global digital elevation model (ASTER, version 3). Annual Rainfall values were extracted from weather stations located on-site. Methods of fuel condition sampling are discussed in detail in* ***Section 4.3.1, Chapter 4****.*

Site	Altitude (m)	Mean Gradient ± SD (%)	Annual Rainfall (mm)	Area (ha)	No. of Exp. Plots	Mean Fuel Load ± SD (t/ha)	Curing ± SD (%)
1	1100	29.7 ± 9.5	800	54.2	22	7.228 ± 1.551	61 ± 9.5
2	1100	32.2 ± 12.6	800	20	21	4.055 ± 1.091	65 ± 10.1
3	1600	37.3 ± 10.7	1000	91.8	22	5.935 ± 1.297	80 ± 6.3
4	1600	23.5 ± 13.4	1000	62.3	22	5.269 ± 0.938	77 ± 6.6
5	1700	19.3 ± 5.8	1000	57.7	20	6.035 ± 1.274	71 ± 13.6
6	1400	42.2 ± 10.5	800	24	14	5.332 ± 1.091	77 ± 10.8
7	1800	45.7 ± 16.3	900	26.6	22	8.601 ± 0.967	77 ± 13.7
Total	–	–	–	336.6	143	–	–
Mean	1471.4	32.3	900	48.1	20.4	6.065	72.6

3.2 Weather conditions & fire behaviour:

3.2.1 Boschberg fires:

Fire 1

The approximate mean weather conditions prevailing for the duration of each prescribed burn are summarised below in **TABLE 3.2**. Weather conditions prevailing during the 1st prescribed burn (MW1, Boschberg) on 11 September 2019 began mild, gradually becoming more conducive to the ignition and spread of grass fires by late morning. In terms of the formal Fire Danger Rating System (Lowveld) for the Republic of South Africa (Government Gazette Notice 1099 of 2013), weather conditions recorded for the duration of the 1st prescribed fire (MW1, Boschberg) translate to Fire Danger Indices (FDIs) ranging between 33 and 44, in the upper "GREEN" zone.

Lowveld FDI scores between 21 and 45 fall within the "GREEN" zone and are termed "Low Ratings" (Government Gazette Notice 1099 of 2013). In this zone, fire danger is considered "Moderate" (Government Gazette Notice 1099 of 2013). In terms of fire behaviour, the Government Gazette Notice (1099 of 2013) states that "Fires likely to ignite readily but spread slowly." & "Flame lengths in grassland and plantation forest litter lower than 1.0 m and rates of forward spread between 0.3 and 1.5 kilometres per hour."

It is noted that in this context, the term "Lowveld" (Government Gazette Notice 1099 of 2013) refers to the name of the fire danger rating system, and should not be confused with a term of the same name used to distinguish general climatic/regional vegetation types (savanna) at low altitudes.

TABLE 3.2: *Summary of approximate mean weather conditions and Lowveld Fire Danger Index (FDI) scores with standard deviations (SD), for duration of prescribed burns at each site in the Greater Winterberg Escarpment, Eastern Cape, South Africa. Methods of weather condition sampling are discussed in detail in* ***Section 4.3.1, Chapter 4.*** *Lowveld FDI scores were calculated according to the methods stipulated in Government Gazette Notice 1099 of 2013 for the Republic of South Africa.*

Site	Date	Air Temperature ± SD (ºC)	Wind Speed (km/h)	Relative Humidity ± SD (%)	Lowveld FDI Score ± SD
1	11 Sept 2019	24 ± 0.78	4–14	60 ± 0.47	39 ± 2.7
2	17 Sept 2019	23 ± 0.71	7–14	57 ± 0.23	46 ± 3.5
3	15 Oct 2019	17 ± 1.34	2–15	55 ± 0.41	37 ± 2.7
4	16 Oct 2019	26 ± 1.2	5–14	55 ± 0.3	44 ± 3.4
5	4 Nov 2019	19 ± 0.39	8–16	49 ± 0.21	42 ± 1.1
6	8 Nov 2019	18 ± 0.54	7–21	49 ± 0.54	40 ± 2.5
7	12 Nov 2019	24 ± 0.89	13–42	51 ± 0.25	54 ± 7.2

FIGURE 3.4: *Head fire spreading upslope and with the wind in a Cymbopogon dominated fuel stand, in the lower slopes of Site 1, Boschberg, Eastern Cape, South Africa. Prescribed burn MW1, 11 September 2019.*

FIGURE 3.5: *Fire spread in medium to upper slopes of Site 1, Boschberg. Wind direction left to right. Head fire spreading left to right, having been inserted along contour road. Back fire spreading right to left, having been inserted along fence-line firebreak (right of image). Prescribed burn MW1, 11 September 2019, Boschberg, Eastern Cape, South Africa.*

Fire 2

Prevailing weather conditions for the duration of the 2nd prescribed burn (MW2, Boschberg) on 17 September 2019 were somewhat more conducive to the ignition and spread of grass fires than those experienced during the 1st prescribed fire (MW1, Boschberg). The Lowveld Fire Danger Rating System score (or FDI) ranged between 37 (upper "GREEN" zone) and 49 (lower "YELLOW" zone) (Government Gazette Notice 1099 of 2013).

Lowveld FDI scores between 46 and 60 fall within the "YELLOW" zone and are termed "Medium Ratings" (Government Gazette Notice 1099 of 2013). In this zone, fire danger is considered "Dangerous" (Government Gazette Notice 1099 of 2013). In terms of fire behaviour, the Government Gazette Notice (1099 of 2013) states that "Fires ignited readily and spread rapidly, burning in the surface layers below trees." & "Flame lengths in grasslands and plantation forests between 1 and 2m, and rates 0.3 and 1.5 kilometres per hour."

The large size (up to ±100 ha in some cases) and rugged topography of the fire sites meant that in some cases, a degree of deviation existed between prevailing weather conditions recorded at the portable weather station and localised weather conditions experienced through each 10 x 10 m plot. An example of where localised conditions differed from prevailing conditions was the channelling effect in valley winds, influencing wind speed and direction. During the day, valley winds almost always blow upslope (anabatic) and at greater speeds than prevailing conditions (Cheney & Sullivan, 2008). Valley winds had a strong influence on conditions at the 2nd prescribed fire site (MW2, Boschberg).

3.2.2 Katberg fires:

Fire 3

Weather conditions prevailing during the 3rd prescribed burn (DE1, Katberg) on 15 October 2019 were mild, yet still conducive to the ignition and spread of grass fires. The Lowveld FDI score ranged between 30 and 40 (mid to upper "GREEN" zone) (Government Gazette Notice 1099 of 2013).

Fire 4

Prevailing weather conditions for the duration of the 4th prescribed burn (BE1, Katberg) on 16 October 2019 were somewhat more conducive to the ignition and spread of grass fires than those experienced during the 3rd prescribed burn (DE1, Katberg). The Lowveld FDI score ranged between 39 (upper "GREEN" zone) and 48 (lower "YELLOW" zone) (Government Gazette Notice 1099 of 2013).

Fire 5

Weather conditions prevailing during the 5th prescribed burn (BE2, Katberg) on 4 November 2019 were mild. Weather conditions recorded for the duration of the prescribed fire translate to FDI scores ranging between 41 and 47 (on the boundary between "GREEN" and "YELLOW" zones) (Government Gazette Notice 1099 of 2013). It is noted, however, that the author's observations of actual conditions prevailing during the prescribed burn on 4 November 2019 were less conducive to the ignition and spread of grass fires than the calculated Lowveld FDI scores imply. The fire burnt as a low intensity fire, with short flame lengths, and was often patchy and incomplete. The mild burning conditions may be accounted for by fuel conditions and cautious burning techniques. The 5th site is at higher elevation relative to neighbouring sites and is located along the precipice of the Katberg escarpment, with a higher density of woody shrubs than the other six sites. Fuel moisture content in the woody component of the fuel may have perhaps been higher than the other six sites, which under the above circumstances, may have had a dampening effect on the grass fire. The presence of commercial forestry plantations (*Pinus sp.*) beyond the precipice of the paddock poses an inherent fire risk, as firebrands could easily be lifted and deposited downslope to kindle a new fire (spotting), without the need for strong winds or convective updrafts. The fire officer in charge on 4 November 2019 therefore exercised more than the usual level of caution in order to mitigate the potential risk. This increased level of exercised caution inevitably resulted in milder fire conditions (fires were at low intensity and not allowed to develop large flames).

Fire 6

In contrast, observed weather conditions prevailing during the 6th prescribed burn (BE3, Katberg) on 8 November 2019 appeared to be more conducive to the ignition and spread of grass fires than those recorded by the weather station for the duration of the prescribed burn. Recorded weather conditions translate to Lowveld FDI scores ranging between 35 and 42 (mid to upper "GREEN" zone) (Government Gazette Notice 1099 of 2013). Despite the "low" FDI rating, channelled valley winds in combination with steep slopes created conditions very conducive to the ignition and spread of fire, facilitating high intensity fires with long flame lengths (up to 10 m in some cases). The 6th prescribed fire was the only burn to take place in the afternoon (the other six took place in the morning).

3.2.3 Winterberg fires:

Fire 7

Prevailing weather conditions for the duration of the 7th prescribed burn (CB1, Winterberg) on 12 November 2019 were very conducive to the ignition and spread of vegetation fires, and the most severe of the seven experimental fires. In terms of the formal Fire Danger Rating System (Lowveld) for the Republic of South Africa (Government Gazette Notice 1099 of 2013), weather conditions recorded for

the duration of the 7th prescribed fire (CB1, Winterberg) translate to FDI scores ranging between 47 (lower "YELLOW") and 72 (upper "ORANGE") (Government Gazette Notice 1099 of 2013).

Lowveld FDI scores between 61 and 75 fall within the "ORANGE" zone and are termed "High Ratings" (Government Gazette Notice 1099 of 2013). In this zone, fire danger is considered "Very Dangerous" (Government Gazette Notice 1099 of 2013). In terms of fire behaviour, the Government Gazette Notice (1099 of 2013) states that "Fires ignited readily and spread very rapidly, with local crowning and short-range spotting." & "Flame lengths between 2 and 5m, and rates of forward spread between 1.5 and 2.0 kilometres per hour."

The high FDI rating observed in the seventh prescribed burn (CB1, Winterberg) can be attributed to high wind speeds, and not unusually high temperatures or low humidity.

From visual assessment of degree of curing at site 7 on the day of the prescribed burn (CB1, Winterberg, 12 November 2019) it appeared as though percent curing may have decreased since fuel sampling several days earlier (it is not uncommon for grasses in this region to 'green-up' rapidly during spring). This, however, cannot be corroborated. Decreased curing percent would result in lower rates of spread and intensities.

FIGURE 3.6: *Example of line ignition of controlled fuel management burn at Festuca dominated Site 7, Winterberg. Wind direction bottom right to top left. Fire ignited using drip torch (right of image), and back fire immediately extinguished using bowser (right of image). Personnel equipped with swatters follow up with 'mop-up' operations to ensure reignition does not occur along ignition line (out of picture). Prescribed burn CB1, 12 November 2019, Winterberg, Eastern Cape, South Africa.*

A phenomenon known as the lee-slope eddy effect (**FIGURE 3.7**) was prevalent at site 7 on 12 November 2019. This phenomenon resulted in notable localised deviation from prevailing weather conditions. A lee-slope eddy occurs when, under recurved airflow conditions, the prevailing wind separates and lifts away from a slope, creating eddies on the leeward side of a hill, which blow back upslope, in the opposite direction to the prevailing wind (**FIGURE 3.7**).

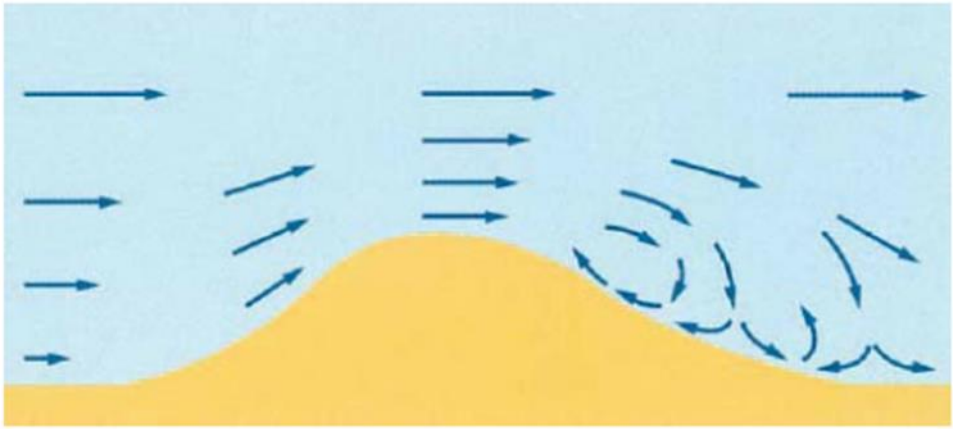

FIGURE 3.7: *Schematic diagram illustrating the lee-slope eddy effect. Separation of wind flowing over a hill creating eddies which flow back up-slope. Reprinted from "Grassfires: fuel, weather and fire behaviour (2nd ed.)", by Cheney, P., & Sullivan, A., 2008, pp. 76, Australia: CSIRO Publishing. Copyright 2008 by CSIRO.*

The Lowveld FDI rating system in Government Gazette Notice 1099 of 2013 to a large degree under-predicted flame length for all seven sites. Recorded head fire flame lengths ranged between 0.5 and 3 m during the 1st prescribed fire (upper "GREEN" zone); 2–7 m during the 2nd prescribed fire (lower "YELLOW" zone); 1.75–3 m during the 3rd prescribed fire (mid to upper "GREEN" zone); 1.5–3 m during the 4th prescribed fire (upper "GREEN" to lower "YELLOW"); 1 m during the 5th prescribed burn (on the boundary between "GREEN" and "YELLOW" zones); 2–10 m during the 6th prescribed burn (mid to upper "GREEN" zone); and 2–8 m during the 7th prescribed burn ("YELLOW" and "ORANGE" zones).

Recorded head fire flame lengths did not only exceed Government Gazette Notice 1099 of 2013 predicted values, but also appeared to not be correlated with Lowveld FDI scores (see **Chapter 4**). This is to be expected, because intensity, and thus flame length, is not solely determined by weather conditions, but in fact, is determined to greater degree by fuel conditions (fuel load, fuel moisture, heat yield). Lowveld FDI calculations do not take fuel conditions into account, other than indirectly, in that humidity and temperature affect fuel moisture content. Large moribund fuel loads (3–5 years accumulation) in combination with steep slopes are likely responsible for large flame lengths (high

intensity) observed at several sites. Despite occasional very large flame lengths, conditions remained under control and were not considered dangerous.

Combustion temperatures were recorded at various points throughout each of the seven prescribed burn sites using a handheld infrared thermometer. There was little variation in combustion temperatures between sites. Flame temperatures were around 300–400ºC, with smouldering temperatures ranging between 125–200ºC.

As previously stated, the primary purpose of this study is to investigate the reliability and accuracy of fire models and *post-hoc* indicators to diagnose fire behaviour. From perusal of the above fuel and weather data, it can be seen that the independent variables (fuel & weather conditions) recorded during prescribed burns in this study fall within a restricted range. This is logical, because while pastoralists desire reasonably intense fires to assist with removal of woody species (if removal of woody species is the objective), the overriding consideration is that fire conditions are considered safe. So, it is very unusual for extreme weather conditions to be experienced during prescribed burns. Having said that, conditions that would result in very cool fires or incomplete burns would also usually be avoided, as the prescribed burn would not achieve its purpose. Even if the purpose is just to remove grass only, cool fires tend to be patchy and result in incomplete burns.

An incidental advantage in terms of this study (investigating the reliability and accuracy of *post-hoc* indicators to diagnose fire behaviour (**Chapter 5**)), is that the restricted range of conditions provided a low indicator variance. *Post-hoc* wildland fire pattern indicators occur through a wide range of fire conditions, but are usually applicable in 'runaway' scenarios. Those indicators that occur during intense fires are likely to be more pronounced than those measured in this study (**Chapter 5**).

The significance of the above is, that provided with this dataset, one needs to exercise caution when making deductions about the proportion of variation in fire behaviour (intensity, ROS) accounted for by each independent variable (fuel and weather conditions), s a full range of independent variable measures has not been recorded.

Chapter 4:
HOW DO VARIOUS FIRE BEHAVIOUR PREDICTION MODELS COMPARE WITH RECORDED GRASSFIRE CONDITIONS?

4.1 Chapter Summary:

Wildland fire managers and practitioners in southern Africa use fire as a management tool in grassland and savanna systems to achieve a range of management goals for ecological, agricultural, and safety purposes. However, the occurrence of uncontrolled wildland fires and subsequent damage to property, is inevitable. Acknowledging that there is always risk that prescribed burns can get out of control, an important safety consideration for wildland fire managers and pastoralists is whether to conduct prescribed burns under the prevailing weather and fuel conditions. When making decisions in this regard, one of the tools available to fire practitioners, are mechanistic fire behaviour prediction models. Given their increasing credibility and value in predicting and forecasting fire behaviour, mathematical fire models can also be useful aids in the reconstruction of fire conditions of past fire events, in forensic wildfire investigations, conducted in contemplation of litigation. Given the risks involved in conducting prescribed burns, it is important that these models be considered accurate and reliable for local conditions. Equally, given the weight forensic reports can hold in legal matters, it is critical that the evidence used in these reports (simulated fire behaviour) be considered credible and accurate. While there have been several studies which have constructed and tested site appropriate fuel models in South Africa, few, if any, have shown accurate application (simulation) over a range of conditions. Fewer have compared various models or model configurations against each other, or over a range of input (fuel model) assumptions. This chapter aimed to test the accuracy of model outputs (rate of spread, fire intensity, & flame length) under a range of model configurations, from five widely used practical fire behaviour prediction base models, in mesic montane grasslands of the Eastern Cape, South Africa. Base models were arranged into a total of 20 configurations based on several existing fuel models, various input assumptions, and the inclusion or exclusion of supplementary slope correction functions. Simulated fire behaviour values were generated *post-hoc*, from fuel, weather, and topographical conditions prevailing at the time of combustion and compared with real-time actual fire behaviour data, collected from 143 fires. Slope proved to be a critical driver of fire behaviour in the mountainous Eastern Cape grasslands. Fire behaviour models (encompassing a wide range of fuel model configurations constructed for southern African grassland systems), did not suitably predict (or retrodict) actual fire conditions, generally under-predicting rate of spread, fire intensity, & flame length values. McArthur models, derived from field-based data, proved to be the most suitable predictors of fire behaviour in Eastern Cape montane grasslands. It is recommended that current fuel model and input assumptions which exist for southern African grassland and savanna systems be re-evaluated.

4.2 Introduction:

Wildland fires are an ever-present feature in African vegetation systems. African grasslands and savannas, in particular, have the highest representation of cool, frequent fires, globally (Archibald *et. al.*, 2013). In many of the grassland and savanna systems of southern Africa, fire managers and pastoralists aim to emulate and control the natural effects of fire which maintain these systems, by implementing controlled fire regimes (Teie, 2003; Trollope, 2011; Nieman *et. al*., 2021). There is a long history of wildfire management in southern Africa, with evidence that South African pastoralists have been implementing prescribed burning (as a management tool), at least as early as the 15th century (Alberti, 1968; Wilson, 1969; Bradlow & Bradlow, 1979; Forbes, 1986; Trollope, 2011), while human influence on fire regimes in an African context likely extends back thousands of years (Archibald *et. al.*, 2012).

However, the threat posed by wildfires is becoming increasingly relevant with the rapidly expanding wildland-urban interface and changing climate (Trollope *et. al.*, 2004; Bowman *et. al*., 2009; Flannigan *et. al*., 2009; Moritz *et. al*., 2012; Jolly *et. al.*, 2015; Doerr & Santin, 2016).

Perhaps the most common recurring challenges faced by fire managers and practitioners is the age-old safety consideration of whether or not to conduct prescribed burns under the prevailing weather and fuel conditions (Van Wilgen & Wills, 1988; Trollope *et. al.*, 2004). These decisions are made easier when equipped with accurate and reliable data (Van Wilgen & Wills, 1988; Trollope *et. al.*, 2004).

For many years, wildland fire practitioners have used fire danger rating systems and fire behaviour prediction models as aids when making important safety decisions or contemplating management strategies (Van Wilgen & Wills, 1988; Anderson *et. al.*, 2011; Andrews, 2018). Rapid technological advancements and the emergence of open-access software have increased the range, scope, availability, and promptness of fire behaviour mapping and forecasting. However, despite these tremendous recent modelling advances, basic empirical fire research into the mechanics and processes of fire behaviour and spread has largely been neglected (Finney *et. al.*, 2013).

Given their increasing credibility and value in predicting and forecasting fire behaviour, mathematical models should also be useful tools for the retrodiction of fire conditions, and aid in the reconstruction of fire behaviour. Provided with fuel and weather boundary conditions for any past fire event, it should be possible to reconstruct the behaviour and passage of past wildfires. This technique has been applied as a useful aid in forensic investigations of runaway fires, conducted in contemplation for litigation. However, for this to be considered reliable evidence in the court of law, fire behaviour prediction models' output values need to accurately retrodict actual fire conditions. A clear idea of which variables are critical for credible retrodiction (simulation) is also needed.

Current application of fire models in private sector forensic wildfire investigations entails the determination of fire rate of spread (ROS) and intensity from simulated values, to gain an understanding of how a fire might have behaved and spread. Investigators use simulated ROS in combination with ground-truthing from direct evidence, to determine the passage or path of fires (Danckwerts J.E. (PhD), personal communication, 2019). This technique allows wildfire investigators to build a timeline of events and can contribute towards explaining where and when a fire originates, and how it spreads.

Fireline intensity values (either simulated or calculated from known values) are used to determine whether a fire could cross barriers (firebreaks), as well as to aid in judgement of the level of difficulty involved to suppress or extinguish fires. These are important considerations for legal teams when building cases in contemplation of litigation. Luke & McArthur, (1978), found that at intensities in excess of 4000 kJ/s/m, it is difficult to bring wildfires under control. This is widely considered to be an accurate guideline and is corroborated by anecdotal observations from wildfire practitioners.

Spotting and convection fires are examples of two mechanisms by which grassfires cross firebreaks. They both require sufficient fire intensities to occur. The process of spotting involves the upliftment of firebrands from convective heat currents, which are then carried by the prevailing wind, and deposited ahead of the fire front to kindle a new fire (Trollope, 1984; Teie, 2003; Van Wagtendonk, 2006; Cochrane & Ryan, 2009; Scott *et. al*., 2014). Although usually attributed to woodland and macchia systems, Luke & McArthur, (1978), note that spotting is common in grassfires. However, spotting distances in grass fires are considerably shorter, commonly up to 100m ahead of the flame front (Luke & McArthur, 1978). A likely explanation as to why spotting is generally not associated with grassfires, is that due to the relatively short distances of firebrand deposition, newly kindled fires ahead of the fire front are usually enveloped by the main fire, leaving little to no evidence of spotting. Spotting is exacerbated at higher intensities when convective updrafts are stronger. According to Trollope, (1989), grassfires above 3000 kJ/s/m are considered extremely hot fires.

At very high intensities (above 10 000 kJ/s/m), grassfires can also cross firebreaks around 10 m wide by means of long convection flames or pockets of flame flashes ahead of the fire (Wilson, 1988; Cheney & Sullivan, 2008).

The relevance of the above in terms of fire modelling (*post-hoc* or otherwise), is that accurate determination and/or simulation of ROS and fireline intensity is critical for wildland fire investigators in their endeavours to determine fire suppression difficulty and efficacy of firebreaks.

Similarly, before wildland fire practitioners can make model-based management decisions, predictions need to be suitable for local conditions (Van Wilgen & Wills, 1988; Trollope *et. al*., 2004).

Therefore, before implementation, models need to be considered accurate for subject site, and based on site-appropriate fuel properties of dominant vegetation (Van Wilgen & Wills, 1988; Trollope *et. al*.,

2004). To achieve this, site-specific empirical research is required to investigate which models and fuel properties (assumptions) work best in specific environments or systems.

Predictive mechanistic models also need to be based on fundamental fire behaviour theory (Finney *et. al.,* 2013). Many models are based on a variety of assumptions, making it difficult to accurately represent real fire conditions (Finney *et. al.,* 2013). It has further been noted that there seems to be a lack of common understanding of what processes occur, and how they occur (Finney *et. al.,* 2013). This is exacerbated in Africa, where various authors have identified a serious lack of quantitative data on factors influencing fire behaviour in African conditions, compared to Australia and the USA (Trollope *et. al*., 2004).

To prove the credibility of wildland fire behaviour prediction models under various conditions, researchers have published studies which show how well model outputs fit with actual fire conditions (Sneeuwjagt & Frandsen, 1977; Van Wilgen *et. al.*, 1985; Everson *et. al*., 1988; Van Wilgen & Wills, 1988; Cruz *et. al*., 2020). Several of these model fit studies have been conducted in South African savanna and grassland systems (Everson *et. al*., 1988; Van Wilgen & Wills, 1988), but none in mesic montane grasslands of the Eastern Cape. However, Cruz *et. al.,* (2020), suggests that given the degrees of freedom that exist in mathematical fire behaviour models, it is not difficult to achieve a model fit to experimental fire conditions. Cruz *et. al.,* (2020), goes on to say that given the uncertainties involved in fire modelling (*e.g.*, fire behaviour processes, critical drivers, sampling error, & input assumptions) (Trollope *et. al*., 2004; Finney *et. al.,* 2013), they recommend that researchers should attempt to show how models fail to accurately predict or retrodict observed behaviour, rather than continual validation of models with observed conditions (by adjusting input variables or assumptions). Identifying the shortfalls and the failures in predictive fire behaviour modelling will likely be a more powerful driver of model improvement and development (Cruz *et. al.,* 2020), ultimately contributing towards improved model performance over a broad range of conditions.

Few studies have shown accurate application (simulation) of fire behaviour prediction models over a range of fuel, weather, and topographical conditions. Fewer still, have made comparisons between several models or model configurations, covering a range of fuel model and input assumptions, within a single fuel system (Weise & Biging, 1997). There has also been a paucity of wildfire modelling work in the Eastern Cape montane grasslands.

The purpose of this chapter is to identify suitable fire models, as well as appropriate fuel model and input assumptions, for accurate simulation and credible retrodiction of fire conditions in mesic montane grasslands surrounding the Greater Winterberg area of the Eastern Cape, South Africa. In doing so, contributing towards a greater understanding of which fire models, fuel models, and input assumptions are relevant in southern African grassland and savanna systems. This chapter also investigated the potential of char height as a practical *post-hoc* indicator of flame length.

I aimed to achieve the above by simulating rate of spread, fireline intensity, and flame length from five widely used, practical fire models, arranged into a total of 20 configurations, using fuel, weather, and topographical data collected from 143 controlled burns, across seven sites, in montane grasslands of the Boschberg, Katberg, & Winterberg mountain ranges. These data were then used to evaluate and assess the accuracy, and suitability of various fire models, input assumptions, and fuel model configurations to predict and retrodict actual wildfire conditions in this grassland ecosystem. These results were then used to verify which particular fire behaviour parameters are critical for accurate simulation of fire behaviour in southern African grassland and savanna systems. The relevant base models are: BehavePlus V6.0.0 (Andrews & Bevins, 2018); Rothermel R package (Rothermel, 1972; Vacchiano & Ascoli, 2015); McArthur's grassland fire spread models Mk3 & Mk5 (McArthur, 1966; McArthur, 1967; McArthur, 1977; Noble *et. al*., 1980); & CSIRO modified McArthur Mk4 grassland fire spread calculator (CSIRO, 1999).

I hypothesised that the input parameters critical for accurate simulation of fire behaviour (primary drivers of fire behaviour) in Eastern Cape montane grasslands, would not differ significantly from those in other similar grassland and savanna systems in southern Africa.

It was hypothesised further, that models either developed specifically for grassland conditions, using data collected from numerous field trials, or developed for wildland fires in general, from artificially reconstructed fuel conditions, would differ significantly in their ability to project and thus to retrodict actual wildfire behaviour (recorded fire conditions).

4.3 Methods:

Pre-fire data, active fire conditions, and post-fire data were collected from a total of 143 ten-by-ten-meter (100 m^2) experimental burn plots across seven montane grassland sites in the Eastern Cape (see **Chapter 3**).

4.3.1 Fuel, weather, & topography:

Fuel load

Fuel load measurements were sampled within a week prior to commencement of prescribed burns (September, October, November 2019). Fuel load was estimated using a disc pasture meter (DPM), developed by Bransby & Tainton, (1977) (**FIGURE 4.4**). A DPM is one of the most widely used, practical and efficient methods for estimating fuel loads in grass dominated ecosystems (Trollope, 1983; Trollope & Potgieter, 1986; Harmse *et. al.*, 2019). Its appeal lies in the rapid and non-destructive nature of sampling (Trollope, 1983; Trollope & Potgieter, 1986; Harmse *et. al.,* 2019). In their description of the DPM, Bransby & Tainton, (1977), initially suggested that it could be a useful tool in pasture research (Danckwerts & Trollope, 1980). The DPM has subsequently been used on various natural veld types and found to be a reliable technique for fuel load estimation in grassland and savanna ecosystems (Danckwerts & Trollope, 1980; Trollope & Potgieter, 1986; Harmse *et. al.,* 2019).

A number of calibrations for general use of the DPM have been developed for various regions of Southern Africa (Trollope, 1983; Trollope & Potgieter, 1986; Dörgeloh, 2002; Zambatis *et. al.*, 2006; Harmse *et. al.,* 2019). Nonetheless, subsequent research has found that the Kruger National Park calibration developed by Trollope & Potgieter, (1986), does not differ significantly from calibrations developed in Eastern Cape Province (Trollope, 1983); Caprivi Region, Namibia; Ngorongoro Crater, Tanzania; central highlands of Kenya; and tall grass prairies in Kansas, USA (Trollope & Trollope, 2016). This study has therefore used the Kruger National Park calibration developed by Trollope & Potgieter, (1986), as recommended by Trollope & Trollope, (2016), for general use for DPM calculations when estimating grass fuel loads in African grasslands and savannas.

Disc pasture meter (DPM) general calibration for African grasslands & savannas:

$$\mathbf{y = -3019 + 2260*\sqrt{x}}$$

Where: y = mean fuel load (kg/ha)

x = mean disc height (cm)

(Trollope & Potgieter, 1986)

Estimations of fuel load were made by sampling 30 random DPM readings throughout the area of each 100 m^2 burn plot (n = 30 x 143). Each DPM reading returns a value for disc height (cm). The mean disc height (cm) for each plot was then calculated and used in the above regression to produce a value for mean fuel load (kg/ha).

Curing

Curing state measurements were sampled within a week prior to commencement of prescribed burns. The curing state of burn sites was expressed as percent curing which represents the fraction of dead material within the sward (Cheney & Sullivan, 2008). The conventional method of percent curing determination in South Africa is by visual observation. While this method of assessment is quick and easy, it is also subjective and often inaccurate, requiring experience and expert judgement (Millie & Adams, 1999; Anderson & Pearce, 2003; Anderson *et. al*., 2011). Destructive sampling and sorting of dead (cured) and live material provides a more accurate measure of curing state (Anderson *et. al*., 2011). As grass curing is influenced by seasonal growth cycle, the curing state of grassland swards is fairly constant throughout regional areas. For this reason, and due to the time constraints associated with destructive sampling process (Anderson *et. al*., 2011), percent curing was estimated for the entire burn site, rather than for each 10 x 10 m plot.

To estimate percent curing, 20 random samples of herbaceous plant material were randomly harvested throughout each of the seven burn sites (paddocks). For each destructive sample, all above aboveground plant material was harvested from within a 0.01m^2 frame (Anderson *et. al*., 2011). Following harvest, living and cured (dead) herbaceous plant material in each sample were separated by hand in the laboratory (Anderson *et. al*., 2011; Kidnie *et. al*., 2015). Samples were then sun dried for a minimum of 24 hours, before undergoing oven drying at 80 degrees Celsius for 10 hours. Following oven drying, corresponding living and cured samples were weighed, using a balance, accurate to 0.001 grams (Radwag scale). Sample curing percent was calculated as the fraction of oven-dried cured mass over oven-dried total mass (cured + living), expressed as a percentage (Anderson *et. al*., 2011):

$$\%\ \mathbf{Curing} = \frac{\mathbf{Oven\ dried\ cured\ mass}}{(\mathbf{Oven\ dried\ cured\ mass} + \mathbf{Oven\ dried\ living\ mass})} * \mathbf{100}$$

The curing percent of all 20 destructive samples were then averaged to calculate percent curing for the entire burn site.

Fuel moisture

Fuel moisture content measurements were sampled within a week prior to commencement of prescribed burns. For similar reasons to percent curing, fuel moisture content was estimated for entire burn sites (seven), rather than for each 10 x 10 m plot (143). The same 20 stratified, random samples of herbaceous plant material used for curing state calculations were used to estimate fuel moisture content. Immediately after harvesting, samples were placed into plastic zip-lock bags, sealed, and marked. These marked samples were placed into black bags, which were subsequently placed into a cooler box, in order to minimize moisture loss after harvest. After living and cured (dead) herbaceous plant material was separated, corresponding samples were weighed to record pre-oven-dried fuel moisture content of samples (Cruz *et. al*., 2015; Kidnie *et. al*., 2015). These weights were then used in correspondence with the oven-dried weights (recorded for percent curing) to calculate live and dead (cured) fuel moisture contents (Cruz *et. al*., 2015; Kidnie *et. al*., 2015). Fuel moisture values were averaged for each entire burn site.

Weather data

For the full duration of all prescribed burns, weather data was recorded at one-minute intervals. Wind speed and direction, ambient air temperature, and relative humidity were recorded on location, near the fire site, using a portable weather station (Campbell Scientific; R.M. Young Company) (**FIGURE 4.1**). Portable weather station placement locations were chosen for suitability and capacity to represent prevailing weather conditions for the entire fire site, usually located near the highest point of the paddock. Careful consideration was made to ensure that no obstacles, objects or landmarks such as buildings, vehicles, woody thickets, or rocky outcrops were in the vicinity of the portable weather station, such that they interfere with wind readings. In cases where localised conditions within the fire site differed from prevailing conditions throughout the fire site (such as lee-slope eddies and valley winds), observed wind direction through said locality (10 x 10 m plot) was noted and recorded.

Topography

The presence of hills and slopes were noted, along with their respective **gradients** and **aspects**. Coordinates were recorded at centre of each 10 x 10 m plot, using a handheld GPS (Garmin). Slope gradient and aspect of each burn plot was measured remotely in QGIS (QGIS Development Team, 2020), using a global digital elevation model (ASTER, version 3), extracted, and verified with observed on-site estimations. The method of gradient determination can be described as taking elevation change between the neighbouring cells directly above and below the relevant cell, divided by the horizontal width or length of the relevant cell, multiplied by 100 to attain a percentage gradient.

FIGURE 4.1: *Photograph showing portable weather station (Campbell Scientific; R.M. Young Company) used to record wind speed & direction, ambient air temperature, and relative humidity.*

4.3.2 Observed fire conditions:

Real-time fire behaviour conditions were observed and recorded for each 10 x 10 m experimental fire. The prescribed burns used in this study follow burn protocols and safety precautions, which require that back burns be inserted first, along the leeward edges of the paddock and gradually along the lateral edges, in order to widen the fire breaks (Trollope, 1989) (**FIGURE 4.2)**. Only once the safety officer is content that the fire breaks have been widened sufficiently and that conditions are not dangerous, is a head fire inserted on the windward side of the paddock to burn the remaining vegetation (Trollope, 1989) (**FIGURE 4.3**). This results in multiple points of fire origin and an assortment of fire conditions throughout the entire burn area (site). It was therefore important to record **direction of fire passage**, **type of fire spread** (head, back & flank), and the **time at which combustion occurred** through each 100 m^2 experimental plot (n = 143), across the seven paddocks/sites. The exact time of day (accurate to a minute) at which combustion took place through each 10 x 10 m burn plot was recorded and matched up with weather data for that corresponding time period. This yielded specific weather conditions for each 100 m^2 plot. Locations of ignition points and lines (fire origin) were also recorded, as well as locations and extent of area experienced by each fire spread type (head, back, or flank).

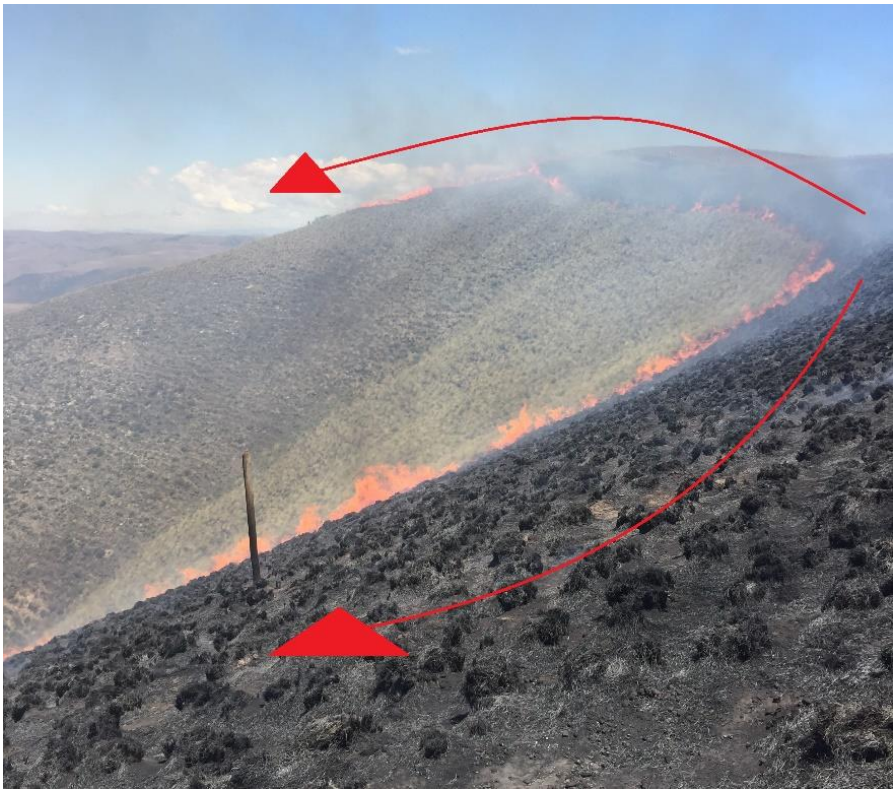

FIGURE 4.2: *Annotated photograph showing gradual back fire ignition along leeward and lateral edges of paddock. Wind direction left to right. Precribed burn CB1, Winterberg, EC, South Africa, 12 November 2019.*

FIGURE 4.3: *Photograph showing head fire burning up-slope (centre), after being inserted on windward side (left), and following back burning of leeward and lateral edges of paddock. Wind direction left to right. Prescribed burn CB1, Winterberg, EC, South Africa, 12 November 2019.*

Fire intensity

Measurements of fire intensity were made for each 10 x 10 m plot (n = 143), across all seven burn sites. Measuring wildfire intensity can be a tedious and time-consuming process and empirical evaluations of intensity are not often conducted as result (Van Wilgen, 1986; Schwilk, 2003; Scott *et. al*., 2014). **Three** different methods were used in this study to estimate, record, and calculate real-time fireline intensity: **Steam-releasing open-can calorimetry (Hydropyrometer)** (Webber & Trollope, 1997); **flame length** (Van Wilgen, 1986); and **Byram's (1959) equation for Fireline intensity**.

1.) **Steam-releasing open-can calorimetry** as a measure of fire intensity is based on the principles of latent heat of vaporisation. One can measure the amount of heat energy released at a point in the fire, by determining the amount of water lost by vaporisation (Webber & Trollope, 1997; Schwilk, 2003). A number of studies have shown that there is a highly correlated relationship between the amount of water loss from vaporisation and fire intensity (Viegas *et. al.*, 1994; Webber & Trollope, 1997; Perez & Moreno, 1998).

    Several differing methods of steam-releasing open-can calorimetry have been applied globally across a handful of studies, with varying success (Viegas *et. al.*, 1994; Webber & Trollope, 1997; Perez & Moreno, 1998; Schwilk, 2003; Gorgone-Barbosa *et. al*., 2015). Application of steam-releasing calorimetry in a diverse assortment of fuel types, with different fire behaviour characteristics, may explain why methods differ markedly amongst studies. Studies conducted in conifer forests of Portugal and Spain used large containers, sometimes sealed, with 250ml of water or more (Viegas *et. al.*, 1994; Perez & Moreno, 1998). This method cannot be replicated in relatively cool, fast-moving grassfires, as there may not be sufficient time or heat energy available for 250ml of water to heat up to boiling point. On the other hand, if the 20ml of water proposed by Webber & Trollope, (1997), for grassfire steam-releasing calorimeters in southern Africa was used in intense forest fires, all water would vaporise before measurements of intensity could be calculated.

    Steam-releasing calorimetry is an efficient, practical, and cost-effective alternative to conventional (often problematic) fire intensity measures (Webber & Trollope, 1997). There is a gap for research in wildfire related steam-releasing calorimetry, and a need for fuel-type appropriate 'standard' methods.

    The use of steam-releasing open-can calorimeters (also referred to as **hydropyrometers** (Trollope W.S.W. (PhD), personal communication, 2019)) in this study followed similar methods to those proposed by Webber & Trollope (1997), and Perez & Moreno (1998). Hydropyrometers were made from 410 g (400 cc) tin cans (70 mm basal diameter, ±100 mm depth) filled with 20ml of water (Webber & Trollope, 1997). A hydropyrometer was placed within each 10 x 10 m plot across the

burn site, 30 minutes before commencement of the prescribe fire. Once the fire was extinguished and it was safe to enter the fire scar, the volume of remaining water in each hydropyrometer was measured using a 20ml plastic livestock dosing syringe with a metal needle. For each hydropyrometer, the mass of water lost (g) was calculated by subtracting the recorded water volume (ml) from the original 20ml. The latent heat (kJ) captured by each 410 g tin can was calculated by multiplying the mass of water lost (g) by the latent heat of vaporisation (2.571kJ/g) (Weast, 1987; Webber & Trollope, 1997). Fire intensity was then calculated by multiplying latent heat captured (kJ) by rate of spread (ROS) (m/s) of fire front, divided by basal area (m^2) of container (3.84845 x 10^{-3} m^2) (Webber & Trollope, 1997). This formula is summarised below:

Fire intensity (kJ/s/m) = latent heat captured (kJ) * ROS (m/s) / area of container (m^2)

(Webber & Trollope, 1997)

2.) **Flame length** was used as proxy for fire intensity. It has long been accepted that direct correlations exist between flame length and fireline intensity (Byram, 1959; Brown & Davis, 1973; Chandler *et. al.*, 1983; Van Wilgen *et. al.*, 1985; Van Wilgen, 1986; Kremens *et. al.*, 2003; Cochrane & Ryan, 2009; Scott *et. al.*, 2014; Andrews, 2018). The following formula was developed from Byram's (1959) original equation for the relationship between flame length and fireline intensity:

$$\mathbf{I = 273 * (h)^{2.17}}$$

(Brown & Davis, 1973)

Where: **(I)** is fireline intensity (kJ/s/m) and **(h)** is flame length (m).

Flame length measurements were made observationally for each 10 x 10 m plot (n = 143), using objects of known heights (planted fence posts) in the fire's path as visual aids (Van Wilgen, 1986) (**FIGURE 4.4**). Corresponding fireline intensity values were calculated from flame length measurements, using Byram's (1959), formula (above) for the relationship between flame length and fireline intensity.

Char height was used as an additional *post-hoc* indication of flame length (Williams *et. al.*, 2003). Based off data collected from a series of fire experiments between 1990 and 1994 in eucalypt savannas at the Kapalga research site, Williams *et. al.*, (2003), proposed char height on trees as a practical post-fire indicator of flame height and fireline intensity. Height of char was recorded on pre-planted fence posts at the centre of each 100 m^2 plot (n = 143) (**FIGURE 4.4**). Measurements were made in centimetres, from the base of the pole at the soil surface, to the maximum height of char on the fence post, following methods similar to those proposed by Williams *et. al.*, (2003).

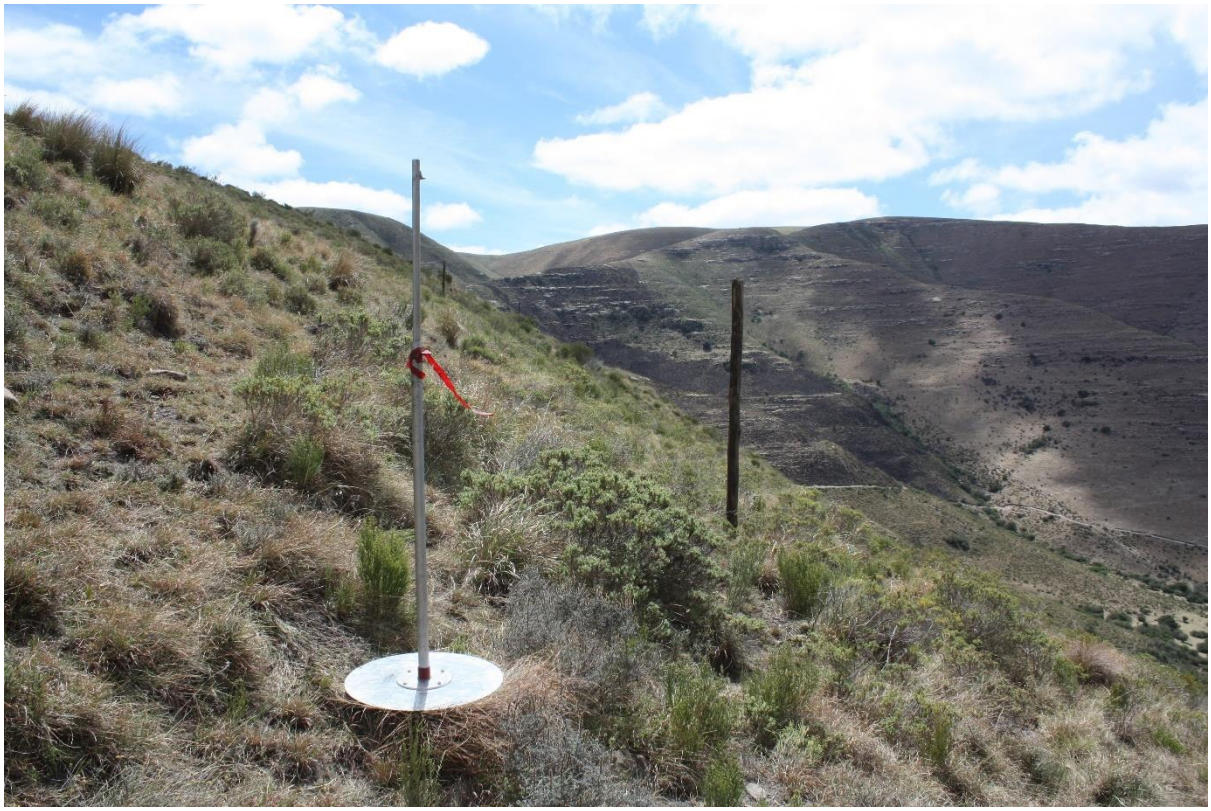

FIGURE 4.4: *Photograph showing example of fence post of a known height planted at centre of 100 m^2 burn plot. Pre-planted fence posts were used for both active flame length visual observation and post-fire height of char measurements. Disc pasture meter (DPM) used for fuel load estimations is shown in foreground and to left of fence post. Prescribed burn BE3, 8 November 2019, Katberg, Eastern Cape.*

3.) **Byram's (1959) Fireline Intensity** calculations were made post-fire, from recorded real-time fire data, using the following formula:

$$\mathbf{I = H * w * r}$$

(Byram, 1959)

Where: **Intensity (I)** represents the heat released per second, per meter of fire front (kJ/s/m) and is calculated by multiplying the **heat yield (H)** of fuel (kJ/kg) with the **mass of available fuel (w)** (kg/m^2) and **rate of spread (r)** of fire front (m/s) (Byram, 1959).

Individual calculations of Byram's (1959) Fireline Intensity were made for each 10 x 10 m plot within the fire site.

Heat yields for southern African grasses have been determined in previous studies by Smith, (1982), Trollope, (1983) and others. Trollope, (1983), investigated the heat yield of fine grass fuels in savanna areas of the Eastern Cape Province and attained values of **16 890 kJ/kg** for head fires and **17 781 kJ/kg** for back fires. These values of heat yield are similar to those commonly used in

USA and Australia, as well as the values determined by Smith, (1982), for herbaceous fine fuels in shrublands of the Drakensberg mountain range in KwaZulu-Natal, South Africa (Trollope, 1983; Trollope, 1984; Trollope *et. al*., 2004). The heat yields recommended by Trollope, (1983), for estimation of fire behaviour parameters are therefore considered appropriate for Eastern Cape montane grasslands.

Fuel loads estimated for each 10 x 10 m plot (n = 143), using the DPM method (Bransby & Tainton, 1977) (**Section 4.3.1, *Fuel, weather, & topography***), were used as values for mass of available fuel.

The amount of fuel consumed by fire (severity) was considered as an alternative measure to mass of available fuel and was calculated by subtracting post-fire fuel load from pre-fire fuel load, using a disc pasture meter (DPM) (Bransby & Tainton, 1977) (see methods for calculation of burn severity below).

A rate of spread (ROS) value was calculated for each 10 x 10 m plot using best fit model configuration (see methods for ROS calculation below).

Burn severity

Burn severity was measured as amount of fuel consumed by fire in kg/ha. The amount of fuel consumed in each 100 m^2 plot was calculated by subtracting post-fire fuel load from pre-fire fuel load. Post-fire fuel load was estimated using a disc pasture meter (DPM) (Bransby & Tainton, 1977). The same procedure used to estimate pre-fire fuel load (detailed above) was used to sample and estimate post-fire fuel load. Burn severity DPM readings were the final field samples measured at each prescribed burn (after all fire pattern indicator data had been sampled (**Chapter 5**)), as the DPM damaged brittle grass stubble during the process of sampling.

This method of measuring post-fire fuel load with a DPM is novel, and was applied with the assumption that it would be an appropriate technique. It is recognized however, that this method likely overestimates the amount of residual material remaining, due to the brittleness of the residual stubble. While the DPM calibration used was appropriate for the presiding unburnt vegetation, the same calibration would not be appropriate for hard and brittle residual grass stalks remaining after combustion. These hard and brittle residual grass stalks would have generated, in relative terms, taller height measurements (and thus fuel loads) for the available fuel compared to flexible live grass. However, this problem can be rectified with the development of a post-fire calibration for relevant herbaceous vegetation.

Rate of spread

Measuring **ROS** of fires is a challenging task (especially for multiple plots within a burn site) under normal circumstances. For this reason, it is not uncommon to incorporate spread models to simulate ROS. The challenging nature of measuring ROS was exacerbated in this study due to rugged terrain, impaired visibility, and limited availability (incl. cost) of equipment (Scott *et. al.*, 2014). To overcome this, ROS was simulated from a number of spread models, simulated outputs tested for suitability against a subsample dataset, and the most appropriate model chosen as representative for entire dataset.

Where possible, ROS was measured between landmarks of a known distance, yielding a subsample of 28 recorded ROS observations across five burn sites. Using corresponding subsample fuel, weather, and topographical data (n = 28), ROS was simulated from a number of recognized fire spread models. From the same subsample dataset of recorded conditions (fuel, weather, fire, & topography), several linear and non-linear fire spread models were constructed using R Studio software (R Core Team, 2020). The proportion of variation of fire behaviour (ROS) accounted for by each independent variable (fuel, weather & topography) from the subsample dataset (n = 28) was also investigated. The various models' (pre-existing & constructed) simulated rates of spread were then compared with the subsample real-time recorded rates of spread, and the best fit model configuration was chosen and used to simulate ROS for entire set of 143 observations. Model inputs, general assumptions and the various model configurations are discussed in detail in **Section 4.3.3**, ***Modelled fire behaviour***, of this chapter. The proportion of variation of fire behaviour (ROS) accounted for by each independent variable (fuel, weather & topography) from the subsample dataset (n = 28) was also investigated.

4.3.3 Modelled fire behaviour:

A number of fire behaviour prediction models (arranged in numerous configurations) were used to simulate certain aspects of fire behaviour, specifically **rate of spread (ROS), fireline intensity, and flame length**. **TABLE 4.1** is a list of the various fire models used in this study, showing the respective output variables produced by each model. The various models require a range of different input variables. **TABLE 4.2** is a detailed list of the different input variables required for each fire model. Where possible, sampled fuel, weather, and topographical data (input variables), collected for **each** 10 x 10 m plot (n = 143) were used as relevant input variables (*i.e.*, 143 different fuel, weather, & topographical scenarios). Specific emphasis was put on using sampled data ahead of generalised, previously derived (*i.e.*, fuel model), theoretical, or assumed values for the specific fuel type or region.

Various pre-existing fire spread models can be assembled into a number of configurations based on a range of input variable assumptions or arrangements (*i.e.*, fuel models). Some of these input variables (dead fuel moisture of extinction (MOE) (the theoretical moisture content of fine dead fuels, above

which fires no longer spread (Van Wilgen & Wills, 1988; Scott *et. al*., 2014)); and fuel (live & dead) surface area to volume (SA/V) ratio) are difficult or impossible to measure or specify (Scott *et. al*., 2014), and as a result are usually based on either previously determined or theoretical values (of which, several may exist). Other input variables which may alter model configuration include the presence or absence of correction functions for the influence of slope, and method of fuel moisture value determination. An incidental advantage of the above, is that several fuel model arrangements (configurations) of the same base models (*e.g.,* BehavePlus) could be, and were, developed for each 100 m^2 burn plot. The performance of these various fuel model arrangements were then compared.

A total of 22 model configurations were used to simulate **ROS** for the subsample dataset (n = 28). Of these, 19 model arrangements were configured from five pre-existing spread models. The remaining three configurations (one linear model & two general additive models (GAM's)) were built from the subsample dataset using R Studio software (R Core Team, 2020). The five pre-existing models used were: BehavePlus V6.0.0 (Andrews & Bevins, 2018); Rothermel R package (Rothermel, 1972; Vacchiano & Ascoli, 2015); McArthur's grassland fire spread models Mk3 & Mk5 (McArthur, 1966; McArthur, 1977; Noble *et. al*., 1980); & CSIRO modified McArthur Mk4 grassland fire spread calculator (CSIRO, 1999). **TABLE 4.3** is a list of the various model configurations and respective distinguishing input variables used in this study (only configurations 1-19 were used to simulate ROS).

Thirteen model configurations from three prediction models (six BehavePlus, six Rothermel, & Trollope's (2004), regression equation for fireline intensity) were used to simulate **fireline intensity** for each 100 m^2 plot (n = 143), throughout the seven prescribed burn sites. See **TABLE 4.3** for list of various model configurations and respective distinguishing input variables (only configurations from BehavePlus, Rothermel, & Trollope (2004) regression were used to simulate fireline intensity).

Sixteen model configurations from three prediction models (four McArthur Mk5, six BehavePlus, & six Rothermel) were used to simulate **flame length** for each 10 x 10 m plot (n = 143) throughout the seven prescribed burn sites. See **TABLE 4.3** for list of the various model configurations and respective distinguishing input variables (only McArthur Mk5, BehavePlus, & Rothermel configurations were used to simulate flame length). Additionally, Lowveld (Government Gazette Notice 1099 of 2013) Fire Danger Index (FDI) associated flame lengths were generated from each 100 m^2 burn plot's FDI score.

TABLE 4.1: *Output variables produced by each of the six fire behaviour prediction models used in this study. These models are: BehavePlus V6.0.0 (Andrews & Bevins, 2018); Rothermel R package (Rothermel, 1972; Vacchiano & Ascoli, 2015); McArthur's grassland fire spread models Mk3 & Mk5 (McArthur, 1966; McArthur, 1977; Noble et. al., 1980); CSIRO modified McArthur Mk4 grassland fire spread calculator (CSIRO, 1999); & Trollope's (2004), regression equation for fireline intensity.*

	Output		
Model	Rate of Spread	Fireline Intensity	Flame Length
McArthur Mk3	✓		
CSIRO Modified Mk4	✓		
McArthur Mk5	✓		✓
BehavePlus	✓	✓	✓
Rothermel (1972)	✓	✓	✓
Trollope (2004)		✓	

Model inputs & general assumptions

The fire behaviour prediction models used in this study range in their complexity and number of input parameters required. A list of model input variables can be found in **TABLE 4.2**. For the most part, requisite input variables differ in fuel moisture content (FMC) determination. The McArthur based Australian models account for fuel moisture through temperature, relative humidity, and curing input variables (Noble *et. al*., 1980; McCaw & Catchpole, 1997; Cheney & Sullivan, 2008). The American Rothermel based models require direct fuel moisture input values (Andrews & Bevins, 2018; Vacchiano & Ascoli, 2015). In addition to the listed model inputs, several assumptions were made based on specific fuel properties. I elaborate:

Fuel models can be considered **static** or **dynamic**, based on types of fuels present in the fuel stand. Dynamic fuel models allow for a portion of the live fuel load to be transferred to dead fuel load as a result of living fine fuels drying out and 'curing' during the preheating phase of combustion (Everson *et. al*., 1988, Andrews & Bevins, 2018). Grasslands (herbaceous fine fuels) are considered dynamic since a portion of the live component may 'cure' during combustion (Everson *et. al*., 1988). Where selection was required (BehavePlus & Rothermel), fuel models in this study were considered dynamic.

It is largely acknowledged that woody cover in grassland and savanna systems has little contribution to fire behaviour in these relatively cool, fast-moving fires (Trollope W.S.W. (PhD), personal communication, 2019). However, unlike savanna systems, the woody component (Amathole montane Fynbos (*e.g., Cliffortia paucistamina*)) in mesic montane grasslands of the Eastern Cape is very

susceptible to fire (Trollope, 1970; Trollope, 1972), and when present, has a significant contribution to the behaviour of surface fires in these systems (Trollope W.S.W. (PhD), personal communication, 2019). This study specifically focussed on grass fire behaviour. While there was a **woody component** present in the montane grasslands of the Boschberg, Katberg, & Winterberg, for the purposes of this study, fuel was considered fine and herbaceous in its entirety. Where possible, 10 x 10 m burn plots were placed in such a manner as to largely avoid the woody component.

Flammable fuel can be divided into **fuel (size) classes**, based on time lag related to moisture transfer (wetting and drying) in and out the fuel (Cochrane & Ryan, 2009; NWCG, 2016; NWCG, 2018), referred to earlier in **Chapter 2**. In this context, time lag is defined as the amount of time it takes a piece of dead fuel to transfer two thirds from its current moisture content towards equilibrium FMC (Andrews & Bevins, 2018). Rothermel based fuel models divide live fuels into a woody and herbaceous component, and dead fuels into 1-hour, 10-hour, & 100-hour fuel size classes (Andrews & Bevins, 2018). Fuels larger than three inches in diameter (100-h) are considered to have negligible effect on surface fire behaviour (ROS & intensity), and are thus not included in Rothermel based model calculations (Andrews & Bevins, 2018). The three dead fuel size classes considered are grouped by the following diameters: < ¼ in (needles, leaves, & herbaceous plants); ¼ - 1 in; & 1 - 3 in (Cochrane & Ryan, 2009; Andrews & Bevins, 2018; NWCG, 2018). Fuel size classes with smaller SA/V ratios (*i.e.*, 1-hour fuels) are considered to have greater influence on surface fire spread model calculations, with larger fuel size classes having less influence (Andrews & Bevins, 2018). For the purposes of this study, all fuels were considered as either live herbaceous or dead 1-hour fuels.

BehavePlus and Rothermel (1972) models require a **fuel heat content (heat of combustion)** input value. (Not to be confused with heat yields. See **Section 2.1.7, *Intensity and severity*, Chapter 2**). Trollope, (1983), previously investigated the heat of combustion of various grass species in savanna areas of the Eastern Cape Province and attained a mean heat content value of **18024 kJ/kg**. This value is similar to those determined for similar fuel types in other studies (Smith, 1982; Trollope, 1983; Trollope, 1984; Trollope *et. al*., 2004). Trollope's (1983) heat content value for Eastern Cape grass species was considered appropriate for this study and thus was used for all fuel models.

In addition, BehavePlus and Rothermel (1972) models also require a **fuel bed depth** measurement for their respective fuel models. Fuel bed depth was measured for each 10 x 10 m plot from ground level to grass canopy, ignoring occasional taller individuals (Everson *et. al*., 1988). Montane sourveld grasslands are particularly suitable for these measurements, as open spaces between plants are infrequent (Everson *et. al*., 1988).

The McArthur and Rothermel spread models do not consider the directional value associated with vector predictor variables (*e.g.*, wind direction, fire spread direction, aspect) as an input value in their respective functions. These models assume wind blows in the direction of fire spread, and in the case

of Rothermel, that spread is upslope. To account for this in this study, wind speed was assumed to be 0 km/h in back fire scenarios for McArthur Mk3, Mk5, and Rothermel models, and 5 km/h (minimum input) in CSIRO modified Mk4 models. For head and flank fire scenarios, the full wind speed value was assumed, regardless of wind direction. McArthur models account for up and down slope inputs, but not diagonal spread. These slope directional inputs for McArthur and Rothermel models were, however, accounted for in this study, and are discussed in more detail in the following section (*Model configurations*). In the case of BehavePlus model configurations, all directional vector values were accounted for and entered as recorded through each 10 x 10 m burn plot.

TABLE 4.2: *Detailed list of input variables required for each of the six fire behaviour prediction models used in this study, namely McArthur's grassland fire spread models Mk3 & Mk5 (McArthur, 1966; McArthur, 1967; McArthur, 1977; Noble et. al., 1980); CSIRO modified McArthur Mk4 grassland fire spread calculator (CSIRO, 1999); BehavePlus V6.0.0 (Andrews & Bevins, 2018); Rothermel R package (Rothermel, 1972; Vacchiano & Ascoli, 2015); & Trollope's (2004) regression equation for fireline intensity.*

	Input Variable												
Model	Wind Speed	Wind Direction	Relative Humidity	Temperature	Degree of Curing	Fuel Moisture Content (FMC)	Fuel Load	Fuel Heat Content	Fuel Bed Depth	Fuel SA/V Ratio	Dead Fuel Moisture of Extinction	Slope Gradient	Slope Aspect
McArthur Mk3	✓		✓	✓	✓								
CSIRO Modified Mk4	✓		✓	✓	✓								
McArthur Mk5	✓		As part of FMC calculation	As part of FMC calculation	As part of FMC calculation	Can be entered directly or calculated with built in function	✓					As part of supplementary function	
BehavePlus	✓	✓				For each class	For each class	For each class	✓	For each class	✓	✓	✓
Rothermel (1972)	✓					For each class	For each class	For each class	✓	For each class	✓	Upslope only	
Trollope (2004) Regression	✓		✓	✓		Single value	Single value						

Model configurations

Fire behaviour prediction models can be arranged into a number of configurations based on various distinguishing input variables (usually fuel model arrangements). The pre-existing models used in this study were arranged into a total of 20 configurations according to four distinguishing factors: fuel (live & dead component) SA/V ratio; dead fuel moisture of extinction (MOE); method of fuel moisture value derivation; & the inclusion or exclusion of a slope correction function. **TABLE 4.3** is a list of the 20 model configurations and respective distinguishing input variables used in this study. Individual model configurations were given a shorthand code (Model Configuration Code) to distinguish between different configurations of the same base model. Configurations for the three constructed models (one linear model and two GAM's) were based on significance values of independent variables.

Rothermel based models require **dead fuel MOE** and **SA/V ratio** values as fuel model input variables. Field based methods of fuel SA/V ratio determination are difficult, while lab-based alternatives are tedious and impractical. The consequence is, that most applications of the BehavePlus and Rothermel models use predefined values for fuel SA/V ratios, even when defining custom fuel models (Everson *et. al*., 1988; Van Wilgen & Wills, 1988).

While moisture in the fuel certainly impedes fire spread, it is difficult to specify a FMC threshold above which, fires will self-extinguish (Scott *et. al*., 2014). Rothermel, (1972), termed this threshold value as 'moisture of extinction' (MOE). However, dead fuel MOE is in fact a theoretical value, with little use or application outside of fire modelling (Trollope W.S.W. (PhD), personal communication, 2019). It has been found from both lab and field studies, that dead fuel MOE values depend on the amount and structure of fuel, as well as wind speed (Wilson, 1985; Burrows, *et. al*., 2009; Scott *et. al*., 2014). Nevertheless, it is largely acknowledged that grassfires spread poorly at dead FMC above 30% (McArthur, 1977; Scott *et. al*., 2014), although there have been few empirical studies which verify this.

Currently, no Rothermel based fuel models have specifically been developed for the mesic montane grasslands of Boschberg, Katberg, & Winterberg. Although several fuel models have been developed for functionally and structurally similar fuel types in southern Africa (De Ronde, 1988; Everson *et. al*., 1988; Van Wilgen & Wills, 1988; Trollope *et. al.*, 2004). **Six** dead fuel MOE and fuel SA/V ratio fuel model configurations, derived from appropriate existing fuel models (De Ronde, 1988; Everson *et. al*., 1988; Van Wilgen & Wills, 1988), were developed for the montane grasslands of Boschnerg, Katberg, & Winterberg. The six fuel model configurations intentionally incorporated a wide range of values for fuel model comparisons. Using these fuel models, BehavePlus and Rothermel base models were each arranged into **six** unique configurations according to different dead fuel MOE and SA/V ratio values. These configurations (fuel models) are detailed in **TABLE 4.3**.

The McArthur based Australian models account for fuel moisture through temperature, relative humidity, and curing input variables (Noble *et. al*., 1980; McCaw & Catchpole, 1997; Cheney & Sullivan, 2008). The McArthur Mk5 grassland fire spread model (McArthur, 1977), like its predecessor (McArthur Mk3 (McArthur, 1966; McArthur, 1967)) uses temperature, humidity, and degree of curing to calculate fuel moisture content (Noble *et. al*., 1980). Unlike its predecessors, this is done in a separate function, and is not built-in (Noble *et. al*., 1980). The resultant calculated FMC is then entered into the main ROS function (Noble *et. al*., 1980). Incidentally, this affords users the opportunity to enter a value for **dead fuel moisture (DFM)** content directly into the ROS function, without the need for relative humidity, temperature, or curing values. It is unclear whether McArthur intended for this to be the case — curing, temperature, and relative humidity inputs could be similarly bypassed in CSIRO published nomograms (Cheney & Sullivan, 2008). Nevertheless, it allows for the comparison of model outputs from field sampled DFM contents and self-generated FMC values. It has also been acknowledged that methods of indirect fuel moisture estimation from meteorological data (*i.e.,* function for fuel moisture determination) are not always accurate and effective (Dexter & Williams, 1976; Noble *et. al.*, 1980). In this study, McArthur Mk5 model configurations were generated for both field sampled DFM content values and built-in function calculations (relative humidity, temperature, curing state) (**TABLE 4.3**).

That slope gradient influences the ROS of wildland fires, is widely acknowledged and well documented (Luke & McArthur, 1978; Trollope, 1984; Cheney & Sullivan, 2008; Sullivan *et. al.*, 2014; Leavell *et. al*., 2017). An interpretation (based on empirical data) of this relationship is shown in **FIGURE 4.5**. Various **slope correction functions** have been developed which adjust modelled ROS values, to account for influence of slope (Noble *et. al.*, 1980; Weise & Biging, 1997; Sharples, 2008; Sullivan *et. al.*, 2014). BehavePlus V6.0.0 accounts for both upslope and downslope effects with built in functions (Andrews & Bevins, 2018), while the Rothermel R package only accounts for upslope effects (Vacchiano & Ascoli, 2015). A slope correction function exists for McArthur based models (McArthur, 1967; Noble *et. al.*, 1980), but must be applied to already modelled ROS values manually. This function is illustrated graphically in **FIGURE 4.5**.

The Rothermel R package (Vacchiano & Ascoli, 2015) and McArthur based slope correction function (Noble *et. al.*, 1980) do not account for the influence of directional vectors (fire spread, wind, aspect) on slope gradient (Sharples, 2008). They assume that (A): fires are spreading either directly up or downhill, and not at an oblique angle; and (B): that wind direction is aligned with the axis of fire spread (coming from directly behind direction of fire spread). In reality however, fires usually spread at relative angles (oblique angles) up or down slope and/or compared to wind direction (*e.g.*, a head fire spreading with the wind, but diagonally up a slope). This means that a fire spreading at relative angles to wind direction or slope aspect, does not experience the full effect of wind speed or slope gradient on its relative ROS.

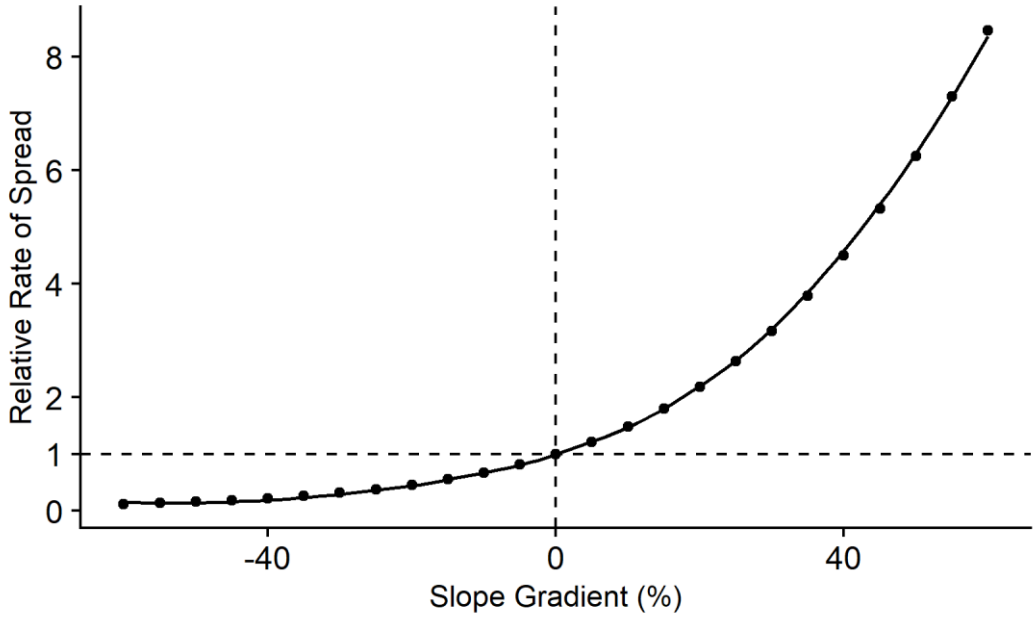

FIGURE 4.5: *The influence of slope gradient on rate of spread, according to McArthur, (1967). Where dashed lines represent relative rate of spread on level ground (no slope influence). Curve constructed using slope correction formula specified by Noble et. al., (1980). Illustration inspired from pp. 43, Cheney & Sullivan, (2008).*

With specific reference to slope, a fire spreading horizontally across a slope, is effectively spreading on a level gradient. Similarly, the **effective gradient** realised by a forward moving fire, spreading diagonally up a slope, will be less than the overall gradient of the slope, relative to aspect. When conducting studies comparing fire spread model (those which incorporate slope gradient effects) performance to observed actual fire conditions, it is therefore critical that direction of fire spread and slope aspect, in conjunction with gradient and wind direction, are recorded.

To address the above issues surrounding directional vectors, Sharples, (2008), developed a **slope-corrected scaler function** for the McArthur based slope factor function (Noble *et. al.,* 1980), which accounted for directional spread relative to aspect and associated effective gradients.

In this study, configurations for McArthur Mk4 & Mk5 models were made with, and without the Sharples, (2008), adapted slope-corrected function applied (**TABLE 4.3**). Since the Rothermel R package (Vacchiano & Ascoli, 2015) did not account for downslope effects, the Sharples, (2008), adapted McArthur slope correction function was applied to downslope fire spread scenarios. This was considered an important deviation from the original model, as the characteristically steep slopes of the Boschberg, Katberg, & Winterberg study sites would have had a significant effect on fire behaviour.

TABLE 4.3: *List of various model configurations and respective distinguishing input variables used in this study. Fire behaviour prediction models are arranged into a number of configurations based on differing fuel model and/or input variable assumptions, as well as the inclusion or exclusion of slope factor functions. BehavePlus and Rothermel models were each arranged into six different configurations according to fuel model differences in dead fuel moisture of extinction (MOE) and surface area to volume (SA/V) ratio. McArthur based models were arranged into several configurations according to the inclusion or exclusion of a slope factor function and method of fuel moisture derivation. Individual model configurations were given a shorthand code (Model Configuration Code) to distinguish between different configurations of the same base model.*

Count	Model Configuration Code	Base Model	Fuel Moisture	Slope Correction Factor	Dead Fuel Moisture of Extinction (%)	1h Fuel SA/V Ratio (m^2/m^3)	Live Herbaceous Fuel SA/V Ratio (m^2/m^3)
1	McA_Mk3	McArthur Mk3	–	No	–	–	–
2	McA_Mk4	CSIRO Modified Mk4	–	No	–	–	–
3	McA_Mk4_Slp	CSIRO Modified Mk4	–	Yes	–	–	–
4	McA_Mk5	McArthur Mk5	Simulated	No	30	–	–
5	McA_Mk5_Slp	McArthur Mk5	Simulated	Yes	30	–	–
6	McA_Mk5_DFM	McArthur Mk5	Dead fraction	No	30	–	–
7	McA_Mk5_DFM_Slp	McArthur Mk5	Dead fraction	Yes	30	–	–
8	BH20_4949	BehavePlus	–	Yes	20	4900	4900
19	BH20_6649	BehavePlus	–	Yes	20	6600	4900
10	BH20_6659	BehavePlus	–	Yes	20	6600	5900
11	BH30_4949	BehavePlus	–	Yes	30	4900	4900
12	BH30_6659	BehavePlus	–	Yes	30	6600	4900
13	BH30_6659	BehavePlus	–	Yes	30	6600	5900
14	RT20_4949	Rothermel	–	Yes	20	4900	4900
15	RT20_6649	Rothermel	–	Yes	20	6600	4900
16	RT20_6659	Rothermel	–	Yes	20	6600	5900
17	RT30_4949	Rothermel	–	Yes	30	4900	4900
18	RT30_6649	Rothermel	–	Yes	30	6600	4900
19	RT30_6659	Rothermel	–	Yes	30	6600	5900
20	WSWT04	Trollope (2004)	–	No	–	–	–

4.3.4 Data analyses:

All statistical data analyses were performed in R Studio (R Core Team, 2020) and where relevant, statistical significance was set at $P < 0.05$, unless specifically stated otherwise.

Rate of spread

Rate of spread (ROS) values were calculated for each 10 x 10 m plot using best fit model configuration for subsample dataset (n = 28) (see *Rate of spread*, **Section 4.3.2*, Observed fire conditions***).

A linear model for ROS was constructed using slope gradient, wind speed, air temperature, relative humidity, & percent curing data collected from the subsample dataset. Fire spread type (head, back, flank) and site were also included, as a factor and random effect variable, respectively.

Similarly, a generalised additive model (GAM) (non-linear) was also constructed using slope gradient, wind speed, air temperature, relative humidity, & percent curing data collected from the subsample dataset. Again, fire spread type and site were also included, as a factor and random effect variable, respectively.

A second GAM was constructed based on significance level of each contributing independent variable. A manual stepwise backward elimination of non-significant variables was performed to determine which variables should be removed from the original GAM. This was based off contributory significance of random and fixed effect terms.

The three constructed models were then used to simulate ROS for subsample dataset (n = 28). An additional five pre-existing spread models, arranged into a total of 19 configurations (**TABLE 4.3**) (see *Model configurations*, **Section 4.3.3*, Modelled fire behaviour***), were also used to simulate ROS for subsample dataset.

Linear regressions were performed to compare simulated various ROS model (22 configurations) outputs with actual ROS values recorded for each observation in the subsample dataset (n = 28). The best performing model (based off a combination of slope, intercept, & R^2 values) was chosen to simulate ROS for each 10 x 10 m burn plot of entire dataset (n = 143).

Cook's Distance tests were conducted to identify outliers in the best performing spread model linear regressions, as well as the influence any outliers might have on the linear regressions.

Measured fire behaviour

Kruskal-Wallis (rank sum) tests for non-parametric data were performed to identify differences in fireline intensity values between head, back & flank fires (fire spread type). Wilcoxon (Mann-Whitney U) *post-hoc* analyses were then run to determine between which fire spread types or sites differences (if they existed) occurred.

ANOVA tests for parametric data were performed to identify differences in fire severity values between head, back & flank fires (fire spread type), with site included as a variable to account for site affects. Tukey's HSD (honestly significant difference) *post-hoc* analysis was performed to determine between which fire spread types or sites differences (if they existed) occurred.

To test performance of alternative measures of fireline intensity, linear regressions comparing various (alternative) measures (Hydropyrometers, flame length, & Byram's intensity using severity) against Byrams's (1959) calculated fireline intensity for each 100 m^2 plot (n = 143), were performed.

Modelled fire intensity & flame length

Modelled fire behaviour output values (flame length & fire intensity) (n = 143), from various model configurations (**TABLE 4.3**), were compared with real-time observed fire conditions, recorded through each 10 x 10 m plot within the seven prescribed burn sites.

Following similar methods to Everson *et. al.*, (1988), & van Wilgen & Wills, (1988), model performance was tested by conducting linear regression analyses comparing simulated model outputs (predicted fire conditions) (flame length & intensity) from various model configurations (**TABLE 4.3**) with recorded real-time fire conditions (flame length & intensity).

To test if height of char on pole-type fuels is an appropriate *post-hoc* measure of flame length, linear regression analyses were performed, comparing char height and double (2x) char height against recorded real-time flame lengths.

Spearman's rank correlations (non-parametric) were performed to validate associations between double (2x) char height and flame length.

4.4 Results:

Mean fuel, weather, and topographical data for each site are summarised in **TABLE 3.1** & **TABLE 3.2** of **Chapter 3**.

4.4.1 Rate of spread:

Predicted/simulated versus observed actual rates of spread for subsample dataset (n = 28) for various spread model configurations are shown in **FIGURE 4.6** & **FIGURE 4.7**. Spread model (linear regression) performance of all 22 model configurations is summarised in **TABLE 4.4**. Adjusted R^2 values cannot be taken in isolation and need to be considered in combination with linear regression intercepts and slope coefficients. Perfect agreement is indicated by an R^2 value of one, an intercept of zero, and a slope coefficient of one. The McArthur Mk5 spread model, using field sampled value of dead fuel moisture content, with the slope factor correction function (Noble *et. al*., 1980) applied (McA_Mk5_DFM_Slp) (**A** in **FIGURE 4.7**), proved to be the best fit ROS model configuration for the subsample dataset (n = 28). Cook's Distance test showed that outliers had little influence on the results of the linear regression. Removal of outliers did not significantly change the linear regression equation.

Fire spread type ($P < 0.001$), followed by slope gradient ($P < 0.01$), air temperature ($P < 0.034$), and relative humidity ($P < 0.053$) were found to best explain ROS in a linear model run for subsample dataset of 28 fires in Eastern Cape montane grassland. While in the two generalised additive models (GAM's), fire spread type ($P < 0.029$ & 0.006), slope gradient ($P < 0.001$), air temperature ($P < 0.017$ & 0.002), and percent curing ($P < 0.1$ & 0.052) were found to be the most significant predictor variables of ROS for subsample dataset of 28 fires in Eastern Cape montane grassland. Admittedly, there was a level of uncertainty with regards to percent curing, but less so than with wind speed ($P > 0.4$), relative humidity ($P > 0.78$), and site ($P > 0.89$).

McArthur based spread model configurations performed significantly better (when compared to observed ROS) with slope factor correction functions applied (McA_Mk4_Slp; McA_Mk5_Slp; McA_Mk5_DFM_Slp (**B, D, F, FIGURE 4.6**)) than configurations which did not take slope gradient into account (McA_Mk4; McA_Mk5; McA_Mk5_DFM (**A, C, E, FIGURE 4.6**)) (**TABLE 4.4**).

Looking now at BehavePlus and Rothermel spread model configurations which require dead fuel moisture of extinction (MOE) and 1h & live fuel surface area to volume (SA/V) ratio as input variables. Fuel model configurations with greater SA/V values (1h fuel SA/V: 6600 m^2/m^3; live fuel SA/V: 5900 m^2/m^3) (**D** & **F** in **FIGURE 4.7**) performed better than fuel model configurations with lower SA/V values (1h fuel SA/V: 4900 m^2/m^3; live fuel SA/V: 4900 m^2/m^3) (**C** & **E** in **FIGURE 4.7**) when simulating observed ROS (**TABLE 4.4**). BehavePlus and Rothermel fuel model configurations which used a dead fuel MOE value of 30% (**D** & **F** in **FIGURE 4.7**) produced better ROS results than fuel model configurations which used a dead fuel MOE value of 20% (**C** & **E** in **FIGURE 4.7**) when

simulating observed ROS (**TABLE 4.4**). The combined fuel scenario of 6600 m^2/m^3 1h fuel SA/V, 5900 m^2/m^3 live fuel SA/V, and 30% dead fuel MOE performed significantly better when simulating for ROS than fuel scenario of 4900 m^2/m^3 1h fuel SA/V, 4900 m^2/m^3 live fuel SA/V, and 20% dead fuel MOE for both BehavePlus and Rothermel spread models for subsample dataset of 28 fire in Eastern Cape Montane grassland vegetation. Rothermel spread model configurations' regression equations (**E** & **F** in **FIGURE 4.7**) produced better fits to observed ROS than BehavePlus spread model configurations (**C** & **D** in **FIGURE 4.7**) (**TABLE 4.4**).

TABLE 4.4: *Rate of spread (ROS) simulation model linear regression performance of 22 model configurations for 28 fires in Eastern Cape montane grassland vegetation. Nineteen configurations were adapted from five pre-existing models. Three additional model configurations were constructed from fuel, weather and topographical variables sampled from 28 fires in the Greater Winterberg region of the Eastern Cape. For details on ROS Model Configuration codes, refer to* ***TABLE 4.3****.*

ROS Model Configuration	Adjusted R^2 Value	Intercept	Slope Coefficient
McA_Mk3	0.501	-0.07078	14.72712
McA_Mk4	0.5071	-0.2502	4.8615
McA_Mk4_Slp	0.9662	-0.08389	2.16416
McA_Mk5	0.3633	-0.6215	2.8016
McA_Mk5_Slp	0.9289	-0.13699	1.32676
McA_Mk5_DFM	0.4414	-1.6414	2.4550
McA_Mk5_DFM_Slp*	**0.9162***	**-0.4358***	**0.9051***
BH20_4949	0.8618	-0.3129	2.4973
BH20_6649	0.8825	-0.2048	1.6554
BH20_6659	0.8843	-0.2313	1.6126
BH30_4949	0.8472	-0.5144	2.1911
BH30_6649	0.8738	-0.4121	1.4624
BH30_6659	0.8734	-0.4046	1.4150
RT20_4949	0.8686	-0.2461	2.0075
RT20_6649	0.8867	-0.17103	1.32981
RT20_6659	0.8874	-0.1669	1.2893
RT30_4949	0.8494	-0.4052	1.7485
RT30_6649	0.8734	-0.31236	1.16298
RT30_6659	0.8736	-0.30647	1.12651
Linear Model	0.873	-0.20186	0.57288
GAM 1	0.9776	-0.01704	0.40875
GAM 2	0.9761	-0.03857	0.42248

***** *Best fit ROS model configuration*

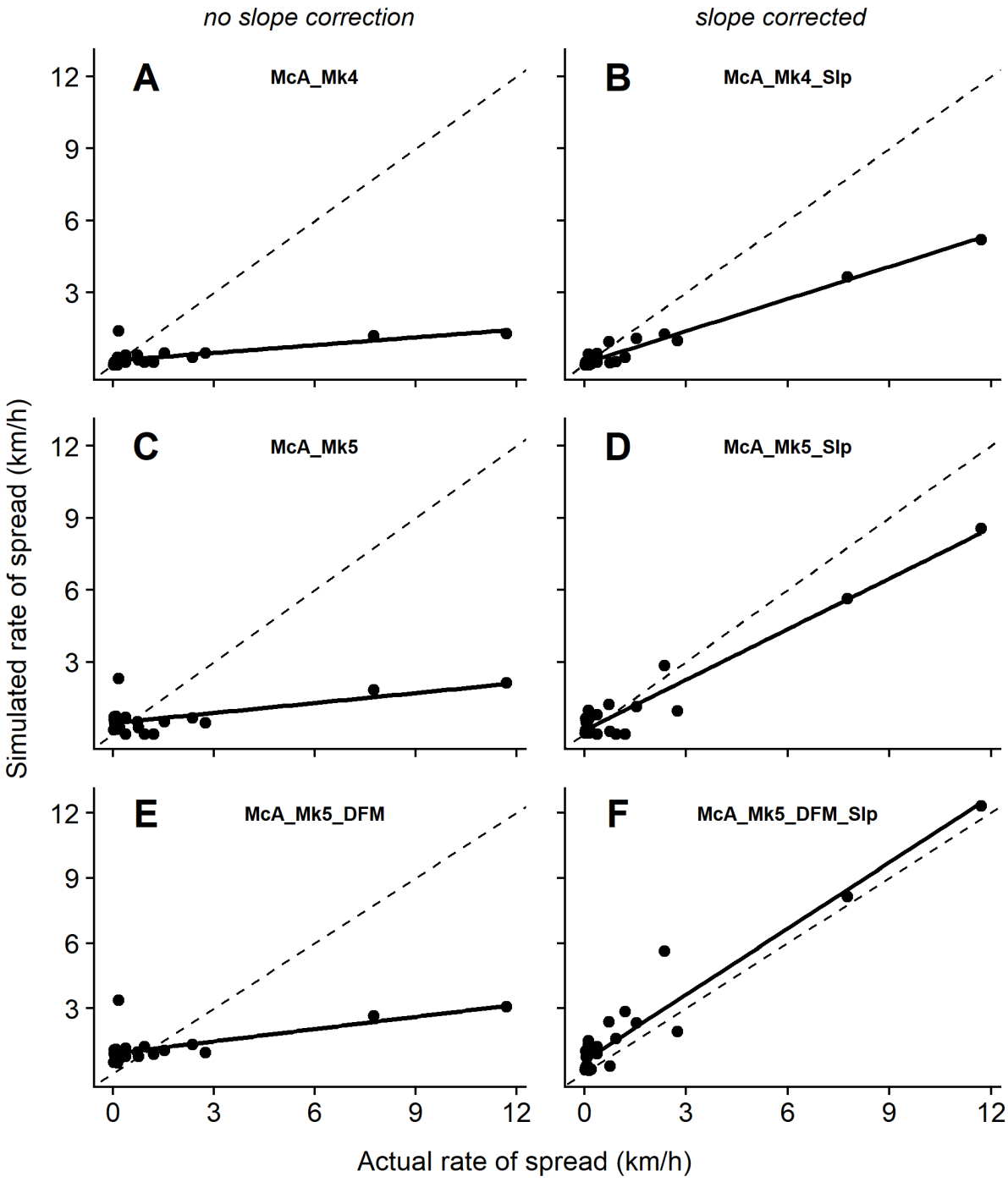

FIGURE 4.6: *Comparison of spread model performance between configurations with (right) and without (left) slope correction functions applied. Observed actual rates of spread (ROS) versus simulated ROS outputs from various spread model configurations for 28 fires in Eastern Cape montane grassland vegetation. Dashed lines indicate perfect agreement between observed actual ROS and simulated values. Solid lines are linear regressions, details of which are shown in* ***TABLE 4.4.*** *Various spread model configurations A-F: (A): CSIRO modified Mk4 spread calculator, no slope factor function applied. (B): CSIRO modified Mk4 spread calculator, with a slope correction factor function (Noble et. al., 1980) applied. (C): McArthur Mk5 spread model, using built-in function for fuel moisture determination, no slope factor function applied. (D): McArthur Mk5 spread model, using built-in function for fuel moisture determination, with a slope correction factor function (Noble et. al., 1980) applied. (E): McArthur Mk5 spread model, using field sample value of dead fuel moisture content, no slope factor function applied. (F): McArthur Mk5 spread model, using field sample value of dead fuel moisture content, with a slope correction factor function (Noble et. al., 1980) applied.*

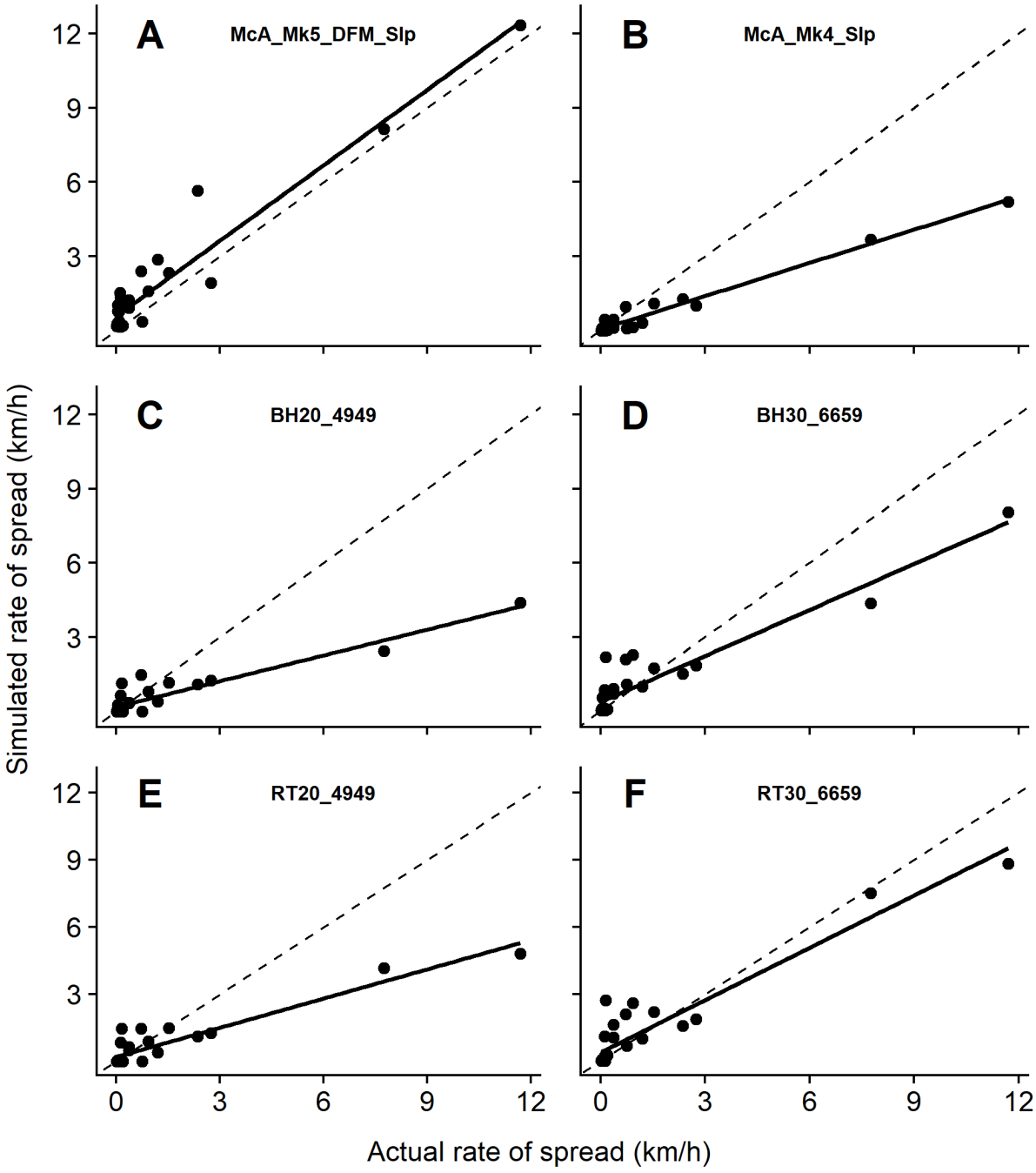

FIGURE 4.7: *Comparison between observed actual rates of spread (ROS) versus simulated ROS outputs from various spread model configurations for 28 fires in Eastern Cape montane grassland vegetation. Dashed lines indicate perfect agreement between observed actual ROS and simulated values. Solid lines are linear regressions, details of which are shown in* ***TABLE 4.4****. Various spread model configurations A-F: (A): McArthur Mk5 spread model, using field sample value of dead fuel moisture content, with a slope correction factor function (Noble et. al., 1980) applied. (B): CSIRO modified Mk4 spread calculator, with a slope correction factor function (Noble et. al., 1980) applied. (C): BehavePlus V6.0.0, dead fuel moisture of extinction (MOE): 20%, surface area to volume ratio (SA/V) of dead component: 4900 m^2/m^3, SA/V of live component: 4900 m^2/m^3. (D): BehavePlus V6.0.0, dead fuel MOE: 30%, SA/V of dead component: 6600 m^2/m^3, SA/V of live component: 5900 m^2/m^3 (E): Rothermel (1972) (Vacchiano & Ascoli, 2015), dead fuel MOE: 20%, SA/V of dead component: 4900 m^2/m^3, SA/V of live component: 4900 m^2/m^3. (F): Rothermel (1972) (Vacchiano & Ascoli, 2015), dead fuel MOE: 30%, SA/V of dead component: 6600 m^2/m^3, SA/V of live component: 5900 m^2/m^3.*

4.4.2 Measured fire behaviour:

Byram's, (1959), fireline intensities (kJ/s/m) were significantly lower ($P < 0.001$) in back fires (mean of 1 896 kJ/s/m) than head (mean of 12 787 kJ/s/m) and flank fires (mean of 8 597 kJ/s/m) for all 143 burn plots in the montane grasslands of the Boschberg, Katberg, & Winterberg mountains (**FIGURE 4.8**).

Fire severities (kg/ha) (fuel consumed), estimated using a disc pasture meter (Bransby & Tainton, 1977), were significantly lower in head fires (mean of 2 624 kg/ha) than back ($P < 0.031$) (mean of 3 218 kg/ha) and flank fires ($P < 0.001$) (mean of 3 495 kg/ha) for all 143 burn plots in the Eastern Cape montane grassland sites (**FIGURE 4.9**).

Simulated (n = 143) and observed (n = 28) rates of spread (km/h) relationship with effective slope gradient (%), for entire (A) and subsample (B) dataset, are shown in (**FIGURE 4.10**).

The distribution of fire spread types along a range of effective slope gradients (%), for 143 fires in mesic montane grasslands of the Eastern Cape, is shown in (**FIGURE 4.11**). Head fire spread did not occur below -25% effective gradient. Back fire spread did not occur above 23% effective gradient.

Byram's (1959), fireline intensity versus three alternative methods of fireline intensity determination — steam releasing open-can calorimetry (Hydropyrometer); Byram's (1959) flame length – fireline intensity correlation equation; & Byram's (1959) fireline intensity equation using fuel consumed (severity) as an input value in place of fuel load — for 143 fires in Eastern Cape montane grassland vegetation are shown in **FIGURE 4.12**. Alternatively derived fireline intensity (linear regression) performance of three alternative methods is summarised in **TABLE 4.5**. As with modelled ROS, adjusted R^2 values cannot be taken in isolation and need to be considered in combination with linear regression intercepts and slope coefficients. Perfect agreement is indicated by an R^2 value of one, an intercept of zero, and a slope coefficient of one.

While none of the three alternative methods of fireline intensity determination performed particularly well against Byram's (1959) fireline intensity for the 143 fires in Eastern Cape Montane grassland vegetation, the steam releasing open-can calorimetry (Hydropyrometer) method performed the best (**A** in **FIGURE 4.12**).

All three alternative methods of fireline intensity determination underestimated fire Byram's (1959) fireline intensity.

Observed flame length versus post-fire char height and double (2x) char height for 83 fires is shown in **FIGURE 4.22**. See **Section 4.4.4, *Modelled flame length*** for further details on height of char.

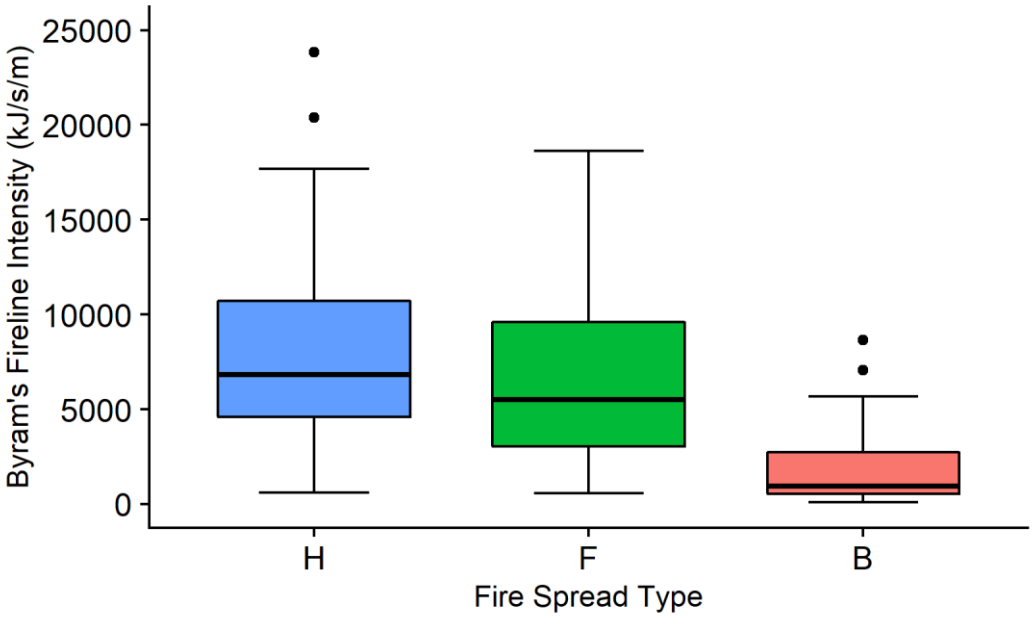

FIGURE 4.8: *Boxplot comparing Byram's (1959) fireline intensity (kJ/s/m) values between head (H), back (B), and flank (F) fire spread types, from 143 fires in Eastern Cape mesic montane grasslands.*

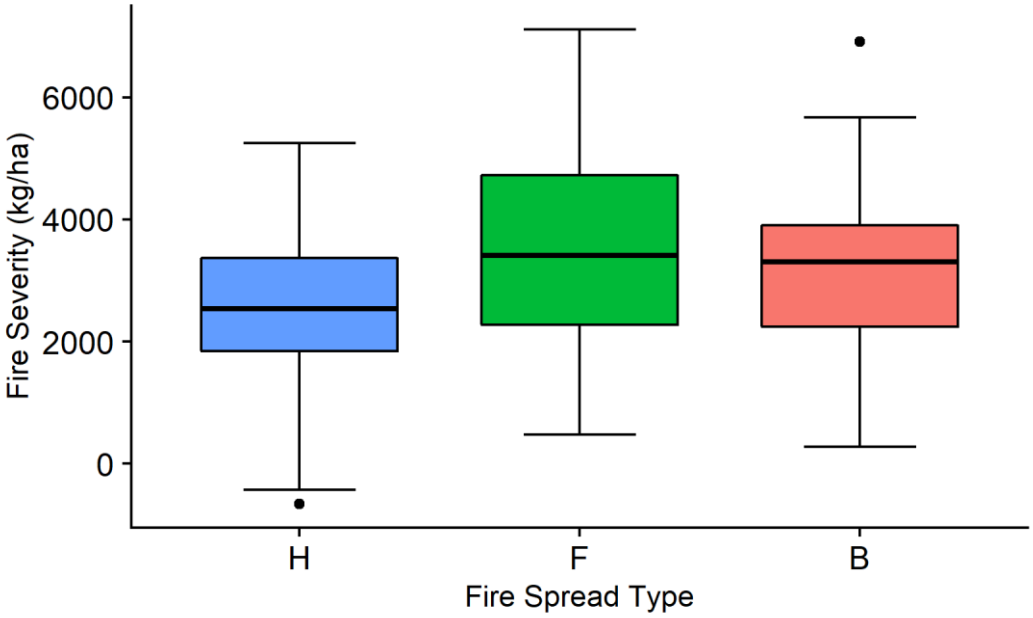

FIGURE 4.9: *Boxplot comparing fire severity (kg/ha) (fuel consumed) values, estimated using a disc pasture meter (Bransby & Tainton, 1977), between head (H), back (B), and flank (F) fire spread types, from 143 fires in Eastern Cape mesic montane grasslands.*

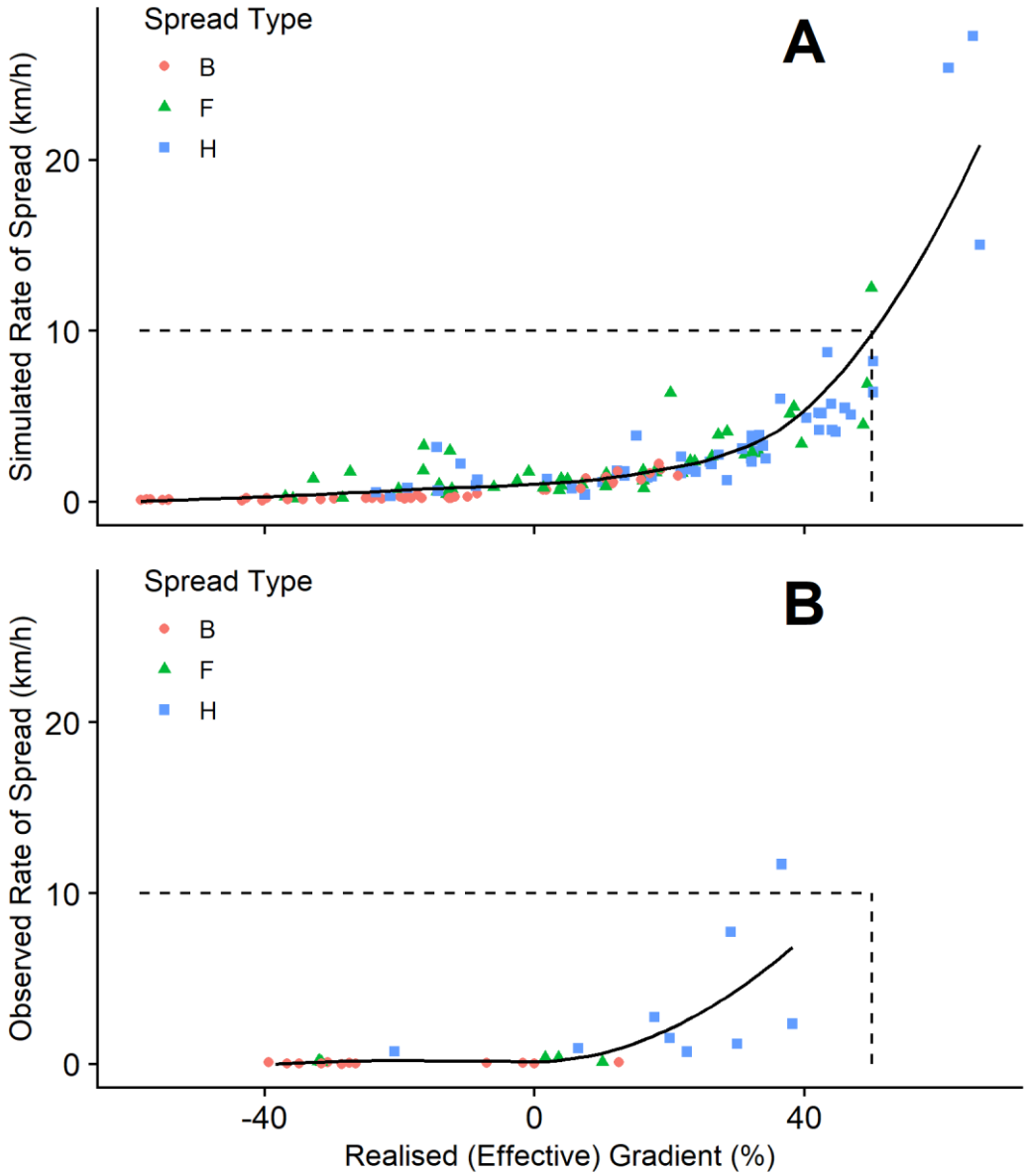

FIGURE 4.10: *Realised (effective) gradient (%) versus (A) simulated rate of spread (km/h) for 143 fires in Eastern Cape mesic montane grasslands, and (B) observed rate of spread (km/h) from subsample dataset of 28 fires in Eastern Cape mesic montane grasslands. Simulated values generated from McArthur Mk5 spread model, using field sampled value of dead fuel moisture content, with the slope factor correction function (Noble et. al., 1980) applied. Solid lines indicate general trend of data. Dashed lines indicate same position of 50% effective gradient and 10 km/h rate of spread.*

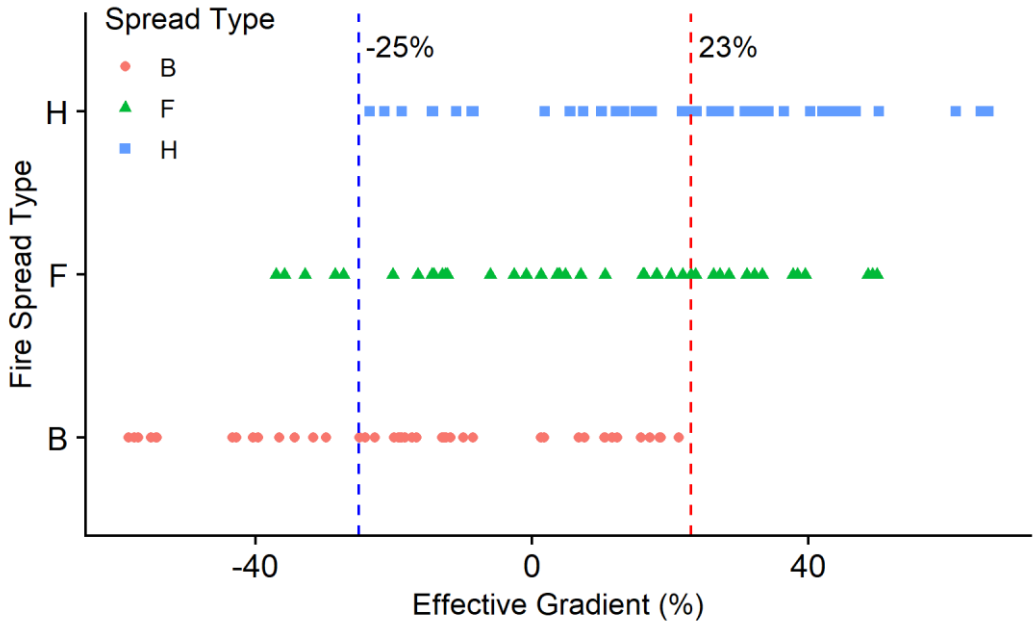

FIGURE 4.11: *Scatterplot showing distribution of fire spread types (head (H), back (B), & flank (F)) along a range of effective gradient (%), for 143 fires in Eastern Cape mesic montane grasslands. Vertically positioned dashed lines (blue & red) indicate potential effective gradient thresholds for head (-25%) and back (23%) fire spread, respectively.*

TABLE 4.5: *Alternatively derived fireline intensity linear regression performance of three alternative methods of fireline intensity determination against Byram's (1959) fireline intensity for 143 fires in Eastern Cape montane grassland vegetation. Alternative methods: Steam releasing open-can calorimetry (Hydropyrometers); Byram's (1959) flame length – fireline intensity correlation equation; & Byram's (1959) fireline intensity equation using fuel consumed (severity) as an input value in place of fuel load.*

Method of Intensity Determination	Adjusted R^2 Value	Intercept	Slope Coefficient
Steam releasing open-can calorimetry (Hydropyrometer).	0.9397	1121.0	1.113
Byram's flame length correlation.	0.3367	3651.8	1.376
Byram's fireline intensity equation using fuel consumed in place of fuel load.	0.8905	-263.75	2.381

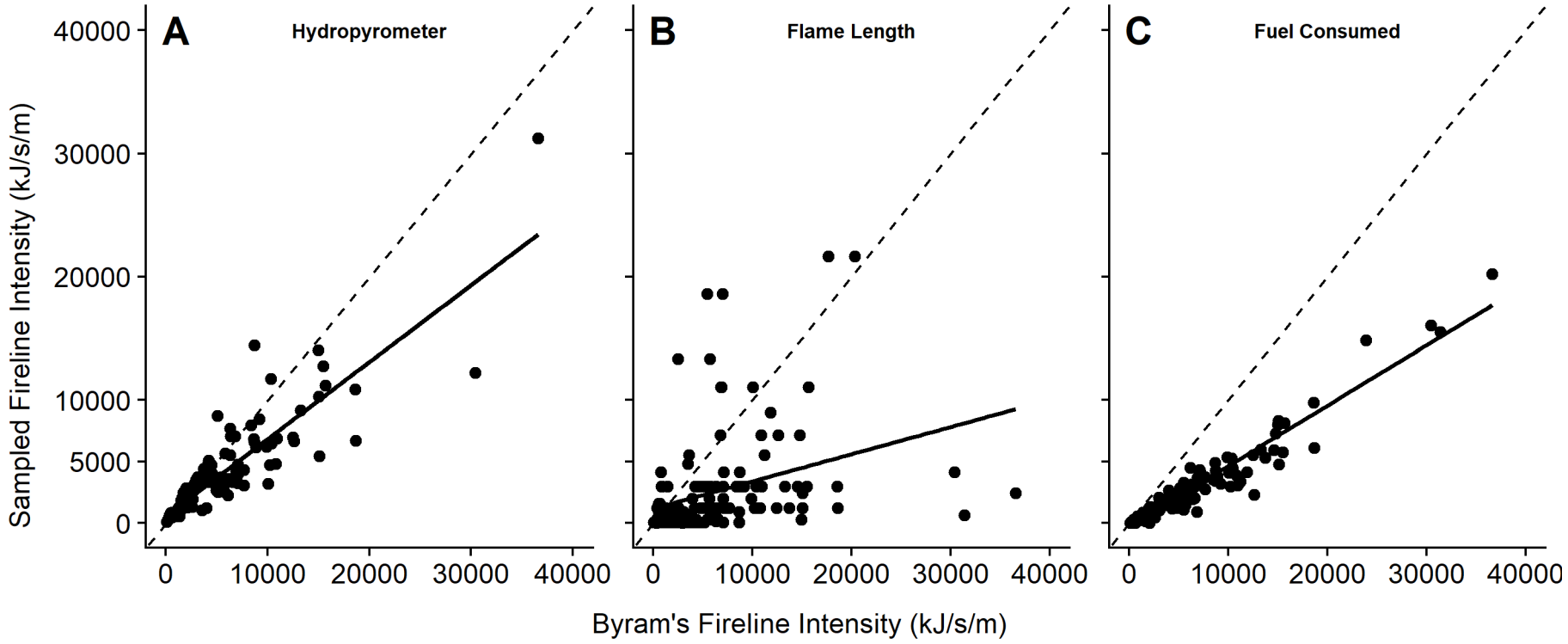

FIGURE 4.12: *Byram's (1959), fireline intensity versus three alternative methods of fireline intensity determination for 143 fires in Eastern Cape montane grassland vegetation. Dashed lines indicate perfect agreement between Byram's (1959), fireline intensity and alternative method values. Solid lines are linear regressions. Refer to* ***TABLE 4.5*** *for slope and coefficient values. Various methods of fireline intensity determination A-C: (A): Steam releasing open-can calorimetry (Hydropyrometer). (B): Byram's (1959) flame length – fireline intensity correlation equation. (C): Byram's (1959) fireline intensity equation using fuel consumed (severity) as an input value in place of fuel load. Axis scaled down to 40 000 kJ/s/m for visual enhancement. Several observations lie outside of graph area but are still included in analyses.*

4.4.3 Modelled fire intensity:

Byram's (1959), fireline intensity versus simulated values for 143 fires in Eastern Cape montane grassland vegetation, from various fuel configurations of BehavePlus V6.0.0 (Andrews & Bevins, 2018) and Rothereml (1972) R package (Vacchiano & Ascoli, 2015) fire behaviour prediction models are shown in **FIGURE 4.13** & **FIGURE 4.14** respectively. Fireline intensity prediction model (linear regression) performance of 13 model configurations is summarised in **TABLE 4.6**. As with modelled ROS, adjusted R^2 values cannot be taken in isolation and need to be considered in combination with linear regression intercepts and slope coefficients. Perfect agreement is indicated by an R^2 value of one, an intercept of zero, and a slope coefficient of one. None of the 13 model configurations performed well against Byram's (1959) fireline intensity for the 143 10 x 10 m fire plots in Eastern Cape Montane grassland vegetation. In fact, all the fire intensity model configurations used in this study performed simulated particularly badly when simulating Byram's (1959), fireline intensity (**TABLE 4.6**).

Looking at BehavePlus and Rothermel fireline intensity model configurations which require dead fuel MOE and 1h & live fuel SA/V ratio as input variables. Fuel scenarios with 30% dead fuel MOE (**B, D**, & **F** in **FIGURE 4.13** & **FIGURE 4.14**) produced partially better fits to Byram's (1959), fireline intensity than 20% dead fuel MOE scenarios (**A, C**, & **E** in **FIGURE 4.13** & **FIGURE 4.14**) for both BehavePlus and Rothermel model configurations in 143 fires in Eastern Cape Montane grassland vegetation. No significant differences ($P > 0.1$) were observed between different SA/V fuel scenarios when simulating fireline intensity from both BehavePlus and Rothermel fire models for 143 fires in Eastern Cape Montane grassland vegetation (**FIGURE 4.13** & **FIGURE 4.14**).

Rothermel fireline intensity model configurations' regression equations (**FIGURE 4.14** & **TABLE 4.6**) produced perhaps marginally better fits to Byram's (1959), fireline intensity than BehavePlus model configurations (**FIGURE 4.13** & **TABLE 4.6**).

Similar to the BehavePlus and Rothermel intensity models, W.S.W Trollope's (2004), regression did not predict well for Byram's (1959), fireline intensity ($y = 3.132x - 1024.5$, where y is the simulated and x is the calculated fireline intensity; $R^2 = 0.094$) (**TABLE 4.6**).

Despite underpredicting fireline intensity as a whole, Rothermel configurations simulated fireline intensity better for flank fire scenarios than head and back fire scenarios (overpredicted for flank fire scenarios in comparison to head fire scenarios) (**FIGURE 4.15**).

For both BehavePlus and Rothermel fireline intensity model configurations, Site 7 (Winterberg) fireline intensity observations and simulated outputs were far removed from the other six sites (**FIGURE 4.16**). Several outliers may be responsible for this outcome.

On the whole, fire behaviour prediction models (BehavePlus, Rothermel, & Trollope (2004) regression) underestimated when simulating for fireline intensity (**FIGURE 4.13** & **FIGURE 4.14**).

TABLE 4.6: *Fireline intensity simulation model linear regression performance of 13 model configurations against Byram's (1959) fireline intensity for 143 fires in Eastern Cape montane grassland vegetation. Nineteen configurations were adapted from five pre-existing models. For details on Intensity Model Configuration codes, refer to* ***TABLE 4.3****.*

Intensity Model Configuration	Adjusted R^2 Value	Intercept	Slope Coefficient
BH20_4949	0.2894	4686.0857	2.5375
BH20_6649	0.2566	5143.9497	1.7139
BH20_6659	0.2532	5182.4346	1.6681
BH30_4949	0.2934	3852.2747	1.9867
BH30_6659	0.2603	4485.8525	1.3391
BH30_6659	0.2567	4542.5160	1.3020
RT20_4949	0.3994	3182.2092	2.9636
RT20_6649	0.3662	3695.3068	2.0716
RT20_6659	0.3627	3737.7915	2.0242
RT30_4949	0.4295	1389.1517	2.3887
RT30_6649	0.3928	2184.6393	1.6652
RT30_6659	0.3890	2256.8550	1.6260
WSWT04	0.09446	-1024.5089	3.1321

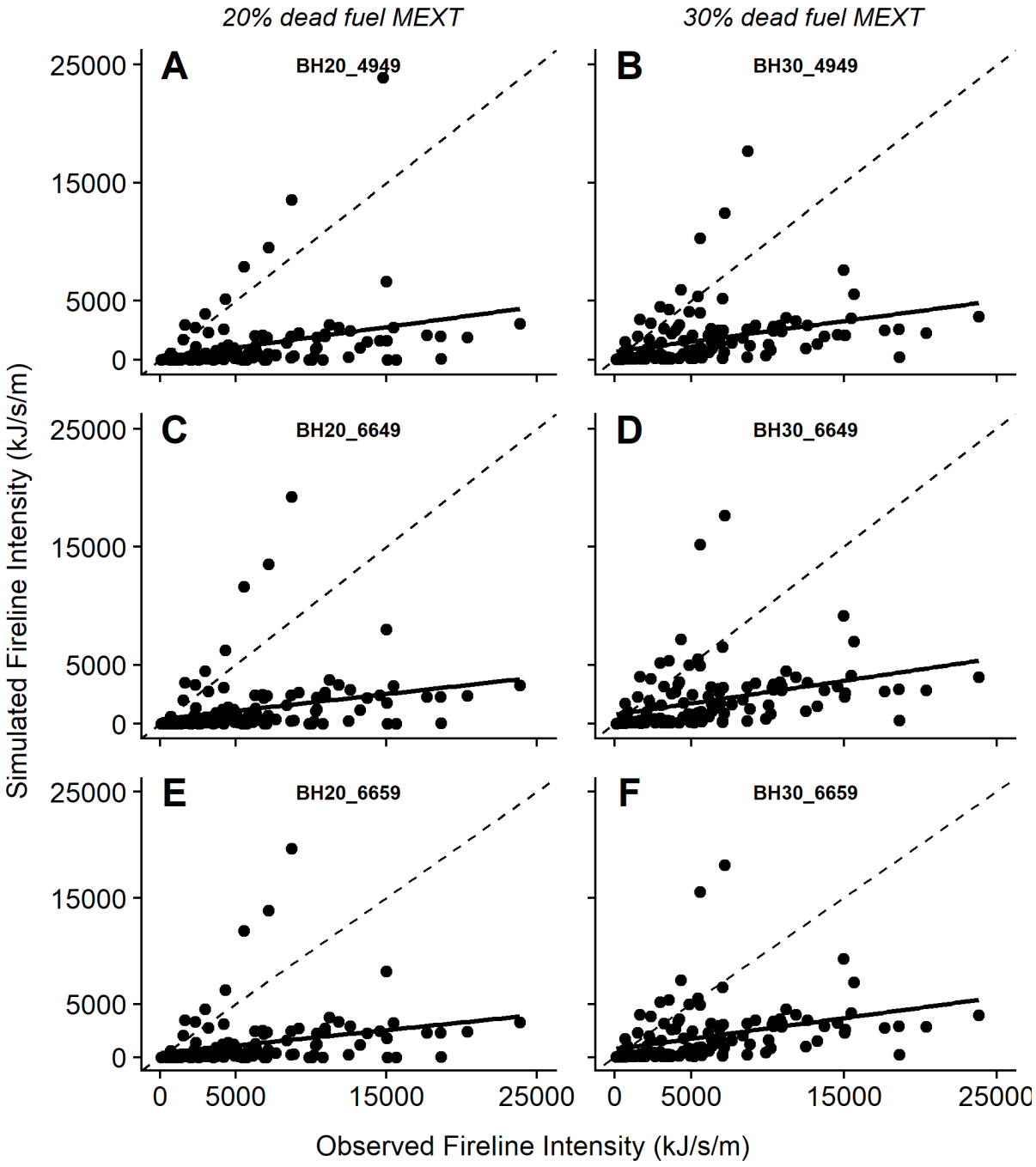

FIGURE 4.13: *Comparison of intensity model performance between six BehavePlus V6.0.0 fuel configurations. Byram's (1959), fireline intensity versus simulated outputs for 143 fires in Eastern Cape montane grassland vegetation. 20% dead fuel moisture of extinction (MOE) left, 30% dead fuel MOE right. Dashed lines indicate perfect agreement between Byram's (1959), fireline intensity and simulated values. Solid lines are linear regressions, details of which are shown in* ***TABLE 4.6****. Various BehavePlus fuel model configurations A-F: (A): Dead fuel moisture of extinction (MOE): 20%, surface area to volume ratio (SA/V) of dead component: 4900 m^2/m^3, SA/V of live component: 4900 m^2/m^3. (B): Dead fuel MOE: 30%, SA/V of dead component: 4900 m^2/m^3, SA/V of live component: 4900 m^2/m^3. (C): Dead fuel MOE: 20%, SA/V of dead component: 6600 m^2/m^3, SA/V of live component: 4900 m^2/m^3. (D): Dead fuel MOE: 30%, SA/V of dead component: 6600 m^2/m^3, SA/V of live component: 4900 m^2/m^3. (E): Dead fuel MOE: 20%, SA/V of dead component: 6600 m^2/m^3, SA/V of live component: 5900 m^2/m^3. (F): Dead fuel MOE: 30%, SA/V of dead component: 6600 m^2/m^3, SA/V of live component: 5900 m^2/m^3. Axis scaled down to 25 000 kJ/s/m for visual enhancement. Several observations lie outside of graph area but are still included in analyses.*

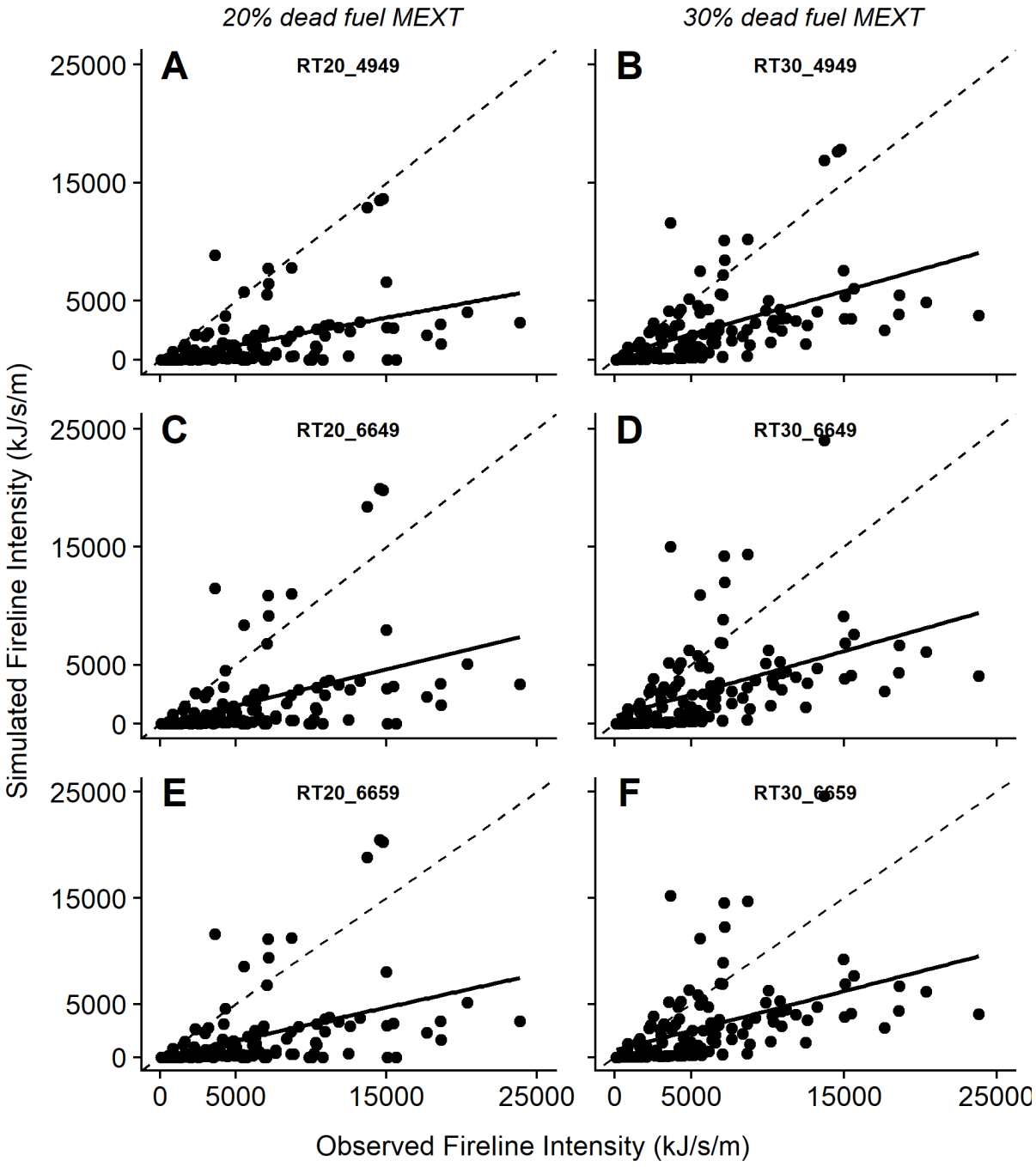

FIGURE 4.14: *Comparison of intensity model performance between six Rothermel (1972) (Vacchiano & Ascoli, 2015), fuel configurations. Byram's (1959), fireline intensity versus simulated outputs for 143 fires in Eastern Cape montane grassland vegetation. 20% dead fuel moisture of extinction (MOE) left, 30% dead fuel MOE right. Dashed lines indicate perfect agreement between Byram's (1959), fireline intensity and simulated values. Solid lines are linear regressions. Various Rothermel fuel model configurations A-F: (A): Dead fuel moisture of extinction (MOE): 20%, surface area to volume ratio (SA/V) of dead component: 4900 m^2/m^3, SA/V of live component: 4900 m^2/m^3. (B): Dead fuel MOE: 30%, SA/V of dead component: 4900 m^2/m^3, SA/V of live component: 4900 m^2/m^3. (C): Dead fuel MOE: 20%, SA/V of dead component: 6600 m^2/m^3, SA/V of live component: 4900 m^2/m^3. (D): Dead fuel MOE: 30%, SA/V of dead component: 6600 m^2/m^3, SA/V of live component: 4900 m^2/m^3. (E): Dead fuel MOE: 20%, SA/V of dead component: 6600 m^2/m^3, SA/V of live component: 5900 m^2/m^3. (F): Dead fuel MOE: 30%, SA/V of dead component: 6600 m^2/m^3, SA/V of live component: 5900 m^2/m^3. Axis scaled down to 25 000 kJ/s/m for visual enhancement. Several observations lie outside of graph area but are still included in analyses.*

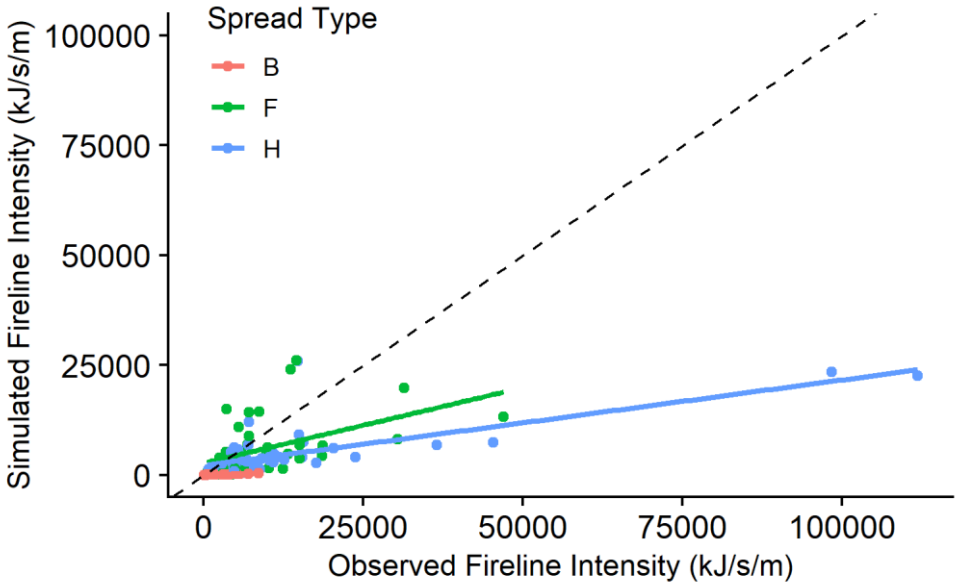

FIGURE 4.15: *Byram's (1959), fireline intensity versus simulated outputs from Rothermel (1972) (Vacchiano & Ascoli, 2015), fire behaviour model separated by fire spread type (head, back, or flank), for 143 fires in Eastern Cape montane grassland vegetation. Dashed line indicates perfect agreement between Byram's (1959), fireline intensity and simulated values. Solid lines are linear regressions for each fire spread type (head, back, or flank). Fuel model configuration: RT30_6649; dead fuel moisture of extinction: 30%; surface area to volume ratio (SA/V) of dead component: 6600 m^2/m^3, SA/V of live component: 4900 m^2/m^3.*

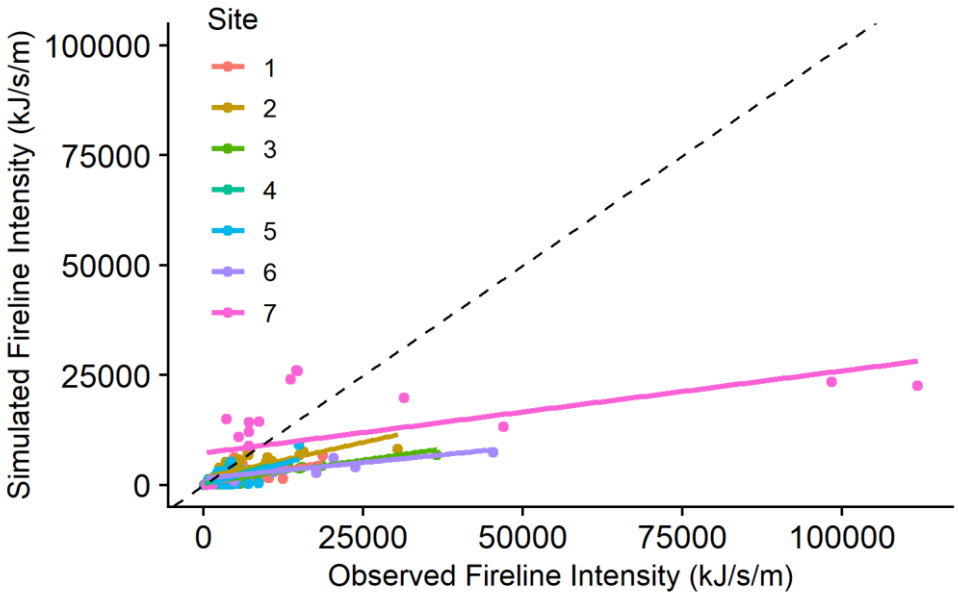

FIGURE 4.16: *Byram's (1959), fireline intensity versus simulated outputs from Rothermel (1972) (Vacchiano & Ascoli, 2015), fire behaviour model, separated by site, for 143 fires in Eastern Cape montane grassland vegetation. Dashed line indicates perfect agreement between Byram's (1959), fireline intensity and simulated values. Solid lines are linear regressions for each site 1-7. Fuel model configuration: RT30_6649; dead fuel moisture of extinction: 30%; surface area to volume ratio (SA/V) of dead component: 6600 m^2/m^3, SA/V of live component: 4900 m^2/m^3.*

4.4.4 Modelled flame length:

Observed flame length versus simulated values for 143 fires in Eastern Cape montane grassland vegetation, from various configurations of McArthur Mk5 (McArthur, 1977), BehavePlus V6.0.0 (Andrews & Bevins, 2018), and Rothereml (1972) R package (Vacchiano & Ascoli, 2015) flame length prediction models are shown in **FIGURE 4.17**, **FIGURE 4.18**, & **FIGURE 4.19** respectively. Flame length prediction model (linear regression) performance of 16 model configurations is summarised in **TABLE 4.7**. Additionally, Lowveld (Government Gazette Notice 1099 of 2013) FDI score associated flame length prediction as well as post-fire height of char and double (2x) char height versus observed flame length linear regression performance are also summarised in **TABLE 4.7**. As with modelled ROS and fireline intensity, adjusted R^2 values cannot be taken in isolation and need to be considered in combination with linear regression intercepts and slope coefficients. Perfect agreement is indicated by an R^2 value of one, an intercept of zero, and a slope coefficient of one. None of the 16 model configurations performed particularly well against observed flame length of the 143 10 x 10 m fire plots in Eastern Cape Montane grassland vegetation.

McArthur Mk 5 flame length model configurations did not perform better (when compared to observed flame lengths) when slope correction factor functions were applied (**B** & **D** in **FIGURE 4.17**). In fact, if anything, McAthur Mk 5 model configurations performed better (when compared to observed flame lengths) without slope correction factor functions were applied (**A** & **C** in **FIGURE 4.17**) for 143 fires in Eastern Cape Montane grassland vegetation.

Looking at BehavePlus and Rothermel flame length model configurations, which require dead fuel MOE and 1h & live fuel SA/V ratio as input variables. Fuel scenarios with 30% dead fuel MOE (**B, D**, & **F** in **FIGURE 4.18** & **FIGURE 4.19**) produced significantly better fits to observed flame lengths than 20% dead fuel MOE scenarios (**A, C**, & **E** in **FIGURE 4.18** & **FIGURE 4.19**) for both BehavePlus and Rothermel model configurations in 143 fires in Eastern Cape Montane grassland vegetation. No significant differences were observed ($P > 0.25$) between different SA/V fuel scenarios when simulating flame length from both BehavePlus and Rothermel fire models for 143 fires in Eastern Cape Montane grassland vegetation (**FIGURE 4.18** & **FIGURE 4.19**).

Rothermel flame length model configurations' regression equations (**FIGURE 4.19** & **TABLE 4.7**) produced marginally better fits to observed flame lengths than BehavePlus model configurations (**FIGURE 4.18** & **TABLE 4.7**). Both BehavePlus and Rothermel flame length model configurations performed particularly badly when simulating back fire flame lengths, compared to head and flank fire scenarios (**FIGURE 4.20**).

Lowveld FDI score associated flame length predictions did not fit well with observed flame lengths from 143 fires in Eastern Cape Montane grassland vegetation (**FIGURE 4.21** & **TABLE 4.7**). Lowveld FDI associated flame lengths mostly under-predicted observed flame length for head fire scenarios.

Observed flame length versus post-fire char height and double (2x) char height for 83 fires in Eastern Cape Montane grassland vegetation is shown in **FIGURE 4.22**. Double (2x) char height produced a more precise fit to observed flame lengths ($y = 0.711x + 0.971$; $R^2 = 0.609$) than char height itself, particularly in head fire scenarios, showing a strong positive correlation (rho = 0.807; $P < 0.001$). Back fire char heights and double (2x) char heights did not show any significant association with flame lengths (rho < 0.15; $P > 0.567$). Double (2x) char height in flank fires appeared to have a moderate positive correlation with flame length (rho = 0.532; $P < 0.005$).

TABLE 4.7: *Predicted flame length linear regression performance of 16 simulation model configurations and Lowveld (Government Gazette Notice 1099 of 2013) FDI associated flame lengths for 143 fires in Eastern Cape montane grassland vegetation. For details on Flame Length Model Configuration codes, refer to* ***TABLE 4.3****. Char height was recorded on pre-planted fence posts and compared to corresponding observed flame length for 83 fires. Double (2x) char height was also compared to corresponding observed flame length.*

Flame Length Model Configuration	Adjusted R^2 Value	Intercept	Slope Coefficient
McA_Mk5	0.0731	2.00895	0.19702
McA_Mk5_Slp	0.3089	1.86475	0.11976
McA_Mk5_DFM	0.0758	1.80145	0.14645
McA_Mk5_DFM_Slp	0.3531	1.63236	0.08543
BH20_4949	0.0416	1.99339	0.22806
BH20_6649	0.0408	2.00896	0.19868
BH20_6659	0.0412	2.00780	0.19870
BH30_4949	0.2609	1.00600	0.65280
BH30_6659	0.2530	1.09473	0.55942
BH30_6659	0.2486	1.10697	0.55093
RT20_4949	0.1332	1.65901	0.44032
RT20_6649	0.1301	1.69213	0.38241
RT20_6659	0.1301	1.69484	0.37948
RT30_4949	0.3382	0.85544	0.64629
RT30_6649	0.3199	0.95738	0.54587
RT30_6659	0.3190	0.96610	0.54070
Lowveld FDI predicted flame length	0.0396	1.54950	0.57890
Char height	0.6091	0.97120	1.42190
2x char height*	**0.6091***	**0.97115***	**0.71093***

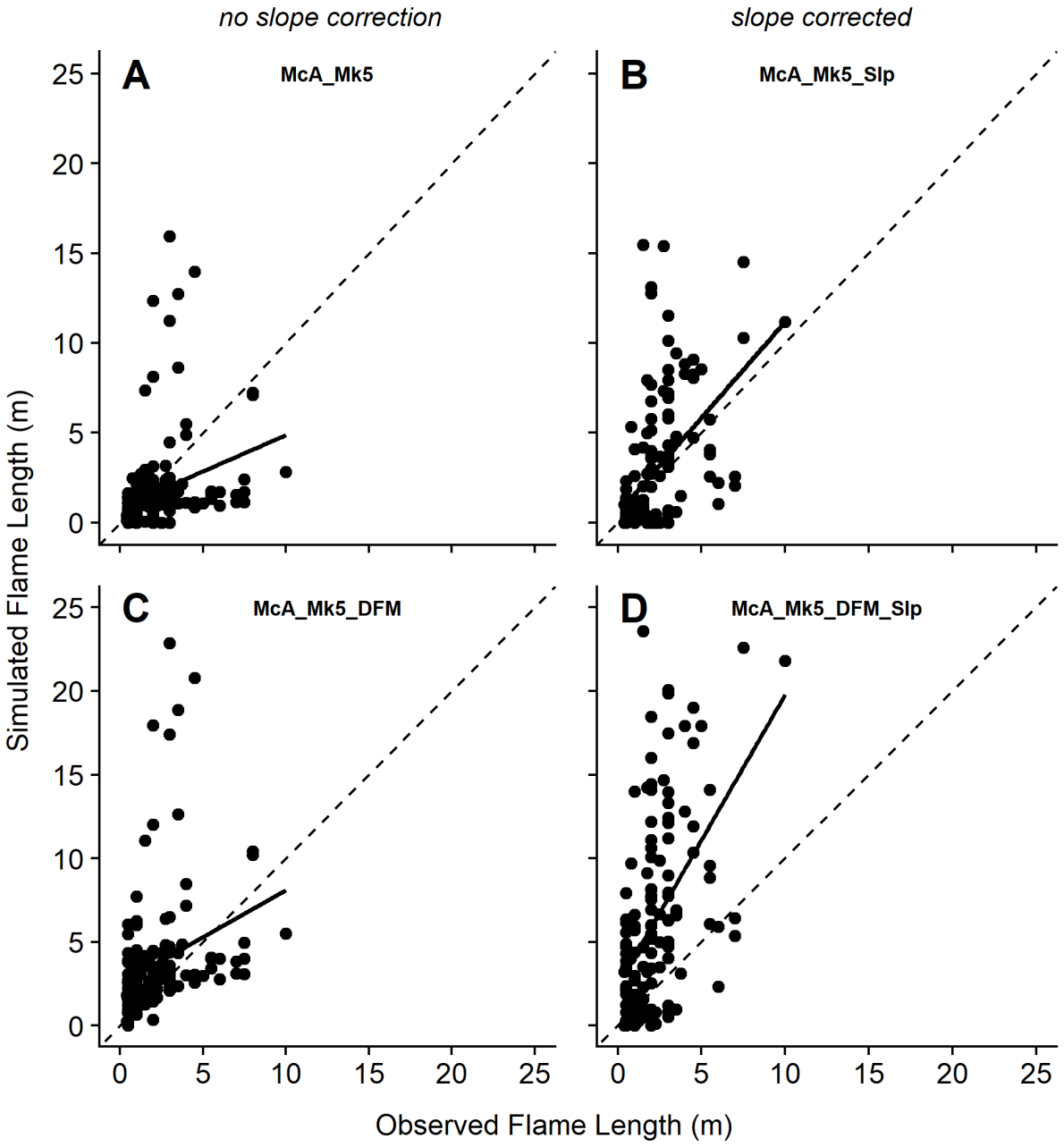

FIGURE 4.17: *Comparison of flame length model performance between four McArthur Mk5 model configurations. Observed flame length versus simulated outputs for 143 fires in Eastern Cape montane grassland vegetation. Dashed lines indicate perfect agreement between observed flame length and simulated values. Solid lines are linear regressions, details of which are shown in* ***TABLE 4.7****. Various McArthur model configurations A-D: (A): McArthur Mk5 flame length model, using built-in function for fuel moisture determination, no slope factor function applied. (B): McArthur Mk5 flame length model, using built-in function for fuel moisture determination, with a slope correction factor function (Noble et. al., 1980) applied. (C): McArthur Mk5 flame length model, using field sample value of dead fuel moisture content, no slope factor function applied. (D): McArthur Mk5 flame length model, using field sample value of dead fuel moisture content, with a slope correction factor function (Noble et. al., 1980) applied. Axis scaled down to 25 m for visual enhancement. Several observations lie outside of graph area but are still included in analyses.*

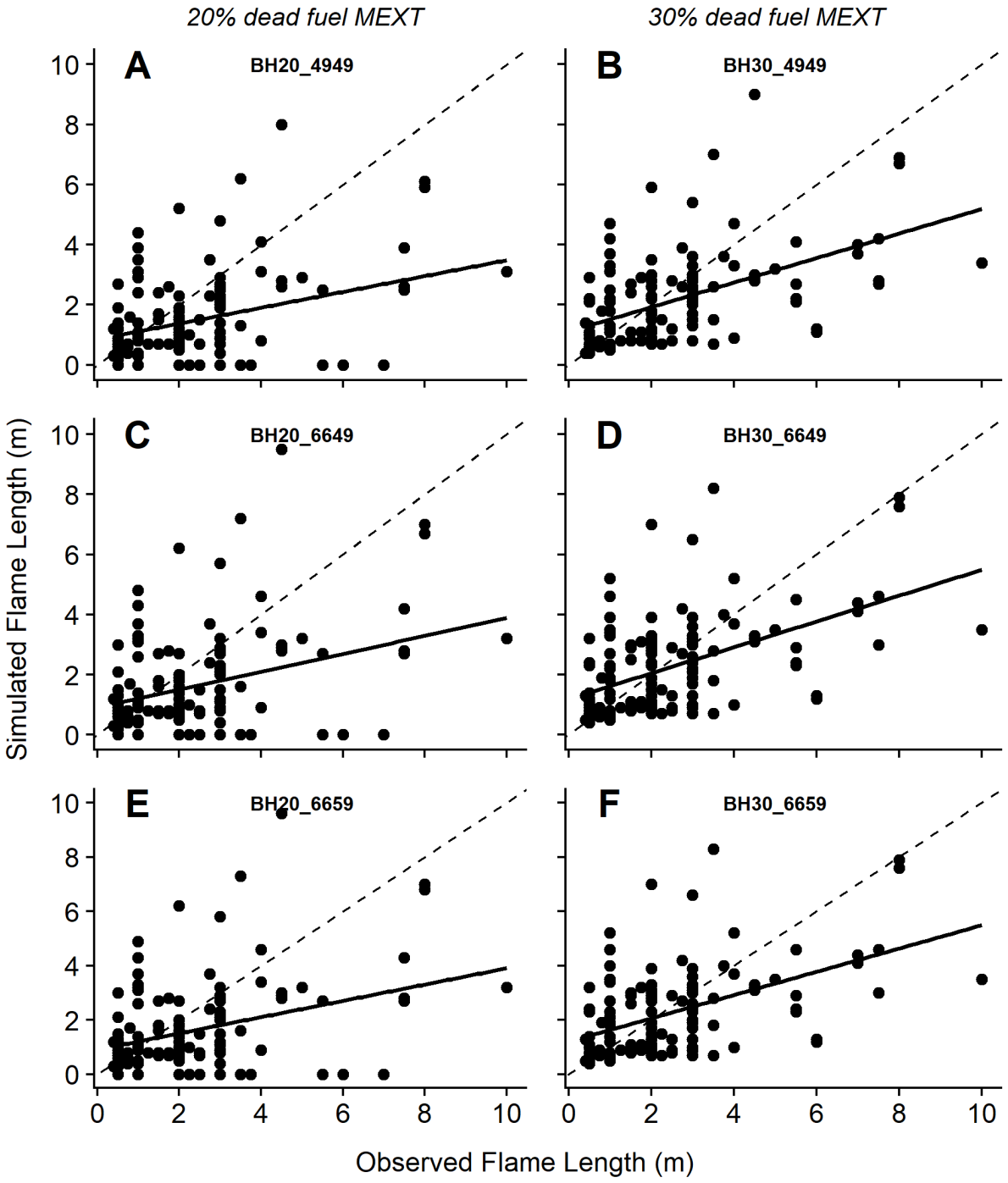

FIGURE 4.18: *Comparison of flame length model performance between six BehavePlus V6.0.0, fuel configurations. Observed flame length versus simulated outputs for 143 fires in Eastern Cape montane grassland vegetation. 20% dead fuel moisture of extinction (MOE) left, 30% dead fuel MOE right. Dashed lines indicate perfect agreement between observed flame length and simulated values. Solid lines are linear regressions, details of which are shown in* ***TABLE 4.7****. Various BehavePlus fuel model configurations A-F: (A): Dead fuel moisture of extinction (MOE): 20%, surface area to volume ratio (SA/V) of dead component: 4900 m^2/m^3, SA/V of live component: 4900 m^2/m^3. (B): Dead fuel MOE: 30%, SA/V of dead component: 4900 m^2/m^3, SA/V of live component: 4900 m^2/m^3. (C): Dead fuel MOE: 20%, SA/V of dead component: 6600 m^2/m^3, SA/V of live component: 4900 m^2/m^3. (D): Dead fuel MOE: 30%, SA/V of dead component: 6600 m^2/m^3, SA/V of live component: 4900 m^2/m^3. (E): Dead fuel MOE: 20%, SA/V of dead component: 6600 m^2/m^3, SA/V of live component: 5900 m^2/m^3. (F): Dead fuel MOE: 30%, SA/V of dead component: 6600 m^2/m^3, SA/V of live component: 5900 m^2/m^3. Axis scaled down to 10 m for visual enhancement. Several observations lie outside of graph area but are still included in analyses.*

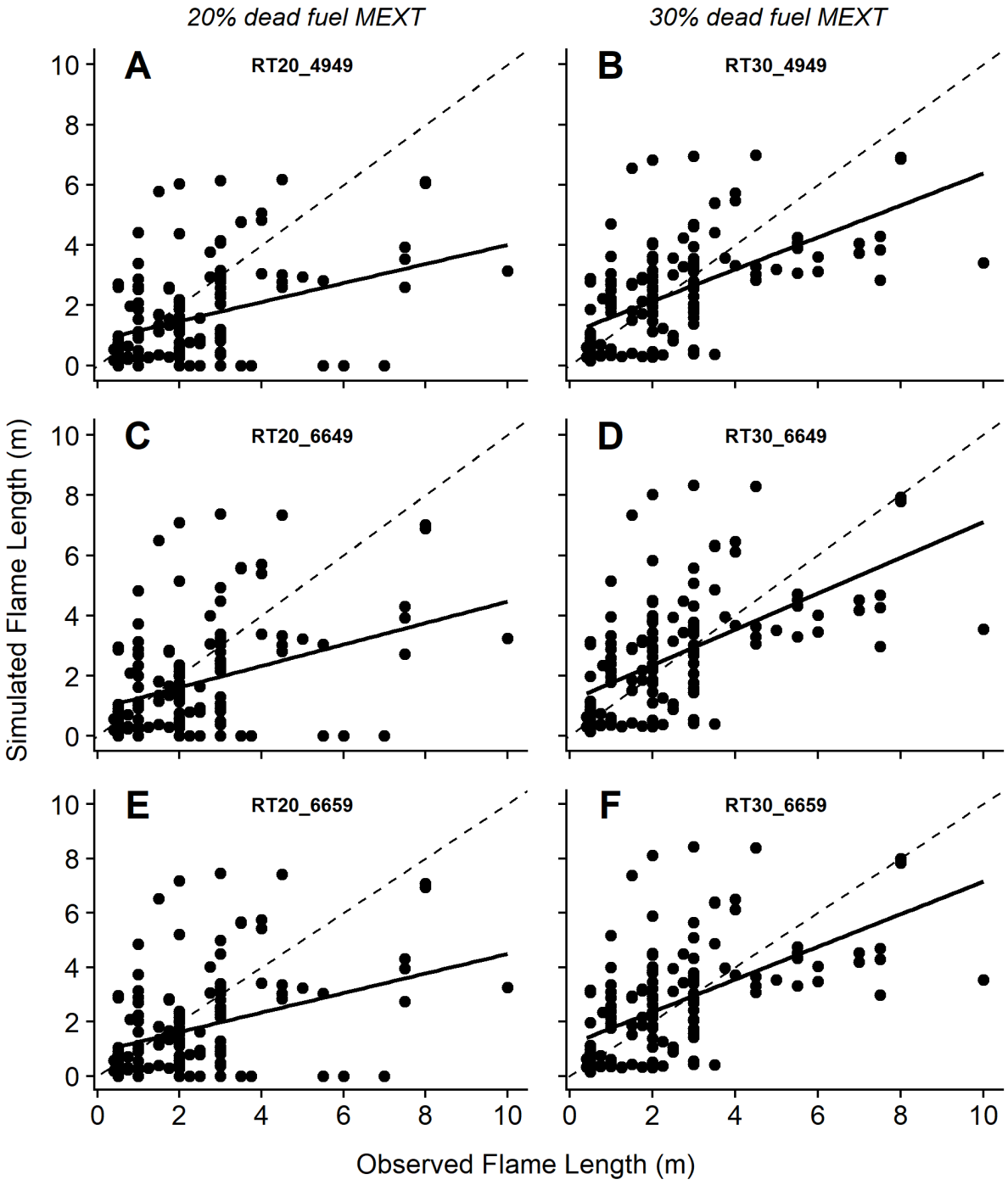

FIGURE 4.19: *Comparison of flame length model performance between six Rothermel (1972) (Vacchiano & Ascoli, 2015), fuel configurations. Observed flame length versus simulated outputs for 143 fires in Eastern Cape montane grassland vegetation. 20% dead fuel moisture of extinction (MOE) left, 30% dead fuel MOE right. Dashed lines indicate perfect agreement between observed flame length and simulated values. Solid lines are linear regressions. Various Rothermel fuel model configurations A-F: (A): Dead fuel moisture of extinction (MOE): 20%, surface area to volume ratio (SA/V) of dead component: 4900 m^2/m^3, SA/V of live component: 4900 m^2/m^3. (B): Dead fuel MOE: 30%, SA/V of dead component: 4900 m^2/m^3, SA/V of live component: 4900 m^2/m^3. (C): Dead fuel MOE: 20%, SA/V of dead component: 6600 m^2/m^3, SA/V of live component: 4900 m^2/m^3. (D): Dead fuel MOE: 30%, SA/V of dead component: 6600 m^2/m^3, SA/V of live component: 4900 m^2/m^3. (E): Dead fuel MOE: 20%, SA/V of dead component: 6600 m^2/m^3, SA/V of live component: 5900 m^2/m^3. (F): Dead fuel MOE: 30%, SA/V of dead component: 6600 m^2/m^3, SA/V of live component: 5900 m^2/m^3.*

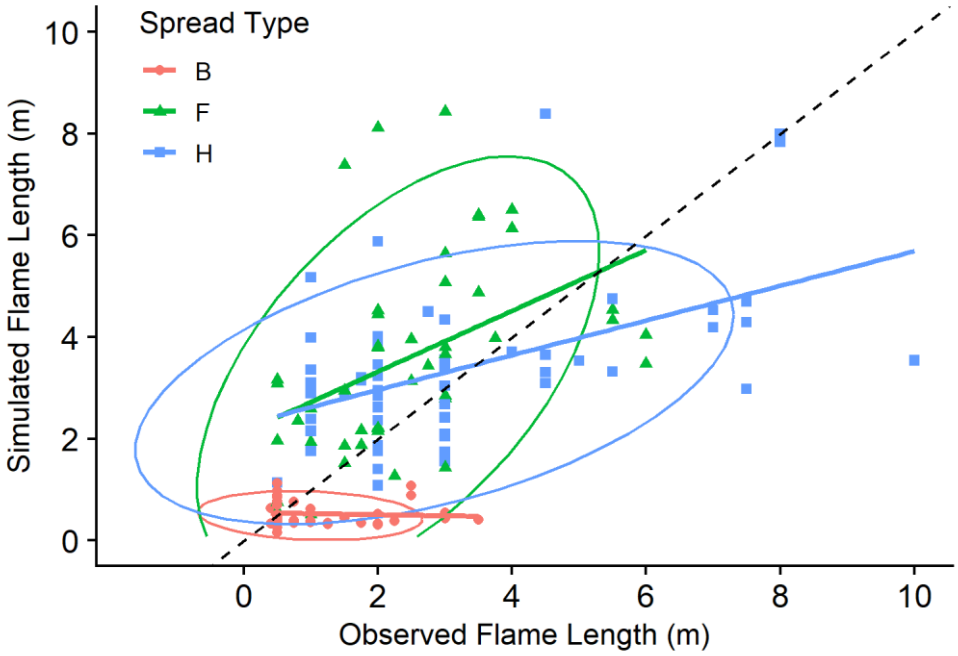

FIGURE 4.20: *Observed flame length versus simulated outputs from Rothermel (1972) (Vacchiano & Ascoli, 2015), fire behaviour model, separated by fire spread type (head, back, or flank), for 143 fires in Eastern Cape montane grassland vegetation. Dashed line indicates perfect agreement between observed flame lengths and simulated values. Solid lines are linear regressions for each fire spread type (head, back, or flank). Ellipses indicate general axis of data point distribution for each fire spread type. Fuel model configuration: RT30_6659, details can be found in* ***TABLE 4.3****.*

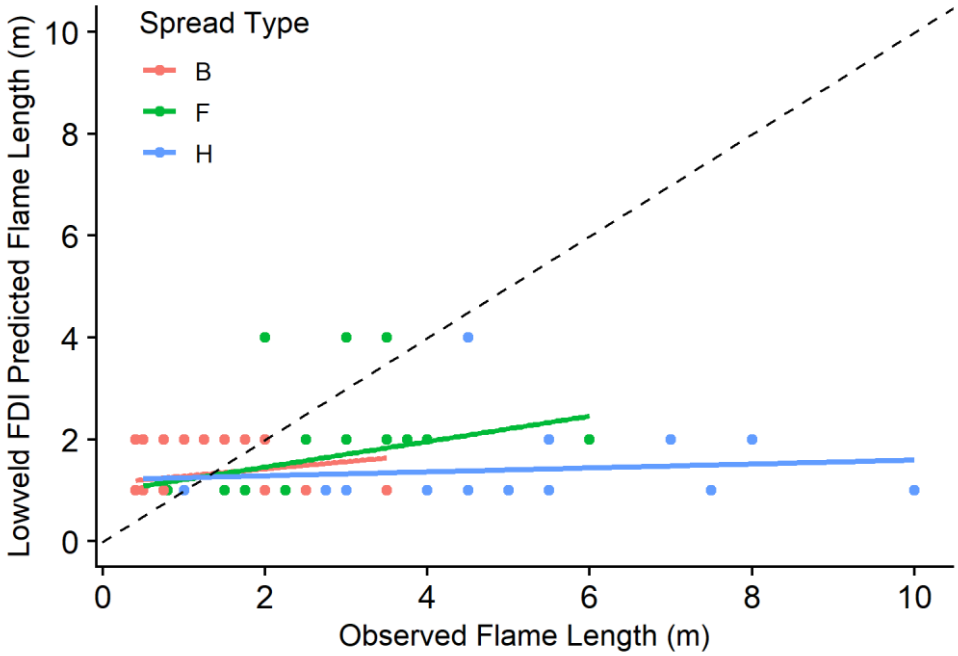

FIGURE 4.21: *Observed flame lengths versus Lowveld (Government Gazette Notice 1099 of 2013) FDI score associated flame lengths, separated by fire spread type (head, back, or flank), for 143 fires in Eastern Cape montane grassland vegetation. Dashed line is the line of perfect agreement between observed flame length and predicted values. Solid lines are linear regressions for each fire spread type (head, back, or flank).*

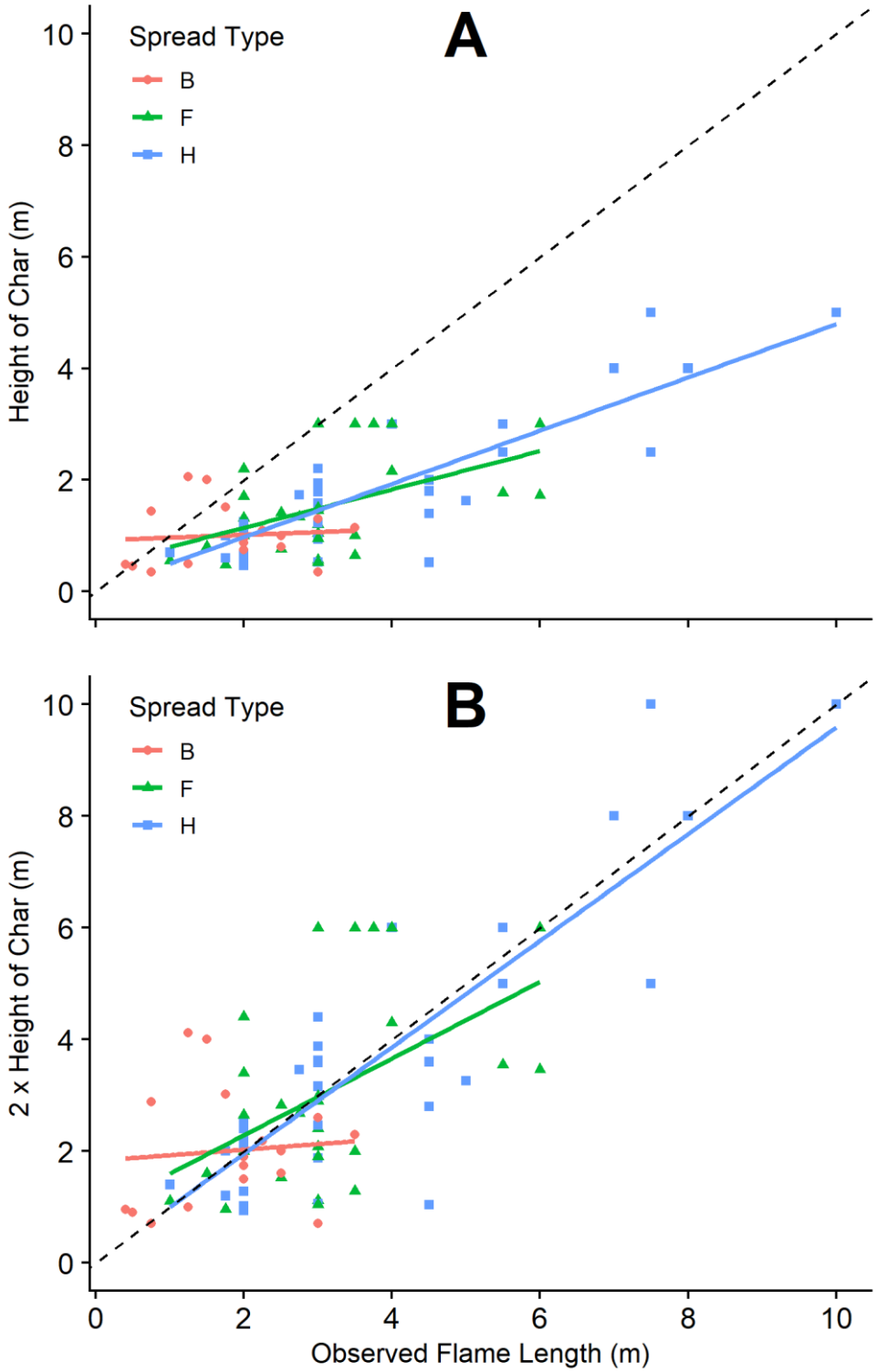

FIGURE 4.22: *Observed flame lengths versus height of charring (A) & double (2x) the height of charring (B) measured on pre-planted fence poles, separated by fire spread type (head, back, or flank), for 83 fires in Eastern Cape montane grassland vegetation. Dashed lines indicate perfect agreement between observed flame lengths and char height values. Solid lines are linear regressions for each fire spread type (head, back, or flank). Linear regression for all observations in scatterplot A: $y = 1.42x + 0.971$; $R^2 = 0.609$, where y is char height and x is the observed flame length. Linear regression for all observations in scatterplot B: $y = 0.71x + 0.971$; $R^2 = 0.609$, where y is double (2x) char height and x is the observed flame length. Smaller sample size (n = 83) due to absence of charring on fence posts in 60 fires.*

4.5 Discussion:

4.5.1 Rate of spread:

Rate of spread (ROS) is an important measure of fire behaviour for both scientific and practical purposes. However, measuring ROS in wildland fires can be a challenging task, especially for multiple burn plots (up to 22), over a large area (~100 ha), in a rugged landscape, as was the case in the study sites of this project (Boschberg, Katberg, & Winterberg). To overcome the challenges of sampling ROS, it was decided that ROS would be simulated, from an appropriate spread model, chosen from a selection of spread models, verified against a subsample dataset (n = 28) of observed ROS. An additional three models (one linear and two general additive models (GAM's)) were also constructed using observed data from the subsample dataset. It is recognised that the subsample dataset (n = 28) did not have enough observations from which to construct accurate linear or GAM ROS models for the montane grassland study sites of this study. And indeed, the three constructed models were almost certainly not suitable to simulate ROS from (**TABLE 4.4**). However, while the sample size was not ideal, it was large enough to be used for validation of simulated ROS values from pre-existing models, and aid in the selection of a site appropriate spread model for this study.

It has been noted previously (**Chapter 3)** that the experimental burns in this study were not conducted for the purpose of investigating the proportional influence independent variables (fuel, weather, & topography) have on fire behaviour (this has been done before, and is well documented). Instead, the burns were conducted with the primary purpose of implementing rangeland management practices, as mentioned previously. The consequent restricted range of independent variables (fuel & weather conditions) (due to seasonality, safety, *inter alia*) were suitable, and provided a low indicator variance for this study (**Chapter 5**). It was noted further (**Chapter 3**), that with specific reference to this study's dataset, one should exercise caution when determining the proportion of variation in fire behaviour (intensity, ROS) accounted for by each independent variable (fuel, weather, & topography). (This is because a full range of fuel, weather, and topographical conditions was not accounted for in this study's experimental burns.).

Nevertheless, investigation into the proportion of variation of fire behaviour (ROS) accounted for by each independent variable (fuel, weather & topography), from the subsample dataset (n = 28), was done as an exercise in scientific procedure — good practice when conducting studies relating to wildfire behaviour (see **Section 4.4.1, *Rate of spread***).

The results showed that fire spread type, followed by slope gradient, and air temperature were the three most significant descriptors of ROS for the subsample dataset of 28 fires in Eastern Cape montane grasslands. Note that fire spread type (direction in which flames lean) is a categorization of convective

heat transfer and thus cannot be described by wind direction or effective slope alone. In terms of fire behaviour, fire spread type is therefore considered an input rather than an output.

These results, however, should be interpreted with caution. While fire spread type (convection) was quite appropriately found to be the biggest driver of ROS (Trollope, 1989), we know that, in reality, slope gradient and air temperature are not the greatest predictors of ROS in grassland fires (Cheney *et. al.*, 1993; Trollope *et. al.*, 2004; Cheney & Sullivan, 2008). The restricted range of predictor variables means that the full effects of parameters such as curing (fuel moisture) and relative humidity could not be accounted for. For example, percent curing would be relatively high in spring, before the summer rains, with little deviation between sites. However, when curing is much lower, say towards the end of a wet summer, a green grass sward full of live herbaceous material, will likely not burn, and the dampening effect of fuel moisture will certainly slow rate of spread. So, without conducting burns throughout the year, covering a full range of fuel, weather, and topographical conditions, it is difficult to determine the proportion of influence each predictor variable has on ROS and other fire behavioural parameters.

Nevertheless, for the subsample dataset (under prevailing conditions) of this study, after fire spread type, slope gradient appears to have described ROS best. This is somewhat logical, as the particularly steep gradients and rugged terrain, in combination with relatively mild weather conditions (for obvious safety reasons, wind speeds and temperatures could not be too high, and humidity could not be too low.), prevailing at and during prescribed burns would lead to a more slope driven fire (*i.e.*, slope drives convective movement more than wind).

Slope correction functions were therefore considered to be appropriate inclusions to spread model configurations in this study (**TABLE 4.3**). It should be noted though, that current literature has recognized, that existing slope correction functions may not be as accurate at accounting for influence of slope gradient, as we would like them to be (Weise & Biging, 1997; Sullivan *et. al.*, 2014). With respect to this, they advised that slope correction functions be applied with caution (Sullivan *et. al.*, 2014). Taking into consideration the particularly steep gradients, and extent to which slope might influence fire behaviour in the study sites at Boschberg, Katberg, & Winterberg, it was determined that slope correction functions would be a crucial inclusion and likely to yield more accurate ROS simulations (results) than models without slope correction functions applied (**TABLE 4.3**).

Indeed, this proved to be the case, spread models with slope correction functions applied performed significantly better than model configurations which did not correct for the influence of slope (**FIGURE 4.6** & **TABLE 4.4**).

Nevertheless, all 19 pre-existing model configurations, except one, under-predicted for observed actual ROS for the 28 montane grassland fires in the Eastern Cape.

ROS simulations from the **McArthur Mk5 spread model** (McArthur, 1977), using **field sampled value of dead fuel moisture** (DFM) content, with the **slope factor correction function** (Noble *et. al*., 1980) applied (McA_Mk5_DFM_Slp) (**A** in **FIGURE 4.7** & **TABLE 4.4**), were found to be the most representative of observed actual ROS for the subsample dataset of 28 fires in Eastern Cape montane grasslands. This spread model configuration was deemed to have appropriately simulated ROS, with a small amount of error, and as a result, was chosen to simulate ROS for entire sample of 143 plots, across the seven montane grassland sites.

Interestingly, Cheney & Gould, (1995), no longer recommend the use of the McArthur Mk5 model, because of questions of validity raised around the influence of fuel load on ROS (Cheney *et. al.*, 1993; McCaw & Catchpole, 1997) (see *Rate of spread*, **Section 2.1.8, Chapter 2**). Nevertheless, I found it to be the most accurate of the three McArthur models (Mk3, CSIRO modified Mk4, & Mk5) at predicting fire spread in the Eastern Cape montane grasslands study sites (**TABLE 4.4**). Importantly though, this was with field measured dead fuel moisture (DFM) entered instead of the built-in function for fuel moisture content (FMC) determination (**TABLE 4.3**). This was a deviation from the original model, which yielded significantly more accurate results (**TABLE 4.4** & **FIGURE 4.6**).

In this regard, McCaw & Catchpole, (1997), identified a discrepancy between FMC calculated using Noble *et. al.*, (1980), equations, and FMC calculated from the original Mk5 slide rule (McArthur, 1977), particularly at low temperatures (~20^{o}C) and high humidity's (~40%) (such as was the case in this study). McCaw & Catchpole, (1997), went on to note that despite this discrepancy, it is unlikely to result in substantial differences in predicted rates of spread. Nevertheless, it does go some way to explaining why I found more accurate results for the McArthur Mk5 model when field sampled DFM was applied (C, D, E, & F in **FIGURE 4.6** & **TABLE 4.4**).

The McArthur models also appeared to be very sensitive to curing state adjustments, particularly at lower levels of curing (<75%). Research has shown that that McArthur models under predict for ROS of grass fires in partially cured grasslands (Cruz *et. al*., 2015). This was corroborated by the findings from this study, which yielded similar results from partially cured grasslands (largely under-predicted ROS for swards between 60 – 80% curing) (**FIGURE 4.6**). Other studies have found that the influence of grass curing on fire behaviour appears to be less than currently accounted for in McArthur models (Cheney *et. al.*, 1993).

It is also worth noting that the CSIRO modified Mk4 spread calculator has a built-in minimum wind speed contribution of 5 km/h (CSIRO, 1999). While not explicitly stated in the original models, Cheney & Sullivan, (2008), suggest that this is to account for variable gusts and movement of air flow around flame structures, as well as anemometer stall speeds of around 3 km/h. It is unclear whether this minimum wind input was also intended to be applied to the McArthur Mk 3 and Mk 5 spread models. The spread model functions developed by Noble *et. al.*, (1980), do not automatically account for a

minimum input, however, one could easily be manually applied. In this study, minimum wind speed inputs were not applied to McArthur Mk3 & Mk5 configurations. Judging by the poor model performance in back fires (wind speed assumed to be 0 km/h), it is likely that inclusion of a 5 km/h minimum wind speed would have improved simulations of back fire spread.

While the slope factor correction functions certainly improved McArthur based model performance (**FIGURE 4.6**), a possible reason for poor McArthur Mk3 and CSIRO modified Mk4 spread model performance is likely the particularly steep gradients present at the Boschberg, Katberg, & Winterberg montane grassland sites. The Mk3 and Mk4 models were developed form field data (prescribed burns) collected from Australian grassland sites with relatively gentle gradients (McArthur, 1966; McArthur, 1967). These models are therefore unlikely to perform well when steep slope gradients are involved. One might expect these two models to perform better in relation to the BehavePlus and Rothermel based models on level ground surfaces. In fact, I have personal professional experience of the CSIRO modified Mk4 spread model performing reliably on a number of occasions in grasslands throughout the Freestate province of South Africa, under conditions of high curing (>70%) and gentle gradients — simulated fire timelines (simulations of ROS) are validated (match up) with eyewitness accounts (fire timelines) (*i.e.*, fire reached point X at a specific time).

The BehavePlus (Andrews & Bevins, 2018) and Rothermel (Rothermel, 1972; Vacchiano & Ascoli, 2015) configurations had mixed results when modelling ROS for the subsample dataset of 28 fires in Eastern Cape montane grasslands. All configurations under-predicted for ROS. Performance of these two base models was mostly centred around dead fuel moisture of extinction (MOE) and fuel surface area to volume (SA/V) ratio input assumptions (**TABLE 4.3** & **TABLE 4.4**). BehavePlus and Rothermel configuration performance improved with increasing dead fuel MOE and SA/V ratio (both live & 1h fuels) values (C, D, E, & F in **FIGURE 4.7** & **TABLE 4.4**). The Rothermel based models also generally performed better than the BehavePlus based models.

The fuel SA/V ratio values used in this study (4900 – 6600 m^2/m^3) fall within the medium to finer grass coarseness category, as stipulated by the BehavePlus computation program (Andrews & Bevins, 2018). The grass species prevailing in the mesic montane grasslands study sites (*Cymbopogon* & *Festuca*), at the time of prescribed burns, are courser in structure relative to most other Southern African grass species. This is of particular interest, as the BehavePlus and Rothermel model configurations, somewhat contradictorily, performed better when simulating ROS for finer coarseness of herbaceous material (incr. SA/V ratio values). The SA/V ratio values used in this study were based off existing fuel model configurations developed for similar southern African grassland and savanna systems (De Ronde, 1988; Everson *et. al*., 1988; Van Wilgen & Wills, 1988; Trollope *et. al.,* 2004). So, since SA/V ratio values of the grass fuel was not directly measured in this study, it is unclear whether the base models themselves, or the previously constructed fuel models for southern African conditions are responsible

for the observed error in ROS simulation. Since it is unlikely that the computation models will make adjustments in this regard, it is recommended that existing fuel model configurations for southern African grassland and savanna systems be revised. Cognizance of this relationship between fuel SA/V ratio values, southern African grasses, and the Rothermel based models should be acknowledged by wildland fire practitioners.

There is, however, a caveat in Rothermel's (1972), relationship between fuel SA/V and ROS in grassfires. In a study comprising 121 grass fires, spanning 2500 ha in Northern Territory, Australia, *circa* 1986, it was found that grass SA/V ratio did not have a significant influence on fire spread (Cheney *et. al.*, 1993). As Rothermel's (1972), spread model was mostly developed for woody systems in the USA, it is likely that fuel SA/V ratio has a bigger influence on spread those systems. Indeed, this makes logical sense, as fuels need to preheat before they release flammable hydrocarbons (Byram, 1959; Trollope, 1984; Trollope *et. al.*, 2004; Van Wagtendonk, 2006; Cheney & Sullivan, 2008; Cochrane & Ryan, 2009; Scott *et. al*., 2014) (see *Phases of combustion*, **Section 2.1.3, Chapter 2**). Large woody fuels, with smaller SA/V ratios, will require a great amount of heat to raise fuel temperature to appoint where flammable hydrocarbons are released. This process takes time, and thus slows the rate of spread of fires in these systems. By contrast, grasses are fine and herbaceous, and ignite readily when cured. There is not much of a discrepancy in SA/V ratio values between grasses, compared to woody fuels. Therefore, it is quite reasonable to expect fuel SA/V ratio values to have little influence on ROS in grassfires.

Dead fuel moisture of extinction (MOE) is a theoretical FMC threshold value, above which fires self-extinguish (Scott *et. al*., 2014). Rothermel, (1972), conceptualised and coined the term during development of his fire spread model. However, while moisture in the fuel certainly impedes fire spread, it is difficult to specify moisture threshold above which, fires will self-extinguish (Scott *et. al*., 2014). Studies have shown that dead fuel MOE values may vary within the same site, depending on fuel and weather conditions such as fuel load and wind speed (Wilson, 1985; Burrows, *et. al*., 2009; Scott *et. al*., 2014). Whether or not a grass sward can carry a fire (without self-extinguishing) is dependent on many more factors than just the moisture content of the cured (dead) fraction of the fuel. Parameters such as proportion of live and dead fuel, live fuel moisture, fuel load, and weather conditions are important factors determining whether a grass sward will carry a fire (Cheney *et. al.*, 1993; Cheney & Sullivan, 2008). The proportion of live and dead fuel in grasslands changes with season, depending on factors such as rainfall, senescence, minimum temperatures (frost), and disturbance (grazing & fire). For example, if a moribund grass fuel stand is burned, the resultant new growth will have a lower dead fuel MOE value than before the fire, as the overall FMC of the sward has risen. Similarly, after a 'sourveld' rangeland paddock has been eaten out (presuming livestock will favour live herbaceous fuel ahead of cured fuel), the proportion of cured fuel will rise. The resultant 'eaten out' paddock would have a larger

dead fuel MOE threshold value, as the overall FMC of the paddock would have dropped, reducing its dampening effect on fire.

The conclusion to be drawn from above, is that it is very difficult to define dead fuel MOE value for a site-specific fuel model, without also stipulating a season and condition of the fuel, particularly grassland and savanna systems. In other words, dead fuel moisture of extinction is a theoretical value which could be encompassed in a generalization for a particular fire situation (fuel, weather, & topographical conditions), rather than a threshold value for a particular fuel type. Nevertheless, it is largely acknowledged that grassfires generally spread poorly at dead FMC above 30% (McArthur, 1977; Scott *et. al*., 2014), although there have been few empirical studies which verify this. In fact, the McArthur Mk5 model has a built-in dead fuel MOE of 30% (McArthur, 1977; Noble et. al., 1980).

In this study, model configurations with a dead fuel MOE value of 30% produced better simulations for ROS than those with dead fuel MOE values of 20%. Due to the generalized under-prediction of these models, it is likely that dead fuel MOE values higher than 30%, say ~40%, would yield more accurate simulations for ROS.

While I have no evidence to support that a cured grass sward with dead fuel MOE value of 40% could carry a fire (dead FMC in this study ranged between 10 – 23%), from anecdotal observations and personal 'feel', I think 40% is likely a more accurate value for fully cured fine herbaceous fuels in southern African grasslands. Certainly, more research is required to investigate these relationships between fuel conditions and fire behaviour.

Nevertheless, based off model configuration performance in this study, we may need to re-evaluate some of the existing fuel models constructed for southern African grassland and savanna systems (De Ronde, 1988; Everson *et. al*., 1988; Van Wilgen & Wills, 1988; Trollope *et. al*., 2004), and adjust them accordingly. Certainly, a dead fuel MOE value of 20% is too low for these systems, as recorded values for dead FMC at Site 2 (Boschberg) of this study exceeded 20% and fires did not self-extinguish.

To conclude, while the CSIRO modified McArthur Mk4 spread model did not yield the most accurate simulations for ROS, it is noted that the Mk4 calculator is by far the most practicable spread model of the selection investigated in this study (5 models). It is the easiest to apply and requires few inputs based on standard meteorological weather data and simple fuel assessment (Cheney & Sullivan, 2008). These inputs are easily and rapidly measured by practitioners, researchers, or investigators. The CSIRO modified Mk4 model is recommended for rapid simulation, and might be of practicable use to firefighting personnel and fire managers, provided curing is above 70% and gradients are not too steep.

By contrast, BehavePlus v6.0.0 (Andrews & Bevins, 2018) and the Rothermel R package (Vacchiano & Ascoli, 2015) are complicated, requiring too many input variables and model assumptions, many of which require tedious methods of sampling. The detailed fuel model inputs required for these models

likely mean that they are not generally applicable or reliable over a wide range of conditions. Fire investigators cannot afford (do not have the time or resources) to develop fuel models for every wildland fire site they investigate.

For the most part, the McArthur based fire models are simpler and easier to use and apply. The equations developed by Noble *et. al.*, (1980), & Sharples, (2008), mean that the models are easily transferred and applied to various computational programs. Due to their simplicity, the McArthur based models are likely more applicable and reliable over a wide range of grassland conditions, although there is no empirical evidence from this study to support this.

For these reasons, it is recommended that wildland fire practitioners use McArthur based models, with appropriate supplementary functions or fuel inputs. However, cognizance of the potential shortcomings of these models should be noted. It is strongly recommended that models are ground truthed for subject site or prevailing fuel conditions before application.

4.5.2 Measured fire behaviour:

Fire intensities were significantly higher in head and flank fires, compared to back fires (**FIGURE 4.8**). Fire severities were significantly lower in head fires compared to back and flank fires (**FIGURE 4.9**). These are rather unsurprising results for grassland fire behaviour, but encouraging, nonetheless.

Rate of spread was simulated for the entire dataset (n = 143), using the McArthur Mk5 spread model, with field sampled DFM and a slope correction function applied, based on best fit model comparison, as mentioned previously (*Rate of spread*, **Section 4.4.1 & 4.5.1**). The relationship between simulated ROS for entire dataset and effective slope gradient — the actual gradient experienced by a fire front (head, back, or flank) in the direction of spread — is shown in A in **FIGURE 4.10**. Unsurprisingly, this relationship matches with the relationship McArthur, (1967), identified for the influence of slope on ROS (**FIGURE 4.5**). This is because the slope correction function used in the Mk5 model configuration makes use of this relationship (Noble *et. al.*, 1980). What is of interest, is the relationship between effective slope gradient and observed ROS from the subsample dataset (n = 28) (B in **FIGURE 4.10**). While it is difficult to extrapolate from a small sample size of 28 observations, this observed slope/ROS relationship (B in **FIGURE 4.10**) does appear to match well with, or at least is similar to, McArthur's, (1967), slope influence on ROS (A in **FIGURE 4.10** & **FIGURE 4.5**). This is an encouraging ground-truthing of the slope factor correction function (Noble *et. al*., 1980), and supports its use in this study as an appropriate configuration parameter (see *Model configurations*, **Section 4.3.3, *Modelled fire behaviour***).

There have been few, if any studies which have investigated the relationship between slope gradient and fire spread type (head, back, flank). The idea here is that beyond a certain degree of gradient (- or

+), a fire's flames will be forced to lean toward (upslope) or away (downslope) from the fuel due to both the physical angle of slope, and the increased convective currents (Trollope, 1984; NWCG, 2016; Leavell *et. al*., 2017; NFPA, 2017). Given that fire spread type is defined by the angle in which flames lean relative to fuel (Cheney & Sullivan, 2008) (**Section 2.1.1**, ***Fire spread type,*** **Chapter 2**), there may exist a gradient threshold above or below which back and head fires can no longer persist. If such a relationship were to exist, it would certainly be dependent on other factors such as wind speed and direction, rather than a set gradient level which applies to all scenarios.

The relationship between effective slope gradient and fire spread type from 143 fires in Eastern Cape montane grasslands is examined in **FIGURE 4.11**. Head fire spread did not occur down slopes steeper than -25% gradients, and back fire spread did not occur when spreading up slopes steeper than 23% gradients. This is perhaps evidence of a slope gradient threshold around -25% & 23% for head and back fire spread respectively, in Eastern Cape montane grasslands (**FIGURE 4.11**). This logical, since at a steep enough gradient, slope driven convection (as opposed to wind driven) will become the primary driver of heat transfer, and thus fire behaviour (Trollope, 1984; Teie, 2003; Trollope *et. al.*, 2004; Van Wagtendonk, 2006; Cochrane & Ryan, 2009; Scott *et. al*., 2014). However, acknowledging that wind speed and direction will inevitably influence fire spread type in combination with slope (Trollope, 1978), these identified gradients should not be construed as exact threshold values for fire spread type. Nevertheless, as approximate slope gradient values, these potential thresholds could be used as a general 'rule of thumb' or guide for wildland fire practitioners.

Three alternate measures of fire intensity were recorded in addition to Byram's fireline intensity (**FIGURE 4.12**). The alternate methods of fireline intensity determination offer various practical and/or theoretical advantages which could benefit wildland fire managers, practitioners, and researchers (Van Wilgen, 1986; Webber & Trollope, 1997).

The idea behind **hydropyrometers** was construed by Webber & Trollope, (1997), and is a method of steam-releasing open-can calorimetry (Viegas *et. al.*, 1994; Perez & Moreno, 1998) designed for grassland and savanna systems in Southern Africa. Its appeal is that it is both low cost and does not require fuel load and heat yield measurements in its calculations of intensity. Hydropyrometers were found to have under-recorded fireline intensity in Eastern Cape montane grassland sites, but was not entirely unreliable, performing better than the other two alternate methods, as well as most model simulations tested in this study (**FIGURE 4.12**). In addition, measurements of fireline intensity in back fire scenarios were more accurate than in head and flank fire scenarios.

Hydropyrometers, however, were not used to their full potential in this study. With few key adjustments to methods and application, hydropyrometers will likely yield very accurate measurements of fireline intensity. Webber & Trollope, (1997), outlined in their description of this method, that open-can calorimeters should be placed both at ground level and canopy height, in order to capture energy of both

heading and back flames, if they persist. This is logical in terms of differences in radiative and convective heat transfer between heading and backing fires (see **Section 2.1.4**, ***Heat transfer,*** **Chapter 2**). Importantly, the ground level tin can should be slightly elevated and not in contact with the ground surface, as it could lose heat energy via conduction (Trollope W.S.W. (PhD), personal communication, 2019)). This set-up (two elevated cans offset from each other) requires the use of a metal stake from which to hang the cans. Due to the number of experimental plots used in this study (n = 143), at the time of prescribed burning, it was not feasible to purchase or construct such devices in short notice. Consequently, a single can, placed on the ground surface, was used for each experimental plot. At ground level, the open-can calorimeters would not have captured the full amount of energy produced by head fires. This likely (or at least partly) explains why, in this study, fireline intensities recorded using steam-releasing open-can calorimetry generally under-recorded, especially in head fire scenarios. Incidentally, this afforded the opportunity to identify shortcomings in this method, and produce empirical results which show why one should persist with Webber & Trollope's original method, and not place cans directly on the ground surface. It is important to note that had I constructed the relevant devices and applied the original method, hydropyrometers would still have been a very cost-effective method of fireline intensity determination.

Other shortcomings in the application of the hydropyrometer method include the amount of water used, and the potential for evaporation in field trials which persist for many hours, although these were not as a result of deviation from Webber & Trollope's, (1997), original methods. Webber and Trollope, (1997), advise 20 ml of water as suitable for grassfires scenarios in southern Africa. In this study, the entire 20 ml of water vapourised on a number of occasions, especially when fires were 'hot'. In these scenarios, any additional heat energy produced by the fire, therefore, could not be captured in any further water loss (vaporisation). This would have contributed to further under-recording in 'hot' head fires. From observations of field trials in this study, it is recommended that perhaps 30 ml of water would be more appropriate for fires in high fuel load moribund mesic grasslands in southern Africa.

It is likely that a portion of the 20 ml of water may have been lost to evaporation before and after fires had passed through. This was certainly the case with two open-can calorimeters in this study, which did not have fire burn passed them ('controls'). This loss of water to evaporation can be accounted for in future studies by following similar methods proposed by Gorgone-Barbosa *et. al.*, (2015), and placing controls outside of the burn area and recording water loss over the period of controlled burning. Or alternatively, and perhaps more simply, sealing the openings of the cans with plastic film wrap secured with elastic bands. The film wrap will prevent evaporation before the fire passes through, and melt away when in contact with flames, allowing vaporisation of water. This method would not, however, account for evaporation after fire passage.

Having identified these shortcomings and taking into consideration the recommendations by Webber & Trollope (1997), as well successful application of steam-releasing open-can calorimetry in woody fuel systems of the Mediterranean, it is quite feasible that the hydropyrometer method of fireline intensity measurement is a suitable for application in southern African grasslands and savannas. Further empirical research is, however, required to verify this.

Fire intensity values derived from recorded **flame lengths**, using Byram's (1959), (flame length) equation, was found to be a poor measurement of fireline intensity Eastern Cape montane grasslands (**FIGURE 4.12**). Whether this due to lack of suitability of Byram's (1959), equation to site conditions, or an inappropriate relationship between flame length and fireline intensity, is unclear. What is certain, is that a large degree of variability in flame length through 10 x 10 m burn plots contributed to misrepresentative recorded flame lengths.

Byram's (1959), equation for fireline intensity makes use of mass of available fuel as an input value in its calculation of fire intensity. Considering that amount of fuel converted to energy (combusted) directly affects the amount of energy (intensity) produced by a fire, and that severity is a direct measure of the amount of fuel consumed by a fire, it is quite possible that fire intensity derived from fire severity (instead of fuel load) could be considered an appropriate alternative measure of fireline intensity. It is acknowledged though that fireline intensity values derived in this manner, will always be somewhat lower than conventional methods, as the total fuel load is almost never entirely consumed by fire. In nature, there is always some element of incomplete combustion (Van Wagtendonk, 2006; Cheney & Sullivan, 2008; Cochrane & Ryan, 2009; Scott *et. al*., 2014). Therefore, application of this method was conducted for comparative purposes, rather than as an accurate to Byram's fireline intensity. The discrepancy between intensity values recorded from the two methods, for 143 fires in Eastern Cape montane grasslands, was greater than expected. There may be several explanations for this. Firstly, the residual fuel load remaining after a fire is not necessarily completely 'unburnt'. Residual 'charred' grass stalks would have, to a certain degree, experienced partial combustion — preheating of fuel and subsequent release of hydrocarbon gases (see **Section 2.1.3, *Phases of combustion*, Chapter 2**). It is, therefore, misrepresentative to disregard remaining post-fire fuel load as a portion of fuel consumed by the fire.

Secondly, residual fuel load was likely overestimated, and thus severity, underestimated for the montane grassfire sites of this study. A novel method of post-fire fuel load estimation, adapted from the existing disc pasture meter (DPM) method (Bransby & Tainton, 1977; Danckwerts & Trollope, 1980) was used in this study. The DPM method is a widely applied pre-fire fuel load estimation method (Trollope, 1983; Trollope & Potgieter, 1986; Harmse *et. al.,* 2019). The DPM, calibrated to site or vegetation type/unit, produces height values which can be entered into an appropriate function to generate estimated fuel loads (Bransby & Tainton, 1977; Danckwerts & Trollope, 1980; Trollope, 1983; Trollope & Potgieter,

1986; Harmse *et. al.*, 2019). The mistake made in this study, was that the same DPM calibration used for pre-fire fuel load estimation, was also used for post-fire fuel load estimation. While the DPM calibration used was appropriate for the presiding unburnt vegetation, the same calibration would not be appropriate for hard and brittle residual grass stalks remaining after combustion. These hard and brittle residual grass stalks would have generated, in relative terms, taller height measurements for the available fuel compared to flexible live grass. Using the pre-fire DPM calibration, these post-fire DPM measurements would produce higher residual fuel load estimations than actual residual fuel load present after combustion. This would result in overall lower fire severity measurements for each 10 x 10 m burn plot, compared to reality.

4.5.3 Modelled fire intensity:

All thirteen model configurations did not produce good simulation fits for fireline intensity, under-predicting in all cases (**FIGURE 4.13** & **FIGURE 4.14**). Behave plus and Rothermel based model configurations were particularly bad at predicting head and back fire intensity (**FIGURE 4.15**). BehavePlus configurations were slightly better than Rothermel at predicting intensity in backfire scenarios. This may perhaps be attributed to a minimum wind speed input in the BehavePlus system. Some models are known to have a minimum wind speed input of around 5 km/h (CSIRO, 1999), thought to account for variable gusts and movement of air flow around flame structures, as well as anemometer stall speeds of around 3 km/h (Cheney & Sullivan, 2008). The BehavePlus system takes all relevant predictor variable vectors as inputs values (*e.g.,* wind direction, fire spread direction, aspect). It is understood that the BehavePlus system scales the associated predictor variables (wind speed & slope gradient) accordingly. This scaling of wind and slope inputs would, in theory, account for oblique back fire spread (not at 180^{o} to wind), which is at least partially influenced by wind.

Perhaps another reason for slightly worse back fire intensity simulations in Rothermel configurations, is due to differences in downslope slope correction functions between Rothermel and BehavePlus models. The McArthur slope correction function was applied to the Rothermel R package model (Vacchiano & Ascoli, 2015), as it does not account for downslope effects on fire behaviour. From observational trial simulations, it appears as though the McArthur downslope correction function reduces ROS, and thus intensity, more harshly than the BehavePlus downslope adjustor.

Rothermel configurations performed marginally better when simulating for flank fire intensity, than head and back fire intensity. **FIGURE 4.15** shows the relative model performance of a Rothermel configuration for each fire spread type. It was stated previously (*Model assumptions*, **Section 4.3.3, *Modelled fire behaviour***) that the Rothermel model does not account for directional vector inputs of wind direction. As a result, the full influence (unscaled) of wind is accounted for in flank fire scenario simulations. Because Rothermel model configurations under-predicted as a whole, the relative 'over-

prediction' of flank fires, accounted for by wind inputs, explains why flank fire intensity simulations were more representative than head fire intensity simulations.

For both BehavePlus and Rothermel model configurations, fireline intensity observations and simulated outputs from Site 7 (Winterberg) were far removed from the other six sites (**FIGURE 4.16**). It appears several outliers above 25000 kJ/s/m observed fireline intensity may be responsible for this outcome. BehavePlus and Rothermel model configurations severely under-predicted for these values. These four outliers originate from extremely intense head fire spread, far removed from typical prescribed burning conditions, levels of which have likely never been reproduced in field or lab fire trials used to develop these models. Disregarding these four outliers, BehavePlus and Rothermel model configurations simulated intensity values for the remainder of Site 7, surprisingly well. Reasons for this are unclear.

With regards to slope factors and simulated and observed fireline intensity, some interesting observations were made during prescribed burns in the rugged topography of the montane grassland sites. A number of high intensity (~3 m flame length) back fires occurred at several of the fire sites. These high intensity back fires could not be simulated for by BehavePlus and Rothermel model configurations. What was observed, was that the intensity of these back fires appeared to be influenced by unaccounted-for slope affects while spreading horizontally (effective gradient of zero) across steep slopes. To the best of my knowledge, this slope affect can be described and explained as follows: A wind driven fire moving horizontally across a steep slope, while experiencing an effective level (or close to level) gradient, will behave more intensely than a fire on a level surface, when all else is equal. This is due to combined wind and slope effects, in different directions. Despite no effective gradient change (wind is driving fire horizontally across slope), flame structures are three dimensional and a portion of the flame flank is burning upslope as a 'slope head'. The increased lateral convective transfer of heat (upslope) leads to increased lateral preheating of fuel and increased lateral fuel bed depth, contributing to larger flames and higher fire intensities than would be expected of a fire with the same fuel and weather condition on a level surface. This is despite the hypothetical 'wind head' fire on the slope moving along an effective level gradient.

Current slope factor correction functions as well as existing theory of slope effects on fire do not account for the above interactions. Further research is required to quantify this theoretical slope effect.

In terms of fire investigations, in addition to aiding in judgement of difficulty involved to suppress fires, wildland fire investigators use fireline intensity values to determine whether a particular fire could cross barriers, usually firebreaks. This is an important consideration for legal teams building cases in contemplation of litigation. When accurate calculation of fireline intensity is not possible, investigators may choose to use fire models to simulate an approximate fireline intensity value.

Judging from the poor performance of intensity simulations fromRothermel and BehavePlus model configuration in this study, and the implications that these values might hold, it is strongly

recommended that investigators do not use these models to simulate fireline intensity for Eastern Cape montane grasslands or similar systems.

4.5.4 Modelled flame length:

All 16 model configurations performed particularly badly when simulating for flame length (**TABLE 4.7**). Simulated flame length values were very erratic for all configurations, widely over and underestimating (**FIGURE 4.17**, **FIGURE 4.18**, & **FIGURE 4.19**).

It is perhaps worth noting that the Noble *et. al*., (1980), paper (which expresses the McArthur Mk3 & Mk5 models as equations) stipulates that the McArthur Mk5 flame length model (four configurations of which are used in this study) simulates flame height, and not flame length) (see **Section 2.1.6, *Flame zone structures,* Chapter 2**). However, this is most likely an oversight, and in practice the authors are likely referring to flame length.

Both BehavePlus and Rothermel flame length model configurations performed particularly badly when simulating back fire flame lengths, compared to head and flank fire scenarios (**FIGURE 4.20**). It is difficult to attribute this to anything, as model performance was also very bad for head and flank fire scenarios. These models were likely not designed to account for fire behaviour without the influence of wind (*i.e.*, back fires).

Lowveld FDI (Government Gazette Notice 1099 of 2013) associated flame length predictions also did not match well with observed flame lengths (**FIGURE 4.21**). this is not surprising, as FDIs only consider weather conditions in their calculations for danger rating. FDIs only account for the influence of fuel on fire behaviour, indirectly through temperature and relative humidity. Fuel load is not accounted for. Fuel load has a significant effect on fire intensity and thus flame length, and therefore its exclusion from FDI ratings, means that FDI' cannot make accurate predictions for fire intensity.

Char height on pole type fuels has previously been identified as a useful *post-hoc* indication of flame length in eucalypt savannas at the Kapalga research site, Australia (Williams *et. al*., 2003). This study found that while there was certainly a relationship between char height and flame length in mesic montane grasslands of the Eastern Cape (A in **FIGURE 4.22**), double the height of char, proved to be an accurate post-hoc indicator of flame length, particularly in head fire scenarios (B in **FIGURE 4.22**, **TABLE 4.7**). This is an exciting and simple relationship which could have very wide practical application in southern African grassland and savanna systems. While it is acknowledged that the relationship is not perfect, as a general guide, this should be useful tool for all wildfire practitioners.

It is noted that the reduced sample size (n = 83) is due to a number of the planted poles showing no evidence of charring. These samples were therefore excluded from the data, rather than assigning charring height values of zero.

4.5.5 General model observations:

Ideally the preferred option would have been for this study to have collected empirical data under fire conditions as close to typical runaway wildfire conditions (high wind speeds, low humidity, high fuel load), as possible. An inevitable consequence of conducting prescribed burns, is that safety takes precedence ahead of desired effect/outcome. Despite endeavouring to emulate runaway conditions, on average, experimental fire conditions in this study were milder than those experienced in typical runaway wildfire conditions. Notwithstanding, a range of high wind speeds (up to 40+ km/h) was achieved. Under runaway conditions, model performance may possibly improve as extreme conditions have a more significant effect on simulated outputs. Further empirical research is required to verify model performance under extreme runaway fire conditions.

The prescribed fires were conducted on privately owned livestock farms (rangelands), so paddocks were regularly grazed, although, there was an abundance of cured flammable material at the sites used in this study, as the paddocks were rested before burning. The consequence is, that on occasion, fuel conditions were patchy. Patchiness of fuel does, of course, affect fire behaviour, with changing fuel loads and moisture.

On the other hand, conducting these prescribed burns on large-scale privately owned agricultural rangelands instead of typical experimental burn plots, added robustness to this study, as the presiding fuel conditions and terrain were representative of the conditions under which wildland fire investigators would conduct investigations of runaway fires.

As previously noted, (*Model configurations*, **Section 4.3.3, *Modelled fire behaviour***) it is largely acknowledged that woody cover has little contribution to fire behaviour in the relatively cool, fast-moving fires of grassland and savanna systems (Trollope W.S.W. (PhD), personal communication, 2019). However, unlike savanna systems, the woody component (Amathole montane Fynbos (*e.g.*, *Cliffortia paucistamina*)) in mesic montane grasslands of the Eastern Cape is very susceptible to fire (Trollope, 1970; Trollope, 1972), and when present, has a significant contribution to the behaviour of surface fires in these systems (Trollope W.S.W. (PhD), personal communication, 2019). This study specifically focussed on grass fire behaviour.

Despite efforts in this study to place 10 x 10 m burn plots in such a manner as to avoid the woody component, there were, in some cases, an element of woody fuel, both highly flammable (*Cliffortia paucistamina*) and resistant to fire present in experimental plots. This woody component would have,

to some degree, contributed to the overall fire behaviour in burn plots. this contribution could have been increased fire intensity, or have a dampening effect on the fire, depending on species present in the sward. This would obviously have affected measurements of fire behaviour, however, on average, over the entire sample (n = 143), this influence would have been low.

For the most part, requisite input variables differ in fuel moisture content (FMC) determination. The grassland functions of the McArthur based Australian models account for fuel moisture through temperature, relative humidity, and curing input variables (McCaw & Catchpole, 1997; Cheney & Sullivan, 2008), assuming all fuel is herbaceous. These fuel and meteorological values are relatively easily derived, whether by *post-hoc* means, or pre-burn (Cheney & Sullivan, 2008). The American Rothermel based models require direct fuel moisture input values for live woody, live herbaceous, and each dead fuel size class (Vacchiano & Ascoli, 2015; Andrews & Bevins, 2018). Accurate fuel moisture content determination is a slow and tedious process, usually requiring fuel sampling and many hours of lab analysis (oven drying) (Cheney & Sullivan, 2008). This means it is particularly difficult to reliably generate FMC values for fire models, both in short notice pre-burn, or post-fire after some length of time has elapsed. The consequence is that BehavePlus & Rothermel based models are less practically applicable for rapid simulation.

In herbaceous fine fuel systems, such as grasslands and savannas, a large proportion of the fuel is cured at times of year when fires occur. In these scenarios, fuel can essentially be split into live herbaceous or cured 1-hour fuels. Dead fuel moisture content is therefore an important driver of fire behaviour in these systems. Hence the use of curing, temperature, and humidity as input variable proxies for FMC (see **Section 2.1.9*, Fuel moisture & curing*, Chapter 2**) in models designed for grassfire spread is more appropriate say, compared to Rothermel based models which may need to be applied in woody systems, where a large proportion of the fuel is live and non-herbaceous. Interestingly, live FMC by itself has not been found to be related to the damping effect of live fuels on the rate of fire spread in grasslands (Cruz *et. al.*, 2015).

Apart from FMC input disparities, one of the key differences between the McArthur based Australian models and Rothermel based models is with regards to the method of data collection used for the development of model functions (Weise & Biging, 1997). The Australian McArthur/CSIRO models were derived from field data collected from multiple field (fire) trials (McArthur, 1966; McArthur, 1967; Weise & Biging, 1997), while the Rothermel (1972) model — and therefore subsequent models based on Rothermel, (1972) — were developed using data collected from fire tunnels (Cheney *et. al.*, 1993). Fire tunnels make use of harvested fuel, collected from the field, and placed in the tunnel to recreate a desired fuel type (Cheney *et. al.*, 1993). Many of these fuel scenarios were based on north American woody fuel systems (Andrews & Bevins, 2018). Fire tunnels are far removed from field

conditions, and for that matter, may be far removed from reality (Weise & Biging, 1997; Trollope W.S.W. (PhD), personal communication, 2019).

The consequence is that Rothermel based models may be less suited to southern African grassland and savanna systems, compared to McArthur based models which were specifically and empirically developed for grassfire scenarios (similar to subtropical African grassland).

It has been mentioned previously that BehavePlus and Rothermel models require fuel SA/V ratio and dead fuel MOE values as input variables. These values are difficult and extremely impractical (or impossible) to measure accurately in the field (Scott *et. al*., 2014). Consequently, most applications of the BehavePlus and Rothermel models use predefined values for SA/V and MOE, sometimes even when building new custom fuel models (Van Wilgen *et. al*., 1985; Everson *et. al*., 1988; Van Wilgen & Wills, 1988; Trollope *et. al.,* 2004). As a result, many custom fuel models may not be entirely accurate representations of relevant fuel scenarios. This would be of little consequence if model outputs did not differ significantly within the range of SA/V and MOE values used in southern African grass fuel systems. However, the ranges of SA/V and MOE values used in modelling of fires in southern African grasslands (20-30% dead fuel MOE; 4900 – 6600 m^2/m^3 fuel SA/V ratio) do significantly effect model output values (**TABLE 4.4**, **TABLE 4.6**, & **TABLE 4.7**). This questions the credibility of custom fuel models developed for southern African grassland and savanna systems.

4.6 Conclusions:

To conclude, McArthur, BehavePlus, & Rothermel model configurations did not perform well when simulating fire behaviour in Eastern Cape mesic montane grasslands. For the most part, models largely under-predicted fire behaviour in these montane rangeland systems.

Existing fuel models constructed for southern African grassland and savanna systems proved to be inappropriate for the Boschberg, Katberg, and Winterberg mountain systems. These fuel models are likely not accurate representations of southern African grassland fuel conditions. It is advised that these existing custom grassland and savanna fuel models be revised. Suggested changes include a higher dead fuel moisture of extinction value, probably close to 40%, and adjusted (perhaps larger) fuel surface area to volume ratios (finer coarseness).

Investigation into which predictor variables drove fire behaviour in the prescribed burns of this study (mesic montane grasslands of the Boschberg, Katberg, & Winterberg) was conducted. While extrapolation of these results is not recommended, it is clear that slope gradient is an important driver of fire behaviour in this system.

Model slope factor correction functions were a crucial configuration inclusion for accurate simulation in this area. This will likely also be the case in other mountainous regions in southern Africa, especially when landscapes are rugged and slope gradients steep.

The McArthur Mk5 grassland model suitably simulated for fire rate of spread in montane grasslands of the Eastern Cape, but not flame length. McArthur based models are recommended for simulation of rate of spread in **cured** (>70%) grassland fuels of southern Africa, but further empirical research is required to confirm credibility of these models in other grassland and savanna systems. Double (2x) char height on pole type fuels such as trees and fence posts was found to be an adequate practical *post-hoc* indicator of head fire flame length in montane rangelands of the Eastern Cape.

Cruz et. al., (2020), stressed the need for researchers to conduct studies which show how models fail to accurately simulate actual fire conditions. By highlighting model flaws, we are able to specifically identify weaknesses and address them accordingly. To that end, this chapter showed that current fire behaviour prediction models widely implemented in various African rangelands are **not** appropriate for mesic montane grassland systems of the Eastern Cape. I encourage modellers to address these issues and improve on model accuracy in these systems.

Furthermore, this chapter examined model performance in head, back, and flank fires. Almost all quantitative fire behaviour studies only assess veldfire conditions in head fire scenarios. This study had an approximately equal split of fire spread types (~50 fires each) (n = 143). The data and findings from

this study may provide valuable insights into how fire behaviour differs between spread type as well as how fire prediction models perform and function in all three fire spread types (head, back & flank).

Regardless of model fit results, from an implementation point of view, several conclusions based on practicability of McArthur, BehavePlus, and Rothermel models, can be drawn. The BehavePlus and Rothermel models are fairly complex and require a multitude of input variables, many of which are difficult or impossible to accurately measure in the field. These models also require tedious and time-consuming application in order to implement appropriately. This is impractical in terms of rapid *post-hoc* forensic analysis of fire behaviour. Investigators do not have time to make precise measurements of fuel characteristics in typical site inspections, which usually last several hours. Recording these numerous fuel parameters would perhaps be justified if it was accompanied with improved simulation, however, this is not the case. BehavePlus exists as its own software program and is difficult to transfer outputs or inputs via external sources.

On the other hand, McArthur based models are easy to apply, and have been converted into mathematical equations which can be included into computational software such as Microsoft Excel or R Studio. These models require few input variables which are easily derived from meteorological data or observational assessments of fuel. This is particularly suitable for rapid simulation and is useful for fire practitioners and investigators.

Chapter 5:

RELIABILITY AND UTILITY OF *POST-HOC* RANGELAND FIRE PATTERN INDICATORS

5.1 Chapter Summary:

This chapter aimed to quantitatively assess the reliability and accuracy of seven existing *post-hoc* wildfire pattern indicators, as well as the viability of two potential novel indicators, in grassfire conditions. Despite the existence of numerous guides and handbooks which catalogue, describe, and offer guidance on implantation of *post-hoc* wildland fire pattern indicators, there have been few, if any quantitative empirical studies on *post-hoc* indicators' performance in reconstructing and interpreting wildfire behaviour. Real-time fire behaviour data were gathered from 143 fires across seven sites in Eastern Cape montane grasslands and compared with corresponding post-fire indicator expression. Residual ash colour, curling, spalling, and residual ash organic carbon content were found to be unreliable indicators of wildfire pattern and spread. Foliage freeze, cupping of grass tussocks, consumption depth of grass tussocks, amount of residual unburnt plant litter, protection, sooting, & staining were considered reliable, but in some cases may be site specific and need to be applied in conjunction with each other to draw accurate and reliable conclusions of fire pattern and spread. The presence of undercut culms and leeside charring on pole-type fuels are almost unequivocal indicators of back fires and wind direction, respectively. These findings suggest that certain *post-hoc* wildland fire pattern and spread indicators must be re-evaluated, and practitioners are advised to adopt an adaptive approach to indicator interpretation, applying fire behavioural science of the processes and drivers of indicator formation and expression, while collectively incorporating several indicators in conjunction with each other before forming conclusions on origin, cause, and spread of runaway wildfires.

5.2 Introduction:

Fire plays a vital role in shaping and maintaining grassland and savanna systems of southern Africa (Bond *et. al*., 2005; Bond & Keeley, 2005; Pausas & Keeley, 2009; Trollope, 2011; Staver *et al.*, 2011a, 2011b). Fire managers and pastoralists aim to emulate and control the natural effects of fire which maintain these systems, by implementing controlled fire regimes (Teie, 2003; Trollope, 2011; Nieman *et. al*., 2021). Notwithstanding, an inevitable consequence of anthropogenic settlement, accompanied by infrastructural development, is damage to property when uncontrolled fires occur. The result is numerous claims for losses, incurred from runaway fires, and many of these lead to litigation.

Legal teams rely on experts in wildland fire behaviour to investigate the origin, cause, spread, and other pertinent aspects of fire behaviour to gain an understanding of potential liability. These investigations are conducted on a *post-hoc* basis and rely on physical evidence left by the fire to explain the origin, cause, and behaviour of the fire. It is therefore imperative that the indicators on which identification of point of origin, cause, and spread are based, are considered accurate and reliable.

Incorrect attribution has significant consequences. For example, in the now well-known fire of 527 Lime Street, Jacksonville, Florida, 1990, an innocent man was charged with arson (and murder) based on anecdotal fire investigation knowledge, which at the time was considered ‘sound’ science. The original investigative teams were unanimous in their conclusions that the residual char patterns on floorboards, and rate of spread of fire were clear indicators of the presence of an accelerant, and thus arson (DeHaan, 1992; Lentini, 1992). However, a follow-up investigative team proposed a full-scale recreation of the fire in an identical abandoned neighbouring house, 525 Lime Street. An almost exact replication was constructed, using, where possible, identical contents to 527 Lime Street (DeHaan, 1992; Lentini, 1992). Two fire scenarios were replicated, with and without accelerant (and two points of origin) (DeHaan, 1992; Lentini, 1992). Surprisingly, both scenarios showed very similar fire behaviour (rapid rate of spread and fire growth) and left behind almost exact post-fire burn patterns (DeHaan, 1992; Lentini, 1992). Importantly, the findings did not refute nor prove the presence or absence of an accelerant at the scene of the fire, but rather exposed the unreliability of anecdotal fire behaviour indicators of the time (DeHaan, 1992; Lentini, 1992). The consequence was a complete overhaul of forensic structural fire investigation science, with the adoption of a more scientific approach, based on empirical evidence (Lentini, 2019).

Wildland fire forensic science, however, has not yet been held to the same standard as the above example. Despite recent advances in structural fire forensic science, and in ecological understanding of fire behaviour, empirical research in wildland fire forensic science has largely been neglected and unsupported.

Nevertheless, there has been a recent increase in publications of wildland fire investigation guides and handbooks (Cheney & Sullivan, 2008; NFPA, 2008; NFPA, 2011; De Haan & Icove, 2013; NFPA, 2014; De Ronde & Goldammer, 2015; NWCG, 2016; NFPA, 2017; IAFC *et. al*., 2018; NFPA, 2021), as well as an increasing requirement from litigants for investigators to be considered experts in their field (forensic science), as opposed to previously accepting fire incident, or 'fire chief' reports, usually written by persons unqualified in forensic science. These handbooks provide guidance on the systematic approach to conducting wildland fire origin and cause investigations and, in most cases, are widely accepted by fire investigators as the 'standard' (Simeoni *et. al*., 2017). Upon review, however, many of these guides and handbooks are often inconsistent with one another, and in some cases, factually incorrect.

The approach to conducting investigations inro origin, cause, and spread of fire (as stipulated by the handbooks), involves a stepwise process, first determining the axis or direction of spread of the fire, then tracing your way back towards the approximate area of origin, where the head fire meats the back fire (Cheney & Sullivan, 2008; NFPA, 2017). Whilst tracing your way back towards the origin area, physical evidence left by the fire (known as *post-hoc* wildland fire pattern indicators) is collected to reconstruct the fire's passage and determine area or point of origin (NWCG, 2016; NFPA, 2017).

Post-hoc wildland fire pattern indicators are the physical objects or visual remains persisting after a fire's passage (NWCG, 2016; NFPA, 2017; Simeoni *et. al*., 2017; NWCG, 2018). Collectively they reveal the progress, action, and overall pattern of the fire (NWCG, 2016; NFPA, 2017; Simeoni *et. al*., 2017; NWCG, 2018). These visual remains are the observable and/or quantifiable changes caused to partially burned fuels and incombustible objects when exposed to fire (NWCG, 2016). Information gathered from indicators is usually simplified to at least one of three critical aspects of fire behaviour: **fire spread type** (head, back, or flank fire); **direction of fire passage**; and **wind direction** at the time of combustion. **Chapter 2** contains a detailed list of *post-hoc* indicators of wildland fire pattern and spread relevant to wildfire investigations.

When determining origin and spread of fire, it is recommended that indicators be interpreted in groups or clusters in close proximity to each other, which collectively portray a consistent vector (NWCG, 2016). This practice reduces the probability of inaccurate conclusions on behaviour of the entire fire, arising from a single indicator (vector) which may have experienced idiosyncratic circumstances as a result of temporary fluctuations in local conditions from those prevailing at the time.

Despite the existence of a number of these wildfire investigation handbooks and guides, there have been few, if any empirical studies quantifying the efficacy of forensic *post-hoc* indicators in determining wildfire pattern, spread, and behaviour. The literature and knowledge on the topic is almost entirely anecdotal.

The demand for a universally accepted standard for wildland fire origin and cause investigation is increasing, especially considering the information inferred from *post-hoc* wildland fire pattern indicators often influence the outcome of claims for damages (insurance & litigation) and are regularly invoked in the court of law. Much of the current evidence (indicators) used charge defendants (arson or negligence), is not based on quantified empirical scientific data. The consequence is, that there is potential for innocent people to be found liable for civil offences, or even the conviction of innocent people for criminal offences (arson), based on anecdotal knowledge. We may be at risk of encountering a rangeland fire equivalent of the '527 Lime Street Fire'.

It is therefore imperative that wildfire indicators be considered accurate and reliable forensic evidence in wildfire investigations. The purpose of this chapter is to contribute to resolving the above-mentioned issues by quantitatively assessing the reliability and accuracy of various *post-hoc* wildland fire pattern and spread indicators as aids in wildfire origin and cause investigations in mesic montane grasslands of the Eastern Cape, South Africa. And, in doing so, establish a scientific framework and procedure for quantitative assessment of wildfire indicators in future studies.

I aimed to achieve this by gathering real-time fire behaviour data and *post-hoc* fire indicator data from 143 controlled burns, across seven sites, in montane grasslands of the Boschberg, Katberg, & Winterberg mountain ranges. This information was then used to evaluate and assess the reliability, accuracy, and suitability of seven existing, and two novel *post-hoc* indicators to accurately retrodict and reveal aspects of actual wildfire conditions in this grassland ecosystem. And using these results to verify which particular fire behaviour parameters are revealed by each indicator, with anecdotal literature, as well as investigate two additional measures for feasibility as novel indicators. These indicators were: *Consumption depth of grass tussocks; Undercutting of grass culms; Ash colour; Leeside charring on pole type fuels; Protection; Sooting; Staining; Amount of unburnt plant litter; & Ash total organic carbon (TOC) content.* Additionally, I also aimed to identify the conditions (fuel, weather, topography, & fire behaviour) required for the formation of each of the indicators listed above, in montane grassland fuels, as well as make visual assessments of presence and absence of a further four indicators (*Foliage freeze; Cupping in grass tussocks and on terminal ends of woody branches, Curling* and *Spalling*).

My primary hypothesis is that some of the selected indicators will be more sensitive and reliable for the purposes of reconstructing and interpreting wildfire behaviour, and my objective is to determine which of these have utility for forensic purposes

5.3 Methods:

5.3.1 Fuel, weather, & topography:

The same methods as those proposed in **Chapter 4** were used to collect fuel, weather and topographical data. See **Section 4.3.1 *Fuel, weather, & topography*** in **Chapter 4** for more details.

5.3.2 Observed fire conditions:

The same methods as those proposed in **Chapter 4** were used to collect data on observed fire conditions. See **Section 4.4.2 *Observed fire conditions*** in **Chapter 4** for more details.

5.3.3 Post-hoc fire pattern indicators:

The 17 *post-hoc* wildland fire pattern indicators listed in **Section 2.4, *Post-hoc* wildland fire pattern indicators** in **Chapter 2**, vary considerably in terms of their scale, occurrence and degree of detail. Some indicators, such as *shape of fire scar*, *partial burning in fire scar* and *ash patterns*, need to be observed from afar to be interpreted accurately, such as in satellite or aerial images, or from atop a large hill or mountain. Other indicators require more careful examination from a close-up position. The presence or absence of indicators can be affected by vegetation type, ignition procedure, fire behaviour and weather conditions (Simeoni *et. al*., 2017). Due to these variations of scale, occurrence and degree of detail, it is not possible to test all 17 indicators for their reliability. The indicators tested in this study were chosen for their suitability within grassland vegetation as well as for their ease of analysis.

The following 7 of the 17 wildfire pattern indicators were tested for their reliability in this study*: Consumption depth of grass tussocks; Undercutting of grass culms; Ash colour; Leeside charring on pole type fuels; Protection; Sooting; & Staining*. While *Foliage freeze; Cupping in grass tussocks and on terminal ends of woody branches, Curling* and *Spalling* indicators were not quantitatively tested in this study, the presence or absence of any of these indicators within the fire scar were recorded and various visual patterns or observations noted. An array of information can be inferred from individual indicators, however, most indicators are characterised by indicating at least one of the following: **fire spread type** (heading, backing or flanking fire); **wind direction**; & **fire spread direction.**

In addition to 7 of the 17 *post-hoc* wildland fire pattern indicators identified in the literature, a further two indicators, namely *Amount of unburnt plant litter,* and *Ash total organic carbon (TOC) content* were also tested for their suitability as 'novel' indicators. While the use of these 'novel' methods as indicators of fire behaviour is not novel *per se*, their use as indicators in wildfire investigations has not yet been mentioned in the literature.

Post-hoc indicator pattern data was recorded within 143* 10 x 10m experimental burn plots, randomly placed throughout the seven prescribed burn sites, such that heading, backing and flanking fire spread types were equally (roughly) represented, amongst the plots. Some indicators require the presence of supporting items for the formation of certain fire pattern indicators (Simeoni *et. al*., 2017). A 330 ml glass bottle was placed at ground level within each of the plots as a supporting item for *sooting, staining* and *protection* indicators. The 410 g (400 cc) tin cans used as hydropyrometers in each 10 x 10m burn plot were also used as supporting items for *sooting, staining* and *protection* indicators. An untreated *Eucalyptus* fence post (~3 m) was planted at the centre of each 10 x 10m burn plot as a supporting item for the *leeside charring on pole type fuels* indicator. Fence posts were chosen as they are the most common supporting item for leeside charring in runaway rangeland fire scenarios (fence posts, telephone poles, & wooden pylons in agricultural rangeland settings). The planting of fence posts was done in the week leading up to prescribed burns.

* It is noted that several response variables (indicators) varied in sample size. While this was not an intended outcome, it was unavoidable for several reasons. Firstly, some indicators only form under specific conditions (*e.g.*, head or back fires), This presence or absence of indicator expression results in a number of various sample sizes. Incidentally, the presence or absence of indicator expression is, in and of itself useful and insightful data. Another reason for mixed sample sizes of response variables (indicators) was due to interference of supporting items and/or experimental plots from wildlife (*e.g.*, baboons), which resulted in several samples being spoiled, destroyed, or removed (*e.g.*, 330ml glass bottles & 410g tin cans). Special reference is made of two experimental burn plots (10 x 10 m) within Site 6 (n = 14 fires), in which the entire ground surface and residual vegetation was compromised from wildlife activity. The only post-fire data salvageable from these two plots were that which was collectable from the planted fence posts (*i.e.*, char height and direction of char). Additionally, all ash samples collected from Site 6 (n = 12) were unfortunately lost in transit. Fortunately, Site 6 comprised the fewest burn plots, and thus had little bearing on overall sample size.

Measurements of *ash colour, undercutting, sooting, staining* and *unburnt plant litter* indicators were recorded as soon as possible after the fire was extinguished, as these indicators can, in some cases, be sensitive to certain weather conditions such as heavy rains and strong winds. Measurements of *leeside charring on pole type fuels; foliage freeze; consumption depth of grass tussocks; cupping; & protection;* are less weather sensitive and were sampled during the week following the prescribed burn. All directional measurements were made using a 360° handheld compass and were recorded within 5-degree increments.

Indicators of fire spread type (head, back & flank)

- For ***consumption depth of grass tussocks***, the stubble height of 30, randomly selected, remaining grass tussocks within each plot (n = 141) was recorded in centimetres, using a stainless steel one-meter ruler. Consumption depth measurements were averaged for each plot.

- ***Undercutting*** of grass culms was sampled the day following prescribed burns. The total number of unburnt culms lying on burnt ground in each plot (n = 141) was recorded.

- ***Ash colour*** was measured using two separate methods: Munsell colour score (Munsell Colour co., 1975) and surface cover fraction of plots.

  Munsell colour score method: Ash samples were collected from 126 10 x 10m plots and placed in test tubes. When collecting samples, careful consideration was made to select a sample representative of the entire 10 x 10 m burn plot, avoiding large stumps or areas of prolonged combustion. Munsell colour scores were determined *post-hoc* for each sample (plot) (n = 126) using a Munsell Soil Colour Chart (Munsell Colour co., 1975), following similar methods proposed by Ubeda *et. al*., 2009; Bodi *et. al*., 2011; Bodi *et. al*., 2012; Pereira *et. al*., 2012; Bodi *et. al*., 2014. A second Munsell colour score was determined for each of the 126 ash samples after 'complete combustion' in a muffle furnace. Samples were placed in aluminium cups and dried for three hours at 105^{o}C before undergoing five hours of combustion at 500^{o}C. All Munsell score colour measurements were done by the same person, in the same location, and under the same artificial light conditions. Munsell colour scores are divided into three components: hue, chroma (colour intensity), & value (lightness or darkness). Additionally, a colour class (*e.g.*, dark grey) can be determined based on the combination of the previous three values (Munsell colour score). It is noted that ash colour does not always fall within the grey spectrum and may often comprise an element of colour (yellows and oranges) (Ubeda *et. al*., 2009; Pereira *et. al*., 2012; Bodi *et. al*., 2014). It is also true that ash colour often has a chroma score of zero, which is equivalent to a neutral hue.

  Surface cover fraction method: Following similar methods to Hudak *et. al.*, (2013), cover fractions were estimated for 139 10 x 10m experimental fire plots, recording percent cover of the following elements: white ash; black soot; bare ground; & unburnt plant material.

Indicators of direction (wind & fire spread)

- ***Leeside charring on pole type fuels***. The presence or absence of charring on fence posts within each the 143 10 x 10m plots was recorded. The direction of the side of the fence pole that had experienced the greatest height of charring was also recorded. A pole was considered 'charred' if charring was present above the first 30 cm from the ground surface.

- ***Foliage freeze***. Total number of tall woody plants (bushes) in each plot were counted and classified into either: unburnt; scorched; or charred. The number of scorched bushes that displayed leaf freeze was recorded. For each plot, foliage freeze incidence was expressed as percentage of scorched bushes that displayed leaf freeze.

- ***Cupping*** was sampled on both grass tussocks and charred woody plant (tall bush) "skeletons".

  Grass tussocks: The total number of grass tussocks present in each plot were counted. The number of tussocks in each plot that expressed cupping were counted. For each plot (n = 141), cupping incidence was expressed as percentage of tussocks displaying cupping.

  Tall woody plant 'skeletons': As with Foliage freeze, total number of bushes in each plot were counted and classified as either: unburnt; scorched; or charred. The number of charred bush skeletons that displayed cupping were recorded. For each plot, cupping incidence was expressed as percentage of charred bushes that displayed cupping.

- The presence or absence of ***protection*** was recorded around the 330 ml glass bottle within each plot. When protection occurred, the direction of the protected side of the object was recorded.

- ***Sooting*** and ***staining*** was sampled on the day following prescribed burns. The presence or absence of ground level sooting or staining on supporting items (330 ml glass bottle & 410 g (400 cc) tin can) was recorded within each plot (n = 127). If sooting or staining had occurred, the direction of the side of the object that had experienced the sooting or staining, was recorded.

Potential novel indicators

- Amount of residual ***unburnt plant litter*** was sampled on the day following each prescribed burn. For each 10 x 10m plot a litter sample was collected within a 29 x 25cm quadrat (725cm^2) with rounded edges (**FIGURE 5.1**). Importantly, the quadrat was 20 cm high for ease of distinction between fragile material inside and outside the quadrat. Samples were collected by sweeping the contents of the small quadrat into a zip-lock bag, using a paint brush. Caution was taken during litter collection to only sweep up the loose remains of partially combusted plant material, and to not include soil or remaining grass stubble and tussocks which were still intact and attached to the ground surface. Litter samples were weighed using a balance, accurate to 0.001 grams (Radwag scale), thus obtaining a litter weight (g) per 725cm^2. Litter weights were then converted to g/m^2.

FIGURE 5.1: *Photograph showing quadrat (29 x 25cm with rounded edges (725cm^2) and 20 cm high) used to collect residual plant litter samples.*

- ***Ash total organic carbon content.*** Ash samples from 126 10 x 10m plots were analysed for total organic carbon (TOC) content. The same ash samples taken for Munsell colour score estimations were also used for TOC content calculations. Ash TOC content was calculated using the Loss on Ignition technique (Nelson & Sommers, 1996; Bodi et. al., 2014), following similar methods to

Burns, (2007). Loss on Ignition technique was chosen, as it is a relatively simple and inexpensive method to determine carbon content (Burns, 2007).

The Loss of Ignition technique works on the basis that inorganic carbon combusts at a much higher temperature (roughly 600 – 800^{o}C) than organic carbon (roughly 150 – 400^{o}C) (Bodi *et. al*., 2014). In theory, this allows for the complete combustion of organic carbon, without a loss in inorganic carbon.

Ash samples were placed in aluminium cups and initially oven dried at 105^{o}C for three hours to drive off excess moisture. Ash samples were then weighed using a balance accurate to 0.001 grams (Radwag scale) and recorded as total carbon (TC) weight. Ash samples were then placed in a muffle furnace for a second time, now at 500^{o}C for five hours in order to combust all remaining organic carbon. Ash samples were then weighed for a second time, and weights recorded as total inorganic carbon (TIC) weight. The difference in TC and TIC weights was recorded as amount of TOC and was expressed as a percentage of total weight (TC weight).

$$\mathbf{TOC = TC - TIC}$$

(Bodi *et. al.*, 2014)

5.3.4 Data analyses:

All statistical data analyses were performed in R Studio (R Core Team, 2020) and where relevant, statistical significance was set at $P < 0.05$, unless specifically stated otherwise.

Indicators of fire spread type (head, back & flank)

ANOVA tests for parametric data and Kruskal-Wallis (rank sum) tests for non-parametric data were performed to identify differences in indicator values between head, back & flank fires (fire spread type), with site included as a variable to account for site affects. These indicator measures included: *Consumption depth of grass tussocks; Number of unburnt culms lying on burnt ground; Munsell colour value of ash; Amount of unburnt plant litter; & Ash TOC content*. *Post-hoc* analyses (Tukey's HSD (honestly significant difference) for ANOVA's and Wilcoxon (Mann-Whitney U) for Kruskal-Wallis tests) were then run to determine between which fire spread types or sites differences (if they existed) occurred.

Indicators of direction (wind & fire spread)

It is important to understand that directional (circular) data cannot be interpreted or expressed on a linear scale. Circular data is vector interval data with no true zero. (*e.g.*, the difference between 5 degrees and 355 degrees is 10 degrees, **not** 350 degrees). Therefore, linear interpretation of circular data will result in incorrect mean and median values. While this may seem self-evident, the significance of this is that circular data is interpreted using unique statistical tests which make use of values such as circular means, circular medians, and resultant vector lengths (R). When calculating circular means and circular medians, a vector is produced. In addition to an angular value, an associated length of angle is also produced. This length value is known as the Resultant Vector Length (R) and is an indication of the spread of the circular data. R is a value between zero and one, with a value of one indicating a clustered or unimodal distribution and a value of zero indicating a uniform distribution around a circle.

Another aspect in which circular statistics differs from regular statistics is with regards to data distributions. Circular data distributions are usually grouped as either uniformly distributed (around a circle) or unimodally distributed (clustered around a point). The Von Mises distribution is a type of unimodal distribution which is the circular analogy of the normal distribution (Ruxton, 2017).

Here indicator directions are expressed as angles in relation to a reference direction (wind direction, fire spread direction, aspect), and not in relation to north. This is done so as to avoid overlap of non-corresponding dependent variables with independent variables when conducting statistical analyses of entire dataset. This is critical, because wind direction, fire spread direction and aspect values differ for each of the 143 observations. Indicator directional expression was grouped into 22.5^{o} increments.

Watson goodness of fit tests for circular uniformity or Von Mises distributions were performed on relevant directional data in order to test for acceptable deviation away from Von Mises data distribution.

In order to test various indicator directional distributions against *a priori* predictions of unimodal clustering around expected directions, Rayleigh tests, with specified expected mean directions (mu) for the alternative hypothesis, were conducted (Ruxton, 2017). While Rayleigh tests are most efficient when applied to Von Mises data distributions, their performance on most unimodal data distributions is sufficient (Ruxton, 2017). No alternative test is in common usage (Ruxton, 2017).

In scenarios where dependent variable directional data distributions deviated very significantly from Von Mises distributions, Rao's & Kuiper's tests for uniformity were performed to test for uniformity or clustering around an angle.

Dependant variables: *Leeside charring on pole type fuels* (char direction)*; Protection* (protected side direction)*; Sooting* (direction of sooting)*; Staining* (direction of staining).

Independent variables: Wind direction; fire spread direction; aspect.

Other analyses

Pearson's (linear) correlations (parametric) and Spearman's rank correlations (non-parametric) were performed between effective gradient experienced by each fire and *consumption depth of grass tussocks*. These same correlations were performed between *ash TOC content* and fire severity and Munsell value.

Welch two sample T-test was performed on residual ash field samples to determine if a difference existed between Munsell values before and after complete combustion at 500ºC for five hours.

5.4 Results:

Mean fuel, weather, and topographical data for each site are summarised in **TABLE 3.1** & **TABLE 3.2** of **Chapter 3**.

5.4.1 Indicators of fire spread type:

Consumption depth of grass tussocks

Residual grass stalk stubble height (cm) values for head, back, & flank fire spread types from 141 fires in Eastern Cape mesic montane grasslands are summarised in **TABLE 5.1**. Residual grass stubble height data was positively skewed away from normal distribution. Grass stubble height was found to differ significantly in means ($P < 0.001$) between fire spread type, and perhaps also differ in medians ($P < 0.007$) (**FIGURE 5.2**). Mean residual grass stubble height in back fires (9.658 cm) was significantly shorter than mean stubble height in head and flank fires ($P < 0.004$). According to the Wilcoxon rank sum test, consumption depth of grass tussocks in flank fires differed significantly from consumption depth in back fires ($P < 0.003$).

Residual grass stubble height (for all three spread types) was significantly higher ($P < 0.001$) in sites 1 & 2 (Boschberg) (**FIGURE 5.4**) than sites 3 – 7 (Katberg & Winterberg) (**FIGURE 5.5**) (**FIGURE 5.3**). The difference in residual stubble height between fire spread types was also more pronounced in these two sites (1 & 2 at Boschberg) (**FIGURE 5.3**).

Residual grass stubble height (cm) versus the effective slope gradient (%) realised by forward moving fire through each 10 x 10 m experimental burn plot, and separated by fire spread type is shown in **FIGURE 5.6**. There appeared to be no significant associations between residual grass stubble height and effective gradient for all three fire spread types ($rho < \pm 0.237$; $P > 0.1$). A weak linear correlation may perhaps exist between residual grass stubble height and effective gradient in flank fire scenarios ($rho = 0.295$; $P < 0.05$), although the positively skewed data distribution likely influences this result.

TABLE 5.1: *Residual grass stubble height (cm) standard deviation, median, mean & standard error (se) values for head, back, & flank spread types from 141* fires in Eastern Cape montane grasslands.*

Fire Spread Type	Standard Deviation	Median	Mean ± se
Head (*n = 52*)	6.058	9.578	12.069 ± 0.840
Flank (*n = 45*)	5.703	12.703	13.510 ± 0.850
Back (*n = 44*)	3.114	9.681	9.658 ± 0.470

**n = 141 (residual vegetation of two out of total 143 burn plots compromised from wildlife interference)*

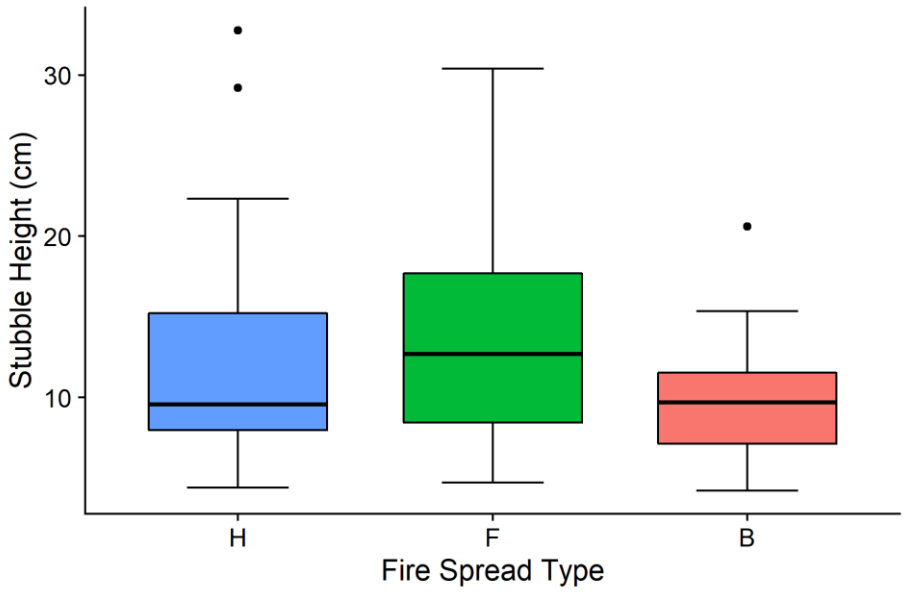

FIGURE 5.2: *Boxplot comparing residual grass stubble height (cm) between head (H), back (B), & flank (F) fire spread types from 141 fires in Eastern Cape mesic montane grasslands.*

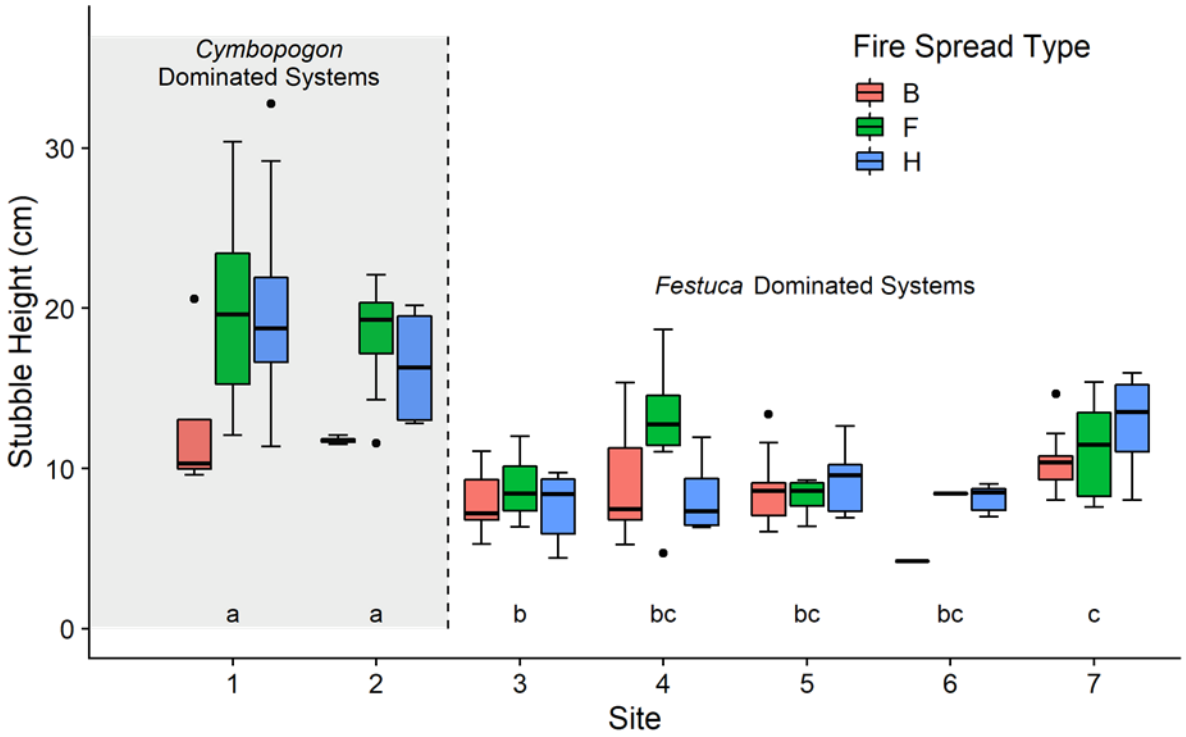

FIGURE 5.3: *Boxplot comparing residual grass stubble height (cm) between sites (1 – 7) and separated by head (H), back (B), & flank (F) fire spread types from 141 fires in Eastern Cape mesic montane grasslands. Greyed out area (Sites 1 & 2) highlights Cymbopogon dominated systems, while the remaining sites (3 – 7) are Festuca dominated systems. Lower case letters (a, b, & c) represent significant differences ($P < 0.02$) between sites.*

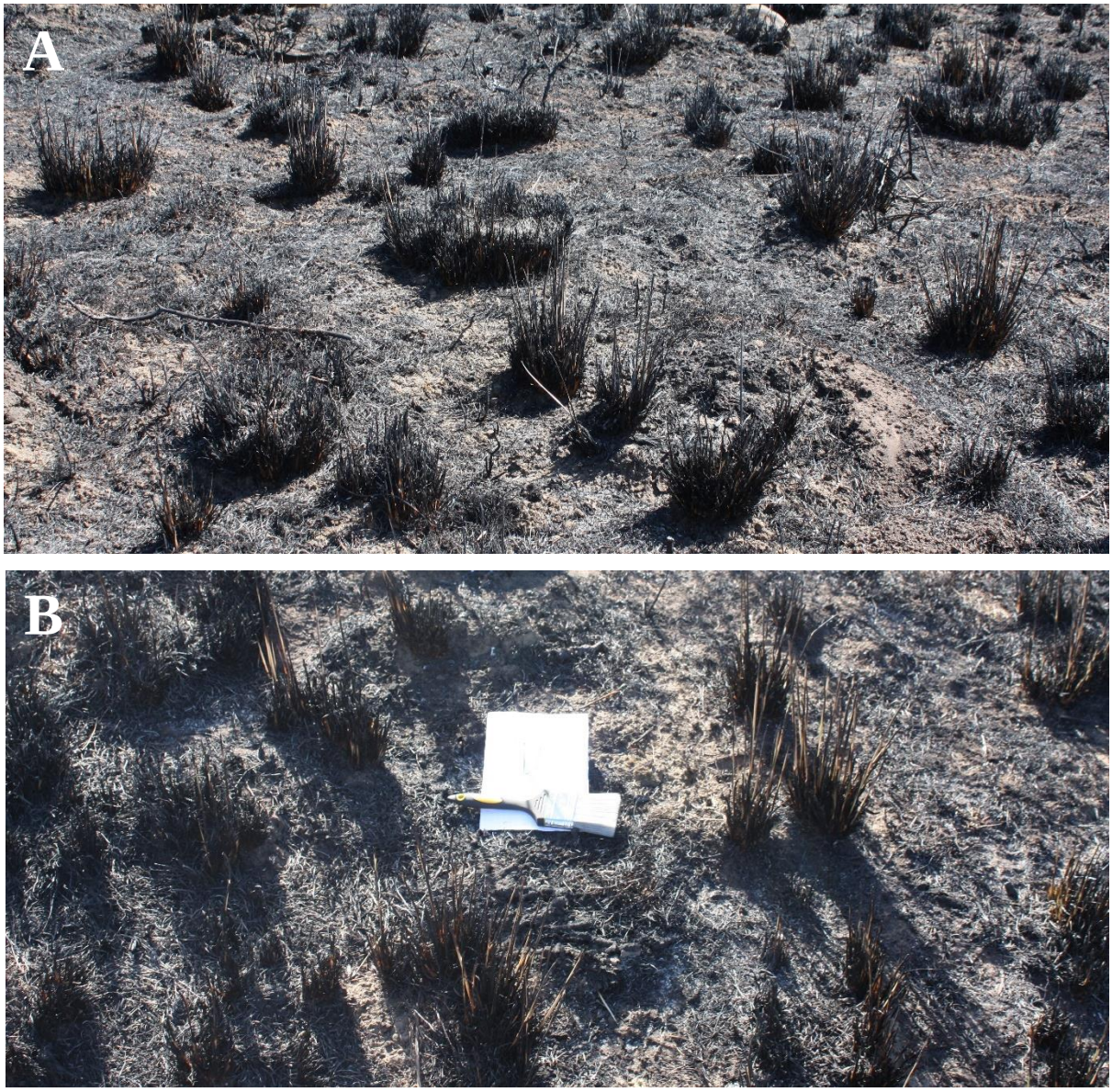

FIGURE 5.4: *Photographs showing examples of partially burnt (A) and unburnt (B) residual Cymbopogon grass stubble after head fire passage at Site 1. Note the unburnt (brown) stalks in photograph B, which were live green basal portions of Cymbopogon tillers before fire passage. Prescribed burn MW1, Boschberg, EC, South Africa, 13 September 2019.*

FIGURE 5.5: *Photograph showing example of partially burnt residual Festuca grass stubble at Site 4, one week after fire passage. Note how close to the ground surface grass tussocks have been consumed. Green Festuca shoots have emerged in the week following prescribed fire. Prescribed burn BE1, Katberg, EC, South Africa, 16 October 2019.*

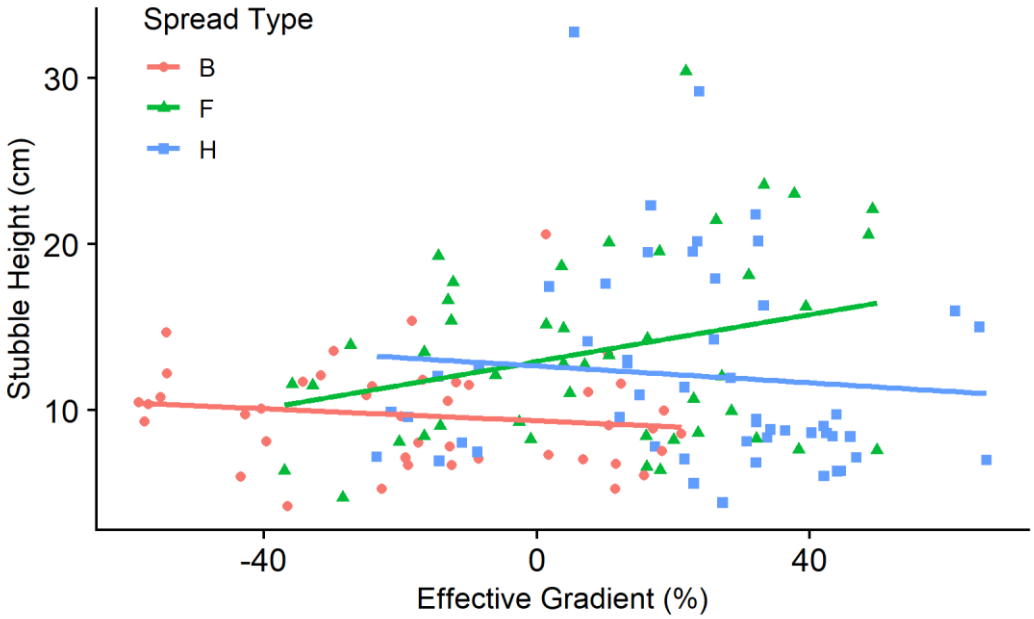

FIGURE 5.6: *Residual grass stubble height (cm) versus the effective gradient (%) realised by forward moving fire through each 10 x 10 m plot, separated by fire spread type (head (H), back (B), & flank (F)), from 141 fires in Eastern Cape mesic montane grasslands. Solid lines indicate regression equations for each fire spread type (head, back, & flank).*

Undercutting of flowering culms

Number of unburnt grass culms lying on burnt ground per *100 m^2* values for head, back, & flank fire spread types from 141 fires in Eastern Cape mesic montane grasslands are summarised in **TABLE 5.2**. Number of unburnt undercut culms data was distributed exponentially and positively skewed.

In all cases (sites and grass species), the flowering culms present in the grass sward were from the previous season's growth, as it was too early in the current season for new tillers to have produced flowering culms. If any new culms had been produced, they were of fresh growth and therefore non-flammable. As such, all undercut flowering culms were dry and flammable.

Unburnt undercut culm density was found to differ significantly between fire spread type ($P < 0.001$) (**FIGURE 5.7**). A Wilcoxon rank sum *post-hoc* analysis determined that culm densities in head, back, & flank fires were all independent of each other ($P < 0.001$). Undercut culms were present on burnt ground after fire passage, in 86.4% of all back fires, 40% of all flank fires, and in only one instance out of 52 head fires (< 2%).

Only two sites differed significantly from each other in culm density ($P < 0.006$). Number of unburnt undercut culms (for all three spread types) was significantly higher ($P < 0.029$) in Site 5 than Site 6.

TABLE 5.2: *Number of unburnt grass culms lying on burnt ground per 100 m^2 standard deviation, median, mean & standard error (se) values for head, back, & flank fire spread types from 141 fires* in Eastern Cape mesic montane grasslands.*

Fire Spread Type	Standard Deviation	Median	Mean ± se
Head (*n = 52*)	0.555	0	0.077 ± 0.077
Flank (*n = 45*)	46.525	0	25.578 ± 6.936
Back (*n = 44*)	143.453	80	138.500 ± 21.626

**n = 141 (ground surface and residual vegetation of two out of total 143 burn plots compromised from wildlife interference)*

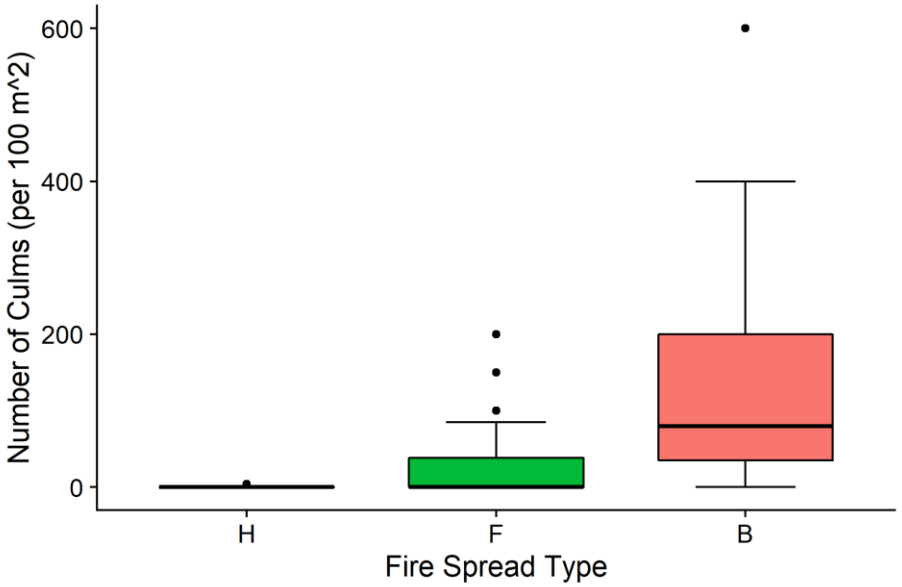

FIGURE 5.7: *Boxplot comparing number of unburnt undercut flowering grass culms lying on burnt ground per 100 m^2 between head (H), back (B), & flank (F) fire spread types from 141 fires in Eastern Cape mesic montane grasslands.*

FIGURE 5.8: *Photograph showing example of an unburnt undercut flowering Cymbopogon culm, two days after back fire passage. Pen denoting direction of fire approach (left). Back fire passage left to right. Undercut culm has fallen in direction of, and pointing towards back fire approach. Prescribed burn MW2, Boschberg, EC, South Africa, 17 September 2019.*

Ash colour

Munsell colour score

Field sampled residual ash sample Munsell values (darkness/lightness) before and after complete combustion in muffle furnace (5 hours at 500ºC) for head, back, & flank fire spread types from 126 fires in Eastern Cape mesic montane grasslands are summarised in **TABLE 5.3**. Munsell value data for residual ash field samples was positively skewed away from normal distribution. There was no significant difference in Munsell value between fire spread type for field sampled residual ash in these grasslands ($P > 0.309$) (A in **FIGURE 5.9**). There was, however, a difference in Munsell value of residual ash field samples between sites ($P < 0.001$). Site 1 had a significantly higher Munsell value (lighter in colour) than Sites 3, 4, & 7 ($P < 0.007$).

After combustion in a muffle furnace at 500ºC for five hours, Munsell values of completely combusted residual ash samples (B in **FIGURE 5.9**) were significantly higher (lighter in colour) than Munsell values of field sampled residual ash before complete combustion (A in **FIGURE 5.9**) ($P < 0.001$).

Distribution of residual ash field sample Munsell colour class between head, back, & flank fire spread types is illustrated in **FIGURE 5.10**. There did not appear to be any discrepancy in Munsell colour class distribution between fire spread type.

TABLE 5.3: *Field sampled residual ash Munsell value (darkness/lightness) standard deviation, median, mean & standard error (se) values, before and after complete combustion (five hours at 500ºC), for head, back, & flank fire spread types from 126 fires* in Eastern Cape mesic montane grasslands.*

Fire Spread Type	Standard Deviation	Median	Mean ± se
Field sample:			
Head (*n = 42*)	1.908	3	3.232 ± 0.294
Flank (*n = 43*)	1.561	2.5	2.855 ± 0.278
Back (*n = 41*)	1.803	3	3.357 ± 0.238
After Complete Combustion:			
Head (*n = 42*)	0.958	7	7.095 ± 0.148
Flank (*n = 43*)	0.947	7	7.035 ± 0.144
Back (*n = 41*)	0.862	7	6.890 ± 0.135

**n = 126 (no samples exist from Site 6, three samples spoiled in the lab)*

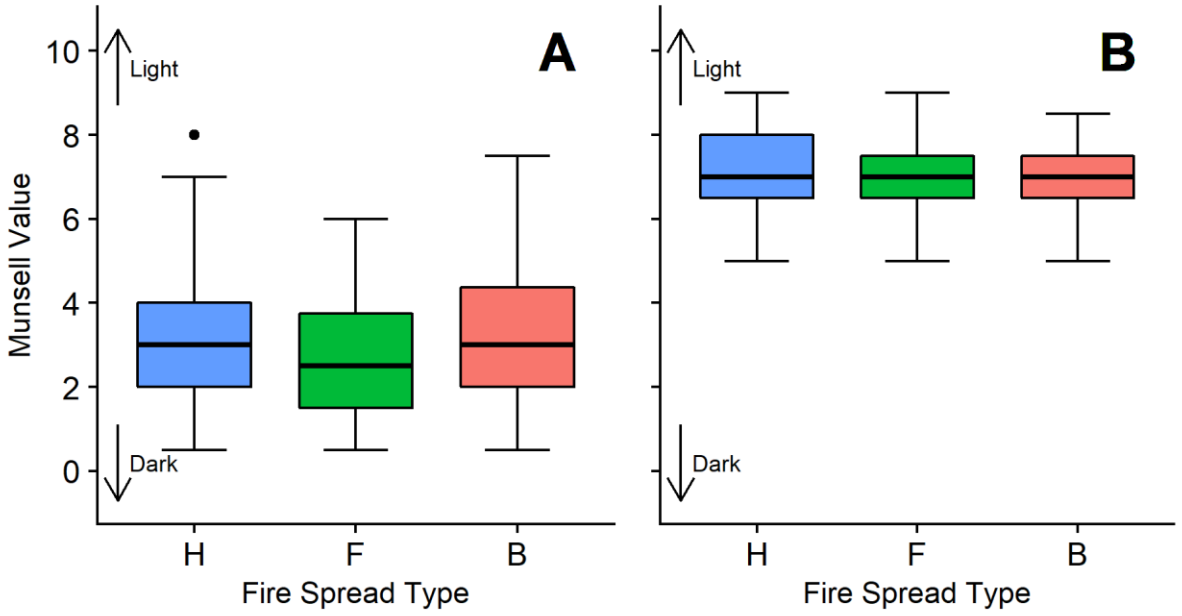

FIGURE 5.9: *Boxplot comparing Munsell value (darkness/lightness) of (A) field sampled residual ash, and (B) completely combusted (five hours at 500°C) ash samples between head (H), back (B), & flank (F) fire spread types from 126 fires in Eastern Cape mesic montane grasslands. High values indicate lighter colours, while low values indicate darker colours.*

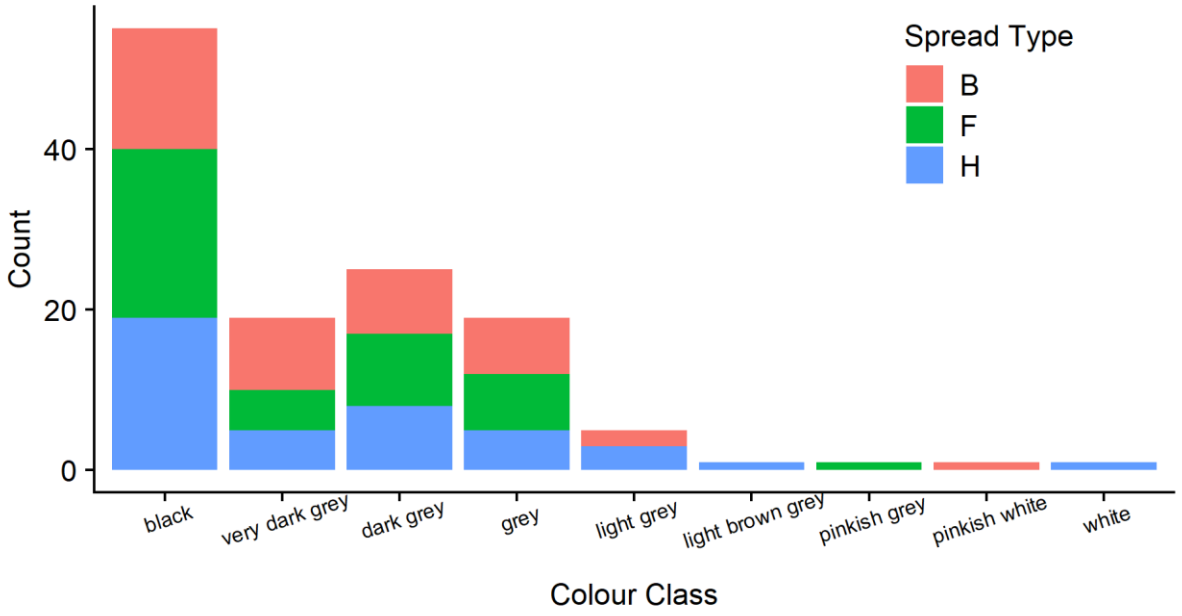

FIGURE 5.10: *Bar graph comparing proportional distribution of residual ash sample Munsell colour class between head (H), back (B), & flank (F) fire spread types, collected from 126 fires in Eastern Cape mesic montane grasslands.*

Surface cover fractions

Surface cover fraction (%) values for head, back, & flank fire spread types from 139 fires in Eastern Cape mesic montane grassland are summarised in **TABLE 5.4**. From perusal of **TABLE 5.4** there appeared to be no significant differences in surface cover fraction proportions between head, back, & flank fire spread types. Statistically, no difference could be found between individual cover fraction components from different fire spread types ($P > 0.137$).

TABLE 5.4: *Percentage cover fraction standard deviation, median, mean & standard error (se) values of four surface materials (white ash; black soot; bare ground; unburnt plant material), visually estimated after prescribed fires, for head, back, & flank fire spread types from 139 fires* in Eastern Cape mesic montane grasslands.*

Fire Spread Type	Standard Deviation	Median	Mean ± se
Head Fire (*n = 52*)			
White Ash	7.062	8.5	9.413 ± 0.979
Black Soot	13.437	43.25	43.731 ± 1.863
Bare Ground	16.008	25	25.077 ± 2.220
Unburnt Plant Material	14.272	25	21.817 ± 1.979
Flank Fire (*n = 44*)			
White Ash	6.846	10	11.148 ± 1.032
Black Soot	10.891	44	42.011 ± 1.642
Bare Ground	18.876	16.25	23.443 ± 2.846
Unburnt Plant Material	16.125	25	23.398 ± 2.431
Back Fire (*n = 43*)			
White Ash	10.263	10	13.035 ± 1.565
Black Soot	13.172	40	39.128 ± 2.009
Bare Ground	16.788	15	20.523 ± 2.560
Unburnt Plant Material	18.070	30	27.314 ± 2.756

**n = 139 (four out of total 143 burn plots compromised from wildlife disturbance of ground surface)*

5.4.2 Indicators of direction (wind & fire spread):

Leeside charring on pole type fuels

Charring (above 30 cm from ground surface) was present on 83 of total 143 pre-planted fence posts (58%). Charring on fence posts occurred in 72.2% of all head fires, in 60% of all flank fires, and in 38.6% of all back fires. Incidence of leeside charring was more prevalent at higher wind speeds (**FIGURE 5.11**) and steeper slope gradients (**FIGURE 5.12**).

Charring direction (°) on 83 fence posts (side of post on which highest point of charring occurred) relative to wind direction (A), fire spread direction (B), and aspect (C) from 83 fires in Eastern Cape montane grasslands is illustrated in **FIGURE 5.13**, and various values summarised in **TABLE 5.5**. Charring direction on fence posts relative to wind direction was found to be very strongly clustered towards the leeward side (180°) for all three fire spread types ($P < 0.001$), with very little variation in direction ($R = 0.669$) (A in **FIGURE 5.13**). This directional pattern (unimodal distribution) was strongest in head and flank fires (A in **FIGURE 5.13**).

Similarly, the distribution of charring direction on fence posts relative to aspect was found to be clustered towards the upslope side (180°) for all three fire spread types ($P < 0.001$) (C in **FIGURE 5.13**), although less strongly so, and with greater variation ($R = 0.555$) than when compared to charring direction relative to wind direction (A in **FIGURE 5.13**). Again, this directional pattern was strongest in head and flank fires (C in **FIGURE 5.13**).

Looking at charring direction on fence posts relative to fire spread direction (B in **FIGURE 5.13**). Charring in head fire scenarios, for the most part, occurred in the direction of fire spread ($P < 0.001$), with little variation ($R = 0.827$). Charring direction in flank fire scenarios mostly clustered at right angles to fire spread direction ($P < 0.001$), although with some degree of variation ($R = 0.468$). Charring direction on fence posts in back fire scenarios relative to fire spread did not display unimodal distribution around the *a priori* expected mean direction (180°) ($P > 0.232$). Nor did it appear to be clustered in any specific direction ($P > 0.316$), showing a uniform distribution ($P > 0.1$) ($R = 0.262$).

TABLE 5.5: *Means, medians, and resultant vector length (R) values for relative direction of char (°) on pre-planted fence posts in relation to wind direction, fire spread direction, & aspect from 83* fires in Eastern Cape mesic montane grasslands.*

Relative Direction	R	Median	Mean
Relative to Wind	0.669	185	189.550
Relative to Fire Spread	0.429	15	22.645
Relative to Aspect	0.555	205.236	211.206

**n = 83 (leeside charring only present in 83 of total 143 fires)*

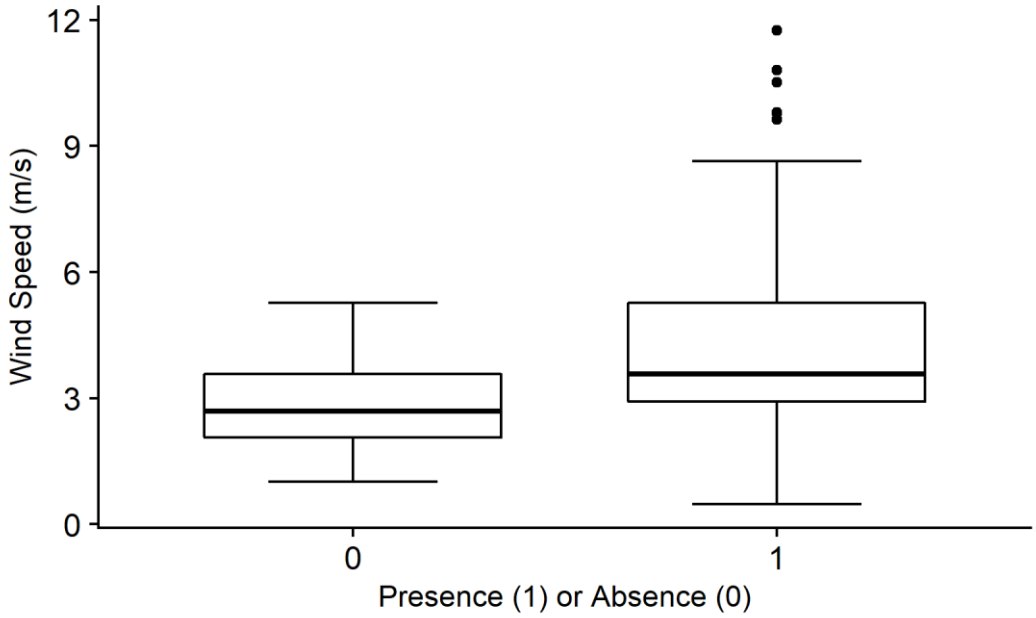

FIGURE 5.11: *Boxplot comparing leeside charring presence (1) and absence (0) at a range of wind speeds (m/s) from 143 fires in Eastern Cape montane grasslands.*

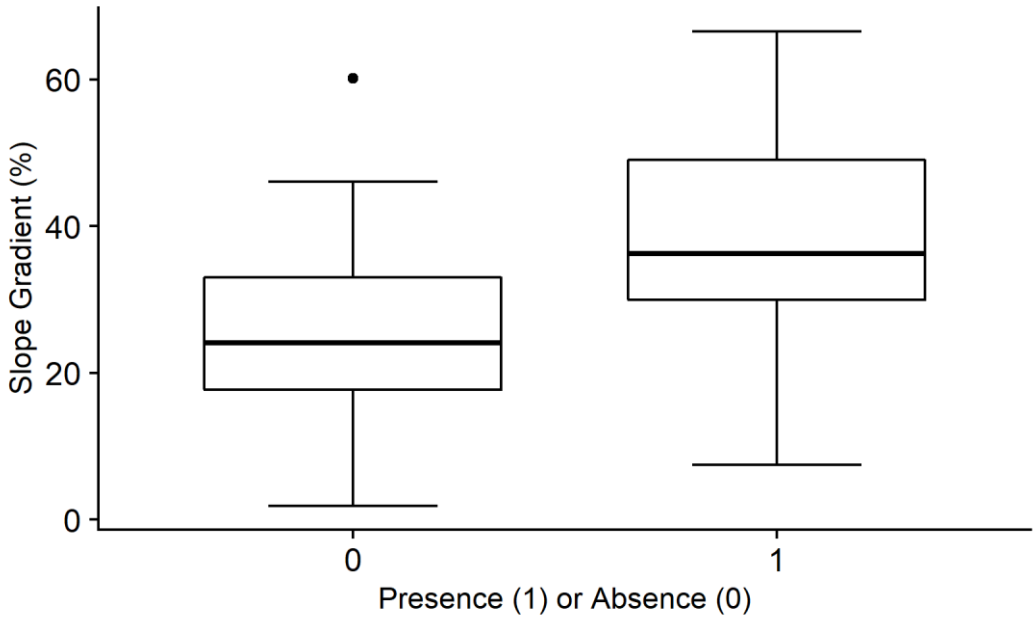

FIGURE 5.12: *Boxplot comparing leeside charring presence (1) and absence (0) at a range of slope gradients (%) from 143 fires in Eastern Cape montane grasslands.*

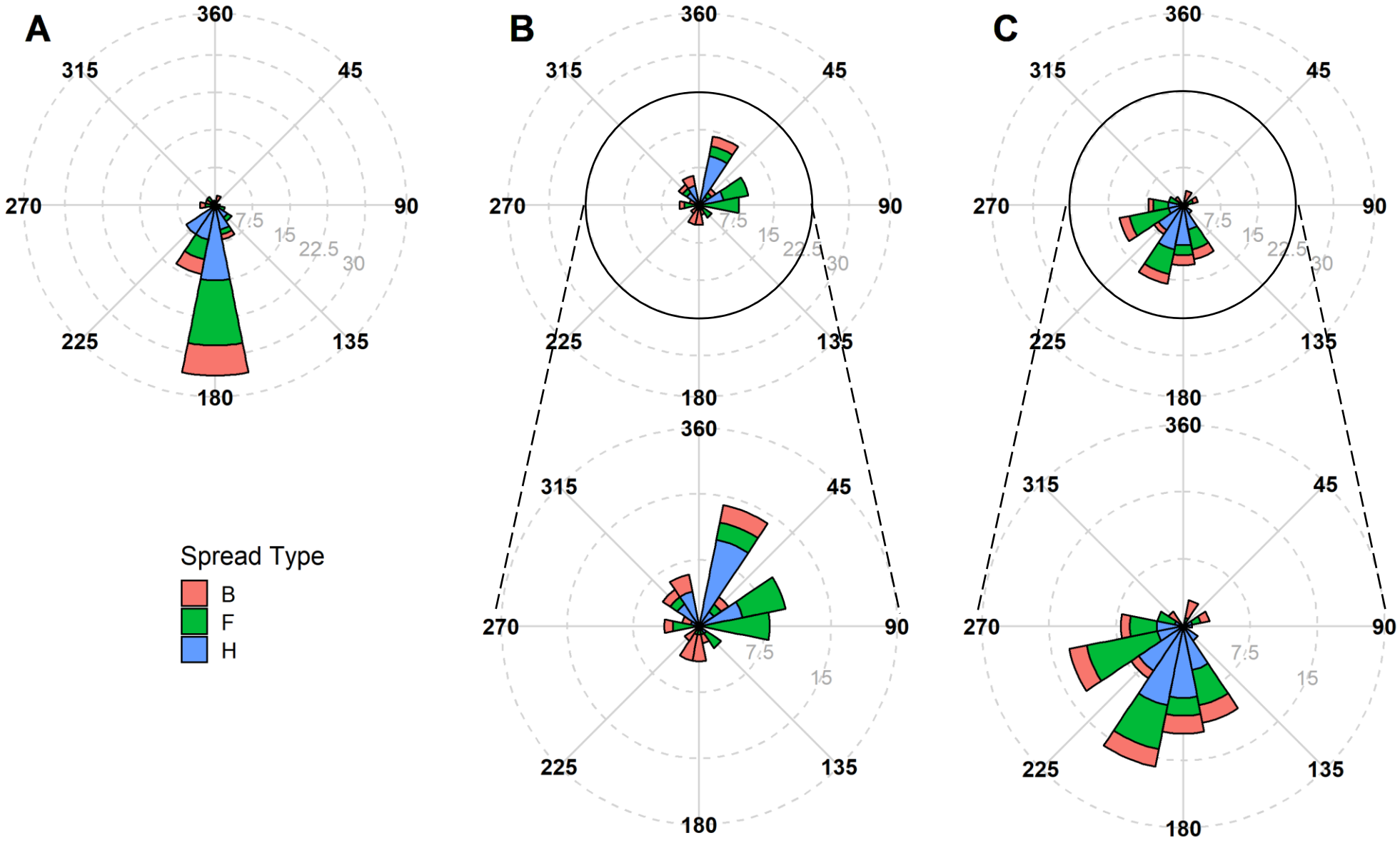

FIGURE 5.13: *Rose plots showing (leeside) charring direction in 22.5 degree (º) increments on ~3 m fence posts relative to (A): wind direction; (B): fire spread direction; & (C): aspect, and grouped by fire spread type from 83 fires in Eastern Cape montane grasslands. r axes are the count of indicator expressions within each 22.5º increment. Upscaling of rose plots B & C is illustrated below respective plots.*

Foliage freeze

Freezing of woody component foliage occurred on 43% of scorched woody species. The presence of leaf freeze on scorched trees and bushes was much higher in head fires (53.9%) than after back fire passage (21.4%) ($P < 0.048$).

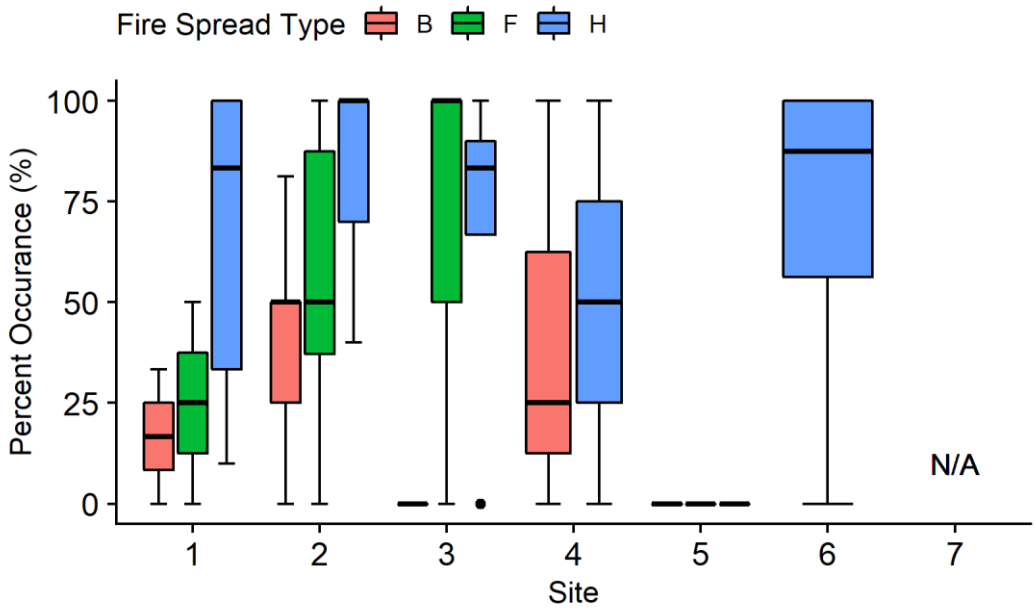

FIGURE 5.14: *Boxplot comparing foliage freeze occurrence (%) in scorched woody species between sites (1 – 7) and separated by head (H), back (B), & flank (F) fire spread types from 61* fires in Eastern Cape mesic montane grasslands. Site 7 had no woody component present within the sward. *Only 61 fires had scorched woody plants present within the plots.*

Cupping

The Eastern Cape montane grassland sites of this study comprised a mean tussock density of 249 ± 10 tussocks per 10 x 10 m burn plot. Cupping of grass tussocks occurred on just over a quarter (28%) of all tussocks. Grass tussock cupping occurrence did not differ significantly between fire spread types ($P > 0.896$). Grass Tussock cupping occurrence was significantly higher at Site 7 than Sites 1, 3, 4, & 6 ($P < 0.038$).

Cupping on terminal ends of woody component branches occurred on only 18.5% of all charred woody species. The presence of cupping on trees and bushes was higher after head fire passage (24%) than in flank (11.7%) and back (16.4%) fires, but not significantly so ($P > 0.155$).

Protection

Direction of protected side of 330 ml glass bottles (°) relative to wind direction (A), fire spread direction (B), and aspect (C) for 62 fires in Eastern Cape montane grasslands are illustrated on **FIGURE 5.15**, and various directional values summarised in **TABLE 5.6**.

17 (of total 143) supporting items (330 ml glass bottles) were spoiled from wildlife interference (*i.e.*, removed from site by curious baboons), which brought the total number of observations down to 126 fires.

Protection from glass bottles occurred in 77.8% of total observations (n = 126) after fire had passed and was no more or less prolific in any particular fire spread type. Of the fires which showed protection, only 63.3% showed a clear direction of protection. Similarly, there were no proportional discrepancies between fire spread types.

The direction of the protected side of glass bottles relative to wind direction showed a weak unimodal distribution ($P < 0.026$) ($R = 0.243$) clustered towards the leeward side (180°) for head and flank fires ($P < 0.017$) (A in **FIGURE 5.15**). This directional relationship did not apply to back fire scenarios ($P > 0.59$), where the direction of the protected side relative to wind direction was uniformly spread ($R = 0.036$).

The direction of the protected side of glass bottles relative to fire spread direction clustered unimodally ($P < 0.001$) towards 45°, although still displayed a strong statistically significant clustering towards the expected *a priori* direction of fire spread (0/360°) ($P < 0.001$) (B in **FIGURE 5.15**). This, however, was not the case in back fire scenarios ($P < 0.268$), which had a fairly uniform distribution ($R = 0.106$).

The direction of the protected side of glass bottles relative to aspect displayed a strong unimodal clustering in an upslope direction (180°) for all three fire spread types ($P < 0.001$), although with some degree of spread in other directions ($R = 0.489$) (C in **FIGURE 5.15**).

TABLE 5.6: *Means, medians, and resultant vector length (R) values for relative direction (°) of protected side of 330 ml glass bottles in relation to wind direction, fire spread direction, & aspect from 62* fires in Eastern Cape mesic montane grasslands.*

Relative Direction	R	Median	Mean
Relative to Wind	0.243	216.98	207.033
Relative to Fire Spread	0.374	43	40.088
Relative to Aspect	0.489	199.382	204.196

**n = 62 (direction of protection was only clear in 62 out of 98 cases of protection (126 total observations))*

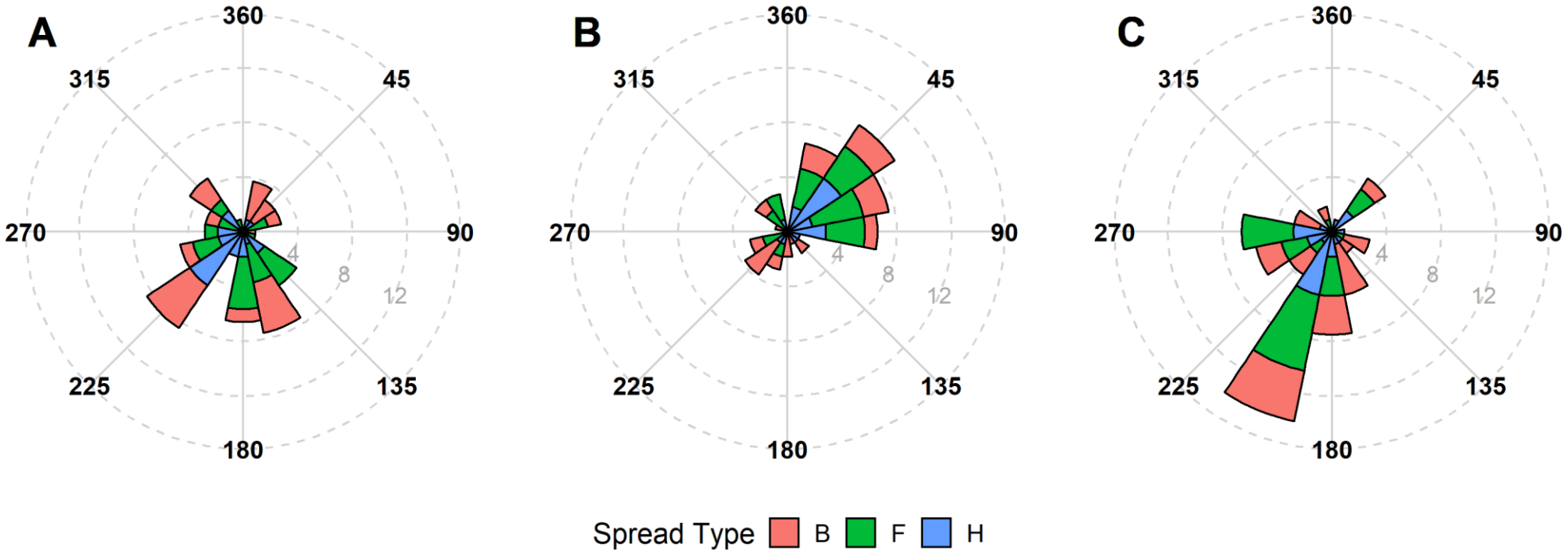

FIGURE 5.15: *Rose plots showing direction of protected side of 330 ml glass bottle in 22.5 degree (º) increments relative to (A): wind direction; (B): fire spread direction; & (C): aspect, and grouped by fire spread type from 62 fires in Eastern Cape mesic montane grasslands. r axes are the count of indicator expressions within each 22.5º increment.*

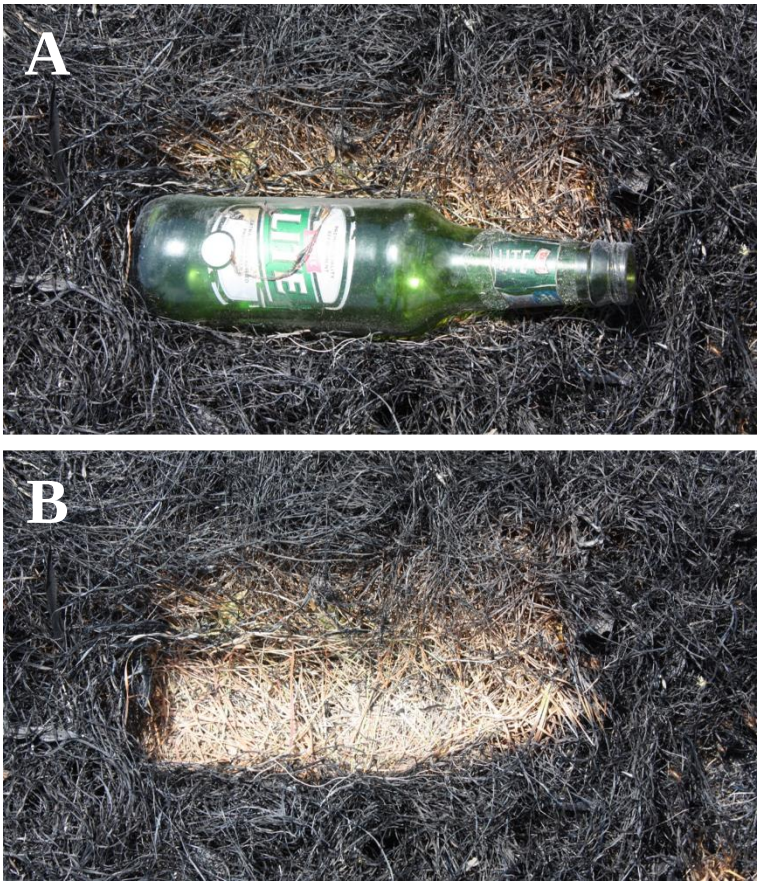

FIGURE 5.16: *Example of protection fire pattern indicator, with (A) and without (B) supporting item (330 ml glass bottle). Fire passage approximately down – up. Experimental burn plot 2, Site 3. Prescribed burn DE1, Katberg, EC, South Africa, 15 October 2019.*

Sooting and staining

Sooting and staining directions (º) at ground level relative to wind direction (A), fire spread direction (B), and aspect (C) for a number of fires in Eastern Cape mesic montane grasslands are illustrated on **FIGURE 5.17**, **FIGURE 5.18**, & **FIGURE 5.19** respectively, and various directional values summarised in **TABLE 5.7**, **TABLE 5.8**, & **TABLE 5.9**.

22 tin cans and 17 glass bottles (samples) were spoiled from wildlife interference (*i.e.*, removed from site by curious baboons), which brought the total number of observations down to 121 and 126 fires respectively.

Ground level sooting of supporting items was present on 62% cans and 48.4% of glass bottles and did not appear to be more or less prolific in any particular fire spread type. Of the cans and bottles covered in soot, only 36% and 37.7% respectively showed a clear direction of sooting. Again, there did not appear to be any proportional discrepancies between fire spread type.

Similarly, ground level staining of supporting items was present on 69% of glass bottles, and was perhaps more prolific in head fires, than back or flank fires. Staining direction was only clear in 50.6% of all instances of staining, but direction was significantly more decipherable (clearer) in back fires (72.4%) than in head (34.3%) or flank (47.8%) fires.

TABLE 5.7: *Means, medians, and resultant vector length (R) values for relative direction (°) of ground level sooting on 410 g tin cans in relation to wind direction, fire spread direction, & aspect from 27* fires in Eastern Cape mesic montane grasslands.*

Relative Direction	R	Median	Mean
Relative to Wind	0.295	350	349.145
Relative to Fire Spread	0.326	215	202.979
Relative to Aspect	0.422	28.408	23.608

**n = 27 (only 27 out of 75 sooted cans (total 121 cans) showed a clear direction of sooting)*

Ground level sooting direction relative to wind direction on both cans and glass bottles did not show unimodal distribution ($P > 0.094$; & 0.464) and was spread fairly uniformly ($R = 0.295$; & 0.184) in most directions for all three fire spread types (A in **FIGURE 5.17** & **FIGURE 5.18**).

Similarly, ground level staining direction relative to wind direction on glass bottles had a weak unimodal distribution ($P < 0.024$), with an almost uniform distribution ($P < 0.025$) ($R = 0.291$) in most directions for all three fire spread types (A in **FIGURE 5.19**).

Ground level sooting direction in relation to fire spread direction on both glass bottles and cans generally clustered towards the direction of the oncoming fire (180°) ($P < 0.014$), although with weak unimodal distributions ($P < 0.056$; & 0.029) and significant variation and spread in other directions ($R = 0.326$; & 0.391) (B in **FIGURE 5.17** & **FIGURE 5.18**).

Ground level staining direction in relation to fire spread direction followed a similar pattern, but with a much stronger unimodal clustering ($P < 0.006$) towards the direction of the oncoming fire (180°) ($P < 0.005$) (B in **FIGURE 5.19**). There was, however, significant distribution of staining in other directions ($R = 0.344$).

Sooting (on both cans and bottles) and staining direction at ground level relative to aspect all clustered strongly towards the downslope side (0/360°) ($P < 0.003$; 0.009; & 0.001 respectively), although staining had a stronger unimodal distribution ($P < 0.001$) than sooting on cans ($P < 0.008$) and bottles ($P < 0.022$) (C in **FIGURE 5.17**, **FIGURE 5.18**, & **FIGURE 5.19**).

As a precautionary measure, assumptions of sooting and staining directional discrepancies between fire spread types were not made, in case potentially inaccurate results arose from the small sample sizes.

TABLE 5.8: *Means, medians, and resultant vector length (R) values for relative direction (°) of ground level sooting on 330 ml glass bottles in relation to wind direction, fire spread direction, & aspect from 23* fires in Eastern Cape mesic montane grasslands.*

Relative Direction	R	Median	Mean
Relative to Wind	0.184	35	23.762
Relative to Fire Spread	0.391	210	214.303
Relative to Aspect	0.404	28.853	29.334

**n = 23 (only 23 out of 61 sooted bottles (total 126 bottles) showed a clear direction of sooting)*

TABLE 5.9: *Means, medians, and resultant vector length (R) values for relative direction (°) of ground level staining on 330 ml glass bottles in relation to wind direction, fire spread direction, & aspect from 44* fires in Eastern Cape mesic montane grasslands.*

Relative Direction	R	Median	Mean
Relative to Wind	0.291	41.741	34.591
Relative to Fire Spread	0.344	214.187	216.009
Relative to Aspect	0.450	13.045	8.62

**n = 44 (only 44 out of 87 stained bottles (total 126 bottles) showed a clear direction of staining)*

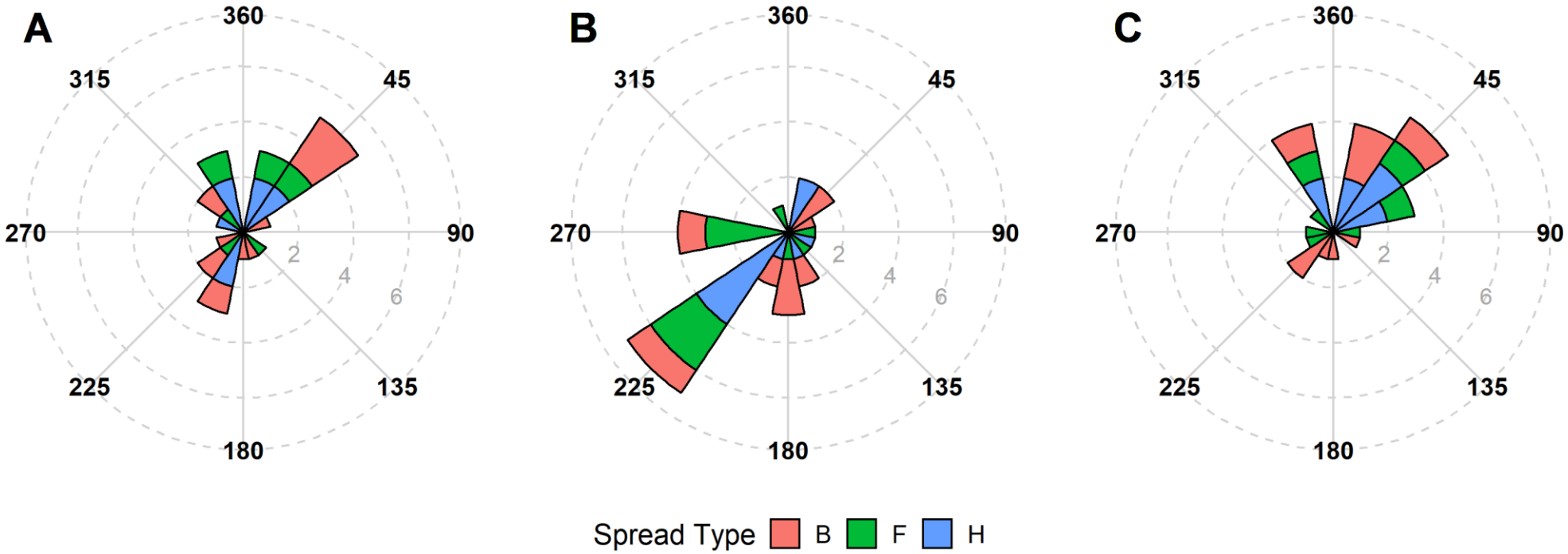

FIGURE 5.17: *Rose plots showing ground level sooting direction in 22.5 degree (°) increments on 410 g (400 cc) tin cans relative to (A): wind direction; (B): fire spread direction; & (C): aspect, and grouped by fire spread type from 27 fires in Eastern Cape mesic montane grasslands. r axes are the count of indicator expressions within each 22.5° increment.*

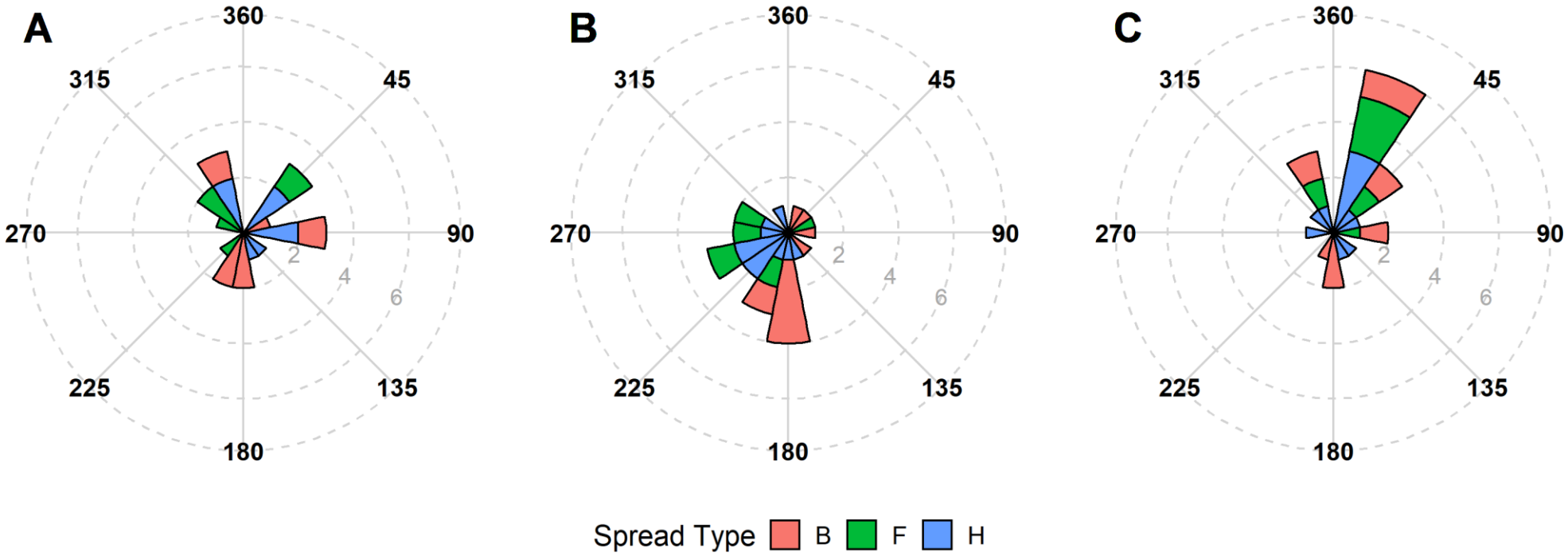

FIGURE 5.18: *Rose plots showing ground level sooting direction in 22.5 degree (°) increments on 330 ml glass bottles relative to (A): wind direction; (B): fire spread direction; & (C): aspect, and grouped by fire spread type from 23 fires in Eastern Cape mesic montane grasslands. r axes are the count of indicator expressions within each 22.5° increment.*

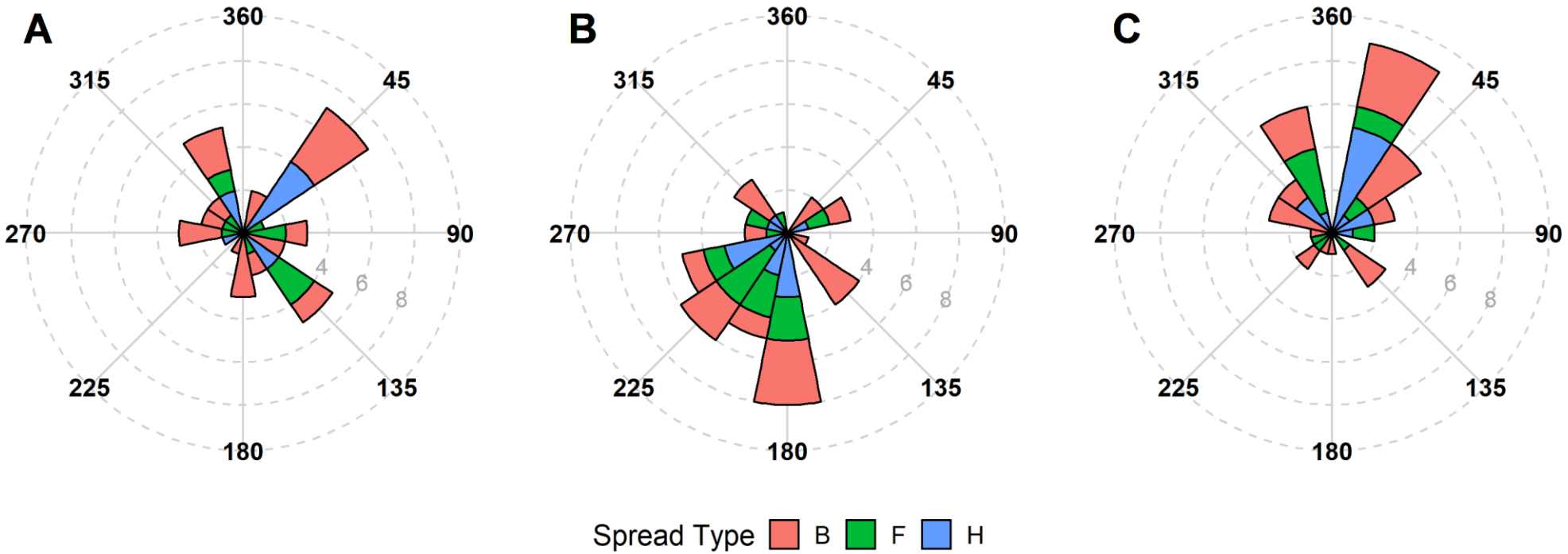

FIGURE 5.19: *Rose plots showing ground level staining direction in 22.5 degree (°) increments on 330 ml glass bottles relative to (A): wind direction; (B): fire spread direction; & (C): aspect, and grouped by fire spread type from 44 fires in Eastern Cape mesic montane grasslands. r axes are the count of indicator expressions within each 22.5° increment.*

FIGURE 5.20: *Example of ash deposit on stained 330 ml glass bottle. Experimental burn plot 17, site 3. Prescribed burn DE1, Katberg, EC, South Africa, 15 October 2019.*

Spalling and curling

No incidents of spalling on rock surfaces were observed within or adjacent to any burn plots, throughout all seven fire sites. Incidents of curling were observed on several scorched woody plants, but were few and far between, and appeared to be in no specific pattern.

5.4.3 Potential novel indicators:

Unburnt plant litter

Residual unburnt (partially burnt) plant litter weight (g/m^2) values for head, back, & flank fire spread types are summarised in **TABLE 5.10**. Plant litter weight data was distributed exponentially and positively skewed. Weight of residual partially or unburnt plant litter differed significantly between fire spread type (head, back, flank) ($P < 0.001$) (**FIGURE 5.21**). Residual plant litter weight in back fires was significantly lower than litter weights in head and flank fires ($P < 0.002$) (**FIGURE 5.21**). A significant difference in residual plant litter weight exists between sites ($P < 0.001$), with Site 7 differing significantly from sites 1 ,2, 3, & 5 ($P < 0.017$) (**FIGURE 5.21**).

TABLE 5.10: *Residual unburnt plant litter weight (g/m^2) standard deviation, median, mean & standard error (se) values for head, back, & flank fire spread types from 141 fires* in Eastern Cape mesic montane grasslands.*

Fire Spread Type	Standard Deviation	Median	Mean ± se
Head (*n = 52*)	112.417	158.793	179.815 ± 15.589
Flank (*n = 45*)	157.483	161.835	208.035 ± 23.476
Back (*n = 44*)	100.648	79.097	114.698 ± 15.173

**n = 141 (ground surface and residual vegetation of two out of total 143 burn plots compromised from wildlife interference)*

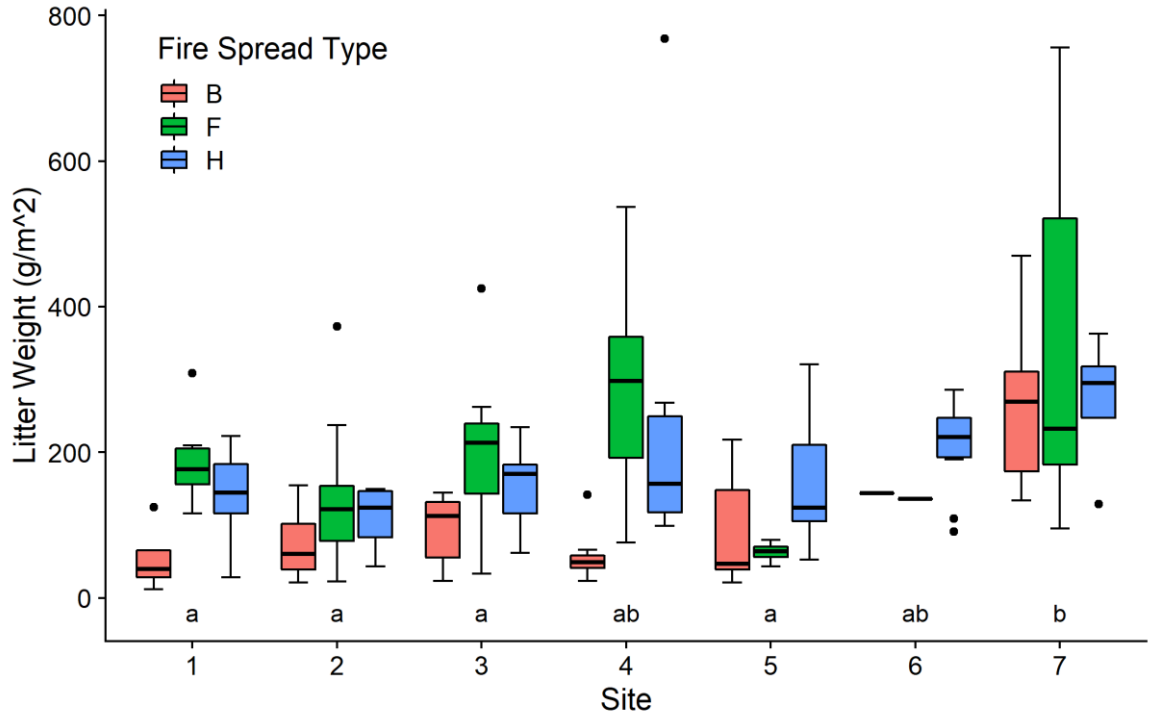

FIGURE 5.21: *Boxplot comparing residual plant litter (unburnt or partially burnt) weights (g/m^2) between head (H), back (B), & flank (F) fire spread types from 141 fires in Eastern Cape mesic montane grasslands. Lower case letters (a & b) represent significant differences ($P < 0.04$) between sites.*

Ash total organic carbon content

Field sampled residual ash total organic carbon (TOC) content (%) values for head, back, & flank fire spread types from 126 fires in Eastern Cape mesic montane grassland are summarised in **TABLE 5.11**. Data distribution for ash TOC content was only slightly positively skewed ($P < 0.009$). The removal of a single outlying observation sufficiently adjusted the data distribution of ash TOC content to a normal distribution ($P > 0.095$).

While mean and median ash sample organic carbon contents (%) were lower in back fires compared to ash samples from head and flank fires, no statistically significant differences in ash organic carbon content could be found between fire spread type ($P > 0.119$) or site ($P > 0.136$), for both untransformed and transformed data. Nevertheless, it certainly appears as though some relationship may possibly exist between ash TOC content and fire spread type in Sites 2, 3, 4, & 7 (**FIGURE 5.22**).

Residual ash sample TOC content (%) versus fire severity (kg/ha), separated by fire spread type from 126 fires in Eastern Cape mesic montane grassland is shown in **FIGURE 5.23**. There appeared to be no significant associations between residual ash sample TOC content and fire severity for all three fire spread types ($rho < \pm 0.208$; $P > 0.186$).

Field sampled residual ash Munsell value (darkness/lightness) versus corresponding sample TOC content (%), separated by fire spread type is shown in **FIGURE 5.24**. Interestingly, a negative corelation existed between residual ash sample TOC content and corresponding Munsell value for all three fire spread types ($rho < -0.475$; $P < 0.002$).

A similar relationship appears to exist between residual ash sample TOC content and Munsell colour class (**FIGURE 5.25**).

TABLE 5.11: *Field sampled residual ash organic carbon content (%) standard deviation, median, mean & standard error (se) values for head, back, & flank fire spread types from 126 fires* in Eastern Cape mesic montane grasslands.*

Fire Spread Type	Standard Deviation	Median	Mean ± se
Head (*n = 42*)	12.092	19.824	21.201 ± 1.866
Flank (*n = 43*)	8.694	22.938	22.670 ± 1.326
Back (*n = 41*)	8.829	15.756	18.978 ± 1.379

**n = 126 (no samples exist from Site 6, three samples spoiled in the lab)*

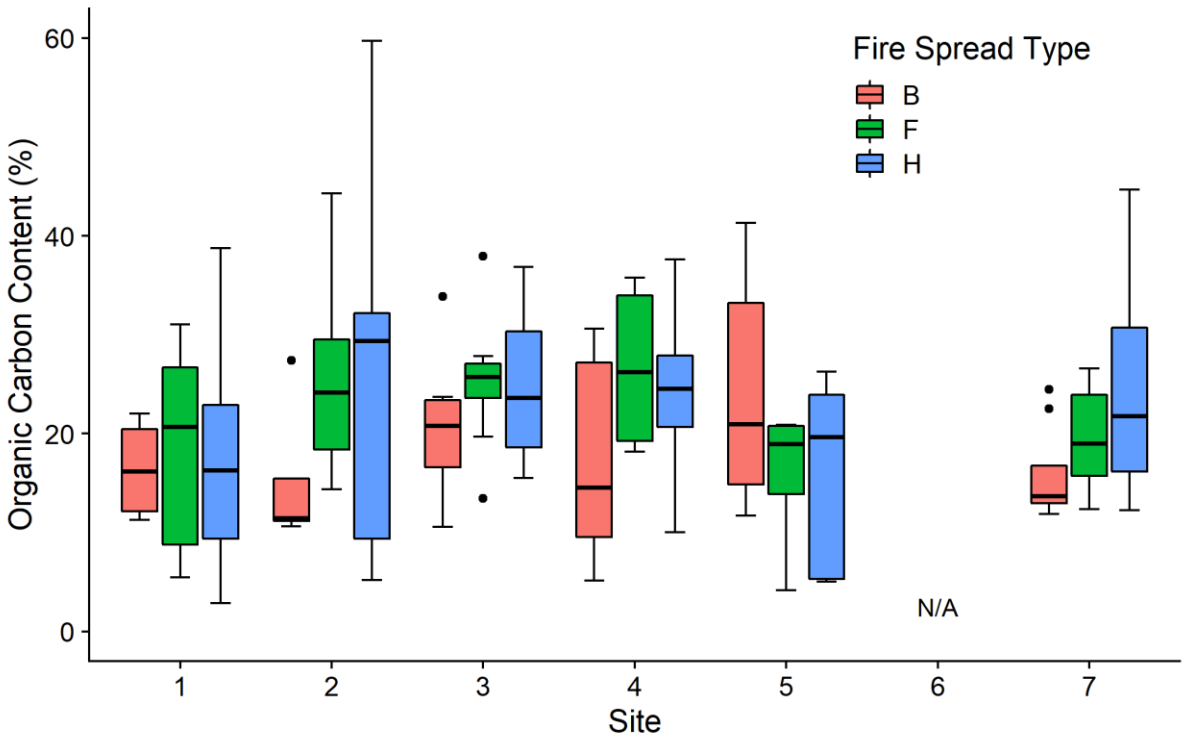

FIGURE 5.22: *Boxplot comparing field sampled residual ash organic carbon content (%) between head (H), back (B), & flank (F) fire spread types from 126 fires in Eastern Cape mesic montane grasslands. No treatments significantly different.*

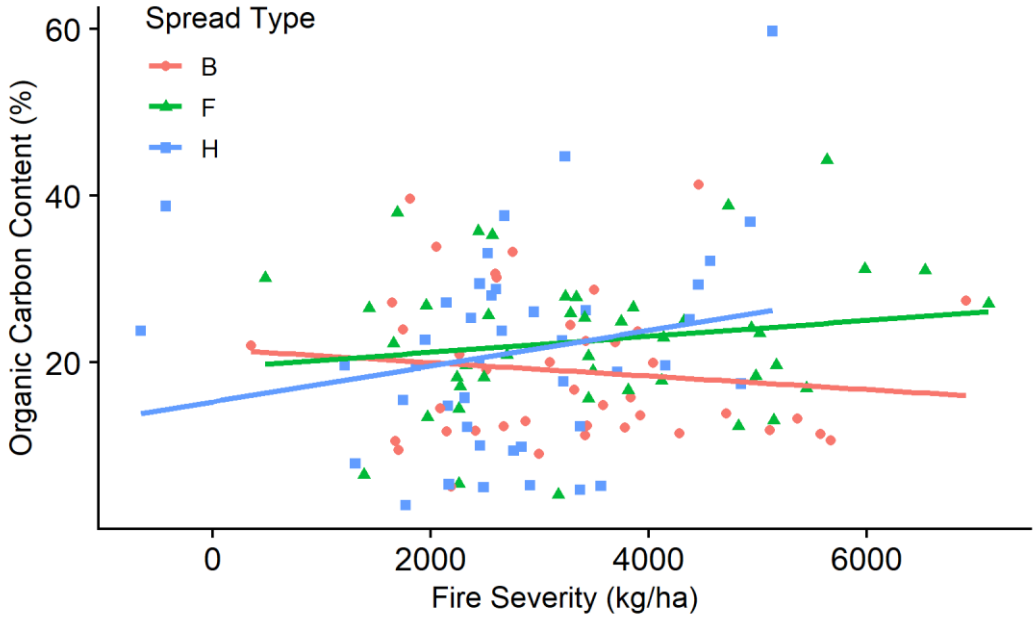

FIGURE 5.23: *Fire severity (kg/ha) versus field sampled residual ash organic carbon content (%), separated by fire spread type (head, back, & flank), from 126 fires in Eastern Cape mesic montane grasslands. Solid lines indicate regression equations for each fire spread type (head, back, & flank).*

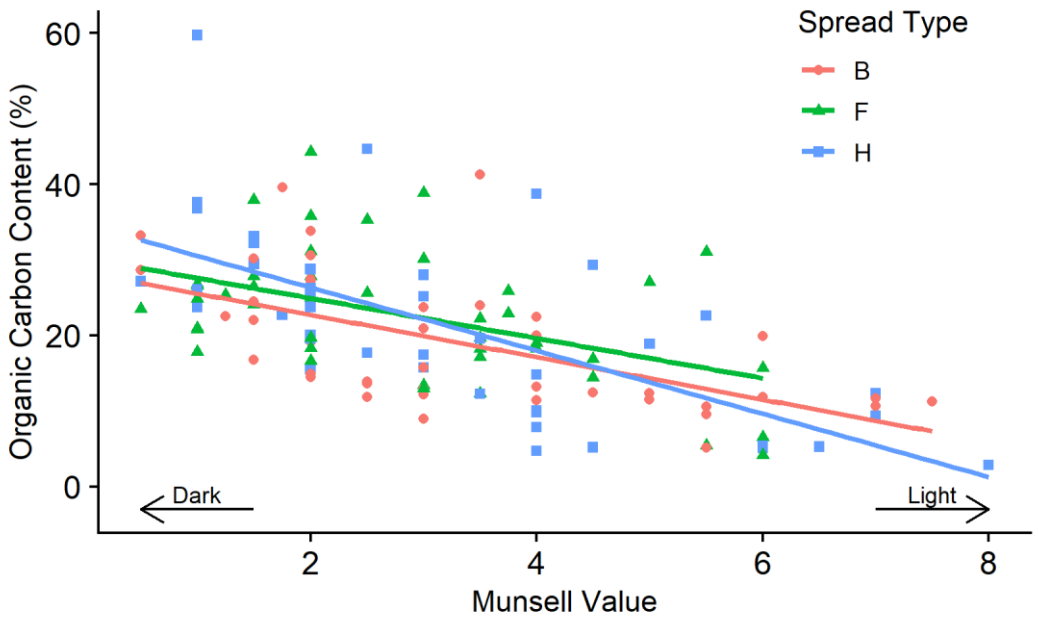

FIGURE 5.24: *Field sampled residual ash Munsell value (darkness/lightness) versus corresponding sample total organic carbon content (%), separated by fire spread type (head (H), back (B), & flank (F)), from 126 fires in Eastern Cape mesic montane grasslands. Solid lines indicate regression equations for each fire spread type (head, back, & flank).*

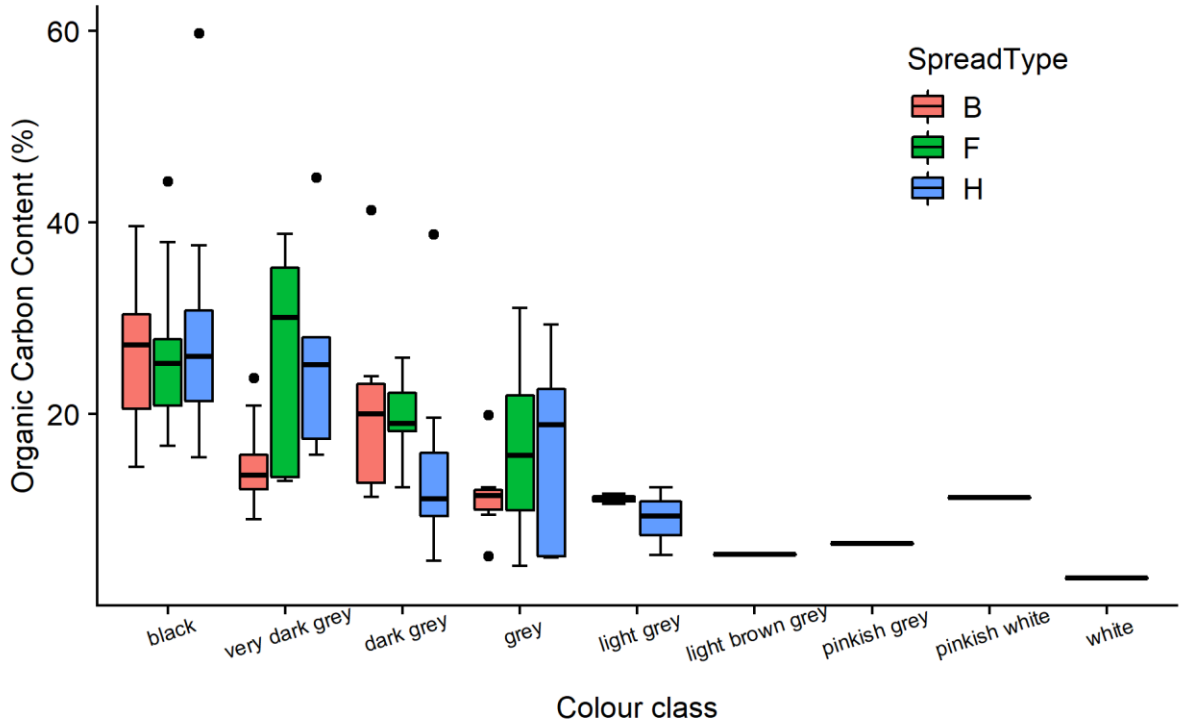

FIGURE 5.25: *Boxplot comparing residual ash sample organic carbon content (%) between Munsell colour classes and separated by head (H), back (B), & flank (F) fire spread types from 126 fires in Eastern Cape mesic montane grasslands.*

5.5 Discussion:

5.5.1 Fuel and weather conditions

Ideally the preferred option would have been for this study to have collected empirical data under fire conditions as close to typical runaway wildfire conditions (high wind speeds, low humidity, high fuel load), as possible. An inevitable consequence of conducting prescribed burns, is that safety takes precedence ahead of desired effect/outcome. Despite endeavouring to emulate runaway conditions, on average, experimental fire conditions in this study were milder than those experienced in typical runaway wildfire conditions. Notwithstanding, a range of high wind speeds (up to 40+ km/h) was achieved. It is likely that under runaway conditions, indicator expression will be more pronounced than under controlled burning conditions. Therefore, it is advised that the results from this study be ground-truthed in extreme runaway conditions to confirm the findings of this study.

As the prescribed fires were conducted on privately owned livestock farms (rangelands), paddocks were often grazed, although, there was an abundance of cured flammable material, as the paddocks were rested before burning. The consequence is, that on occasion, fuel conditions were patchy. Patchiness of fuel does, of course, affect fire behaviour, with changing fuel loads and moisture. This is significant for indicator formation, as continuous fire fronts are often required for thorough and accurate indicator formation. Patchiness of fuel can also affect indicator distribution, as boundaries between heading and backing regions may be blurred by discontinuous and erratic combustion of moribund tufts.

On the other hand, conducting these prescribed burns on large-scale privately owned agricultural rangelands instead of typical experimental burn plots, added robustness to this study, as the presiding fuel conditions and terrain were representative of the conditions under which wildland fire investigators would conduct investigations of runaway fires.

5.5.2 Indicators of fire spread type:

Consumption depth of grass tussocks

Residual grass stalk stubble height data distribution was found to be positively skewed from normal distribution. Data distributions in nature are often non-normal (Stroup, 2015). The positive skewness of residual grass stubble height is easily explained from simple grass fire behaviour. While it has been hypothesised that the consumption depth of grass tussocks in head and back fires differs, for the most part, regardless of fire spread type, the majority of cured (as would be the case in most natural and prescribed grass fires) grass tussocks are consumed relatively close to the ground (< 15 cm), with few tussocks comprising long (> 25 cm) residual partially burnt or unburnt grass stalks.

While overall mean residual grass stubble height in back fires was found to be significantly lower than mean grass stubble heights in head and flank fires (**TABLE 5.1**), one should exercise caution when drawing conclusions form the means, as the distribution of data is positively skewed.

Overall residual grass stubble height showed no difference in medians between head and back fires (**FIGURE 5.2**). Residual stubble height of flank fires was found to be significantly higher than that of back fires, likely a result of inefficient and incomplete combustion prevalent in flank fires (Trollope *et. al.*, 2004; Cheney & Sullivan, 2008).

This perhaps indicates that other variables or interactions may be responsible for differences in consumption depth of grass tussocks. This is self-evident, as various fuel parameters such as fuel moisture, structure, and species, as well as weather conditions most certainly influence the combustion (Trollope *et. al*., 2004; Cheney & Sullivan, 2008; Scott *et. al*., 2014), and thus consumption depth, of grass tussocks.

Interestingly, residual grass stubble height at Sites 1 & 2 were significantly higher and differences in height more pronounced between fire spread types, when compared to Sites 3 – 7 (**FIGURE 5.3**). A likely explanation for this difference in residual grass stubble height may be due to species composition differences between sites. Available fuel at Sites 1 & 2 (Boschberg) comprised mostly of *Cymbopogon* species, while Sites 3 – 7 comprised mostly *Festuca* species. At this time of year (early spring) and time of fire cycle (3 – 5 years since previous burn), moribund *Festuca* species contain more dry flammable plant material within the base of the tussock compared to moribund *Cymbopogon* species, which have a greater proportion of live green material towards the base of each tiller. The presence of this less flammable live material near the base of tussocks at Sites 1 & 2 likely facilitated the expression and accentuation of this indicator, as more residual grass tillers remained unburnt or partially burnt (**FIGURE 5.4**). Conversely, the abundant flammable material near the base of tussocks at Sites 3 – 7 would have facilitated increased consumption and enabled incessant smouldering of plant material after the fire front had passed, resulting in greater consumption depth of grass tussocks (**FIGURE 5.5**) and de-emphasis of the indicator (differences between fire spread type).

The conclusion to be drawn from the above, is that expression of this indicator (pronounced in residual grass stubble height between fire spread types) may vary among different grassland species and/or systems, as fuel parameters differ between said species and/or systems. While this is true for at least two systems (*Cymbopogon* dominated & *Festuca* dominated) within mesic montane grasslands of the Eastern Cape, one might also expect a variation in indicator expression and reliability of consumption depth of grass tussocks to be true for other grassland systems in southern Africa and globally. Expression (and reliability) of this indicator in grasslands may, of course, vary with seasonality (fuel moisture). Future studies will need to be aware of and address these potential variations in consumption depth indicator reliability between different seasons and grassland systems.

It has been posited that interactions between spread type and slope gradient may perhaps influence residual grass stalk stubble height (**Section 2.4.8, *Consumption depth of grass tussocks*, Chapter 2**). (*e.g.*, in head fires advancing upslope with the wind, the combined effect of gradient and wind may reduce the angle between flames and the ground surface, causing increased consumption depth of grass tussocks. Following similar rationale, back fires moving down slope and against the wind, may also result in short residual grass stubble length). However, no such relationship between stubble height and effective gradient could be found within this study (**FIGURE 5.6**).

Drawing from this study's results, one can conclude that the relationship between consumption of grass tussocks and fire spread type are likely overstated in the existing anecdotal literature (Trollope *et. al.*, 2004; Cheney & Sullivan, 2008; NFPA, 2017). Nevertheless, this indicator may have value in a wildland fire investigator's toolbox, provided it is applied within a relevant grassland system (system in which differences in consumption depth of grass stubble between fire spread types are pronounced). Importantly, comparisons of consumption depth of grass tussocks should be applied to adjacent grass swards of equal fuel and weather conditions, and should perhaps be used in conjunction with other indicators to draw more robust conclusions when investigating the origin and spread of grass fires.

Undercutting of flowering culms

The presence of unburnt undercut grass culms lying on burnt ground was found to be an almost unequivocal indicator and characteristic of back fires in mesic montane grasslands of the Eastern Cape. Undercut culms were almost invariably present after backfires had passed (occurring 86.4% of the time), while instances of undercutting were extremely rare in head fires (1/52). Importantly, the absence of unburnt culms on burnt veld (~14% of back fires) is not necessarily indicative of a head fire, as flowering culms may not have been present in the grass sward prior to the fire passing through. The intermediate values for unburnt undercut grass culm density (**TABLE 5.2**) and presence (40%) in flank fires is expected, as flank fires essentially fluctuate between head and back fires with small variations in wind direction (Trollope *et. al.*, 2004; Cheney & Sullivan, 2008), thus producing unburnt undercut culms while behaving as a back fire, and consuming flowering grass culms when behaving as a head fire.

While there was some variation in unburnt undercut culm density between sites, only Sites 5 and 6 differed significantly from each other. This (small) discrepancy in undercut culm abundance between sites may be addressed by a simple explanation. More flowering culms were observed to be present in the swards of Sites 4, 5, & 7 prior to combustion, than Sites 3 & 6, where pre-fire sward culm abundances were noticeably lower. There was also only one back fire out of a total 14 fires at Site 6. This particular back fire could very well be an outlier and misrepresent overall backfire behaviour for Site 6. In hindsight culm density within the sward should have perhaps been measured before prescribed

fires were conducted, however this is peripheral, as the significance and relevance of these findings to wildfire investigators are not related to the abundance of culms, but rather the presence or absence of culms in different fire spread types.

While seasonality is known to affect the abundance of flowering grass culms within the sward (O'Connor & Pickett, 1992; Smith, 2012), previous season's senescent culms will, for the most part, be present within the sward (Hempson *et. al.*, 2015) (considering that grasslands which can carry a runaway grassfire usually comprise medium to high fuel loads and are usually not eaten out, trampled, or inflicted with drought — factors which may affect culm density within the sward (O'Connor & Pickett, 1992; Snyman, 2004; Hempson *et. al.*, 2015). There is no reason to believe this indicator would not be equally reliable in other tussock grassland systems in southern Africa and globally. Further empirical research is required to determine the accuracy of unburnt undercut culm direction as an indicator of back fire direction of spread. This is a difficult task as there are numerous culms per plot. By taking the circular mean culm direction in each plot, one loses valuable directional variation data. It is therefore difficult to quantify error in directional accuracy of undercut culms.

Ash colour

Ash colour, or more specifically the lightness or darkness of ash, was found to be an inconclusive indicator of fire spread type (A in **FIGURE 5.9**). Despite numerous findings and observations in previous studies and literature identifying various relationships between ash colour and completeness of combustion and fire spread type (Goforth *et. al.*, 2005; Lentile *et. al.*, 2006; Cheney & Sullivan, 2008; Ubeda *et. al*., 2009; Bodi *et. al.*, 2011; Bodi *et. al.*, 2014; Dlapa *et. al.*, 2015; NWCG, 2016), no significant Munsell value (darkness/lightness) or ash colour cover fraction differences were found between fire spread types in the mesic montane grasslands of this study.

This inconclusive or non-existent relationship between ash colour and fire spread type found in this study may go some way to explain the confusion and contradictory statements regarding white ash deposit as an indicator, evident in the literature (NWCG, 2016; NFPA, 2017).

It was speculated that perhaps small individual field samples (one for each 10 x 10 m burn plot) would not be accurate or sufficient enough representations for entire 100 m^2 burn plots. In response to this, an alternative method proposed by Hudak *et. al*., (2013), was conducted in the hope that it would offer more insight into ash colour/ fire spread type interactions. The method involved deriving proportional ash composition surface cover fraction values as a measure of residual ash colour. It was deemed an appropriate measure of ash colour for this study, as wildfire investigators, when conducting investigations, are more likely to take in the colour arrangements of a large area (displaying a general trend), than analyse single samples. It was thought that a measure for the entire 100 m^2 would nullify

the chances of extreme local variations in colour influencing results. Despite this, the results from both methods of ash colour determination (surface cover fractions and individual samples) yielded no significant differences in ash colour composition between fire spread types in Eastern Cape montane grasslands (**TABLE 5.4**).

Importantly, however, these results did not contradict the existence of a correlation between completeness of combustion and darkness/lightness of residual ash in herbaceous fuels of mesic montane grasslands of the Eastern Cape. Rather, it suggests that the discrepancy in completeness of combustion between fire spread types in prescribed burns of this study, was not that large. I elaborate:

Ash samples collected from prescribed burn fire scars (A in **FIGURE 5.9**) were much lighter in colour (Munsell value) after undergoing complete combustion in the lab (5 hours at 500^{o}C) (B in **FIGURE 5.9**). One might deduce that this significant change (lightening) in colour is the result of positive correlation between completeness of combustion of fuel and lightness of residual ash colour (Munsell value) for herbaceous fuels in montane grasslands of the Eastern Cape. And indeed, this relationship is identified in the literature. Goforth *et. al*., (2005), & Ubeda *et. al*., (2009), observed positive correlations between lightness of ash and completeness of combustion for both laboratory-generated and wildland fire ash (Bodi *et. al*., 2014), while similarly, Bodi *et. al*., (2011), & Pereira *et. al*., (2012), identified a negative relationship between ash colour (lightness) and organic carbon content — a proxy for completeness of combustion. In this study however, no associations between perceived completeness of combustion (fire spread type) and lightness of residual wildfire ash were identified amongst field samples of residual wildfire ash collected from 126 prescribed fires in montane grasslands of the Eastern Cape.

There may be a simple explanation for this lack of observable discrepancy in completeness of combustion (ash colour) between fire spread types. While it is true that in theory (and reality) herbaceous plant matter in back fires undergo more complete combustion than herbaceous plant matter in head fires (Trollope *et. al*., 2004; Cheney & Sullivan, 2008), the difference in completeness of combustion between the two fire spread types is likely not very large when compared to five hours of combustion in a muffle furnace at 500^{o}C. Under real-world grassfire conditions, herbaceous plant matter burns for perhaps less than a minute, at around 300^{o}C (Clements, 2010) — certainly not equivalent to five hours of combustion at 500^{o}C.

This indicator (differences in ash colour between fire spread types) is perhaps more evident in woody systems, where combustion of plant material occurs at higher temperatures (Liodakis *et. al*., 2002) and for longer duration (Systems from which Goforth *et. al*., (2005), & Ubeda *et. al*., (2009), collected their ash and fuel samples). This indicator is certainly not reliable in the relatively fast burning cool grassfires of Eastern Cape montane grassland systems.

It is rather telling that differences in residual grassfire ash colour from this study were greater between sites than fire spread types. Differences in weather and fire conditions, as well as vegetation composition may be a likely explanation for theses apparent significant differences in ash colour between various sites. There are many parameters apart from fire behaviour which might affect ash colour (Bodi *et. al.*, 2014; Dlapa *et. al.*, 2015). It has been noted by various studies that the amount, combustibility, and type of fuel are important components in ash colour formation (Bodi *et. al.*, 2014; Dlapa *et. al.*, 2015).

To conclude, a relationship may exist between ash colour and combustion completeness in various woody systems, but in typical grassfire conditions of Eastern Cape montane grasslands, this indicator was found to be an unreliable determinant of fire spread type.

5.5.3 Indicators of direction:

Leeside charring of pole type fuels

The charring of pole type fuels on the leeward side was found to be a very accurate and reliable indicator of **wind direction** at the time of combustion, in montane grasslands of the Eastern Cape. This was especially true in head fires, where leeside charring on fence posts was a fairly consistent attribute (occurring in almost 75% of all head fires) (A in **FIGURE 5.13**). Evidently supporting the observations of Cheney & Sullivan, (2008).

Of particular significance, was the presence of leeside charring in all three fire spread types, across all seven montane grassland sites of Boschberg, Katberg, and Winterberg. This evidence (the regular presence of leeside charring in back fire scenarios) contradicts the anecdotal postulations offered by the wildland fire investigation handbooks: *NFPA 921, guide for fire and explosion investigations* (2017 ed.); the *Guide to wildland fire origin and cause determination* (2016 ed.); & *Fire Investigator: Principles and Practice to NFPA 921 and 1033* (5th ed.) (2018), that leeside charring does not occur in backing fires. Although leeside charring was more prevalent in head and flank fires, the idea that its presence is an indication of head fires should henceforth be rejected.

Similarly, 'leeside' charring on pole type fuels was found to roughly indicate an **upslope direction** (C in **FIGURE 5.13**). This is expected, as slope's effect on fire behaviour, in particular its influence on convective heat flow, is similar to that of wind (Luke & McArthur, 1978; Trollope, 1984; Cheney & Sullivan, 2008; NWCG, 2016; Leavell *et. al*., 2017; NFPA, 2017). This relationship between slope and 'leeside' charring is acknowledged in the literature (Cheney & Sullivan, 2008; NFPA, 2017; IAFC *et. al*., 2018). It is worth noting though, that (A) the slope gradients of burn plots in this study were particularly steep, and (B) this relationship between leeside charring and aspect did not indicate aspect as accurately or reliably as with wind direction. However, this is immaterial, because it would be an extremely unlikely event in which a wildland fire investigator would need to determine an upslope

direction *post-hoc*. One would assume an investigator would be able to establish aspect visually without much trouble.

Simeoni *et. al.*, (2017), hinted at the existence of a potential wind speed and slope gradient threshold for leeside charring. Their study proposed that at low wind speeds (and presumably gentle gradients) convective heat currents may play a greater role in the formation of leeside charring than was previously understood (Simeoni *et. al.*, 2017). This is of little consequence, because the conditions under which runaway wildfires occur (those relevant to fire investigators), invariably involve high wind speeds. In this study, it was observed that charring on poles in mesic montane grasslands of the Eastern Cape was less prevalent at low wind speeds and at gentle gradients (**FIGURE 5.11** & **FIGURE 5.12**).

Nevertheless, it is acknowledged that high fuel loads or build-up of flammable vegetation adjacent to pole type fuels may result in false expression of this indicator (Cheney & Sullivan, 2008). (*e.g.*, fuel loading on one of the sides of a pole may result in a charring pattern which could appear as though leeside charring had occurred in a certain direction contrary to prevail wind direction).

What is certain, is that leeside charring is not an indicator of **fire spread direction** in montane grasslands of the Eastern Cape. While indeed, charring of fence posts in head fire scenarios did occur in the direction of fire spread, charring direction in flank fire scenarios clustered at right angles to fire spread direction (B in **FIGURE 5.13**). This is a seemingly logical and expected outcome, as in head fire scenarios, fire spread direction, wind direction, and upslope (aspect + 180^{o}) direction are, in most cases, the same direction. In flank fire scenarios, fire spread direction is perpendicular to wind and/or slope direction.

The above directional pattern of charring relative to fire spread exposes caveats in the assertions of the *NFPA 921, guide for fire and explosion investigations* (2017 ed.); the *Guide to wildland fire origin and cause determination* (2016 ed.); & *Fire Investigator: Principles and Practice to NFPA 921 and 1033* (5th ed.) (2018), that leeside charring is an indicator of fire spread direction. While correct for head fire passage, their statement does not hold true for flank and back fires.

Interestingly, in back fire scenarios, charring direction on poles relative to fire spread did not cluster around the expected *a priori* direction, and in fact displayed a uniform distribution in all directions. In theory, one could expect charring on poles in back fire scenarios to be opposite the direction of spread (as a fire backs into the wind or down a slope, the convective heat flow pulls flames into an eddy wrap, charring the pole on the (leeward) side from which the back fire approached). The existence of oblique back fires (back fires which do not spread directly into the wind, but at various indirect angles) may be an explanation as to why a unimodal distribution of charring at 180^{o} relative to fire spread was not observed.

It is unclear what effect chemical treatments of fence posts may have on the flammability or char patterns of poles. Chemical treatments (*i.e.*, creosote and other products) are commonly used in agricultural settings to protect from decay and prolong the lifespan of fence posts (Morrell *et. al*., 1999). If these chemical treatments act as retardants or accelerants, they may contribute towards the inaccurate expression of the leeside charring indicator. Treated fence posts would, under such scenarios be unreliable supporting items (indicators) in wildfire origin, cause and spread investigations.

Livestock farmers, pastoralists, park, and fire managers in fire prone or fire adapted systems encounter frequent fires, whether from accidental, unintentional, and/or natural runaway wildfires, or from prescribed burns. Substantial costs are incurred from the inevitable damage of fence posts and droppers. A suitable fire retardant treatment may help these rangeland and park custodians reduce costs.

To conclude, leeside charring (charring direction relative to wind) on pole type fuels is an accurate and reliable indicator of **wind direction** in all three fire spread types in montane grasslands of the Eastern Cape, but is particularly prolific in head fire scenarios. Nevertheless, this indicator is not unequivocal, and so, in order to reduce potential risk of outlier variance, it is advised that one observe char patterns from a number of supporting items before drawing conclusions of overall wind direction.

Foliage freeze

Woody species do not make up a very large portion of the fuel, but the tall *Cliffortia paucistamina, Leucosidea sericea,* and occasionally at lower altitudes *Vachellia karoo* are interspersed throughout most sites. However, in many cases, any woody component was completely absent from burn plots, for instance Site 7 was completely devoid of any woody species (**FIGURE 5.14**). Incidentally, this interspersal of tall broad leaf woody species is the favourable fuel structure for foliage freeze interpretation. Cheney & Sullivan, (2008), recommend that the *foliage freeze* indicator be applied to isolated and exposed trees and shrubs, in order to avoid blockage of wind from dense stands (*e.g.*, forests) and potential influence from convective heat currents produced from high fuel loads (NWCG, 2016; NFPA, 2017).

Although no quantitate data of freeze direction was produced in this chapter, from visual observation, I have no reason to believe leaf freeze is not an accurate indicator of wind direction at the time of combustion, in montane grasslands of the Eastern Cape. Further research is required to quantify directional accuracy of leaf freeze. Future studies should be cognizant of the difficulties of quantifying error in directional accuracy of grass tussock cupping (similar to those explained for grass culms).

The significantly higher occurrence of foliage freeze found after head fire passage (53.9%) compared to back fires (21.4%) in the montane grasslands of this study (Boschberg, Katberg, & Winterberg) at least partially verify the identified conditions stipulated in the anecdotal literature (proportional

presence in head versus back fires) (Scott *et. al*., 2014; NWCG, 2016; NFPA, 2017; IAFC *et. al.*, 2018), under which foliage freeze formation is purported to occur, certainly in montane grasslands of the Eastern Cape.

This observed relationship between fire spread type and occurrence of leaf freeze is perhaps indicative of a convective heat (intensity) requirement for the formation of this indicator. Indeed, this is the currently accepted explanation for the discrepancy in foliage freeze occurrence between head and back fires (Scott *et. al*., 2014). It is believed that, for the most part, back fires do not produce enough convective heat to induce freezing (Scott *et. al*., 2014; NWCG, 2016). Similarly, very intense fires are thought to produce too much convective heat, freezing foliage in a vertical position (Cheney & Sullivan, 2008; NWCG, 2016; NFPA, 2017).

To conclude, the formation of foliage freeze indicator is common in head fire scenarios in Eastern Cape montane grasslands interspersed with tall woody species. While no relationship was quantified, from visual observation it is believed that foliage freeze is a fairly accurate indicator of wind direction at the time of combustion in this ecosystem. Further research is required to verify this relationship, as well as any potential relationship that may exist between species of woody plant and indicator occurrence.

Cupping

The indicator know as cupping occurs in two very different fuel types, grass tussocks the terminal ends of thin woody branches (NWCG, 2016; NFPA, 2017; IAFC *et. al.*, 2018). While the mechanisms (wind) thought to influence the expression of this indicator in both fuel types are the same (NWCG, 2016; NFPA, 2017; IAFC *et. al.*, 2018), the two versions of this indicator occur at very different elevations within the fuel structure. These two groups of the cupping indicator may therefore not be interchangeable, as the conditions which influence each fuel type (grass tussocks & branches of woody plants) may vary with elevation (Trollope, 1984; Trollope *et. al.*, 2004). The consequence is that the fire behaviour which interpreted *post-hoc* from both fuel types may differ between each other. Therefore, I propose that henceforth these two types of cupping (in grass tussocks & on ends of branches) be separated into two independent indicators to avoid any confusion that may arise from potentially false interpretation from either fuel type.

Cupping of grass tussocks

The proportion of total grass tussocks in each burn plot which expressed cupping was low (28%), but consistent between all three fire spread types in montane grasslands of the Eastern Cape. Although overall cupping occurrence on grass tussocks was low, there was no shortage of tussocks within each

10 x 10 m plot, from which to interpret cupping. The mesic montane grassland burn sites averaged 249 ± 10 tussocks per 10 x 10 m burn plot, with only 14.2% of plots not expressing any tussock cupping.

The higher density of cupping occurrence recorded at Site 7 compared to Sites 1, 3, 4, & 6 is perhaps influenced by the particularly moribund *Festuca* present throughout Site 7, although there is no clear explanation to support this.

A potential caveat that may affect this indicator is with regards to the curing process of grasses. Many tussock grasses cure from the centre out, with new tillers developing along the outer edges of the tussock (Danckwerts, 1989). This process affects the moisture structure of grasses, (particularly moribund grasses at the end/ beginning of a burn cycle), resulting in a tussock which does not have laterally uniform moisture content, with tinder dry material at the centre and live tillers along the outer edge. The consequence with regards to cupping is that the less flammable outer tillers may experience incomplete combustion or less consumption from fire, leaving a pattern or patterns of cupping inconsistent with the expected outcome of cupping that would usually result from flame angle and angle of combustion. Additionally, long residence time of combustion at the centre of dense moribund tussocks may also influence the final pattern of consumption. This pattern of tussock consumption (long residual stalks along the outer edge and deep consumption in the centre) was widely observed throughout all seven montane grassland sites of this study. I also have personal experience of the occurrence of this pattern of consumption in various other tussock grasslands of South Africa.

To conclude, while the proportional occurrence of cupping in montane grasslands of the Eastern Cape is low, the high density of tussocks in these mesic ecosystems means that there is no shortage of tussocks from which to interpret cupping. Nevertheless, it is advised that investigators exercise caution when using this indicator as evidence in wildfire investigations, as the presence of laterally incongruous live herbaceous material (tillers) near the base of grass tussocks may influence the pattern of consumption of these tussocks. Further empirical research is required to determine the efficacy of this indicator as a reliable *post-hoc* descriptor of wind direction. For reasons similar to those explained for culms and leaf freeze, it is difficult to quantify error in directional accuracy of grass tussock cupping.

Cupping on terminal ends of woody plant branches

Cupping occurrence on the charred ‘skeletons’ of woody plants was rare across all montane grassland sites of this study. While a small discrepancy in cupping occurrence between fire spread type was observed, it was not statistically significant. The small sample size of ‘cupped’ terminal ends of branches may be responsible for this lack of statistical significance. Quite dissimilarly to leaf freeze, the relatively low density of interspersed tall woody plant within the montane grasslands of the Eastern Cape likely does not favour the expression of this indicator. Occurring at relatively higher elevation to

the grass sward, the terminal branch ends of tall woody plants may not be enveloped in enough flame, for long enough (Trollope, 1984; Trollope *et. al.*, 2004) to char the branches sufficiently to produce indicator expression. This indicator is perhaps more prevalent in woody scrubland and dry bush systems such as chaparral, macchia, and fynbos, where flames are larger and woody plants more abundant. I have personal experience of prolific cupping of the terminal ends of Protea 'skeletons' in fynbos of the Western Cape (Worcester).

Tin cans and glass bottles as supporting items for protection, sooting, & staining indicators

Reduced sample size from the original 143 observations was a recurring characteristic of most wildland fire pattern indicators measured in this study. The reduction in sample size of response variables because of the presence or absence of indicator expression, a result of conditional indicator formation requirements (*e.g.*, fire behaviour, weather conditions), is inevitable and unavoidable. The worst affected indicators from sample size reduction, were those reliant on supporting items (cans and glass bottles) for their formation — Protection, Sooting, and Staining.

330 ml glass bottles and 410 g tin cans were chosen as supporting items for protection, sooting, and staining in this study for several reasons. Items needed to be readily available and replicable across 146 burn plots (of the same identical structure and material composition) for comparable results. Items also needed to be of appropriate structure and composition to allow for deposition of soot and staining, as well as not burn or denature during combustion. Lastly, they needed to be items which are often found littered around wildland urban interface areas of ignitions. What was not considered, was that curious baboons would take an incessant liking to (the presumably shiny surfaces of) these supporting items.

While little can be done to combat sample size losses resulting from specific fire behaviour and/or weather condition requirements, something can be done to reduce the number of indicator observations lost to spoilage from wildlife interference. The congregation of wildlife on burnt patches is inevitable, as many species seek to take advantage of improved grazing and easy foraging. Future studies should endeavour to find new and ingenuitive methods to reduce interference and removal of supporting items from wildlife, perhaps incorporating new items, which would broaden our knowledge of soot and staining deposition characteristics of these items.

Protection

Protection from glass bottles was a common feature in all three fire spread types, occurring in nearly 80% of all fires. However, direction was only decipherable from around two thirds of all cases of protection. Protection indicator is therefore a common, but not always conclusive indicator.

Protection was found to not indicate the direction of wind in the montane grasslands of the Eastern Cape (A in **FIGURE 5.15**). A somewhat unsurprising finding, as wind effects are largely redundant within the first 15 cm above the ground surface. Any unimodal clustering that was found to exist, was likely in response to wind associated directional spread (head fires).

The direction of the protected side in montane grassland sites of this study was statistically clustered towards the *a priori* expected direction (direction of fire spread) identified in the literature (NWCG, 2016; NFPA, 2017; IAFC *et. al*., 2018), for head and flank fires. This was despite displaying an observed diagonal direction of around 45º (B in **FIGURE 5.15**). This clustering towards 45º is unexplained and likely coincidental. The direction of the protected side of glass bottles in back fire scenarios was uniformly distributed in all directions. An observation which is unidentified in the literature (NWCG, 2016; NFPA, 2017; IAFC *et. al*., 2018). This supposed relationship between protection and fire spread direction is perhaps overstated in the literature (NWCG, 2016; NFPA, 2017; IAFC *et. al*., 2018), certainly so in mesic montane grasslands of the Eastern Cape.

The direction of the protected side of glass bottles displayed a strong unimodal clustering in an upslope direction for all three fire spread types (C in **FIGURE 5.15**). This was a somewhat surprising result which is not referenced in the literature. I could find no explanation as to why this relationship existed. It is unclear how, in a fire moving down a slope (head, back, or flank), flammable material on the side of the approaching fire (upslope) is protected from combustion.

In conclusion, protection was found to be a weak indicator of head and flank fire spread direction in mesic montane grasslands of the Eastern Cape. Furthermore, protection was an unreliable indication of back fire spread direction, however, perhaps further replications of this study, with different supporting items, are required to confirm this relationship. Nevertheless, it is recommended that wildland fire investigators exercise caution when applying this indicator and should most certainly incorporate various other indicators to come to reliable conclusions of fire spread direction.

Sooting & Staining

Ground level sooting and staining on supporting items (330 ml glass bottles & 410 g tin cans) was less prevalent in montane grasslands of the Eastern Cape than protection indicator. Furthermore, only around a third of all sooted items and around half of all stained items displayed a clear direction of expression. There appeared to be no proportional discrepancies of ground level sooting between fire spread types, despite anecdotal observations suggesting sooting is more prolific in head fires (Cheney & Sullivan, 2008; NWCG, 2016). Staining on the other hand, yielded some interesting results.

For the most part, staining is considered a less common indicator than sooting (NWCG, 2016). This was not the case within the numerous montane grassland burn plots of this study. Staining of glass

bottles was certainly more prolific than sooting on both cans and bottles. Interestingly, the *Guide to wildland fire origin and cause determination* (2016 ed.), note that staining is more prevalent an indicator on smaller objects. Perhaps another determinant of staining abundance may be the chemical makeup of the plant material undergoing combustion. Vapours and volatile resins and oils responsible for staining of objects may vary in their amount and conduciveness between various plant species and rangeland systems.

Staining in montane grassland sites of this study was slightly more prolific in head fires compared to back and flank fires, an observation which is supported by anecdotal literature (NWCG, 2016). Despite this observation, staining direction was significantly more decipherable in back fires (72.4%) than in head (34.3%) or flank (47.8%) fires. This was a clear and obvious finding of this study, yet it appears to contradict the anecdotal observations of the *Guide to wildland fire origin and cause determination* (2016 ed.), which ambiguously states that staining is less **pronounced** in back fires. Indeed, staining of 330 ml glass bottles was less **prolific** in back fires compared to head fires in Eastern Cape montane grasslands, but direction of staining was much **clearer** in back fires than in head fires.

The direction of ground level sooting and staining on glass bottles and cans was not related to wind direction in montane grasslands of the Boschberg, Katberg, & Winterberg (A in **FIGURE 5.17**, **FIGURE 5.18**, & **FIGURE 5.19**). One would be forgiven for thinking wind blows vapours, volatile resins, oils, tars, molecular carbon, and other substances responsible for sooting and staining onto the windward side of objects. This, however, was not the case at ground level. Wind activity in the first 15 cm above ground level is almost negligible. Therefore, at ground level, the deposition of various substances responsible for sooting and staining is not influenced by wind. Convective currents likely play a bigger role than wind, and appear to influence the deposition of soot and staining substances at ground level in grassland fires of the Greater Winterberg escarpment.

As a precautionary measure, deductions of sooting and staining directional discrepancies between fire spread types were not made from this study's data, in case inaccurate relationships arose from small sample sizes.

Deposition of soot and staining in the montane grassland burn plots of this study occurred on the side of supporting items (glass bottles and cans) facing the oncoming fire (B in **FIGURE 5.17**, **FIGURE 5.18**, & **FIGURE 5.19**) — the *a priori* expected direction as identified in the anecdotal literature (NWCG, 2016; NFPA, 2017; IAFC *et. al.*, 2018), thus indicating the direction the fire approached from. This pattern, however, did not occur without some degree of variation in other directions. It is likely that ground level convective activity is the important driver of particle deposition here.

I had hypothesised earlier (**Section 2.4.15, Chapter 2**) that this relationship would be opposite in back fire scenarios. I justified this by arguing that in back fires, flames leaning back over burnt ground (Cheney & Sullivan, 2008) would deposit carbon-based particulates as well as vapours, resins, and oils

responsible for sooting and staining, back onto the side of objects opposite the oncoming fire. This theory, however, was proved to be untrue at ground level in montane grassland fires of the Eastern Cape.

Ground level sooting and staining deposition direction relative to aspect clustered strongly towards the downslope direction in the montane grassland burn plots of this study (C in **FIGURE 5.17**, **FIGURE 5.18**, & **FIGURE 5.19**). This pattern of unimodal clustering was stronger than the sooting and staining directional pattern relative to fire spread direction. On the proverbial surface, this relationship between aspect and soot and stain deposition might appear peculiar, as slope's effect on fire behaviour is usually compared to that of wind (Luke & McArthur, 1978; Trollope, 1984; Cheney & Sullivan, 2008; NWCG, 2016; Leavell *et. al*., 2017; NFPA, 2017). Although, a simple explanation for this relationship is likely ground level convective heat transfer. The reader is reminded that convection is the transfer of heat energy through a moving fluid (Teie, 2003; Trollope *et. al.*, 2004; Van Wagtendonk, 2006; Cochrane & Ryan, 2009; Scott *et. al*., 2014). The heated air molecules are low in density (Cochrane & Ryan, 2009), and move **upwards** (Van Wagtendonk, 2006; Cochrane & Ryan, 2009; Scott *et. al*., 2014). It is therefore quite likely that at ground level on steep slopes (as was the case for many burn plots in this study), convection was the primary driver of particle flow, depositing substances responsible for sooting and staining upslope, on the downslope side of objects.

Nevertheless, this relationship between sooting, staining and slope has little overall bearing on wildfire investigations, as it is unlikely an investigator would need to identify an upslope direction from *post-hoc* evidence left by the fire. Presumably this would be possible with simple visual observation of the terrain.

It is important to note that the sooting and observations identified in this study applied to objects within the first 15 cm of the ground surface. While it might be perfectly justifiable to suggest that different patterns of sooting and staining deposition could perhaps occur in different vegetation systems (*e.g.*, woodland, macchia), I propose that it is more likely that differences in sooting and staining pattern behaviour would occur along vertically stratified elevations relative to ground surface and fuel layer 'canopies' (*e.g.*, needle bed, grass sward, woodland), as a result of changing active drivers of convection and particle flow (*i.e.*, switching between wind driven and convection driven). And yes, indeed these changes between wind driven and convection driven fuel elevation layers is likely to change between various vegetation systems. I therefore deduce that it may be quite likely that different patterns of soot and staining deposition could be observed on larger objects (*e.g.*, boulders) within montane grassland systems of the Eastern Cape and across southern Africa.

To conclude, ground level sooting and staining were confirmed to be fairly accurate indicators of fire spread direction in mesic montane grasslands of the Eastern Cape, but should be interpreted in conjunction with various other indicators, taking into account the potential for variation. Discrepancies

in sooting between fire spread types were not observed. On small items, at ground level in grassland systems, the staining indicator is perhaps more common and useful to investigators than is stated in the anecdotal literature, particularly in back fire scenarios.

Spalling

While no incidents of spalling were observed to have occurred in all 143 fires of this study across seven burn sites in mesic montane grasslands of Boschberg, Katberg & Winterberg, the phenomenon has been known to occur in wildland fires of southern Africa, usually under very intense fire conditions or sustained heat (prolonged combustion) (Danckwerts J.E. (PhD), personal communication, 2019). I have personal experience of the occurrence of spalling in fynbos fires of the Western Cape (Worcester), admittedly a very intense fire. There are many factors which may influence the formation of fire-induced spalling, such as type or chemical composition of rock (Shakesby & Doerr, 2006; NWCG, 2016; Buckman *et. al.*, 2021), temperature, intensity, and duration of fires (NWCG, 2016; Buckman *et. al.*, 2021), and positioning and elevation of rocks relative to flame height (Buckman *et. al.*, 2021). Some possible explanations for the absence of spalling in this study, may be that the type or composition of rocks present at this study's fire sites (Dolerite & Basalt intrusions) were not conducive to the formation of spalling, the general absence of rocks or boulders above the first 40 cm of fuel bed (heat zone), or alternatively, perhaps the grassfires in this study did not reach the required temperature (or sustained heat) for spalling to occur. Although it is conceded that this study has little empirical evidence to support these explanations. What can be concluded however, is that fire-induced spalling of rocks is not a regular or extensive *post-hoc* wildland fire behaviour indicator in mesic montane grasslands of Eastern Cape.

Curling

Despite the relatively frequent occurrence of foliage freeze across most sites in this study, curling incidents were too few and infrequent for meaningful analysis. There may be several explanations for this. Firstly, curling may not be a common or extensive indicator, regardless of conditions. Secondly, curling is likely less prevalent in this study due to the lack (or complete absence) of appropriate broad leaf plants (supporting items) in the fuel stands of mesic montane grasslands of the Eastern Cape. Lastly, heat produced from low intensity back fires of grassland fires may be too cool and/or low to the ground (Trollope, 1984; Trollope *et. al.*, 2004), to generate sufficient heat, at high enough elevations in the fuel stand (foliage canopy of woody species), to cause curling of leaves. Although the literature suggests curling is most commonly observed in slow moving, low intensity burns associated with backing and flanking fires (NWCG, 2016; NFPA, 2017; IAFC et. al., 2018). Curling is perhaps more prevalent in woody systems where back fires may be more intense and provide a bigger heat source from which curling can be induced.

5.5.4 Potential novel indicators:

Residual plant litter

The amount of residual unburnt plant litter remaining after fire passage appears to be a fairly reliable indicator of fire spread type in mesic montane grasslands of the Eastern Cape, with back fires producing significantly less residual plant litter (weight) than head and flank fires (**FIGURE 5.21**). In addition to this relationship between residual plant litter weight and fire spread type, there may be various other factors such as fuel conditions, species composition, and weather conditions which could affect the amount (weight) of unburnt or partially burnt litter left remaining after fire has occurred (Trollope *et. al.*, 2004; Cheney & Sullivan, 2008). For this reason, the existence of threshold litter weight values for head and back fires is very unlikely, as residual plant litter production may vary from site to site regardless of fire spread type (**FIGURE 5.21**). Taking this into account, fire investigators should exercise caution when using amount of residual plant litter as an indicator of fire spread type and should apply this indicator in combination with others when determining boundaries between head and back fires. Nevertheless, litter weight comparisons of adjacent patches should still offer valuable insight when distinguishing a boundary between head and back fires in wildland fire point of origin determination.

Ash total organic carbon content

No statistically significant difference in ash total organic carbon (TOC) content existed between fire spread types for ash samples collected from a number of prescribed fires in Eastern cape montane grasslands. However, upon visual perusal of the data (**FIGURE 5.22** & **TABLE 5.11**), one could quite justifiably infer that ash TOC content in back fires was lower than ash TOC content in head and flank fires. Nevertheless, the importance of statistical significance must be upheld. Unfortunately, these results do not concur with those of Trollope, (1983), which found that ash TOC differed between head (~34%) and back (~10%) fires in similar systems in the Eastern Cape province of South Africa.

While there are very few studies which have looked at differences in ash TOC between fire spread types (Trollope, 1983), the concept behind these potential differences is based on sound scientific theory. It is widely accepted that fire spread types differ in completeness of combustion and severity (Trollope *et. al*., 2004; Cheney & Sullivan, 2008). It is also largely accepted that there exists a negative relationship between residual ash TOC content and severity or completeness of combustion (Bodi *et. al.*, 2014; Dlapa *et. al.*, 2015), although few studies have shown this to be true with empirical data (Bodi *et. al.*, 2011; Pereira *et. al*., 2012). I could only find a single study that looked at this relationship in grassland fires (Trollope, 1983). Nevertheless, one might expect to find a similar relationship between fire spread type (a measure of severity) and residual ash TOC content.

From the results of this study, however, no association was found between residual ash TOC content and fire spread type (**FIGURE 5.22**) nor fire severity (**FIGURE 5.23**) for samples collected from prescribed fires in Eastern Cape montane grasslands. This lack of observed association between residual ash TOC and fire severity for samples collected from various montane grassfires might go some way to explaining why there was also no relationship observed between fire spread type and residual ash TOC content in this study.

A possible explanation for this lack of association between residual ash TOC content and fire spread type may be that the actual differences in completeness of combustion between different fire spread types in the prescribed grassfires of this study were perhaps not that great, especially compared to the woodland and forest fires of other studies (Bodi *et. al.*, 2011; Pereira *et. al*., 2012; Bodi *et. al.*, 2014; Dlapa *et. al.,* 2015). Various studies have noted that other factors such as that the amount, combustibility, and type of fuel may be important in determining ash colour (Bodi *et. al.,* 2011; Bodi *et. al.,* 2014; Dlapa *et. al.*, 2015), which could suggest that perhaps the fuel and behaviour of grassfires is not conducive to the production of ash TOC content differences between fire spread types. Although the study by Trollope, (1983), was conducted in similar grassland systems to this study.

A simple explanation for a lack of observed relationship between fire severity and residual ash TOC content may possibly be due to inaccurate method of post fire fuel load (a metric in severity calculations) sampling used in this study. A novel method of post-fire fuel load estimation, adapted from the existing and widespread pre-fire fuel load estimation disc pasture meter (DPM) method (Bransby & Tainton, 1977; Danckwerts & Trollope, 1980; Trollope, 1983; Trollope & Potgieter, 1986; Harmse *et. al.*, 2019) was used in this study. The DPM, calibrated to site or vegetation type/unit, produces height values which can be entered into an appropriate function to generate estimated fuel loads (Bransby & Tainton, 1977; Danckwerts & Trollope, 1980; Trollope, 1983; Trollope & Potgieter, 1986; Harmse *et. al.,* 2019). The mistake made in this study, was that the same DPM calibration used for pre-fire fuel load estimation, was used for post-fire fuel load estimation. While the DPM calibration used was appropriate for the presiding unburnt vegetation, the same calibration would not be appropriate for hard and brittle residual grass stalks remaining after combustion. These hard and brittle residual grass stalks would have generated, in relative terms, taller height measurements for the available fuel compared to flexible live grass. Using the pre-fire DPM calibration, these post-fire DPM measurements would produce higher residual fuel load estimations than actual residual fuel load present after combustion, and thus overall lower fire severity measurements for each 10 x 10 m burn plot than what occurred in reality.

Interestingly though, a correlation (rho < -0.475) between ash colour and TOC content was observed amongst ash samples collected from prescribed burns in montane grasslands of Boschberg, Katberg, & Winterberg (**FIGURE 5.24**). Lighter coloured ash comprised less residual organic carbon than darker coloured ash (**FIGURE 5.24** & **FIGURE 5.25**). This is logical and expected, with numerous studies

identifying the same relationship (Trollope, 1983; Goforth et al. 2005; Bodi *et. al*., 2011; Pereira *et. al*., 2012). Despite this not being a particularly surprising finding, it does add complexity to the lack of relationship between residual ash TOC content and severity (**FIGURE 5.23**) and fire spread type (**FIGURE 5.22**), as well as between ash colour and fire spread type (**Sections 5.4.1** & **5.5.1**) (**FIGURE 5.9** & **FIGURE 5.10**) observed in this study. This might suggest that perhaps small scale-scale completeness of combustion (ash) is largely affected by other parameters beyond fire spread type and fire severity, such as fuel type, species, and chemical composition of fuel. Indeed, at has been acknowledged that there are numerous parameters which affect various aspects (such as colour) of wildfire ash production (Bodi *et. al.*, 2011; Bodi *et. al.*, 2014; Dlapa *et. al.*, 2015). In comparison to woodland and forest fires, levels of completeness of combustion and severity between fire spread types of herbaceous grassland fuels might perhaps be relatively similar, generating very little difference in residual ash TOC content.

To conclude, inconclusive evidence, in combination with time consuming and resource sensitive nature of ash sample analysis for TOC content as an indicator of fire spread type, severity, or completeness of combustion, means that ash TOC content is an unreliable *post-hoc* wildland fire pattern indicator for wildland fire investigators in montane grassland systems of the Eastern Cape.

5.6 Conclusions:

The generally milder conditions of the prescribed burns in this study, and in some cases fuel discontinuity, likely resulted in dampened or reduced indicator expression than what would be expected in typical runaway wildfire conditions. It is encouraged that the empirical results from this study be extended to more extreme wildfires, when they occur, to ascertain the appropriateness these results under the extreme conditions in which these indicators are typically applied. Nonetheless, conducting these prescribed burns on large-scale privately owned agricultural rangelands instead of typical experimental burn plots, added robustness to this study, as the presiding fuel conditions and terrain were representative of the conditions under which wildland fire investigators would conduct many investigations of runaway fires. Convection had a large influence on fire behaviour, even in the presence moderate to strong winds, in the rugged montane sites of this study, which were characterised by very steep gradients. This is a fire behaviour characteristic which is certainly understated in the literature.

Residual ash colour, curling, spalling, and residual ash organic carbon content were found to be unreliable indicators of wildfire pattern and spread in montane grasslands of the Eastern Cape. Foliage freeze, cupping of grass tussocks, and unburnt undercut culms lying on burnt ground are directional indicators which are abundant and widely spread throughout the montane grasslands of Boschberg, Katberg, and Winterberg. Further empirical research is required to determine the accuracy of these indicators as *post-hoc* directional gauges of direction (wind or fire spread).

Consumption depth of grass tussocks was found to be a reliable indicator of fire spread type in *Cymbopogon* grassland systems of the Boschberg, while unreliable in *Festuca* grassland systems of the Katberg and Boschberg. Similarly, the amount of residual unburnt plant litter was found to be a reliable indicator of fire spread type in most grassland systems, of Eastern Cape mountains, but not all. Both of these two indicators should only be applied to adjacent fuel stands where differences between heading and backing regions are clear and obvious. Importantly, amount of residual plant litter and hights of remaining grass stalks do not produce values above which, or below which head and back fires occur.

Protection, sooting, & staining were found to be fairly reliable indicators of fire spread direction, but are not necessarily conclusive on their own. In conjunction with other indicators, however, they may be used reliably to determine the point of origin and other fire behaviour characteristics.

Undercutting of grass culms was shown to be an almost unequivocal diagnostic feature of backfires, and was almost invariably present after back fire passage. Importantly, however, the absence of unburnt undercut culms on burnt ground is **not** an indicator of head fire passage, as culms may not have been present in the sward before combustion.

Similarly, leeside charring on pole-type fuels was found to be an extremely reliable indicator of wind direction in all three fire spread types, but as with all of the above-mentioned indicators, was not without some level of variation.

The recommendation that one should interpret indicators in groups or clusters within a close proximity to each another, in order to avoid drawing false conclusions from idiosyncratic 'outlier' indicators, appears to be a sound conclusion, and is supported by the findings of this chapter. Indeed, it is encouraged that wildfire investigators be aware of, and take into consideration the existence of indicator variability.

To conclude, in order to accurately investigate and interpret wildfire origin, cause and spread, fire investigators need to have broad knowledge and understanding of a number of complex fire behavioural processes and drivers, which affect the formation and expression of numerous *post-hoc* wildland fire pattern indicators.

Chapter 6:
SYNTHESIS

6.1 Summary of findings & implications:

Wildland fires are an intrinsic feature of seasonal grassland and savanna ecosystems, and are thus guaranteed to occur at some frequency in these systems. In addition, fire managers and practitioners in southern Africa use fire as a management tool in these rangeland systems to achieve an array of management goals for ecological, agricultural, and safety purposes. The occurrence of uncontrolled fires potentially attributable to human agency and accompanied by damage to property and associated litigation is an inevitable outcome in these wildland fire systems.

The field of wildfire forensics in southern Africa is still in its infancy, but there is a growing need from litigants for the development of a reliable scientifically and evidence-based practice, based on good theory and observation. There has also been a paucity of recent wildfire model ground truthing and fuel model development in southern African grassland and savanna systems. Eastern Cape mesic montane grassland is one of these identified systems.

A thorough review of wildfire investigation literature (**Chapter 2)** included an overview of the science of combustion as it relates to wildfire investigations, a review of various fire behaviour prediction models and their use in fire investigations, an introduction to wildfire investigations, and an extensive list of *post-hoc* wildfire indicators, their descriptions, uses and limitations, as well as some proposed novel indicators. This work identified a comprehensive list of *post-hoc* physical wildfire behaviour indicators relevant to forensic wildfire investigations, informed by applicability, reliability, and potential limitations. This list is one of the first of its kind and is intended to serve as a reference guide for experts in wildfire investigations. Some additional novel indicators are proposed for potential application in investigations going forward. Importantly, this list is not final, but rather a first edition. Updated versions of this list will need to be compiled as further empirical research into the reliability and accuracy of *post-hoc* physical indicators of wildfire pattern and spread is conducted.

My primary hypothesis is that some of the selected indicators will be more sensitive and reliable for the purposes of reconstructing and interpreting wildfire behaviour, and my objective is to determine which of these have utility for forensic purposes.

I hypothesised that the critical input parameters (primary drivers of fire behaviour) required for accurate simulation of fire behaviour in Eastern Cape montane grasslands, will not differ significantly from those in other similar grassland and savanna systems in southern Africa.

I hypothesised further that models developed either specifically for grassland conditions, using data collected from numerous field trials, or for wildland fires in general, from artificially reconstructed fuel

conditions, will differ significantly in their ability to project and thus to retrodict actual wildfire behaviour (recorded fire conditions).

Given fuel and weather boundary conditions for any past fire event, it should be possible to reconstruct the behaviour and passage of past wildfires using fire behaviour prediction models, provided models are considered accurate for local conditions. While indeed this has proven to be a useful method of retrodiction, the results of this study (**Chapter 4**) showed that this technique is largely limited by the suitability of prediction models (and fuel models) to specific sites or site conditions. More specifically, the following conclusions can be supported by the data collected and the associated modelling:

- McArthur, BehavePlus, & Rothermel model configurations did not perform well when simulating fire behaviour (ROS, fireline intensity, & flame length) in Eastern Cape mesic montane grasslands. For the most part, models largely under-predicted fire behaviour in these montane rangeland systems.
- Existing fuel models constructed for southern African grassland and savanna systems proved to be inappropriate for the Boschberg, Katberg, and Winterberg mountain systems. These fuel models are likely not accurate representations of southern African grassland fuel conditions. It is advised that these existing custom grassland and savanna fuel models be revised. Suggested changes include a higher dead fuel moisture of extinction value, probably close to 40%, and adjusted (perhaps larger) fuel surface area to volume ratios (finer coarseness).
- Investigation into which predictor variables drove fire behaviour in the prescribed burns of this study (montane grasslands of the Boschberg, Katberg, & Winterberg) was conducted. While extrapolation of these results is not recommended, it is clear that slope gradient is an important driver of fire behaviour in this system. This highlights the need for models to incorporate slope effects in their calculations of fire behaviour.
- Model slope factor correction functions were a crucial configuration inclusion for accurate simulation in this area. Configurations which did not account for slope effects proved to be unsuitable fire behaviour prediction models in this rugged landscape. This will likely also be the case in other mountainous regions in southern Africa, especially when landscapes are rugged and slope gradients steep.
- The McArthur Mk5 grassland model suitably simulated for fire rate of spread in montane grasslands of the Eastern Cape, but not flame length. McArthur based models are recommended for simulation of rate of spread in **cured** (>70%) grassland fuels of southern Africa, but further empirical research is required to confirm credibility of these models in other grassland and savanna systems.
- Double (2x) char height on pole type fuels such as trees and fence posts was found to be an adequate practical *post-hoc* indicator of head fire flame length in montane rangelands of the Eastern Cape.

- Cruz et. al., (2020), stressed the need for researchers to conduct studies which show how models fail to accurately simulate actual fire conditions. By highlighting model flaws, we are able to specifically identify weaknesses and address them accordingly. To that end, **Chapter 4** showed that current fire behaviour prediction models widely implemented in various African rangelands are **not** appropriate for mesic montane grassland systems of the Eastern Cape. I encourage modellers to address these issues and improve on model accuracy in these systems.
- Furthermore, **Chapter 4** examined model performance in head, back, and flank fires. Most quantitative fire behaviour studies only assess veldfire conditions in head fire scenarios. This study had an approximately equal split of fire spread types (~50 fires each) (n = 143). The data and findings from this study may provide valuable insights into how fire behaviour differs between spread type as well as how fire prediction models perform and function in all three fire spread types (head, back, & flank fires).
- BehavePlus and Rothermel models are relatively complex and require a multitude of input variables, many of which are difficult or impossible to accurately measure in the field. These models also require tedious and time-consuming application in order to implement appropriately. This is impractical in terms of rapid post-hoc forensic analysis of fire behaviour. Investigators do not have time to make precise measurements of fuel characteristics in typical site inspections, which usually last several hours. BehavePlus exists as its own software program and is difficult to transfer outputs or inputs via external sources.
- McArthur based models are easy to apply and have been converted into mathematical equations which can be easily included into computational software such as Microsoft Excel or R Studio. These models require few input variables which are easily derived from meteorological data or observational assessments of fuel. This is a particularly useful attribute which is suitable for rapid simulation and therefore favourable for fire practitioners and investigators.

Considering the above conclusions, from an implementation point of view retrodiction of fire conditions (behaviour) from fire behaviour prediction models is a useful tool for rangeland fire investigators, but is not unequivocally reliable or precise. Therefore, before model-based management decisions and/or conclusions of past or potential fire behaviour can be made, practitioners should be cognizant of limitations of fire behaviour prediction models. It is also important that fire managers and practitioners (including investigators) be aware of which parameters are critical for accurate prediction and retrodiction of fire conditions in relevant fire prone systems.

The numerous input variables and time-consuming implementation of the BehavePlus and Rothermel models is not accompanied by increased accuracy and precision compared to simpler McArthur based models, in the montane grasslands of the Eastern Cape. **The McArthur Mk5 grassland model with slope factor correction functions applied** is both simpler and easy to apply, as well as more accurate and reliable than the relatively complex American BehavePlus and Rothermel models in Eastern Cape

montane grassland systems. It is therefore recommended that fire managers and practitioners utilize this fire behaviour model when simulating fire spread southern African montane grassland systems.

Nine *post-hoc* indicators of wildfire pattern and spread used in forensic rangeland fire investigations were tested in this study (**Chapter 5**) for their reliability and utility in montane grasslands of the Eastern Cape. The conclusions were as follows:

- Residual ash colour, curling, spalling, and residual ash organic carbon content were found to be unreliable indicators of wildfire pattern and spread in montane grasslands of the Eastern Cape. Foliage freeze, cupping of grass tussocks, and unburnt undercut culms lying on burnt ground are directional indicators which are abundant and widely spread throughout the montane grasslands of Boschberg, Katberg, and Winterberg. Further empirical research is required to determine the accuracy of these indicators as post-hoc directional gauges of direction (wind or fire spread).
- Consumption depth of grass tussocks was found to be a reliable indicator of fire spread type in *Cymbopogon* grassland systems of the Boschberg, while unreliable in *Festuca* grassland systems of the Katberg and Boschberg. Similarly, the amount of residual unburnt plant litter was found to be a reliable indicator of fire spread type in most grassland systems, of Eastern Cape mountains, but not all. Both of these two indicators should only be applied to adjacent fuel stands where differences between heading and backing regions are clear and obvious. Importantly, amount of residual plant litter and hights of remaining grass stalks do not produce values above which, or below which head and back fires occur.
- Protection, sooting, & staining were found to be fairly reliable indicators of fire spread direction, but are not necessarily conclusive on their own. In conjunction with other indicators, however, they may be used reliably to determine the point of origin and other fire behaviour characteristics.
- Undercutting of grass culms was shown to be an almost unequivocal diagnostic feature of backfires, and was almost invariably present after back fire passage. Importantly, however, the absence of unburnt undercut culms on burnt ground is **not** an indicator of head fire passage, as culms may not have been present in the sward before combustion.
- Similarly, leeside charring on pole-type fuels was found to be an extremely reliable indicator of wind direction in all three fire spread types, but as with all of the above-mentioned indicators, was not without some level of variation.

These findings suggest that certain *post-hoc* wildland fire pattern and spread indicators must be re-evaluated, and practitioners are advised to adopt an adaptive approach to indicator interpretation, applying fire behavioural science of the processes and drivers of indicator formation and expression, while collectively incorporating several indicators in conjunction with each other before forming conclusions on origin, cause, and spread of runaway wildfires.

Importantly, while retrodiction of fire conditions from fire behaviour prediction models is a useful technique for rangeland fire investigators, appropriately interpreted *post-hoc* physical evidence remaining after fire passage is a more reliable *post-hoc* indication of fire pattern, spread, and behaviour than modelled outputs.

6.2 Limitations, improvements, & future research:

One of the biggest areas of limitation in this study, was with regards to measurements for rate of spread (ROS). It is notoriously difficult to accurately measure or determine the ROS of wildland fires. Due to the rugged topography, scale of the study sites (~100 ha), impaired visibility, and limited availability (incl. cost) of equipment, ROS was only recorded for a subsample dataset of 28 fires. As mentioned previously the subsample dataset was then used to choose the most appropriate spread model for subject site and prevailing conditions. Using the most suitable spread model, ROS was simulated for the entire dataset of 143 fires. Accurate real-time measurements of ROS for each of the 143 fires in this study would certainly have been more favourable than modelled values, and would have likely contributed to more robust results and conclusions.

For the subsample dataset (n = 28), ROS was recorded by measuring the time taken for fires to travel between two landmarks (trees, boulders etc.) of a known distance apart. One of the limitations of recording ROS in this manner, apart from the obvious potential lack of appropriate landmarks, is that the direction of travel of fires is not always directly parallel to the line that joins two landmarks. Similarly, when trying to measure ROS through a square plot (10 x 10 m), fire spread is not always perpendicular to/through the plot. Therefore, the distance travelled through the plot is influenced by the angle of approach of the fire. Obvious solutions include circular, octagonal, or similarly shaped plots. However, it is not guaranteed that fire will pass directly through the centre of a plot. An innovative solution has been to arrange thermocouples in an octagonal arrangement and measure the time elapsed for fire spread between two thermocouples of know distance apart, based on temperature readings along a time scale. This method is relatively accurate, accounts for variable direction of spread, and allows for accurate *post-hoc* analysis (researchers/spotters are not required at each plot for duration of fire). However, this method requires numerous thermocouples and is limited by monetary cost. A potentially cheaper solution may be to use ibuttons, protected from fire (perhaps buried 5 cm in the soil surface) as low-cost alternatives to thermocouples. This method will need to be tested for suitability in future studies.

Another limitation in this study was, in some cases, the determination of fire spread type through each 100 m^2 plot. On occasion, fire spread type fluctuated with changing wind conditions when passing

through burn plots. This resulted in some plots which were partly burnt as head fires and partly as back fires. Observer discretion and large sample sizes appear to be the only feasible solutions.

Similarly, due to the rugged topography, variable wind conditions between adjacent valleys, as well as the phenomenon known as the lee-slope eddy effect, on occasion, resulted in differences between actual wind direction occurring through a plot and wind direction recorded by the anemometer. Variable wind conditions are a common attribute of irregular (rugged) landscapes. Wind is often channelled up or down valleys and can differ from general prevailing conditions. The portable weather station was usually placed at the highest position for each site, in order to record prevailing conditions for entire site and avoid small scale influences from outcrops, vehicles etc. In scenarios where conditions through a plot differed from prevailing conditions, smoke direction was used to gauge actual wind direction and where relevant was manually altered in the dataset. The placement of brightly coloured flags atop planted fence posts in future studies may improve recording of wind direction in variable scenarios. Video recording of experimental fires may also be advantageous for post-hoc referral.

Flame length in this study was measured by means of ocular estimation, using planted fence posts of know heights as visual aids. An alternative method exists, which makes use of tall metal rods taped at incremental heights above the ground surface (Anderson *et. al.*, 2003). Tape is burnt when it comes in contact with flame, indicating height reached by flames. A problem with this method is that it measures flame height, and not flame length.

The application of the hydropyrometer (or steam-releasing open-can calorimetry) method of fire intensity determination could also have been improved. With few key adjustments to methods and application, hydropyrometers could likely yield more accurate measurements of fireline intensity, than was the case in this study. Webber & Trollope, (1997), outlined in their description of this method, that open-can calorimeters should be placed both at ground level and canopy height, in order to capture energy of both heading and back flames, if they persist. This is logical in terms of differences in radiative and convective heat transfer between heading and backing fires. Importantly, the ground level tin can should be slightly elevated and not in contact with the ground surface, as it could lose heat energy via conduction (Trollope W.S.W. (PhD), personal communication, 2019)). This set-up (two elevated cans offset from each other) requires the use of a metal stake from which to hang the cans. Due to the number of experimental plots used in this study (n = 143), at the time of prescribed burning, it was not feasible to purchase or construct such devices in short notice. Consequently, a single can, placed on the ground surface, was used for each experimental plot in this study. At ground level, the open-can calorimeters would not have captured the full amount of energy produced by head fires. Incidentally, this afforded the opportunity to identify shortcomings in this method, and produce empirical results which show why one should persist with Webber & Trollope's original method, and not place cans directly on the ground surface. It is important to note that had I constructed the relevant devices and

applied the original method, hydropyrometers would still have been a very cost-effective method of fireline intensity determination.

Other shortcomings in the application of the hydropyrometer method in this study include the amount of water used, and the potential for evaporation in field trials which persist for many hours, although these were not as a result of deviation from Webber & Trollope's, (1997), original methods. Webber and Trollope, (1997), advise 20 ml of water as suitable for grassfires scenarios in southern Africa. In this study, the entire 20 ml of water vapourised on a number of occasions, especially when fires were 'hot'. In these scenarios, any additional heat energy produced by the fire, therefore, could not be captured in any further water loss (vaporisation). This would have contributed to further under-recording in 'hot' head fires. From observations of field trials in this study, it is recommended that perhaps 30 ml of water would be more appropriate for fires in high fuel load moribund mesic grasslands in southern Africa.

It is likely that a portion of the 20 ml of water may have been lost to evaporation before and after fires had passed through. This was certainly the case with two open-can calorimeters in this study, which did not have fire burn passed them ('controls'). This loss of water to evaporation can be accounted for in future studies by following similar methods proposed by Gorgone-Barbosa *et. al*., (2015), and placing controls outside of the burn area and recording water loss over the period of controlled burning. Or alternatively, and perhaps more simply, the openings of the cans could be sealed with plastic film wrap secured with elastic bands. The film wrap will prevent evaporation before the fire passes through, and melt away when in contact with flames, allowing vaporisation of water. This method would not, however, account for evaporation after fire passage.

Webber & Trollope, (1997), suggest using 330 ml beverage cans as steam-releasing calorimeters. The smaller openings of beverage cans (compared to 410 g food cans) may reduce the amount of water lost to evaporation, however, further analysis and research are required to investigate this. In this study, 410 g food cans were chosen over 330 ml beverage cans, as it is easier to extract and measure amount of remaining water from the larger opening of food cans. It was also noted from this study, that measuring amount of remaining water using a syringe with a long needle was a more practical method in the field than weighing cans to determine amount of remaining water.

As previously noted, it is largely acknowledged that woody cover has little contribution to fire behaviour in the relatively cool, fast-moving fires of grassland and savanna systems (Trollope W.S.W. (PhD), personal communication, 2019). However, unlike savanna systems, the woody component (Amathole montane Fynbos (*e.g., Cliffortia paucistamina*)) in mesic montane grasslands of the Eastern Cape is very susceptible to fire (Trollope, 1970; Trollope, 1972), and when present, has a significant contribution to the behaviour of surface fires in these systems (Trollope W.S.W. (PhD), personal communication, 2019). This study specifically focussed on grass fire behaviour.

Despite efforts in this study to place 10 x 10 m burn plots in such a manner as to avoid the woody component, there were, in some cases, an element of woody fuel, both highly flammable (*Cliffortia paucistamina*) and resistant to fire present in experimental plots. This woody component would have, to some degree, contributed to the overall fire behaviour in burn plots. this contribution could have been increased fire intensity, or have a dampening effect on the fire, depending on species present in the sward. A potential improvement to this study could have been to measure the fuel load of woody vegetation by means of belt/line transects or Point Centre Quarter method proposed by Cottam & Curtis, (1956).

Ideally the preferred option would have been for this study to have collected empirical data under fire conditions as close to typical runaway wildfire conditions (high wind speeds, low humidity, high fuel load), as possible. An inevitable consequence of conducting prescribed burns, is that safety takes precedence ahead of desired effect/outcome. Despite endeavouring to emulate runaway conditions, on average, experimental fire conditions in this study were milder than those experienced in typical runaway wildfire conditions. Notwithstanding, a range of high wind speeds (up to 40+ km/h) was achieved. It is likely that under runaway conditions, indicator expression and model performance will be differ when compared to controlled burning conditions. Therefore, it is advised that the results from this study be ground-truthed in extreme runaway conditions, where possible, to confirm the findings of this study.

While one of the main objectives of this study was to assess the effects of slope on fire behaviour, prediction models, and indicators, future studies may need to repeat similar experiments in flatter more uniform landscapes. In these landscapes wind will likely contribute more to fire behaviour. Data from a range of conditions (rugged and flatter landscapes) will contribute to our understanding of what drives fire behaviour, and which parameter are critical for indicator formation and model predictions

Similarly, future studies should also repeat similar studies in different vegetation types, such as fynbos (macchia), savanna, and woodland/forest systems, where drivers of fire behaviour, and thus indicator formation and model outputs, differ from grassfire conditions.

Perhaps one of the most significant aspects of rangeland fire forensic indicators which was not investigated in this study, is with regards to deterioration of indicator evidence over time. *Post-hoc* physical indicators of wildland fire pattern and spread deteriorate in response to *inter alia* weathering (*e.g.*, wind and rainfall). While it is certainly favourable to conduct investigations as soon as possible after a fire event, in reality, investigations are regularly conducted weeks, or even several months after a fire has occurred. Some indicators (*e.g.*, ash) are more prone to deterioration than others (*e.g.*, leeside charring). Deterioration of indicators over time has not been quantified and is largely unknown. In this study, it was observed that ash (colour), undercut grass culms, soot, and unburnt plant litter indicators were particularly sensitive to certain weathering from rain and wind. Future studies should track and

quantify deterioration of indicators over time. Based off observations from this study, and personal experience as a rangeland fire investigator, suggested timescale of indicator data collection in future studies should perhaps sample at one day, one week, two weeks, six weeks, and 12 weeks after the fire event. Research in this regard should offer valuable insight into the accuracy and reliability of indicators over time will have practical implications for fire investigations and the legal system.

6.3 Final conclusions

Despite the above-mentioned limitations, the main objectives and research questions of this study were addressed effectively. The critical input parameters required for accurate simulation of fire behaviour in Eastern Cape montane grasslands, for the most part, did not differ significantly from those in other grassland and savanna systems in southern Africa and Australia. However, slope was identified to be a key driver of fire behaviour in these montane systems, and it is critical that it be included as a parameter when simulating fire conditions in rugged landscapes. Specialised models, developed empirically from field trials, specifically for grassfires, performed significantly better than generalised models, developed from artificially reconstructed fuel conditions, when simulating fire behaviour in Eastern Cape montane grasslands. *Post-hoc* indicators of wildfire pattern and spread differed in their reliability and accuracy for the purposes of reconstructing and interpreting wildfire behaviour. I was able to identify a selection of indicators which have varying levels of utility for forensic rangeland fire investigation purposes.

LIST OF APPENDICES

Attached appendices can be found at the end of this document, following reference list.

Appendix 1: Government Gazette. Notice 1099 of 2013. Publication of the Fire Danger Rating System for General Information in terms of Section 9(1) of the National Veld and Forest Fire Act, 1998. (Act No. 101 of 1998). *Republic of South Africa*.

Appendix 2: Webber, L. N., & Trollope, W. S. W. (1997). A simplified method for measuring fire intensity in grassland fires in the False Thornveld of the Eastern Cape. *Unpublished manuscript.* 22 River Road, Kenton On Sea, 6191, South Africa.

REFERENCES

Acocks, J. P. H. (1975). *Veld Types of South Africa* (2nd ed.). Memoirs of the Botanical Survey of South Africa No. 40. South Africa: Botanical Research Institute, Department of Agricultural Technical Services.

Alberti, L. (1968). *Ludwig Alberti's Account of the Tribal Life & Customs of the Xhosa in 1807*. Cape Town, South Africa: A. A. Balkema.

Anderson, S. A., Anderson, W. R., Hollis, J. J., & Botha, E. J. (2011). A simple method for field-based grassland curing assessment. *International Journal of Wildland Fire, 20*(6), 804-814.

Anderson, S. A., & Pearce, H. G. (2003) Improved methods for the assessment of grassland curing. In *Proceedings: International Wildland Fire Conference, 2003*.

Andrews, P. L. (1986). *BEHAVE: fire behavior prediction and fuel modeling system: BURN subsystem, Part 1* (Vol. 194). USDA Forest Service, Intermountain Research Station.

Andrews, P. L. (2014). Current status and future needs of the BehavePlus Fire Modeling System. *International Journal of Wildland Fire, 23*(1), 21-33.

Andrews, P. L., & Bevins, C. D. (2018). *BEHAVEPLUS: fire behavior prediction and fuel modeling system: SURFACE module, V6.0.0.* USDA Forest Service, Rocky Mountain Research Station.

Andrews, P. L. (2018). The Rothermel surface fire spread model and associated developments: A comprehensive explanation. *Gen. Tech. Rep. RMRS-GTR-371. Fort Collins, CO: US Department of Agriculture, Forest Service, Rocky Mountain Research Station. 121 p., 371*.

Anon. (2001). *Wildfire Investigation: A Guide for Determining the Origin and Cause of Fires in Grasslands, Scrub and Forests*. Victoria, Australia: Dept. of Natural Resources and Environment.

Archibald, S., Lehmann, C. E., Gómez-Dans, J. L., & Bradstock, R. A. (2013). Defining pyromes and global syndromes of fire regimes. *Proceedings of the National Academy of Sciences, 110*(16), 6442-6447.

Archibald, S., Staver, A. C., & Levin, S. A. (2012). Evolution of human-driven fire regimes in Africa. *Proceedings of the National Academy of Sciences, 109*(3), 847-852.

ASTER. Advanced Spaceborne Thermal Emission and Reflection Radiometer. Version 3. Land Processes Distributed Active Archive Center (LPDAAC). NASA.

Babrauskas, V. (2003). *Ignition Handbook: Principles and Applications to Fire Safety Engineering, Fire Investigation, Risk Management and Forensic Science* (1st ed.). Society of Fire Protection Engineers. Fire Science Publishers.

Beaufait, W. R. (1965). Characteristics of backfires and headfires in a pine needle fuel bed. In *U.S. Forest Service Internal Research Note* (Vol. 39). Intermountain Forest & Range Experiment Station, Ogden, Utah, USA: U.S. Dept. of Agriculture, Forest Service.

Bodi, M. B., Mataix-Solera, J., Doerr, S. H., & Cerdà, A. (2011). The wettability of ash from burned vegetation and its relationship to Mediterranean plant species type, burn severity and total organic carbon content. *Geoderma, 160*(3-4), 599-607.

Bodi, M. B., Doerr, S. H., Cerdà, A., & Mataix-Solera, J. (2012). Hydrological effects of a layer of vegetation ash on underlying wettable and water repellent soil. *Geoderma, 191*, 14-23.

Bodi, M. B., Martin, D. A., Balfour, V. N., Santín, C., Doerr, S. H., Pereira, P., ... & Mataix-Solera, J. (2014). Wildland fire ash: production, composition and eco-hydro-geomorphic effects. *Earth-Science Reviews*, *130*, 103-127.

Bond, W. J., & Keeley, J. E. (2005). Fire as a global 'herbivore': the ecology and evolution of flammable ecosystems. *Trends in ecology & evolution*, *20*(7), 387-394.

Bond, W. J., Woodward, F. I., & Midgley, G. F. (2005). The global distribution of ecosystems in a world without fire. *New phytologist*, *165*(2), 525-538.

Bourhill, R. (1982). *A guide to natural cover wildfire: fire direction indicators*. Salem, Oregon, USA: Oregon Department of Forestry.

Bowman, D. M., Balch, J. K., Artaxo, P., Bond, W. J., Carlson, J. M., Cochrane, M. A., ... & Johnston, F. H. (2009). Fire in the Earth system. *Science*, *324*(5926), 481-484.

Bradlow, E., & Bradlow, F. (1979). *William Somerville's narrative of his journeys to the Eastern Cape frontier and to Lattakoe 1799-1802*. Cape Town, South Africa: Van Riebeeck Society.

Bransby, D. I., & Tainton, N. M. (1977). The disc pasture meter: possible applications in grazing management. *Proceedings of the annual congresses of the Grassland Society of Southern Africa*, *12*(1), 115-118.

Brown, A. A., & Davis, K. P. (1973). *Forest fire: control and use* (2nd ed.). New York, USA: McGraw-Hill.

Buckman, S., Morris, R. H., & Bourman, R. P. (2021). Fire-induced rock spalling as a mechanism of weathering responsible for flared slope and inselberg development. *Nature communications*, *12*(1), 1-14.

Burgan, R. E. (1984). *Behave: fire behavior prediction and fuel modeling system, fuel subsystem* (Vol. 167). Intermountain Forest and Range Experiment Station, Forest Service, US Department of Agriculture.

Burns, K. A. (2007). The effective viscosity of ash-laden flows (Unpublished master's thesis). The University of Montana, Missoula, Montana, USA.

Burrows, N. D., Ward, B., & Robinson, A. (2009). Fuel dynamics and fire spread in spinifex grasslands of the Western Desert. *Proceedings of the Royal Society of Queensland, The*, *115*, 69-76.

Byram, G. M. (1959). Combustion of forest fuels. In Davis, K. P. (ed.). *Forest fire: control and use* (1st ed.) (pp. 61–89). New York, USA: McGraw-Hill.

Campbell Scientific. Measurement and control datalogger. CR200XLP.

Chandler, C., Cheney, P., Thomas, P., Trabaud, L., & Williams, D. (1983). *Fire in forestry. Volume 1. Forest fire behavior and effects. Forest fire management and organization*. Wiley.

Cheney, N. P., Gould, J. S., & Catchpole, W. R. (1993). The influence of fuel, weather and fire shape variables on fire-spread in grasslands. *International Journal of Wildland Fire*, *3*(1), 31-44.

Cheney, N. P., Gould, J. S., & Catchpole, W. R. (1998). Prediction of fire spread in grasslands. *International Journal of Wildland Fire*, *8*(1), 1-13.

Cheney, P., & Sullivan, A. (1997). *Grassfires: fuel, weather and fire behaviour* (1st ed.). Australia: CSIRO Publishing.

Cheney, P., & Sullivan, A. (2008). *Grassfires: fuel, weather and fire behaviour* (2nd ed.). Australia: CSIRO Publishing.

Clements, C. B. (2010). Thermodynamic structure of a grass fire plume. *International Journal of Wildland Fire*, *19*(7), 895-902.

Cochrane, M. A., & Ryan, K. C. (2009). Fire and fire ecology: Concepts and principles. In Cochrane, M. A. (ed.). *Tropical fire ecology* (pp. 25-62). Heidelberg, Germany: Springer.

Cottam, G., & Curtis, J. T. (1956). The use of distance measures in phytosociological sampling. *Ecology*, *37*(3), 451-460.

Cruz, M. G., Gould, J. S., Kidnie, S., Bessell, R., Nichols, D., & Slijepcevic, A. (2015). Effects of curing on grassfires: II. Effect of grass senescence on the rate of fire spread. *International Journal of Wildland Fire*, *24*(6), 838-848.

Cruz, M. G., Sullivan, A. S., Kidnie, S., Hurley, R., & Nichols, S. (2016). The effect of grass curing and fuel structure on fire behaviour - final report. *CSIRO Land and Water, Client Report No EP 166414.* Canberra, Australia.

Cruz, M. G., Sullivan, A. L., & Gould, J. S. (2020). The effect of fuel bed height in grass fire spread: addressing the findings and recommendations of Moinuddin *et. al.*, (2018). *International Journal of Wildland Fire*, *30*(3), 215-220.

CSIRO Fire Danger and Fire Spread Calculator. CSIRO-modified McArthur Mk 4 Grassland Fire Spread Meter. Copyright 1999 by CSIRO.

Danckwerts, J. E. (1989). Grass growth and response to defoliation. In Danckwerts, J. E., & Teague, W. R. (eds.). *Veld management in the Eastern Cape*. (pp. 8-19). Pretoria, South Africa: Department of Agriculture and Water Supply.

Danckwerts, J. E. (PhD). (2019). Personal communication. Saxfold Park, Adelaide, 5760, South Africa.

Danckwerts, J. E., & Trollope, W. S. W. (1980). Assessment of the disc pasture meter on natural veld in the false thornveld of the eastern province. *Proceedings of the Annual Congresses of the Grassland Society of Southern Africa*, *15*(1), 47-52.

De Haan, J. D. (1992). Fire: Fatal Intensity; A Third View of the Lime Street Fire. *Fire and Arson Investigator*, *43*(1), 55-59.

De Haan, J. D., & Icove, D. J. (2013). *Kirk's Fire Investigation: Pearson New International Edition* (7th ed.). Pearson.

De Ronde, C. (1998). Unpublished Fuel Model File for the Ermelo District, Mpumalanga Highveld, South Africa.

De Ronde, C., & Goldammer, J. G. (2015). *Wildfire investigation: Guidelines for practitioners; a publication of the Global Fire Monitoring Center (GFMC)*. Kessel, Remagen, Germany: Global Fire Monitoring Center (GFMC).

Dexter, B. D., & Williams, D. F. (1976). Direct field estimation of fine fuel moisture content. *Australian Forestry*, *39*(2), 140-144.

Dlapa, P., Bodí, M. B., Mataix-Solera, J., Cerdà, A., & Doerr, S. H. (2015). Organic matter and wettability characteristics of wildfire ash from Mediterranean conifer forests. *Catena*, *135*, 369-376.

Doerr, S. H., & Santín, C. (2016). Global trends in wildfire and its impacts: perceptions versus realities in a changing world. *Philosophical Transactions of the Royal Society B: Biological Sciences*, *371*(1696), 20150345.

Dörgeloh, W. G. (2002). Calibrating a disc pasture meter to estimate above-ground standing biomass in Mixed Bushveld, South Africa. *African Journal of Ecology*, *40*(1), 100-102.

Durigan, G. (2020). Zero-fire: not possible nor desirable in the Cerrado of Brazil. *Flora*, *268*, 151612.

Du Toit, J. C. O. (PhD). (2019). Personal communication. 7 Church Street, Middelburg, 5900, South Africa.

Everson, T. M., Van Wilgen, B. W., & Everson, C. S. (1988). Adaptation of a model for rating fire danger in the Natal Drakensberg. *South African Journal of Science*.

Fidelis, A. (2020). Is fire always the "bad guy"?. *Flora*, *268*, 151611.

Finney, M. A. (1998). *FARSITE, Fire Area Simulator--model development and evaluation* (No. 4). US Department of Agriculture, Forest Service, Rocky Mountain Research Station.

Finney, M. A. (2006). An overview of FlamMap fire modeling capabilities. In*: Andrews, Patricia L.; Butler, Bret W., comps. 2006. Fuels Management-How to Measure Success: Conference Proceedings. 28-30 March 2006; Portland, OR. Proceedings RMRS-P-41. Fort Collins, CO: US Department of Agriculture, Forest Service, Rocky Mountain Research Station. p. 213-220* (Vol. 41).

Finney, M. A., & Andrews, P. L. (1999). FARSITE—a program for fire growth simulation. *Fire management notes*, *59*(2), 13-15.

Finney, M. A., Cohen, J. D., McAllister, S. S., & Jolly, W. M. (2013). On the need for a theory of wildland fire spread. *International journal of wildland fire*, *22*(1), 25-36.

Flannigan, M. D., Krawchuk, M. A., de Groot, W. J., Wotton, B. M., & Gowman, L. M. (2009). Implications of changing climate for global wildland fire. *International journal of wildland fire*, *18*(5), 483-507.

Forbes, V. S. (Ed.). (1986). *Carl Peter Thunberg: Travels at the Cape of Good Hope: 1772-1775*. Cape Town, South Africa: Van Riebeeck Society.

Ford, R. T. (1971). *Fire Scene Investigation of Grassland and Forest Fires*. California, USA: California Department of Forestry.

Ford, R. T. (1995). *Investigation of Wildfires*. Bend, Oregon, USA: Maverick Publication.

Garmin. GPSmap. 60CSx.

Goforth, B. R., Graham, R. C., Hubbert, K. R., Zanner, C. W., & Minnich, R. A. (2005). Spatial distribution and properties of ash and thermally altered soils after high-severity forest fire, southern California. *International Journal of Wildland Fire*, *14*(4), 343-354.

Gorgone-Barbosa, E., Pivello, V. R., Bautista, S., Zupo, T., Rissi, M. N., & Fidelis, A. (2015). How can an invasive grass affect fire behavior in a tropical savanna? A community and individual plant level approach. *Biological Invasions*, *17*(1), 423-431.

Government Gazette. Notice 1099 of 2013. Publication of the Fire Danger Rating System for General Information in terms of Section 9(1) of the National Veld and Forest Fire Act, 1998. (Act No. 101 of 1998). *Republic of South Africa*.

Harmse, C. J., Dreber, N., & Trollope, W. S. (2019). Disc pasture meter calibration to estimate grass biomass production in the arid dunefield of the south-western Kalahari. *African Journal of Range & Forage Science*, *36*(3), 161-164.

Hempson, G. P., Archibald, S., Bond, W. J., Ellis, R. P., Grant, C. C., Kruger, F. J., ... & Vickers, K. J. (2015). Ecology of grazing lawns in Africa. *Biological Reviews*, *90*(3), 979-994.

Hudak, A. T., Ottmar, R. D., Vihnanek, R. E., Brewer, N. W., Smith, A. M., & Morgan, P. (2013). The relationship of post-fire white ash cover to surface fuel consumption. *International Journal of Wildland Fire*, *22*(6), 780-785.

IAFC, IAAI, & NFPA. International Association of Fire Chiefs, International Association of Arson Investigators, & National Fire Protection Association. (2018). *Fire Investigator: Principles and Practice to NFPA 921 and 1033* (5th ed.). Burlington, Massachusetts, USA: Jones & Bartlett Learning.

Jolly, W. M., Cochrane, M. A., Freeborn, P. H., Holden, Z. A., Brown, T. J., Williamson, G. J., & Bowman, D. M. (2015). Climate-induced variations in global wildfire danger from 1979 to 2013. *Nature communications*, *6*(1), 1-11.

Keeley, J. E. (2009). Fire intensity, fire severity and burn severity: a brief review and suggested usage. *International Journal of Wildland Fire*, *18*(1), 116-126.

Kidnie, S., Cruz, M. G., Gould, J., Nichols, D., Anderson, W., & Bessell, R. (2015). Effects of curing on grassfires: I. Fuel dynamics in a senescing grassland. *International Journal of Wildland Fire*, *24*(6), 828-837.

Kremens, R., Faulring, J., Gallagher, A., Seema, A., & Vodacek, A. (2003). Autonomous field-deployable wildland fire sensors. *International Journal of Wildland Fire*, *12*(2), 237-244.

Leavell, D., Berger, C., Fitzgerald, S., Parker, B. (2017). *Fire Science Core Curriculum*. Oregon, USA: Oregon State University.

Lentile, L. B., Holden, Z. A., Smith, A. M., Falkowski, M. J., Hudak, A. T., Morgan, P., ... & Benson, N. C. (2006). Remote sensing techniques to assess active fire characteristics and post-fire effects. *International Journal of Wildland Fire*, *15*(3), 319-345.

Lentini, J. J. (1992). The lime street fire: another perspective. *The Fire and Arson Investigator*, *43*(1), 1-3.

Lentini, J. J. (2019). Fire investigation: Historical perspective and recent developments. *Forensic Sci Rev*, *31*, 37-44.

Liodakis, S., Bakirtzis, D., & Dimitrakopoulos, A. (2002). Ignition characteristics of forest species in relation to thermal analysis data. *Thermochimica Acta*, *390*(1-2), 83-91.

Luke, R. H., & McArthur, A. G. (1978). *Bushfires in Australia.* Canberra, Australia: Australian Government Publishing Service.

McArthur, A. G. (1966). Weather and grassland fire behaviour. *Leaflet No.* 100. *Forestry and Timber Bureau, Department of national Development*. Canberra, Australia.

McArthur, A. G. (1967). Fire behaviour in eucalypt forests. *Leaflet No.* 107. *Forest Research Institute, Forestry and Timber Bureau.* Canberra, Australia.

McArthur, A. G. (1968). The effect of time on fire behaviour and fire suppression problems. In *E.F.S Manual 1968* (pp. 3-13). Keswick, South Australia: Emergency Fire Services.

McArthur, A. G. (1977). Grassland Fire Danger Meter Mark V. Slide rule printed for the Country Fire Authority of Victoria.

McCaw, W. L., & Catchpole, E. A. (1997). Comparison of grass fuel moisture contents predicted using the McArthur Mark V Grassland Fire Danger Meter and an equation derived from the meter. *Australian Forestry*, *60*(3), 158-160.

Millie, S., & Adams, R. (1999). Measures of grassland curing: a comparison of destructive sampling with visual and satellite estimates. In *Proceedings: Australian Bushfire 99 Conference* (pp. 257-263).

Moritz, M. A., Parisien, M. A., Batllori, E., Krawchuk, M. A., Van Dorn, J., Ganz, D. J., & Hayhoe, K. (2012). Climate change and disruptions to global fire activity. *Ecosphere*, *3*(6), 1-22.

Morrell, J. J., Miller, D. J., & Schneider, P. F. (1999). Service life of treated and untreated fence posts: 1996 Post Farm Report. *Research Contribution 26, Forest Research Laboratory, Oregon State University*. USA.

Mucina, L., Rutherford, M. C., & Powrie, L. W. (2006). Vegetation Atlas of South Africa, Lesotho and Swaziland. In Mucina, L., & Rutherford, M. C. (eds.). *The Vegetation of South Africa, Lesotho and Swaziland* (pp. 748-789). Pretoria, South Africa.

Munsell Colour Co., 1975. Munsell Soil Colour Charts. Maryland, USA: Munsell Colour.

National Veld and Forest Fire Act 101 of 1998. Republic of South Africa.

Nelson, D. W., & Sommers, L. E. (1996). Total carbon, organic carbon, and organic matter. In *Methods of soil analysis: Part 3 Chemical methods*, *5*, 961-1010.

NFPA. (2004). *NFPA 921: guide for fire and explosion investigations* (2004 ed.). Quincy, Massachusetts, USA: National Fire Protection Association.

NFPA. (2008). *NFPA 921: guide for fire and explosion investigations* (2008 ed.). Quincy, Massachusetts, USA: National Fire Protection Association.

NFPA. (2011). *NFPA 921: guide for fire and explosion investigations* (2011 ed.). Quincy, Massachusetts, USA: National Fire Protection Association.

NFPA. (2014). *NFPA 921: guide for fire and explosion investigations* (2014 ed.). Quincy, Massachusetts, USA: National Fire Protection Association.

NFPA. (2017). *NFPA 921: guide for fire and explosion investigations* (2017 ed.). Quincy, Massachusetts, USA: National Fire Protection Association.

NFPA. (2021). *NFPA 921: guide for fire and explosion investigations* (2021 ed.). Quincy, Massachusetts, USA: National Fire Protection Association.

NFPA & IAAI. National Fire Protection Association & International Association of Arson Investigators. (2005). *User's Manual for NFPA 921: guide for fire and explosion investigations* (2nd ed.). Sandbury, Massachusetts, USA: Jones & Bartlett Publishing.

Nieman, W. A., Van Wilgen, B. W., & Leslie, A. J. (2021). A review of fire management practices in African savanna-protected areas. *Koedoe*, *63*(1), 1-13.

Noble, I. R., Gill, A. M., & Bary, G. A. V. (1980). McArthur's fire-danger meters expressed as equations. *Australian Journal of Ecology*, *5*(2), 201-203.

NWCG. (2016). *Guide to wildland fire origin and cause determination* (2016 ed.). PMS 412, NFES 1874. USA: National Wildfire Coordinating Group.

NWCG. (2018). *Glossary of wildland fire terminology*. (2018 ed.). PMS 205. USA: National Wildfire Coordinating Group.

O'Connor, T. G., & Pickett, G. A. (1992). The influence of grazing on seed production and seed banks of some African savanna grasslands. *Journal of Applied ecology*, 247-260.

Pausas, J. G., & Keeley, J. E. (2009). A burning story: the role of fire in the history of life. *BioScience*, *59*(7), 593-601.

Pereira, P., Ubeda, X., & Martin, D. A. (2012). Fire severity effects on ash chemical composition and water-extractable elements. *Geoderma*, *191*, 105-114.

Perez, B., & Moreno, J. M. (1998). Methods for quantifying fire severity in shrubland-fires. *Plant Ecology*, *139*(1), 91-101.

QGIS Development Team (2020). QGIS Geographic Information System. Open Source Geospatial Foundation Project.

Prestemon, J. P., Hawbaker, T. J., Bowden, M., Carpenter, J., Brooks, M. T., Abt, K. L., ... & Scranton, S. (2013). Wildfire ignitions: a review of the science and recommendations for empirical modeling. *Gen. Tech. Rep. SRS-GTR-171. Asheville, North Carolina, USA: USDA-Forest Service, Southern Research Station*, *171*, 1-20.

Radwag scale. S/N: 306814/10. Model: PS 200/2000C/1.

R Core Team (2020). *R: A language and environment for statistical computing*. R Foundation for Statistical Computing, Vienna, Austria.

R.M. Young Company. Wind Sentry anemometer and vane. W/J-box. Category number: 03002. Serial number: WS 16998.

Robichaud, P. R., Lewis, S. A., Laes, D. Y., Hudak, A. T., Kokaly, R. F., & Zamudio, J. A. (2007). Postfire soil burn severity mapping with hyperspectral image unmixing. *Remote Sensing of Environment*, *108*(4), 467-480.

Rothermel, R. C. (1972). *A mathematical model for predicting fire spread in wildland fuels* (Vol. 115). Intermountain Forest and Range Experiment Station, Forest Service, United States Department of Agriculture.

Ruxton, G. D. (2017). Testing for departure from uniformity and estimating mean direction for circular data. *Biology letters*, *13*(1), 20160756.

Schwilk, D. W. (2003). Flammability is a niche construction trait: canopy architecture affects fire intensity. *The American Naturalist*, *162*(6), 725-733.

Scott, A. C., Bowman, D. M., Bond, W. J., Pyne, S. J., & Alexander, M. E. (2014). *Fire on earth: an introduction*. Chichester, United Kingdom: John Wiley & Sons.

Shakesby, R. A., & Doerr, S. H. (2006). Wildfire as a hydrological and geomorphological agent. *Earth-Science Reviews*, *74*(3-4), 269-307.

Sharples, J. J. (2008). Review of formal methodologies for wind–slope correction of wildfire rate of spread. *International Journal of Wildland Fire*, *17*(2), 179-193.

Simeoni, A., Owens, Z. C., Christiansen, E. W., Kemal, A., Gallagher, M., Clark, K. L., ... & Hadden, R. M. (2017). A preliminary study of wildland fire pattern indicator reliability following an experimental fire. *Journal of fire sciences*, *35*(5), 359-378.

Smith, A. M., & Hudak, A. T. (2005). Estimating combustion of large downed woody debris from residual white ash. *International Journal of Wildland Fire*, *14*(3), 245-248.

Smith, F. R., (1982). Responses of four shrub species to timing and behaviour of fire in the Natal Drakensburg (Unpublished master's thesis). University of Natal, Pietermaritzburg, South Africa.

Smith, G. (2012). *First Field Guide to Grasses of Southern Africa*. Penguin Random House, South Africa.

Sneeuwjagt, R. J., & Frandsen, W. H. (1977). Behavior of experimental grass fires vs. predictions based on Rothermel's fire model. *Canadian Journal of Forest Research*, *7*(2), 357-367.

Snyman, H. A. (2004). Short-term influence of fire on seedling establishment in a semi-arid grassland of South Africa. *South African Journal of Botany*, *70*(2), 215-226.

Soil Classification Working Group. (1991). *Soil classification: a taxonomic system for South Africa* (2nd ed.). Pretoria, South Africa: Department of Agricultural Development.

Staver, A. C., Archibald, S., & Levin, S. A. (2011a). The global extent and determinants of savanna and forest as alternative biome states. *Science*, *334*(6053), 230-232.

Staver, A. C., Archibald, S., & Levin, S. (2011b). Tree cover in sub-Saharan Africa: rainfall and fire constrain forest and savanna as alternative stable states. *Ecology*, *92*(5), 1063-1072.

Stroup, W. W. (2015). Rethinking the analysis of non-normal data in plant and soil science. *Agronomy Journal*, *107*(2), 811-827.

Sullivan, A. L., Sharples, J. J., Matthews, S., & Plucinski, M. P. (2014). A downslope fire spread correction factor based on landscape-scale fire behaviour. *Environmental modelling & software*, *62*, 153-163.

Teie, W. C. (2003). *Fire Manager's Handbook on Veld and Forest Fires: strategy, tactics and safety* (South African ed.). Menlo Park, South Africa: Southern African Institute of Forestry.

Trollope, W. S. W. (1970). A consideration of macchia (fynbos) encroachment in South Africa and an investigation into methods of macchia eradication in the Amatole Mountains (Unpublished master's thesis). University of Natal, Pietermaritzburg, South Africa.

Trollope, W. S. W. (1972). Fire as method of eradicating macchia vegetation in the Amatole mountains of South Africa--experimental and field scale results. In *Tall Timbers Fire Ecol Conf Proc*.

Trollope, W. S. W. (1978). Fire behaviour–a preliminary study. *Proceedings of the Annual Congresses of the Grassland Society of Southern Africa*, *13*(1), 123-128.

Trollope, W. S. W. (1981). Recommended terms, definitions and units to be used in fire ecology in South Africa. *Proceedings of the Annual Congresses of the Grassland Society of Southern Africa*, *16*(1), 107-109.

Trollope, W.S.W. (1983). Control of bush encroachment with fire in the arid savannas of Southeastern Africa (Unpublished doctoral dissertation). University of Natal, Pietermaritzburg, South Africa.

Trollope, W. S. W. (1984). Fire behaviour. In de Booysen, P. V., & Tainton, N. M. (eds.). *Ecological effects of fire in South African ecosystems* (pp. 199-217). Heidelberg, Germany: Springer.

Trollope, W. S. W. (1989). Veld burning as a management practice in livestock production. In Danckwerts, J. E., & Teague, W. R. (eds.). *Veld management in the Eastern Cape*. (pp. 67-73). Pretoria, South Africa: Department of Agriculture and Water Supply.

Trollope, W. S. W. (2011). Personal perspectives on commercial versus communal African fire paradigms when using fire to manage rangelands for domestic livestock and wildlife in southern and East African ecosystems. *Fire Ecology*, *7*(1), 57-73.

Trollope, W. S. W. (PhD). (2019). Personal communication. 22 River Road, Kenton On Sea, 6191, South Africa.

Trollope, W. S. W., de Ronde, C., & Geldenhuys, C. J. (2004). Fire Behaviour. In Goldammer, J. G., & De Ronde, C. (Eds.). *Wildland fire management handbook for Sub-Sahara Africa* (pp. 27-59). Global Fire Monitoring Centre (GFMC).

Trollope, W. S. W., & Potgieter, A. L. F. (1986). Estimating grass fuel loads with a disc pasture meter in the Kruger National Park. *Journal of the Grassland Society of Southern Africa*, *3*(4), 148-152.

Trollope, W. S. W., & Trollope, L. A. (2016). Fire ecology and management of African grassland and savanna ecosystems. 22 River Road, Kenton On Sea, 6191, South Africa. Unpublished manuscript.in preparation for Working on fire International.

Trollope, W. S. W., Trollope, L. A., & Hartnett, D. C. (2007). Fire—a key factor in the ecology and management of African grasslands and savannas. In *Proceedings of the 23rd Tall Timbers Fire Ecology Conference: Fire in grassland and shrubland ecosystems* (pp. 2-14).

Ubeda, X., Pereira, P., Outeiro, L., & Martin, D. A. (2009). Effects of fire temperature on the physical and chemical characteristics of the ash from two plots of cork oak (Quercus suber). *Land degradation & development*, *20*(6), 589-608.

Vacchiano, G., & Ascoli, D. (2015). An implementation of the Rothermel fire spread model in the R programming language. *Fire Technology*, *51*(3), 523-535.

Van Wagner, C. E., Stocks, B. J., Lawson, B. D., Alexander, M. E., Lynham, T. J., & McAlpine, R. S. (1992). Development and structure of the Canadian forest fire behavior prediction system. *Forestry Canada Fire Danger Group Information Report ST-X-3.(Ottawa, ON)*.

Van Wagtendonk, J. W. (2006). Fire as a physical process. In Sugihara, N. G., Van Wagtendonk, J. W., Fites-Kaufman, J., Shaffer, K. E., & Thode, A. E. (eds.). *Fire in California's ecosystems* (pp. 38-57). Berkeley, California, USA: University of California Press.

Van Wilgen, B. W. (1986). A simple relationship for estimating the intensity of fires in natural vegetation. *South African Journal of Botany*, *52*(4), 384-385.

Van Wilgen, B. W., Le Maitre, D. C., & Kruger, F. J. (1985). Fire behaviour in South African fynbos (macchia) vegetation and predictions from Rothermel's fire model. *Journal of Applied Ecology*, 207-216.

Van Wilgen, B. W., & Wills, A. J. (1988). Fire behaviour prediction in savanna vegetation. *South African Journal of Wildlife Research-24-month delayed open access*, *18*(2), 41-46.

Viegas, D. X., Figueiredo, A. R., Costa, S., & Borges, C. M. (1994). On the use of water containers for the evaluation of the heat release of a spreading fire. In *Proceedings of the II International Conference on Forest Fire Research, Coimbra, Portugal* (pp. 817-832).

Weast, R. C. (1987). Handbook of Chemistry and Physics (1st Student Ed). CRC Press Inc., Florida, USA.

Webber, L. N., & Trollope, W. S. W. (1997). A simplified method for measuring fire intensity in grassland fires in the False Thornveld of the Eastern Cape. Unpublished manuscript. 22 River Road, Kenton On Sea, 6191, South Africa.

Weise, D. R., & Biging, G. S. (1997). A qualitative comparison of fire spread models incorporating wind and slope effects. *Forest Science*, *43*(2), 170-180.

Williams, R. J., Gill, A. M., & Moore, P. H. (2003). Fire behavior. In Andersen, A. N., Cook, G. D., & Williams, R. J. (eds.). *Fire in tropical savannas: the Kapalga experiment* (pp. 33-46). Ecological Studies (Vol. 169). Springer, New York, NY.

Wilson, A. A. (1988). Width of firebreak that is necessary to stop grass fires: some field experiments. *Canadian Journal of Forest Research*, *18*(6), 682-687.

Wilson, M. (1969). The Nguni People. In Wilson, M., & Thompson, L. (eds.). *The Oxford History of South Africa.* Vol. 1, *South Africa to 1970*. Oxford.

Wilson, R. A., Jr. (1985). Observations of extinction and marginal burning states in free burning porous fuel beds. *Combustion Science and Technology*, *44*(3-4), 179-193.

Whitlock, C., Higuera, P. E., McWethy, D. B., & Briles, C. E. (2010). Paleoecological perspectives on fire ecology: revisiting the fire-regime concept. *The Open Ecology Journal*, *3*(1).

Zambatis, N., Zacharias, P. J. K., Morris, C. D., & Derry, J. F. (2006). Re-evaluation of the disc pasture meter calibration for the Kruger National Park, South Africa. *African Journal of Range and Forage Science*, *23*(2), 85-97.

GENERAL NOTICES
ALGEMENE KENNISGEWINGS

NOTICE 1099 0F 2013

DEPARTMENT OF AGRICULTURE, FORESTRY AND FISHERIES (DAFF)

PUBLICATION OF THE FIRE DANGER RATING SYSTEM FOR GENERAL INFORMATION IN TERMS OF SECTION 9(1) ON THE NATIONAL VELD AND FOREST FIRE ACT, 1998 (ACT NO. 101 OF 1998)

I **Avhashoni Renny Madula**, in my capacity of as Director: Forestry Regulation and Oversight, acting in terms of section 9(1) of the National Veld and Forest Fire Act, 1998 (Act no. 101 of 1998) read with the delegations of powers and duties made in terms of this Act, hereby on behalf of the Minister of Agriculture, Forestry and Fisheries make and publish for general information the South African National Fire Danger Rating System, as set out in the Schedule hereto. This notice, replaces notice 1054 of 2005 which was published in government gazette No. 27735.

For more information, please follow the following instructions:

- Step 1: Open the DAFF website, www.daff.gov.za
- Step 2: Click on legislation
- Step 3: Click on Acts
- Step 3: Click on National Fire Danger Rating System

Avhashoni Renny Madula

DIRECTOR: FORESTRY REGULATION AND OVERSIGHT

Date:

SCHEDULE

1. Introduction

Fire Danger Rating System is the system that is used to provide a measure of the relative seriousness of burning conditions and threat of fire by providing an accurate measure as possible of the relative seriousness of burning conditions. The system also serves as an aid to fire control programs. It process and evaluates factors influencing fire danger systematically and represent them in the form of fire indices. The National Veld and Forest Fire Act (Act No. 101 of 1998) obliges the Minister to set up and maintain the system. However, he or she may delegate his or her powers and duties to do so to an organization with the necessary expertise. Through the system, a prohibition on the lighting of fires in the open air comes into force when the Minister warns in the media that fire danger rating is high and/or extreme-high.

To that extent, the National Fire Danger Rating, which is based on the Lowveld Model, has been approved as the official South African Veldfire Danger Rating system to fulfill this mandate.

2. Lowveld Based Model

The model makes calculations of the fire danger and indicate the value calculated daily, using dry bulb and dew point temperature to calculate first the relative humidity and then a Burning Index.

The Burning Index is adjusted according to prevailing wind by speed, while the availability of excess moisture (above the plant fibre saturation point) provided by recent rainfall, is taken into account by multiplying the burning index by rainfall correction factor. The Burning Index, corrected for wind and rainfall, is known as Fire Hazard Index by a rainfall correction factor. The Burning Index states that the Fire Hazard Index is usually calculated at about midday, when it is to at its maximum and therefore most dangerous stage.

3. Initial Fire Danger Indices (FDI)

It is a quantitative indicator of one or more facet of fire danger expressed in an absolute measure. These are:

- Temperature (T = Maximum, expressed in degrees C)
- Relative humidity (RH = Minimum, expressed in percentage %)
- Wind speed (correction factor) and
- Rain (correction factor).

The initial FDI, based on Temperature and RH will be calculated using the following formula:

- FDI = {(T-35) - ((35-T)/30) + ((100-RH)*0.37) + 30}
- T: Temperature, Degrees C
- RH: Relative humidity (%)

4. Calculating the wind correction factor:

Wind speed (km/h)	Add to initial FDI value
0-2	+ nil
3-8	+05
9-16	+10
17-25	+15
26-32	+20
33-36	+25
37-41	+30
42-45	+35
46+	+40

5. Calculating the rain correction factor:

This takes into account the amount of rainfall that has been received in a particular area and the number of days since that rainfall. The value is then multiplied by the FDI value.

	Days since rainfall											
Rain mm	**1**	**2**	**3**	**4**	**5**	**6**	**7-8**	**9-10**	**11-12**	**13-15**	**16-20**	**21+**
0.1 - 2.6	0.7	0.9	1	1	1	1	1	1	1	1	1	1
2.7 - 5.2	0.6	0.8	0.9	1	1	1	1	1	1	1	1	1
5.3 - 7.6	0.5	0.7	0.9	0.9	1	1	1	1	1	1	1	1
7.7 - 10.2	0.4	0.6	0.8	0.9	0.9	1	1	1	1	1	1	1
10.3 - 12.8	0.4	0.6	0.7	0.8	0.9	0.9	1	1	1	1	1	1
12.9 - 15.3	0.3	0.5	0.7	0.8	0.8	0.9	1	1	1	1	1	1
15.4 - 20.5	0.2	0.5	0.6	0.7	0.8	0.8	0.9	1	1	1	1	1
20.6 - 25.5	0.2	0.4	0.5	0.7	0.7	0.8	0.9	1	1	1	1	1
25.6 - 38.4	0.1	0.3	0.4	0.6	0.6	0.7	0.8	0.9	1	1	1	1
38.5 - 51.1	0.1	0.2	0.4	0.5	0.5	0.6	0.7	0.8	0.9	1	1	1
51.2 - 63.8	0.1	0.2	0.3	0.4	0.5	0.6	0.7	0.7	0.8	0.9	1	1
63.9 - 76.5	0.1	0.1	0.2	0.3	0.4	0.5	0.6	0.7	0.8	0.8	0.9	1
76.6+	0.1	0.1	0.1	0.2	0.4	0.5	0.6	0.6	0.7	0.8	0.9	1

6. Official colors of the model

The model has five official colors. Namely: blue, green, yellow, orange and red. These colors rate the level and categories of the likelihood of fires occurring in a given area.

Alert Stages/ Colour codes	**FDI**	**Fire Danger**	**Ratings**
BLUE	0-20	Low	Insignificant
GREEN	21-45	Moderate	Low
YELLOW	46-60	Dangerous	Medium
ORANGE	61-75	Very dangerous	High
RED	76-100	Extremely dangerous	Extremely high

7. How the system will link with fire behavior and suppression measures

The behavior of fire could change from one form to the other depending on the prevailing meteorological conditions. Suppression measures and resources must be aligned accordingly. In the table below, the following are recommended.

INDICATIVE COLOUR	BLUE	GREEN	YELLOW	ORANGE	RED
FIRE BEHAVIOUR	Fires are not likely to ignite. If they do, they are likely to go out without suppression action. There is little flaming combustion. Flame lengths in grassland and plantation forest litter lower than 0.5m and rates of forward spread less than 0.15 kilometres per hour.	Fires likely to ignite readily but spread slowly. Flame lengths in grassland and plantation forest litter lower than 1.0m and rates of forward spread between 0.3 and 1.5 kilometres per hour.	Fires ignited readily and spread rapidly, burning in the surface layers below trees. Flame lengths in grasslands and plantation forests between 1 and 2m, and rates 0.3 and 1.5 kilometres per hour.	Fires ignited readily and spread very rapidly, with local crowning and short-range spotting. Flame lengths between 2 and 5m, and rates of forward spread between 1.5 and 2.0 kilometres per hour.	Conflations are likely in plantation forests, stands of alien invasive trees and shrubs, sugar cane plantations, and fynbos. Long range fire spotting is likely in these fuel types. Rates of forward spread of head fires can exceed 4.0 kilometres per hour and flame lengths will be in order of 5-15m or more.
FIRE SUPPRESSION DIFFICULTY	Direct attack feasible: one or a few field crew with basic fire fighting tools easily suppresses any fire that may occur.	Direct attack feasible: fires safely approached on foot. Suppression is readily achieved by direct manual attack methods.	Direct attack constrained: fires not safe to approach on foot for more than very short periods. Best forms of control should combine water tankers and back burning from fire control lines.	Direct attack not feasible: fires cannot be approached at all and back burning, combined with aerial support are the only effective means to combat fires. Equipment such as water tankers should concentrate efforts on the protection of houses.	Any form of fire control is likely to be precluded until the weather changes. Back burning dangerous and best avoided.

8. Recommended actions for various ratings

INDICATIVE COLOUR	BLUE	GREEN	YELLOW	ORANGE	RED
DANGER RATING	Insignificant	Low	Moderate	High	High-Extreme
FIRE PREVETION AND PREPAREDNESS MEASURES	No precaution is needed	Fires including prescribed burns may be lit, used or maintained in the open air on the condition that persons making fires take reasonable precautions against the fires spreading	No fires may allowed in the open air except those that are authorized by the Fire Protection Officer exists, or elsewhere, the Chief Fire Officer of the local fire service, or fires in designated fireplaces.	No fires may be allowed under any circumstances in the open air.	No fires may be allowed under any circumstances in the open air and Fire Protection Associations and municipal Disaster Management Centres must invoke contingency fire emergency and disaster management plans including extraordinary readiness and response plans. All operations likely to ignite fires halted. Householders placed on alert.
APPLICATION OF THE ACT			Above precautionary measure to be prescribed and made applicable nationally on days rated moderate.	Section 10(1)(b) applies: no person may light, use or maintain a fire in the open air.	Section 10(1) (b) applies: no person may light, use or maintain a fire in the open air.
RELATIONSHIP WITH DISASTER MANAGEMENT				The threat of disastrous wildfires exists at municipal level under these conditions. Municipal Disaster Management Centres must invoke contingency plans and inform National and Provincial Disaster Management Centre. (Section 49 of the Disaster Management Act).	The threat of disastrous wildfires at provincial level exists under these conditions. Municipal Disaster Management Centres must invoke contingency plans and inform National and Provincial Disaster Management Centres. (Section 49 of the Disaster Management Act).

.

9. List of districts and metros that will be covered by the system

Section 9(3) obliges the Minister to divide the entire country into separate regions, each region being one in which the fire danger is usually sufficiently uniform to allow for a single rating which is meaningful for the entire region. To that extent, the District municipal boundaries and the Metropolitan boundaries will represent separate fire region

STATION NO.	FORECAST STATION	DISTRICT/METROPOLITAN
68155	Lephalale	Waterberg
68174	Polokwane Wo	Capricorn
68183	Thohoyandou Wo	Vhembe
68191	Phalaborwa Airport	Mopani
68237	Tosca	Dr Ruth Segomotsi
68242	Mafikeng Wo	Ngaka Modiri Molema
68255	Rustenburg	Bojanala
68262	Pretoria Eendracht	City of Tshwane Metro
68267	Ermelo Wo	Gert Sibande
68286	Oudestad	Sekhukhune
68286	Machadodorp AWS	Nkangala
682290	Kruger Int Airport	Ehlanzeni
68333	Kuruman	John Taolo Gaetsewe
68345	Welkom	Lejweleputswa
68350	Potchefstroom	Dr Kenneth Kaunda
68353	Vereeniging	Sedibeng
68355	Kroonstad	Fezile Qabi

68361	Jhb botanical gardens	City of Johannesburg Metro
68361	Jhb botanical gardens	West Rand
68368	Johannesburg Int Wo	Ekurhuleni Metro
68377	Newcastle	Amajuba
68400	Makatini Research Cntr	Umkhanyakude
68424	Upington Wo	Siyanda
68438	Kimberley Wo	Frances Baard
68442	Bloemfontein Wo	Mangaung Metro
68461	Bethlehem Wo	Thabo Mofutshanyane
68479	Ladysmith	Uthukela
68487	Greytown	Umzinyathi
68493	Ulundi	Zululand
68494	Mandini	ILembe
68497	Mtunzini	Uthungulu
68512	Springbok Wo	Namakwa
68538	De Aar Wo	Pixley ka Seme
68541	Fauresmith	Xhariep
68570	Matatiele	Alfred Nzo
68577	Kokstad	Sisonke
68579	Paddock	Ugu
68581	Pietermaritzburg	UMgungundlovu
68594	Kin Shaka AWOS	eThekwini Metro
68614	Vredendal	West Coast
68647	Queenstown	Chris Hani
68649	Jamestown	Joel Qabi
68668	Umthatha	O.R. Tambo
68718	Robertson	Cape Winelands

68727	Beaufort West	Central Karoo
68754	Dohne Agr	Amathole
68819	Melteno Reservoir (CT)	City of Cape Town Metro
68828	George Wo	Eden
68840	Somerset East	Cacadu
68842	Port Elizabeth Wo	Nelson Mandela Bay Metro
68858	East London Wo	Buffalo City Metro
68925	Elgin exp farm Grabouw	Overberg

10. Map of districts and metropolitan areas

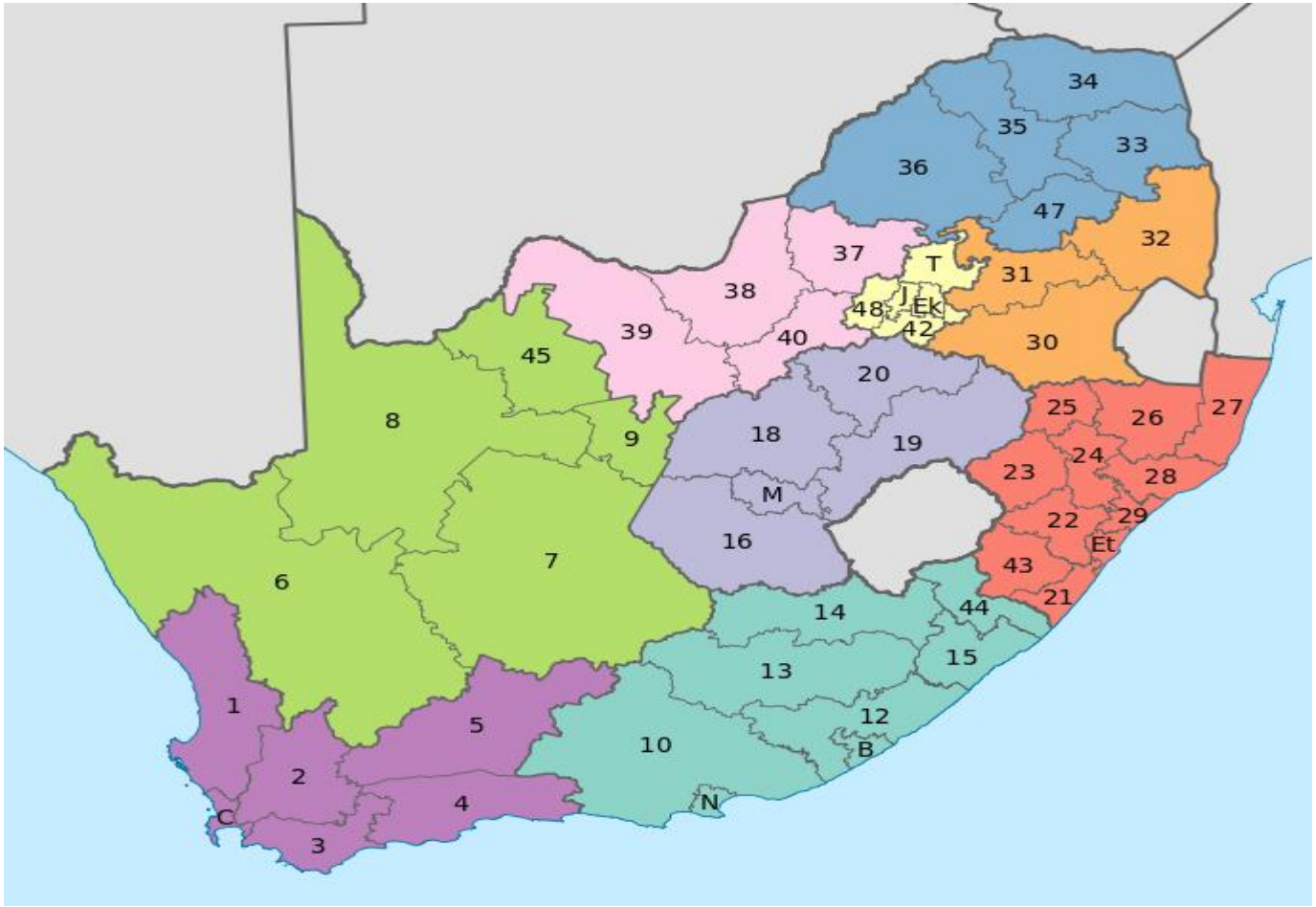

A SIMPLIFIED METHOD FOR MEASURING FIRE INTENSITY IN GRASSLAND FIRES IN THE FALSE THORNVELD OF THE EASTERN CAPE

L.N. Webber* and W.S.W. Trollope
***Department of Livestock and Pasture Science**
Faculty of Agriculture
University of Fort Hare
Private Bag X1314
Alice
5700
South Africa
cell - 0824927466, e-mail - lwebber@eastcape.net

Abstract

Controlled burning is an important, and often essential, management practice in both agricultural and conservation areas. Consequently a thorough understanding of burning and its effects on ecosystems, is essential in order to be able to manage the veld efficiently. In South Africa there is a deficiency of knowledge concerning the behaviour of fires at specific locations in a fire front. Virtually no attempt has been made to quantify the dynamics of the release of heat energy at these specific locations, during a fire, and the subsequent response of plants to it. Fire intensity is defined as the release of heat energy per unit time per unit length of the fire front. Numerically it is the product of available heat energy and the forward rate of spread of the fire front. These parameters can be measured to estimate the mean fire intensity of a free burning fire. Alternatively, fire intensity can be estimated at specific points in a fire front by measuring the amount of water that is converted to steam in a container of known mass and diameter and the rate of spread of the fire front at that particular point. The amount of water which is converted to steam will represent the amount of energy that a specific point is exposed to and when multiplying this by the rate of spread of the fire front divided by the area of the container, this represents the fire intensity for that specific point. By using this technique, fire intensities can be measured at specific sites in the fire front and the subsequent response of the vegetation to it.

Introduction

Controlled burning is an important, and often essential, veld management practice in both agricultural and conservation areas. Consequently a thorough understanding of burning and its effects on ecosystems, is essential in order to be able to manage the veld efficiently. In South Africa there is a deficiency of knowledge concerning the behaviour of fires at specific locations in a fire front. Virtually no attempt has been made to quantify the dynamics of the release of heat energy at these specific locations, during a fire, and the subsequent response of plants to it.

Albini (1976) stated that fire intensity is the heat released per unit time per unit length of fire front. Fire intensity is the product of the available heat energy and the forward rate of spread of the fire front (Byram, 1959) and is described by the following equation:

$$I = H*w*r$$

Where: I = fire intensity - kilojoules second^{-1} metre^{-1} - kJ s^{-1} m^{-1};

H = heat yield - kilojoules kilogram^{-1} - kJ kg^{-1};

w = mass of available fuel - kilogram metre^{-2} - kg m$^{-2;}$

r = rate of spread of the fire front - metre second^{-1} - m s^{-1}.

Trollope (1983) estimated the mean heat yield for grass burning, as a head fire, in the Thornveld areas of the Eastern Cape as 16890 kJ/kg of grass fuel. It was further concluded that the most practical and efficient method for estimating grass fuel loads was with a disc pasture meter developed by Bransby & Tainton (1977). The calibration for the disc pasture meter in the Eastern Cape is (Trollope, 1983):

$$y = 340 + 388.3x$$

where: y = mean fuel load - kg ha^{-1};

x = mean disc height - cm;

Trollope (1983) further developed the procedure whereby the mean rate of spread of the fire front can be measured, by using the following equation:

$$ROS = A(T*L)^{-1}$$

where ROS = mean rate of spread - m s^{-1};

A = area burnt - m^{2};

T = period of flaming combustion - seconds;

L = mean length of the fire front - m.

The aforementioned procedure results in the estimation of the overall mean fire intensity for an area that is being burnt. This is satisfactory when burning small experimental plots that have a uniform fuel load but becomes less meaningful when burning larger areas where there is a considerable variation in the fuel load. However, when studying the effect of fire on different types of vegetation under different conditions , it is necessary to achieve an accurate estimate of the fire intensity at specific points in the fire front because the rate of the release of the heat energy in relation to the location of the growing points of plants, governs the response of plants to fire. For example, the growing points of grasses are located close to ground level whereas those of trees and shrubs are located in the canopies. Consequently an average estimate of the rate at which heat is released during a free burning fire is a rather crude measurement of fire intensity in relation to determining its effect on plants with different growth habits.

More accurate results could be obtained if it were possible to measure the fire intensity at particular points in the fire, relative to the growth habits of the vegetation being studied. To date this could be measured only with specialised equipment such as thermocouples which are both expensive and difficult to manipulate in the field. This conclusion to the formulation of the following key questions was seen as a possible means of solving this problem.

1) Is there any relationship between the amount of water boiled off and the maximum temperature recorded at a specific location during a fire ?
2) Can the heat of vaporisation of water boiled off during a fire be used to estimate the intensity of combustion occurring at different points in a fire ?
3) Can a suitable container in the form of a simple metal container, located at specific points above ground level, be used to estimate the quantity of water vaporised during a fire ?
4) What size and shape of metal container will result in optimum estimates of the quantity of water vaporised during a fire?

The aforementioned key questions were addressed by postulating and testing the following hypothesis: The fire intensity at a particular point in the fire front can be estimated with the aid of a measuring cylinder, enabling one to determine the quantity of water vaporised from a suitable container when located at a particular point in a fire. The resultant fire intensity can be calculated as the product of the

rate of spread of the fire front and the total heat of vaporisation per unit area of the water lost from the container expressed as kilojoules per second per metre - kJ s^{-1} m^{-1} .

Procedure

The research was conducted during July and August, 1996 on an existing long term season of burning experiment at the University of Fort Hare Research Farm located in the False Thornveld of the Eastern Cape. In order to test the aforementioned hypothesis the research was conducted in four phases:

Phase 1:

To determine whether the amount of water lost at specific locations during a fire is correlated with the maximum temperatures recorded at these locations.

In order to provide a control for the experiment, bi-metallic thermometers, which could measure maximum temperatures only, were placed at specific locations in a fire front where metal containers containing water were located. This was done for the following reasons;

The total heat yield and fire intensity of a fire can be estimated by recording the temperature profile during a fire. The area below the temperature curve represents the total amount of heat energy released during a fire and the slope of the curve indicates the rate of release of heat energy during a fire (Tunstal et al 1976).

Although Vines (1981) expressed reservations about the use of temperature measurements for characterising the intensity of fires, Trollope (1983) found that fire intensity was highly significantly correlated with maximum temperatures recorded during surface head fires and that they gave a good indication of the dynamics involved in the release of heat energy in these fires. Tunstal *et al* (1976) further concluded that the total heat yield is also positively correlated with the maximum temperature of a fire. The aforegoing conclusions indicate that maximum temperature can serve firstly, as an index of fire intensity, and secondly, as an index of the total amount of heat energy released during a veld fire.

The following hypothesis was postulated based on the aforegoing conclusions: A positive relationship exists between the amount of water vaporised from metal containers and the maximum temperature recorded with bi-metallic thermometers at specific points in free burning fires.

A field experiment was conducted on the University of Fort Hare Research Farm to test the aforementioned hypothesis and comprised the following procedure:

1) Nine plots with varying fuel loads ranging from 3.1 - 5.1 tons per hectare were burnt as six head and three back fires respectively.
2) Three replications of two metal containers manufactured from tin with a mean mass of 97.93 grams and a basal area of 60.84 cm^2 containing $\pm$ 20 grams of water each were placed at ground level and canopy height in the grass swards in each of the plots.
3) Each individual metal container, plus its contents, was weighed on an analytical balance, both before and after the burn, to determine the exact amount of water converted to steam during each fire.
4) Previous research had found that the maximum temperatures recorded with the bi-metalic thermometers were consistently lower than the actual temperatures occurring in fires. Therefore a regression equation was developed using thermocouple data to convert these temperatures to more realistic values representative of what occurs during a veld fire. Trollope (1983) developed the following regression equation to convert temperatures recorded with the bi-metallic thermometers to corrected temperature values:

$$T = 73.28 + (1.18 * B)$$

Where T = corrected temperature - ^oC

B = bi-metalic thermometer reading - ^oC

Phase 2:

To determine whether fire intensity expressed as the total amount of heat energy released per unit time per unit length of the fire front (kJ s^{-1} m^{-1}) (Byram, 1959) could be derived from the amount of heat required to vaporise known quantities of water from a metal container placed in a free burning fire by means of calorimetry.

The normal procedure used for estimating fire intensity as defined by Byram (1959) comprises the following steps:

i) Estimating the total amount of heat energy released per kilogram of fuel load (kJ kg^{-1}) during a fire;

ii) Estimating the mass of available fuel with the aid of a disc pasture meter (kg m^{-2});

iii) Estimating the mean rate of spread (m s^{-1}) of the fire front;

iv) Calculating the product of the total amount of heat energy released per kilogram fuel load (kJ kg^{-1}) by the mass of available fuel (kg m^{-2}) and the mean rate of spread (m s^{-1}) of the fire front i.e. (kJ kg^{-1}) *(kg m^{-2})* (m s^{-1}) = kJ s^{-1} m^{-1}.

The object in Phase 2 was to determine whether the total amount of heat energy released per kilogram of fuel load (kJ kg^{-1}) during a fire, used in the aforementioned procedure, can also be estimated by calorimetry. This is based on the following theoretical considerations:

- Weast (1987), described the energy required to convert 1 gram of water to steam to be:

$$(2257 + ((100 - \text{ambient temp}) * 4.184))\ J\ (g\ H_2O)^{-1}$$

(For ambient temperature = 25 ^{o}C) $= (2257 + 314)\ J\ (g\ H_2O)^{-1}$

$= 2571\ J\ (g\ H_2O)^{-1}$

$= 2.571\ kJ\ (g\ H_2O)^{-1}$

- The transfer of heat in a moving fire front is mainly due to convection and radiation. Radiation from the flames accounts for most of the preheating of the fuel immediately adjacent to the fire front. It was also found that a grass sward burns from the top down because, as the wind behind the flames pushes the flames towards the ground, it causes the top of the grass sward in front of the fire to ignite first as presented in Figure 1 (Luke & McArthur, 1978).

- As soon as the fire front has passed a specific point, the temperature at that location starts to decrease regardless of the effect of radiation from the receding fire front. This, therefore would make it very difficult to measure the maximum temperature attained by water in a container placed at that specific location in a fire front.

If, however, a limited quantity of water were placed in a metal container at a specific location in a fire front (Figure 1) so that a portion of the water boiled away as the fire passed, it would be possible to

estimate the amount of heat energy released at that point by determining the amount the amount of water lost by vaporisation.

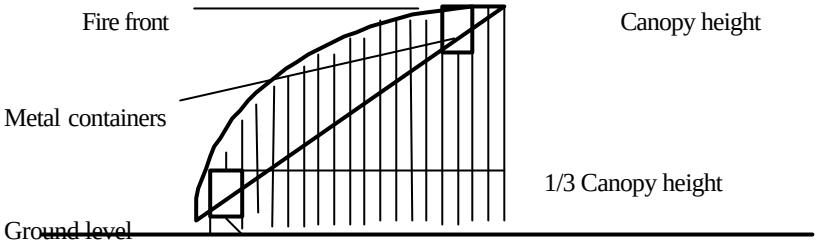

Figure 1: Metal containers used to measure the amount of water lost by vaporisation at specific locations in a grass sward burning from the top down.

Considering the aforementioned points and the insulating nature of dry grass material the following hypothesis was postulated: The amount of energy to which a specific location in a fire front is exposed, is dependent on the amount of heat energy released from the burning fuel in close proximity to that point.

In order to test the above hypothesis the following assumptions were made:

1. The density of the fuel was the same throughout the height of the grass sward. The height of the metal container that was used in the experiments was ten centimetres and the mean height of the grass sward was 30 cm. This implies that only 1/3 of the heat yield from the fuel at a specific location in the grass canopy would have a significant effect on the metal container and its contents. Consequently the calorimetric fire intensity that was calculated for each metal container would have to be multiplied by three for it to be compared with the overall mean fire intensity as defined by Byram (1959).
2. In previous research conducted by Trollope (1983) on the Fort Hare Research Farm, the mean fire intensity and rate of spread of 10 head fires was 1359 $\pm$ 327 kJ s^{-1} m^{-1} and 0.15$\pm$0.03 m s^{-1} respectively.

3. By dividing the energy required to convert 1 gram of water to steam, namely 2.571 kJ, into the mean fire intensity described above being 1359 kJ, it was found that an average of 529 grams of water per ± 15 cm x 1 m strip can be converted to steam per meter of fire front. The area of the metal container that was used was 60.84 cm^2 and the height of the container was on average 1/3 of the mean grass canopy height. This meant that the metal container would be exposed to 1/3 of the heat yield produced by the fuel per unit area. This implies that the mean quantity of water that could be boiled away by the fuel under the metal container was 1/3 of 21.46 grams which was 7.15 grams. It was therefore decided to use 20 grams of water per metal container during Phase 2 of the burning trial.

A field experiment was conducted on the University of Fort Hare Research Farm to test the aforementioned hypothesis and comprised the following procedure:

1) Nine plots, 15m x 15m in size with varying fuel loads were burnt with six head and three back fires.

2) Three replications of two tins with a mean weight of 97.93 grams and a basal area 60.84 cm^2, containing ± 20 grams of water each were placed at ground level and canopy height in the grass swards in each of these plots.

3) At each metal container site a bi-metallic thermometer, which contained an active and a passive needle, was placed to record the maximum temperature of the fire.

4) Each individual metal container, plus its contents, was weighed before and after the fires to determine the amount of water vaporised during the fires.

5) The following measurements were recorded before and during each fire:

i) fuel load;

ii) temperature and relative humidity;

iii) wind speed and direction;

iv) rate of spread;

v) flame height.

6) The fire intensity estimated at ground level and at canopy height with the metal containers was multiplied by three and then compared with the estimations of fire intensity based on the estimation of the fuel load, heat yield and rates of spread of the head and back fires.

Phase 3:

To determine whether the amount of water vaporised from a metal container could be measured simply using an automatic pipette and a measuring cylinder.

Phase 3 of the experiment was conducted at the University of Fort Hare Research and comprised the following procedure;

1) Three by a quarter hectare plots of varying fuel loads were burnt with head fires;
2) Three replications of two tins with a mean weight of 97.93 grams and a basal area 60.84 cm^2 were placed at ground level and canopy height in the grass swards of each of these plots. From an automatic pipette, $\pm$ 20 ml of water was added to each metal container;
3) Each individual metal container, plus its contents, was weighed on an analytical balance both before and after the burn, to determine the amount of water converted to steam during each fire. After the fire the contents of each metal container were also measured in a 20 ml measuring cylinder to determine how many millilitres of water had been converted to steam.

Phase 4:

To determine the size and shape of metal container that would give the optimum estimates of the quantity of water vaporised during a fire.

The following experiment was conducted at the University of Fort Hare Research Farm to determine the size and shape of metal container best able to estimate the quantity of water vaporised during a fire;

1) Six plots 10m x 10m in size, with varying fuel loads were burnt as head fires,
2) Three sets of three replications of two tins with mean dimensions of 88mm x 100mm, 100mm x 100mm and 6.5mm x 40mm (diameter x depth) and a basal area 60.84, 78.53 and 33.18 cm^2 respectively, containing $\pm$ 20 ml of water added with an automatic pipette, were placed at ground level and canopy height in the grass swards of each of these plots.
3) The metal containers together with their contents were accurately weighed before and after the fire to determine the amount of water that had been vaporised during the fire.

Results and Discussion

Phase 1

The relationship between the amount of water vaporised from the metal containers and the maximum temperatures recorded with the bi-metalic thermometers located at these points in the fires is presented in Figure 2.

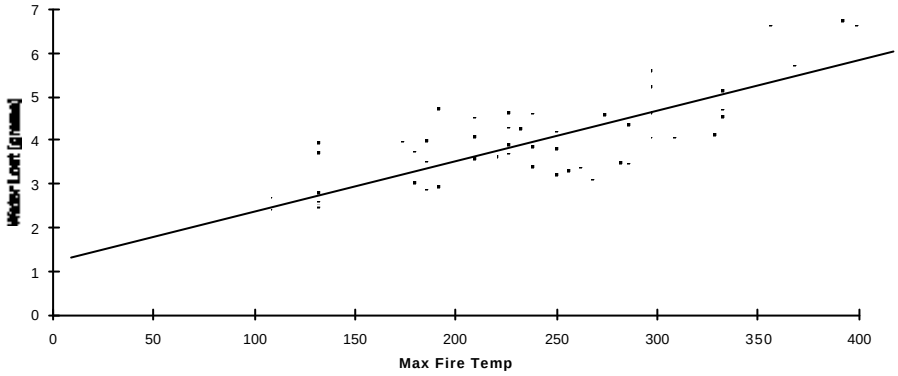

Figure 2: The linear regression between the amount of water vaporised from metal containers and the maximum temperatures recorded with bi-metalic thermometers located at the same points in experimental head fires. ($P < 0.05$; $r^2 = 0.6$; $r = 0.8$; STD ERR = 0.64; df = 51)

The results in Figure 2 indicate a significant positive relationship between the water lost due to vaporisation and the maximum temperature recorded during a fire. Similar results were obtained by Trollope (1983), who estimated using rate of spread, heat yield and fuel load, that fire intensity was significantly correlated with maximum temperatures recorded during surface head fires giving a good indication of the dynamics involved in the release of heat energy in these fires. The fact that the results from the statistical analysis were significant, conceptually meaningful and logical, indicates that it is valid to use the amount of water vaporised as a means of estimating the intensity of a fire.

Phase 2

The results of whether fire intensity expressed as the total amount of heat energy released per unit time, per unit length of the fire front (kJ s^{-1} m^{-1}) (Byram, 1959) could be derived from the amount of heat required to vaporise known quantities of water from a metal container placed in a free burning fire using calorimetry are presented in Figure 3.

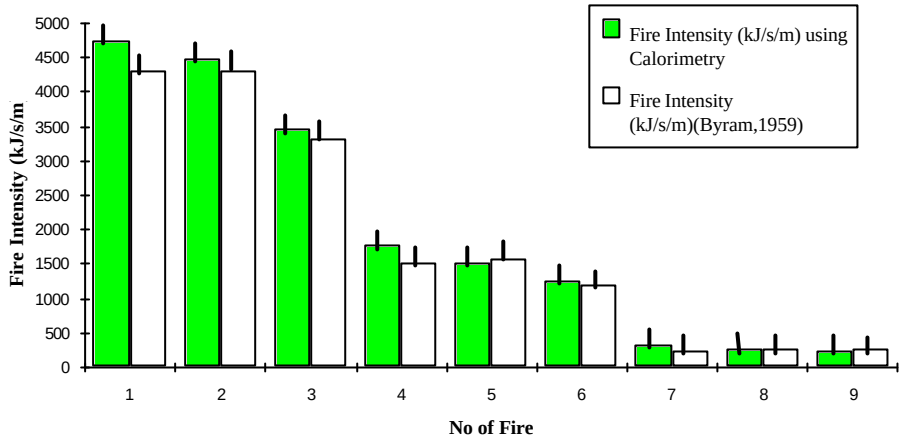

Figure 3 : Relationship between Fire Intensity (Byram, 1959) and Fire Intensity using calorimetry (n = 2, df = 1, SE of mean = 95& $LSD_{(0.05)}$ = 277).

In Figure 3 it can be seen that there are no significant differences between fire intensity as measured using the procedure developed by Byram (1959) and the fire intensity measured by calorimetry. The slight differences can be ascribed to the fact that fire intensity as defined by Byram (1959) is a mean value for the whole area that is burnt. It does not take into account any variation in the flammability of the fuel load due to species diversity, moisture content, age of fuel etc.

Phase 3

The results of whether the amount of water vaporised from a metal container could be measured simply with the aid of an automatic pipette and a measuring cylinder are presented in Figure 4.

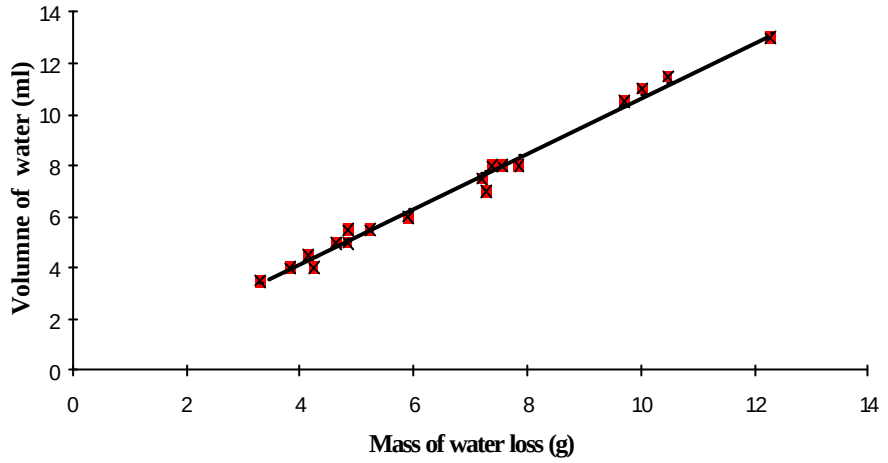

Figure 4: The positive relationship between measuring the amount of water vaporised from a metal container during a fire using measurements of volume and mass. (df = 17; P ≤ 0.05; r = 0.99; r^2 = 0.99; STD ERR = 0.29.)

The results in Figure 10 indicate that there is no significant difference in determining the amount of water converted to steam, either by weighing the metal container on an analytical balance, or by measuring the contents of the metal container in a measuring cylinder. The slight variation in the data between these two methods is understandable because not all the water can be removed from the metal container and added to the measuring cylinder.

By using the following regression equation the actual mass of the water converted to steam can be predicted from the measured amount of water converted to steam;

$y = -0.214 + 0.9494x$

where y = measured amount of water converted to steam - millilitres - ml;

x = mass of water converted to steam - grams - g.

Phase 4

The effect of size and shape of metal container on estimating the quantity of water vaporised during a fire, is presented in Figure 5.

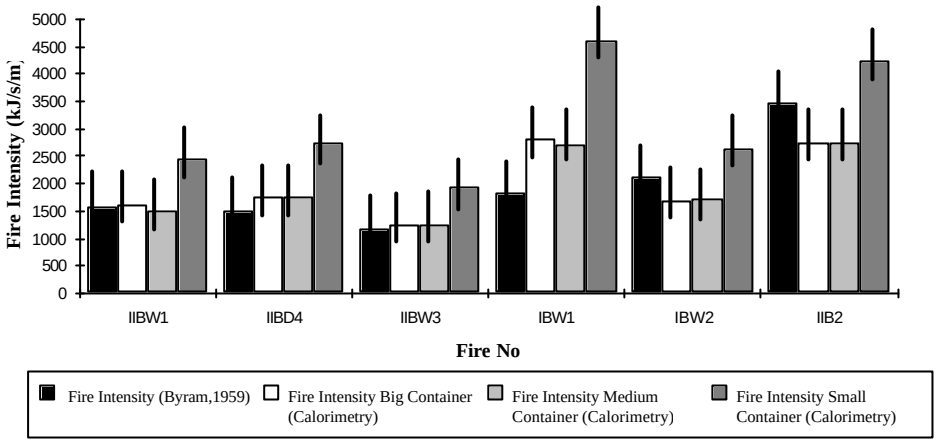

Figure 5: The effect of size and shape of metal container on estimating the quantity of water vaporised during a fire (n = 6, df = 5, SE of mean = 329 & $LSD_{(0.05)}$ = 962).

When comparing the three sets of metal container data it can be seen that they all follow a similar trend except that fire intensities for the small metal containers are greater than the other two by + 1000 kJ s^{-1} m^{-1}. This increase in fire intensity in the small metal container can be attributed to its small size and area. Any error that arises by water splashing out of the metal container during boiling, due to its size, is over emphasised when calculating fire intensity. The results for the two larger metal containers are very similarl.

It is important to note that the diameter of the metal container must be such that when the water is added it comp letely covers the bottom to an appropriate depth otherwise the resultant fire intensity measurement will be inaccurate. This is because if only a portion of the bottom of the container is covered the actual area exposed to the fire front is unknown.

When comparing the results of fire intensity from the medium metal container and the calculated fire intensity, the last three plots vary quiet substantially. However, the two bigger metal container results are virtually the same, indicating that a problem could have arisen with varying fuel load, rates of spread or in measuring the period of flaming combustion for these plots - or a combination of the above. The varying fuel loads and rates of spread have previously been dealt with but the difficulty of measuring the period of flaming combustion will be dealt with below .

The period of flaming combustion is recorded as the time it takes to burn an area once it has been ring fired (Trollope 1983). In other words, it is the time period, from the start of the head fire, to when the head fire meets the back fire. This measurement is subjective and is not always well defined, as most of the time there is no definite indication of when the flames of the head and back fires meet, especially when viewing the fire through the smoke. A small difference in this measurement will create a big difference in the resultant fire intensity. For example, if the time period of the flaming combustion is recorded as five seconds longer for the plot IIB2, the fire intensity calculation would result in a fire intensity of 2824 kJ s^{-1} m^{-1} which would be virtually the same as that recorded by the metal container method.

As stated before, this problem could be overcome if the rate of spread of a free burning fire were to be measured with the aid of stopwatches. This would give a more accurate figure of the actual rate of spread of a fire front at a specific location.

Conclusions

These initial results suggest that:

1) A relationship exists between the amount of water vaporised from metal containers and the maximum temperature recorded with bi-metallic thermometers at specific points in free burning fires. The aforegoing conclusions indicate that maximum temperature can serve firstly, as an index of fire intensity, and secondly, as an index of the total amount of heat energy released during a veld fire.
2) The heat of vaporisation of water boiled off during a fire can be used to estimate the intensity of combustion, as defined by Byram (1959), occurring at different points in a fire. This is evident from the results that there are no significant differences between fire intensity as estimated using the procedure by Byram (1959) and the fire intensity measured by calorimetry.
3) A suitable container in the form of a simple metal container, located at specific points above ground level, can be used to estimate the quantity of water vaporised during a fire. The results indicate that it is reasonable to assume for practical purposes that the amount of energy to which a specific location in a fire front is exposed to, is heat energy released from the burning fuel in close proximity to that location. This implies that if the height of a metal container at ground level is one

third of the canopy height, then the amount of heat energy to which it is exposed is one third of the heat yield of the grass sward.

4) The size and shape of the metal container that resulted in optimum estimates of the quantity of water vaporised during a fire had the following dimensions: 88mm x 100mm (diameter x depth) and a basal area 60.84 cm^2. This size of metal container had a basal area large enough to hold water to a depth of up to 5 mm without water being lost by splashing during the vaporisation process .

From the above it can be concluded that the hypothesis was not disproved: The fire intensity at a particular point in the fire front can be estimated with the aid of a measuring cylinder, enabling one to determine the quantity of water vaporised from a suitable container when located at a particular point in a fire. The fire intensity will be the product of the rate of spread of the fire front and the total heat of vaporisation per unit area of the water lost from the container expressed as kilojoules per second per metre - kJ s^{-1} m^{-1} .

This procedure could be very useful researchers in quantifying the dynamics of the release of heat energy during a fire and the subsequent response of the plants to it.

References

Albini FA 1976. Estimating Wildfire Behaviour and Effects. USDA Forest Service General Technical Report INT-30.

Bransby DI & Tainton NM 1977. The disc pasture meter : Possible applications in grazing management. Proceedings of the Grassland Society of Southern Africa. 12: 115-118.

Byram GM 1959. Combustion of forest fuels. In: Davis KP (ed). Forest fire: control and use. McGraw Hill Book Co, New York.

Luke RH & McArther AG 1978. Bush fires in Australia. Government Publication Service, Canberra.

Trollope WSW 1983. Control of bush encroachment with fire in the arid savannas of southeastern Africa. PhD thesis, Univ. of Natal, Pietermaritzburg.

Tunstall BR, Walker J & Gill AM 1976. Temperature distribution around synthetic trees during grass fires. Journal of Forage Science 22: 269-276.

Vines RG 1981. Physics and rural chemistry of fires. In Gill AM, Groves RH & Noble LR(ed) Fire and the Australian biota. Australian Academy of Science, Canberra.

Weast RC 1987. Handbook of Chemistry and Phisics 1st Student Edition. CRC Press Inc. Boca Raton Florida.